A STUDY OF THE DEFECT NATURE OF IONIC CRYSTALS

Thesis

submitted for the degree of

DOCTOR OF PHILOSOPHY

of the

University of Glasgow

by

Peter J. Harvey B.Sc.

September 1965

ProQuest LLC.
789 East Eisenhower Parkway
P.O. Box 1346
Ann Arbor, MI 48106 – 1346

ACKNOWLEDGEMENTS

I should like to take this opportunity to express my sincere thanks to my supervisor Dr. I. M. Hoodless, to whom I am deeply indebted for his constant help, guidance, and unfailing attention throughout the course of this work.

My thanks are also due to Dr. G. Webb for helpful advice received during the preparation of this manuscript, and to Mr. A. MacQuarrie for technical assistance.

I wish to acknowledge a maintenance grant from D.S.I.R.

SUMMARY

Self-diffusion and ionic conductivity studies have been carried out on 'pure' single crystals of CsCl and on single crystals containing aliovalent impurity ions. The crystals were grown from aqueous solution.

Self-diffusion studies, using radioactive tracers, indicate the existence of two regions in the diffusion plots for both anion (Cl-36) and cation (Cs-137) diffusion, in the approximate temperature range 200-470°C. Below approximately 290°C., the diffusion can be represented by the following equations:-

$$D_{Cl^-}\ (cm^2/sec) = 1.95 \times 10^{-7}.\exp(-0.50/kT)$$

and

$$D_{Cs^+}\ (cm^2/sec) = 9.04 \times 10^{-8}.\exp(-0.60/kT).$$

Between 290-470°C., the diffusion equations have the following form:-

$$D_{Cl^-}\ (cm^2/sec) = 2.1 \exp(-1.30/kT)$$

and

$$D_{Cs^+}\ (cm^2/sec) = 25.3 \exp(-1.54/kT).$$

The diffusion is interpreted in terms of ion movement via Schottky defects. The results indicate that the energy required to create a pair of Schottky defects in CsCl is 1.96 ± 0.04 ev.

Over the complete temperature range studied, the anion is the more mobile ion.

The Cs-137 diffusion coefficient is increased, particularly at higher temperatures, by deliberate addition of divalent cation impurities. Addition of divalent anion impurities lowers the diffusion coefficient over the complete temperature range studied. The Cl-36 diffusion coefficient is lowered by the addition of either divalent cation or divalent anion impurities.

Ionic conductivity studies in 'pure' single crystals of CsCl, in the temperature range 230-470°C., indicate the existence of two regions in the plots of conductivity as a function of reciprocal temperature. The magnitude of the conductivity and the activation energy, in the low temperature region, are dependent upon the origin and pre-treatment of the crystal. In the approximate temperature range 280-470°C., both the magnitude of the conductivity and the activation energy are reproducible from crystal to crystal and independent of the origin and pre-treatment. In this region the conductivity is described by the equation

$$\sigma(\text{ohm}^{-1}\text{cm}^{-1}) = 1.64 \times 10^{5}.\exp(-1.395/kT).$$

In crystals containing divalent cation impurities the existence of a region of conductivity, characteristic of ion movement via impurity-induced vacancies, is not observed. In the approximate temperature range 300-470°C., three regions of conductivity occur. In the approximate temperature range 300-350°C., region I, an activation energy and magnitude of conductivity, similar to those for pure crystals, are observed. In region II, 350-390°C., a rapid increase in conductivity occurs. This is interpreted in terms of impurity dissolution. Above 390°C., region III, the activation energy is dependent upon the impurity concentration.

The general shape of the conductivity plots for crystals containing divalent anion (sulphate) impurity is similar to that for crystals 'doped' with divalent cation impurity. In region I, however, the magnitude of the conductivity decreases with increasing sulphate concentration. It is suggested that the sulphate ion, due to its size, is present in the lattice in the form of impurity-vacancy complexes. The impurity-induced vacancies, therefore, are not available for conduction in this region. The lowering of the magnitude of the conductivity is caused by the suppression of the thermal vacancy concentration. In region II, dissociation of the complexes leads to a rapid increase in conductivity.

The observed activation energies in region III tend to support the interpretation of region II; but the observed effects are less marked than would be expected. It appears, therefore, that only partial dissociation occurs in region II.

Ionic conductivity measurements have also been used to study the phase transition (simple interpenetrating-cubic to face-centred cubic) in caesium chloride. In 'pure' crystals the transition occurs in the temperature range 469 ± 3 — 473 ± 2 °C. The transition temperature is lowered with increasing amounts of divalent cation impurities to a minimum of about 430°C. Further increases in impurity concentration cause the transition temperature to rise again. The transition temperature is raised with increasing amounts of sulphate ion impurity. The highest temperature recorded is 520°C.

It is suggested that the transition in caesium chloride is critically dependent upon the rate of movement of both the caesium and the chloride ions.

CONTENTS

.....

CHAPTER 1.

INTRODUCTION.

1.1 GENERAL INTRODUCTION.

In order to account for the many optical and physical properties of ionic crystals, a departure from the perfect crystalline arrangement is necessary. Without the presence of imperfections, properties which involve migration of atoms or ions, e.g. diffusion and ionic conductivity, are energetically inconceivable.

In 1926, Frenkel[1] proposed that ions sometimes received sufficient energy from thermal vibrations to be pushed from their normal lattice positions to positions in the interstices of the lattice. Further excitation leads to movement from one interstitial ppsition to another until eventually the ion meets a vacant site and drops back into the normal lattice.

In this way diffusion of atoms or ions could take place and ionic movement under the influence of an external field, i.e. ionic conduction, was also explicable. A crystal lattice containing Frenkel defects is illustrated in diagram A.

It has since been shown[2,3] that Frenkel defects are important in the silver halides.

A second type of lattice defect was envisaged by

DIAGRAM A. Illustration of Frenkel Defects.

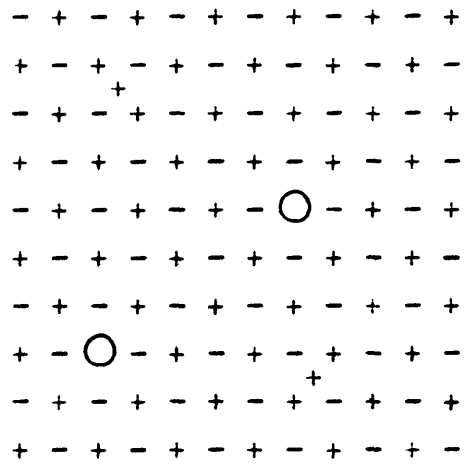

DIAGRAM B. Illustration of Schottky Defects.

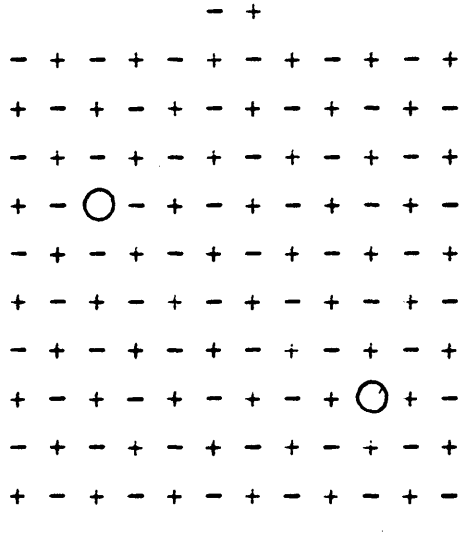

Schottky[4], and is shown in diagram B.

Schottky proposed that a chemically equivalent number of anion and cation vacancies could arise if the ions migrate from their lattice positions to internal or external boundaries.

Although both types of defect can occur in the same crystal, the respective formation energies are such that one type will predominate. In general, Frenkel defect formation is favoured when individual ion sizes are largely dissimilar, and van der Waal's energy and dielectric constant are high. Schottky defects, on the other hand, predominate in the majority of alkali halides, in which the dielectric constant and van der Waal's energy are low.

The number of Schottky or Frenkel defects present can easily be calculated. One method of calculation for Schottky defects proceeds in the following manner[5].

Let us consider that a cation and anion in the lattice react with imaginary sites outwith the lattice and form pairs of ions 'adsorbed' on the surface and a pair of vacancies in the lattice. This can be represented by an equation of the type

Anion and Cation in lattice	+	Imaginary sites outwith lattice	=	Pair of ions adsorbed	+	Pair of vacancies

the surface by N_s, and the number of ion pairs in the lattice by N, then we can apply the Law of Mass Action approach to the equilibrium,

$$n^2 N_s/(N - n)^2(N_s) = K \quad \text{.....(1)}$$

When n is very much less than N, equation (1) reduces to

$$n^2/N^2 = K \quad \text{.....(2)}$$

If W is the energy to create an anion and cation vacancy, i.e. the energy of formation of a Schottky defect, then

$$n = N \exp(-\tfrac{1}{2}W/kT) \quad \text{.....(3)}$$

Equation (3), which illustrates the increase in the concentration of vacancies with temperature, neglects the changes in vibrational frequencies of the ions due to the presence of vacancies, and does not take thermal expansion of the crystal into consideration. The relationship has been modified to allow for these factors[6].

The thermal expansion leads to a decrease in W and may be represented as follows.

$$W_T = W_o + \alpha V_o T(dW/dV) \quad \text{.....(4)}$$

where, W_T is the energy to create a pair of vacancies at temperature T,

W_o = the energy to form the defect at 0^oK,

V_o = the crystal volume at 0^oK,

and α = the coefficient of thermal expansion.

The correction for differing vibrational frequencies introduces a pre-exponential factor, γ, which is given by

$$\gamma = (v/v')^x \qquad \text{.....(5)}$$

where v = the normal lattice frequency,

v' = the frequency of an ion adjacent to a vacancy,

x = the number of nearest neighbours.

Taking these effects into account, equation (3) becomes

$$n = \gamma BN \exp(-\tfrac{1}{2}W/kT) \qquad \text{.....(6)}$$

where $$B = \exp\left(-\frac{\alpha V_o}{2k} \cdot \frac{dW}{dV}\right)$$

Similar relationships can be derived for the concentration of Frenkel defects as a function of temperature.

It should be noted that under constant temperature conditions equation (6) can be represented by

$$n_1 n_2 = K' = n_o^2 \qquad \text{.....(7)}$$

where n_1 and n_2 are the mole fractions of the defects. For Schottky defects, n_1 and n_2 are the mole fractions of cation and anion vacancies which, in a pure crystal,

will be identical and equal to n_o.

1.2 IONIC MIGRATION IN CRYSTALS.

The presence of defects of either Frenkel or Schottky type provides suitable conditions for the movement of ions in the crystal. In a crystal containing Frenkel defects, ions, usually the cation, can migrate by an interstitial mechanism which involves the jumping of the ion to a neighbouring interstitial site. Ions can also move indirectly by knocking an adjacent atom from a lattice site into an interstitial position and occupying the vacated site itself. This is known as the interstitialcy mechanism.

Both anion and cation migration is possible in a crystal containing Schottky defects by the movement of ions from their lattice positions to corresponding vacancies in neighbouring positions.

The phenomenon of ionic conductivity, the movement of ions under the influence of an applied electric field can be represented by equation (8)

$$\sigma = ne\mu \qquad \text{.....(8)}$$

where σ = the specific conductivity measured in $ohm^{-1}cm^{-1}$,

n = the number of vacancies per cm^3, i.e. charge carriers per cm^3,

e = the electronic charge,

and μ = the mobility of the ions, i.e. the

rate of movement under unit field.

This relationship between conductivity and the number of vacancies has led to ionic conductivity studies being widely used for the purposes of learning more about the behaviour of defects in ionic solids.

However, we can only measure the total conductivity of an ionic crystal and the component contributions of the anion and cation must first be determined before any useful information can be derived from such measurements. Transport number determinations[7] have shown that, for the majority of alkali halides, the conductivity is almost exclusively cationic except at temperatures near the melting point.

In such instances ionic conductivity studies have proved invaluable in the quest to understand better the nature and behaviour of lattice defects.

The simple equation (8) can be expanded by introducing the expression for the mobility[5],

$$\mu = (va^2Ce/kT) \exp(-U/kT) \quad \text{.....(9)}$$

where v = vibrational frequency of the ion,

a = the distance between the ions,

and C = a thermal expansion correction to the height of the energy barrier U.

Substituting the value for μ from equation (9),

equation (8) becomes

$$\sigma = (nva^2Ce^2/kT)\exp(-U/kT) \quad \ldots\ldots\ldots(10)$$

Further substitution, this time for n from equation (6), gives

$$\sigma = (\gamma BCNva^2e^2/kT)\exp(-U/kt)\exp(-\tfrac{1}{2}W/kT) \ldots(11)$$

Equation (11) is usually written as

$$\sigma = \sigma_o/T \exp(-E/kT) \quad \ldots\ldots\ldots(12)$$

where $E = U + \frac{1}{2}W$.

Similarly, the diffusion of ions through a lattice can also be represented by equations of this type.

$$D = \gamma BCva^2\exp(-U/kT)\exp(-\tfrac{1}{2}W/kT) \quad \ldots\ldots\ldots(13)$$

and

$$D = D_o\exp(-E/kT) \quad \ldots\ldots\ldots(14)$$

where $E = U + \frac{1}{2}W$,

and D is the diffusion coefficient.

From equations (12) and (14) it is seen that plots of $\log(\sigma T)$ and $\log(D)$ against $(1/T)$ should result in straight lines from which the energy, E, can be calculated.

The early studies[8] of ionic conductivity invariably showed the existence of two regions in the $\log(\sigma)$

versus (1/T) plots. These two regions were defined by a 'knee'. The conductivity at temperatures above the knee, the intrinsic region, was quite reproducible from crystal to crystal. The activation energy for this process is, E, the sum of the energy to create a defect, $\frac{1}{2}W$, and the energy for mobility, U. The region below the knee, the extrinsic region, was found to be dependent upon the purity of the sample and upon its thermal history.

Various reasons were proposed at the time to account for this non-reproducibility and for the lower activation energy in this region.

The first of these was put forward by Smekal[9], who proposed the idea of diffusion of a small number of atoms or ions by means of grain boundaries. Although this theory suffered serious setbacks it has since returned to favour as we shall see later.

The second idea was that of 'frozen-in' defects[10]. It was suggested that on cooling a crystal, vacancies were trapped and consequently a non-equilibrium concentration of vacancies existed in the crystals at the lower temperatures. Temperature changes in this region would only affect the ion mobility.

However, the most-accepted and subsequently verified interpretation (to some extent at any rate)

of the low temperature region was that which attributed the region to the existence of trace amounts of impurity or foreign ions of a different valency to that of the host ions[11]. These will in future be called aliovalent impurity ions. The introduction of aliovalent impurity ions into a crystal lattice leads to the question of electrical neutrality and its subsequent effects. When a divalent cation is introduced into a uni-valent lattice, e.g. Ba^{2+} in NaCl, an unbalance of charge occurs if the Ba^{2+} ion substitutionally replaces a sodium ion. In order to retain electrical neutrality the substitution of the Ba^{2+} ion will be accompanied by the formation of a cation vacancy in the lattice. For example, on the addition of divalent cation impurity of mole fraction c, the maintenance of electrical neutrality requires that,

$$n_1 = c + n_2 \qquad \text{.....(15)}$$

where n_1 and n_2 are the mole fractions of the cation and anion vacancies respectively. Equation (7) can now be written as,

$$n_1(n_1 - c) = n_o^2 \qquad \text{.....(16)}$$

or,

$$n_1 = \tfrac{1}{2}c(1 + (1 + 4n_o^2/c^2)^{\frac{1}{2}}) \qquad \text{.....(17)}$$

Equation (17) illustrates the change over from intrisic conductivity, when $n_o \gg c$, to impurity controlled conductivity when $c \gg n_o$. It also illustrates the suppression of the thermal vacancy equilibrium by the presence of the aliovalent impurities. By substituting values for n_o, the conductivity expression (8) can be shown at low temperatures to be a function only of U, the energy of ion mobility, while at higher temperatures it depends upon the energies for defect formation and for ion mobility, i.e. $U + \frac{1}{2}W$.

This explanation of the two regions in the conductivity plots was first put forward by Koch and Wagner[11] in 19 37. Experimental substantiation of the theory was established in 1949 by Kelting and Witt[12] and by Etzel and Maurer[13] a year later. The former studied the addition of $SrCl_2$ and $BaCl_2$ to KCl, while the latter carried out investigations on Cd^{2+}-doped NaCl.

The phenomenon of single vacancies was sufficient to explain the experimental data available up until some 24 years ago. However, the work of Pohl[14], and later that of Estermann, Leivo and Stern[15], showed the production of F-centres (Farbzentrum) in NaCl and KCl required some modification of theory. These F-centres, which consisted of anion vacancies containing a trapped electron, were instrumental in the proposal

DIAGRAM C. Illustration of Vacancy Pairs.

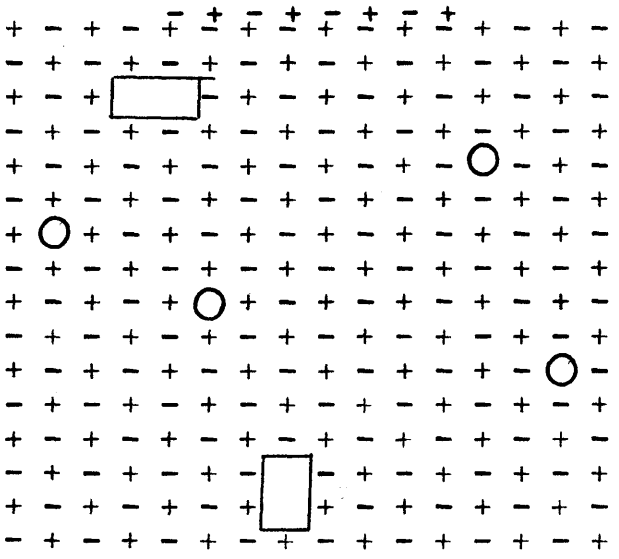

○ Schottky defect.

□ Vacancy pair.

of Seitz[16] of the existence of what has become known as 'vacancy-pairs', (diagram C), neutral entities formed by the association of positive and negative ion vacancies.

Further evidence for the existence of defect entities other than single vacancies became available when detailed studies were made on the ionic conductivity and diffusion in the alkali halides. From a consideration of the conductivity and diffusion equations (11) and (13) a relationship is apparent. This relationship known as the Nernst-Einstein relationship can be written

$$\sigma T(f)/D = Ne^2/k \qquad \ldots\ldots\ldots(18)$$

and is valid so long as the same type of defect is contributing to both conductivity and diffusion*.

A study of conductivity and cation self_diffusion in NaCl and NaBr[18] revealed the validity of the Nernst-Einstein relationship in the intrinsic region above the knee. However, in the region below the knee the measured diffusion coefficient was higher than that

* In cases where tracer diffusion is measured, D must be replaced by D(f) where (f) is a correlation factor which takes into account the deviations of the tracer diffusion from a random walk process. The value of (f) depends on the mechanism of ion movement.

DIAGRAM D. Illustration of Impurity-Vacancy Complexes.

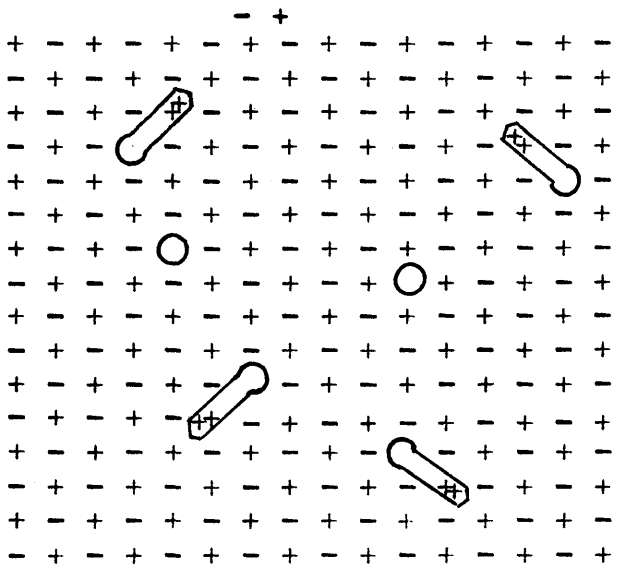

Schottky defect.

Impurity-vacancy complex.

calculated from conductivity results. Similar results were obtained by Aschner[19] on pure and Sr^{2+}-doped KCl. This failure of equation (18) in the extrinsic region necessitated the existence of some neutral entity which contributed to diffusion but not to conductivity. While an obvious explanation was that of vacancy-pairs, the above authors[18] favoured the idea of a second neutral species, which has become known as an impurity-vacancy complex. This is illustrated in diagram D.

Two further pieces of experimental evidence supported the idea of the existence of complexes of this nature. The results of Etzel and Maurer showed that the increase in magnitude of conductivity in the extrinsic part of the conductivity plots in NaCl was not commensurate with the amount of Cd^{2+}-doping. Furthermore, if the non-validity of the Nernst-Einstein relationship is due to impurity-vacancy complexes of this nature, the absolute values for impurity diffusion should be higher than those for self-diffusion. The results of Chemla[20] substantiate this conclusion.

In recent years there have been many investigations of the vacancy-complex formation. A new technique, that of dielectric loss measurements[21], proved a great aid to the studies of lattice disorder at low temperatures, particularly with regards to impurity-vacancy complexes. Dielectric loss, $\tan\delta$, results from the

the re-orientation of the impurity-vacancy complex under the action of an applied filed. Plots of tan δ versus temperature at a fixed frequency or, as is more often employed, tan δ versus frequency at a fixed temperature give rise to peaks. The height and position of the peaks give a measure of the concentration and formation energy of these impurity-vacancy complexes. The existence of such dielectric loss peaks, although at first repudiated[22], has been used by many workers[23-29] and has greatly increased our knowledge of crystal defects.

Further information has been derived from electron spin resonance studies. Measurements on Mn^{2+}-doped NaCl[30,31], in conjunction with dielectric loss measurements, have led to the present-day picture of a crystal lattice in which not only those defects previously mentioned exist; but a lattice in which dimer, trimer and higher order impurity-vacancy complexes, vacancy clusters and impurity aggregates are present.

1.3 ROLE OF GROSS DEFECTS IN CONDUCTIVITY AND DIFFUSION.

The previous section has shown that a reasonably adequate mechanism of ionic conductivity and cation self-diffusion in the alkali halides can be obtained in terms of point defects. i.e. defects whose sphere of influence is restricted to a few ions in the vicinity of the defect. A crystal, however, also contains gross

DIAGRAM E. Regions in conductivity plot (Dreyfus & Nowick)

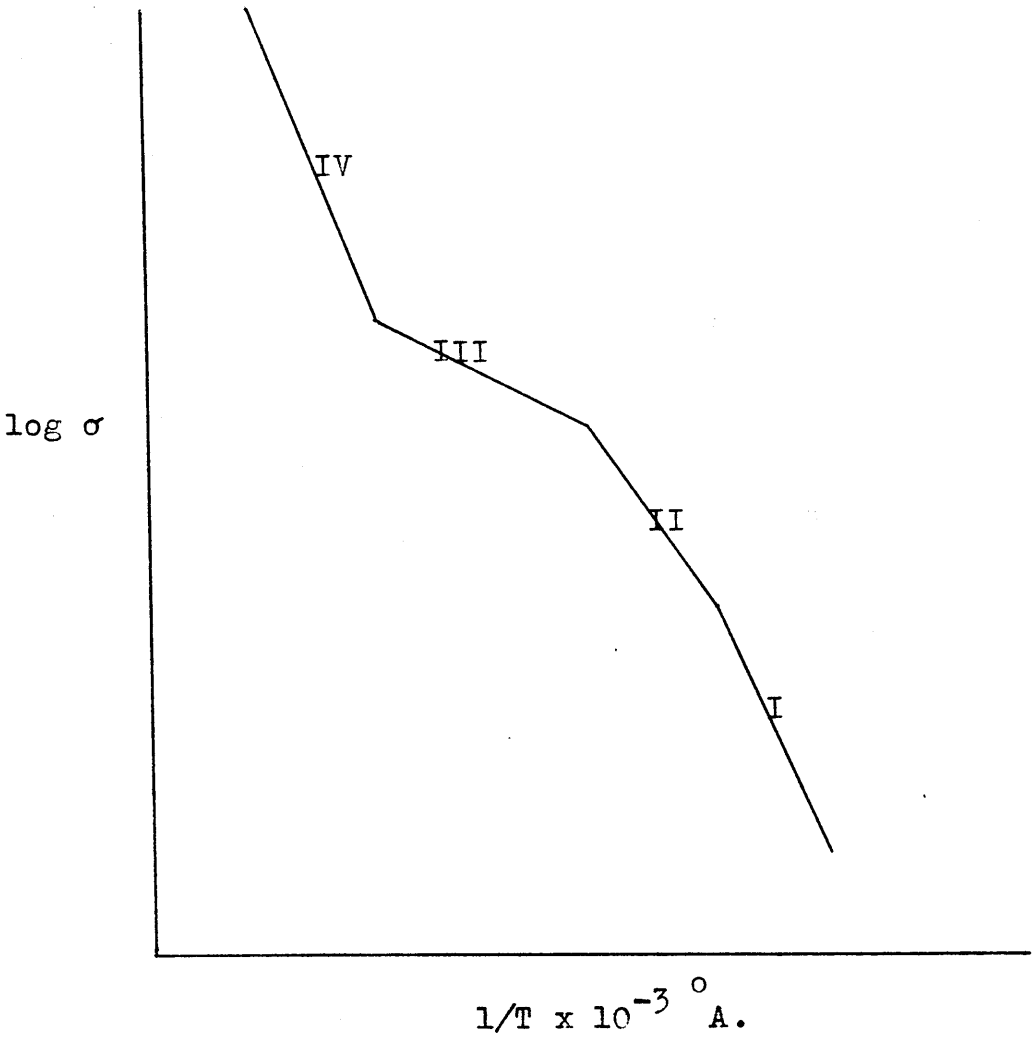

defects which involve large numbers of ions, the most important of these defects being the one-dimensional imperfections, edge and screw dislocations, and the two-dimensional imperfections such as grain boundaries[32].

Structural defects of this type seem to play a minor role in ionic conduction in the alkali halides. This is somewhat unexpected since dislocations can act as either vacancy sources or vacancy sinks. Furthermore, edge dislocations, at low temperatures, do possess a significant charge arising from the difference in mobility of anion and cation vacancies.[33] The main effect of dislocations on ionic conductivity appears to be in their ability to act as impurity aggregation centres[34,35,36].

The previous discussion (1.2) of impurity effects has assumed the complete solubility of the impurities at low temperatures. This is seldom correct. Dreyfus and Nowick[37] have extended the range of conductivity measurements made on aliovalent impurity doped NaCl to lower temperatures. At least four ranges of ionic conductivity can be characterised as shown in diagram E.

Region I corresponds to dissolution of the impurity in the crystal; this is usually accompanied by the formation of vacancy impurity complexes. At higher temperatures (Region II) these complexes

dissociate and the activation energy in this region is given by

$$E_{II} = U + W_a/2$$

where W_a is the dissociation energy of an impurity-vacancy complex.. Regions III and IV correspond to the conductivity ranges discussed in section 1.2 and are characterised by activation energies of U and $(U + \frac{1}{2}W)$ respectively. Values of the impurity-vacancy complex association energy (W_a) have been determined from conductivity studies[38-41], and from impurity diffusion measurements[42-46].

Although gross defects appear to be of minor importance in cation self-diffusion, their role in anion self-diffusion is very significant. Similarly vacancy pairs would appear to be of considerable importance in anion but not in cation self-diffusion.

In 1958, Harrison, Morrison and Rudham[47] investigated chloride ion diffusion in sodium chloride. While Laurent and Bénard[48] seemed to have assumed a diffusion mechanism via single vacancies, Morrison et al postulated the idea of anion impurity-vacancy complexes as being contributory to the chloride diffusion in the extrinsic region. In 1960, Barr, Hoodless, Morrison and Rudham[49] found that the diffusion in the extrinsic region was very much dependent upon dislocations. Lidiard[50], at

this time, interpreted the low temperature diffusion results in terms of vacancy pairs. A few years later, Laurance[51] investigated anion self-diffusion in the intrinsic region in sodium chloride, 'pure' and Ca^{2+}-doped. Laurance's results indicated that the decrease in diffusion coefficients with increasing impurity concentration could not be accounted for in terms of simple vacancy diffusion. He proposed that some of the diffusion was proceeding via vacancy pairs which are independent of impurity concentration. More recently, the study of anion diffusion in sodium chloride has again been undertaken[52]. While at lower temperatures the diffusion is undoubtedly dependent upon the dislocation density in the crystal, it has been found that in the temperature range 450-700°C, the diffusion coefficient could be expressed as the sum of contributions from single vacancies and vacancy-pairs, with the latter being more important at higher temperatures.

The general picture of ion movement in the alkali halides, other than the caesium halides, is one in which the general features of anion and cation self-diffusion are similar but the detailed mechanisms are very different. At low temperatures, cation self-diffusion depends on aliovalent impurities producing

single vacancies and impurity-vacancy complexes. Anion self-diffusion at low temperatures also depends on aliovalent impurities, but in this instance it is the impurity affecting the charge on the dislocation which is important. At high temperatures, both cation and anion self-diffusion are independent of impurity content but while cation diffusion is via a single vacancy, vacancy-pairs appear to be significant in anion diffusion.

1.4 THE CAESIUM HALIDES.

In the previous sections we have indicated the main types of defects present in ionic solids and have discussed their relevance in systems where only the cation is sufficiently mobile to contribute to the conductivity.

The caesium halides, however, present a much more difficult system to study in that both ions contribute to the conductivity. For this reason it would seem, judging by the scarcity of publications in this field, that the conductivity and diffusion studies in caesium halides have been neglected.

In 1955 Harpur, Moss and Ubbelohde[53,54] carried out an investigation of the conductivity of caesium halides in the temperature range 330-470°C. Their reported values for σ_o and E in the equation

$$\sigma T = \sigma_o . \exp(-E/kT)$$

were 50 ($ohm^{-1}cm^{-1}$) and 1.04 eV respectively for caesium chloride in this temperature range. These values, and those for the other caesium halides were very low in comparison with the σ_o and E values for the sodium, potassium and rubidium halides. This apparent anomaly led to these workers proposing a significant electronic contribution to the conductivity.

In the course of a series of self-diffusion studies in the alkali halides, Laurent and Bénard[48] measured the Cs^+ and Cl^- diffusion coefficients in caesium chloride. Their results are of the form

$$D_{Cs^+} = 10^{-5} \exp(-0.70/kT)$$

$$D_{Cl^-} = 1.3 \times 10^{-3} \exp(-0.87/kT)$$

at temperatures below 465°C. The remarkable feature of these results being that although the Cs^+ ion is slower moving it migrates with a lower activation energy than the chloride ion.

In 1959 Lynch[55] studied the ionic conductivity and self-diffusion in caesium bromide and caesium iodide. His conductivity results can be expressed in the form:

$\sigma = 2.48 \times 10^5 \exp(-1.435/kT)$ for CsBr between 475-590°C

$\sigma = 2.51 \times 10^4 \exp(-1.285/kT)$ for CsBr below 475°C

$\sigma = 2.21 \times 10^5 \exp(-1.43/kT)$ for CsI 480-595°C

$\sigma = 1.38 \times 10^4 \exp(-1.25/kT)$ for CsI below 480°C.

At lower temperatures Lynch found the conductivity was impurity dependent and varied from sample to sample At higher temperatures close agreement with the Nernst-Einstein relationship was observed between the diffusion and conductivity results. Lynch concluded that Schottky defects were controlling both processes. This being so, the suggested activation energies for cation and anion mobility were 0.58eV and 0.30eV respectively. Lynch proposed that the results of Harpur, Moss and Ubbelohde were in error due to their method of experimentation in that they placed platinum electrodes into the molten halide salts. It has since been shown that molten halides attack platinum. Lynch's proposal that conductivity was ionic brought the caesium halides into line with the other alkali halides. Even thallium chloride had by this time been shown to contain Schottky defects[56,57], which are responsible for conduction. More recent studies have confirmed this[58,59].

Conductivity and anion self-diffusion in caesium chloride were investigated by Hoodless and Morrison[60]. The close agreement between their results and those of Lynch led them to believe that conduction in caesium

chloride, like the other alkali halides, was ionic.

More recent measurements have been made on caesium iodide[61-63] confirming the ionic nature of the conductivity but failing to produce significant results on the effect of impurities.

The absence of impurity effects has also been noted by Herrington and Staveley[64] who measured the conductivity of pure and Ba^{2+}-doped single crystals of caesium chloride in the temperature region below 190°C.

In view, therefore, of the lack of data on caesium chloride, both pure and doped with aliovalent impurity ions, it seemed desirable to undertake such studies as would lead to a better understanding of the nature of defects in pure and impurity-doped crystals. Furthermore, caesium chloride undergoes a phase transition at high temperatures and very little is known about ion migration in this region. The present work was carried out for these purposes.

1.5 THE PHASE TRANSITION IN CAESIUM CHLORIDE.

It is well known that caesium chloride undergoes a phase transition from a simple interpenetrating cubic lattice (s.i.c.) to a face-centred cubic lattice (f.c.c.) There is considerable disparity in the values reported

Table of Previously Reported Transition Temperatures.

Reference	Method of Study	Transition Temperature (^{o}C)
Zemezuny and Rambach(65)	Cooling curves	451
Sandonini and Scarpa(66)	Cooling curves	451
Korrang(67)	Heating curves	479
Wagner and Lippert(68)	X-rays	450 ± 5
Wagner and Lippert(69)	X-rays	445 ± 5
Menary, Woodward and Ubbelohde(70)	X-rays	469
Johnson, Agron and Bredig(71)	X-rays	470
Wood, Secunda and M^{c}Bride(72)	X-rays	465-472
Hoodless and Morrison(60)	Ionic Conductivity	466-469

.....

for the transition temperature (see Table), but recent careful investigations place the transition in the region 465-472°C.

The transition in caesium chloride is of the first order type with a heat of transition of 700 cals/mole[73]. Transitions of this type are linked with hysteresis effects, the width of the loop depending on the volume change accompanying the transition. In this hysteresis region the phase rule requires that only one form of the crystal lattice should exist. Experiments, however, do not support this view and co-existence of the two phases has been found in this region[74,75].

Experiments involving the deliberate addition of impurities of the second phase form have shown that it is possible to vary the transition temperature. In caesium chloride, the addition of 20 mole per cent of rubidium chloride decreases the transition temperature by 115°C[76]. On the other hand, deliberate addition of impurities of the simple interpenetrating cubic structure, produces the reverse effect; 20 mole per cent of caesium bromide raising the transition by some 20°C[72]. The large variation in transition temperatures recorded in the previous table could, perhaps, be accounted for by the accidental incorporation of large amounts of impurity, as above, or more

likely, the temperature variation is associated with other hysteresis effects.

As a result of their X-ray measurements, Menary, Woodward and Ubbelohde[70] proposed that a significant increase in the number of vacancies arose in the transition region in caesium chloride; the situation being analogous to premelting. It has also been observed that reactivity in some solids is exceptionally high in the region of a first order transition[77-80], and this could be accounted for by large concentrations of vacancies. In the case of caesium chloride enhanced reactivity has been observed at 480°C in neutron-irradiated specimens[81].

These observations, however, have not been substantiated by ion migration studies in caesium chloride. Rather than show a significant increase in the number of vacancies in the transition region, ionic conductivity studies have indicated that the phase transition in caesium chloride is accompanied by a significant decrease in ion mobility[82]. For this reason ionic conductivity methods of following the transition together with self-diffusion measurements are convenient. No pre-transition phenomena have been observed with these types of measurement[53,60], and more recent studies have shown that electronic

conductivity, which could account for the failure to observe such phenomena, is negligible in caesium chloride in this temperature region[60].

It seems probable, therefore, that the transformation does not involve an extensive disruption of the lattice, but rather a simple change, such as dilatation, as has been suggested by Buerger[83]. It should be pointed out, however, that the majority of the previous work has been carried out on powder compacts or polycrystalline specimens and in these circumstances boundary effects could be very significant.

1.6 AIM OF THE PRESENT INVESTIGATION.

It is proposed to investigate three principal aspects of single crystals of caesium chloride.

(a) The measurement of conductivity and self-diffusion in single crystals of caesium chloride.

Very little of the previous work in this system has been concerned with ion movement in single crystals. A few preliminary studies of ionic conduction and some relative anion self-diffusion measurements have been reported[60] but other measurements are restricted to polycrystalline speciemns in which boundary effects could be very important. It is intended to study conductivity and both anion and cation self-diffusion

in single crystals below the transition point. It should be then possible to propose a mechanism for ion movement and to evaluate the effects of boundaries and dislocations.

(b) The measurement of conductivity and self-diffusion in single crystals of aliovalent impurity-doped caesium chloride.

Investigations of systems where both the anion and the cation are significantly mobile are few. This is surprising since relationships of types given in equations (7) and (17) can only be satisfactorily studied in these systems. It is intended to investigate the validity of these equations by measurements in aliovalent impurity-doped crystals.

(c) The measurement of conductivity and self-diffusion in single cystals of caesium chloride in the transition region.

It is the intention to investigate thoroughly the possible existence of pre-transition phenomena. Furthermore the effects of boundaries and aliovalent impurities on the transition temperature will be studied, in an effort to increase our knowledge of the mechanism of this phase transition.

EXPERIMENTAL

CHAPTERS 2-6

EXPERIMENTAL. CHAPTER 2

CRYSTAL GROWTH

2.1 NATURE OF CRYSTALS STUDIED.

In nearly all cases solution grown single crystals of 'pure' and impurity 'doped' caesium chloride were used. A few measurements were made on melt-grown single crystals obtained from Semi-Elements Ltd.

2.2 GROWTH OF SINGLE CRYSTALS FROM AQUEOUS SOLUTION.

The most satisfactory results were obtained by dissolving a known weight of AnalaR caesium chloride, obtained from B.D.H. Ltd, together with ten per cent by weight of urea as an additive in a volume of distilled water equal to the combined weight of caesium chloride and urea.[84]

The containing vessels, 100ml conical flasks, were covered with filter paper and clamped in Dewar flasks containing boiling water. The whole was well lagged with cotton wool and natural cooling allowed to proceed. In this way, the average time of cooling to room temperature was seventy two hours. The rate of cooling was critical in producing good crystals, too rapid cooling, or insufficient solvent, tended to produce a crystalline mass from which the separation of individual single crystals proved difficult. The crystals were filtered under nitrogen and stored in desiccators over silica gel until required.

The method produced good single crystal specimens

of average dimensions, 5 × 5 × 2 mm. In certain instances, larger specimens were obtained, the largest specimen measuring 11 × 10½ × 4 mm. Controlled cooling by means of a thermostatic tank did not improve the size or quality of the single crystals.

2.3 IMPURITY DOPING OF CRYSTALS.

Crystals of caesium chloride containing barium, calcium or sulphate as foreign ions were grown, as described above, with the addition of small amounts (10 - 40 mg) of AnalaR barium or calcium chloride or AnalaR sodium sulphate to the solution of caesium chloride prior to cooling.

The crystals obtained were removed from solution by filtering under nitrogen and stored in desiccators over silica gel until used.

2.4 PRETREATMENT OF SOLUTION GROWN SINGLE CRYSTALS.

All single crystals of 'pure' and 'doped' caesium chloride grown from solution were found to contain a certain amount of occluded water. Two methods have been employed for its removal. The crystals were either heated in an atmosphere of dry nitrogen for several hours at 150°C Centigrade or alternatively dried in vacuum for four to six hours. Subsequent results proved to be independent of the method of pretreatment employed.

FIGURE 1. The Circuit

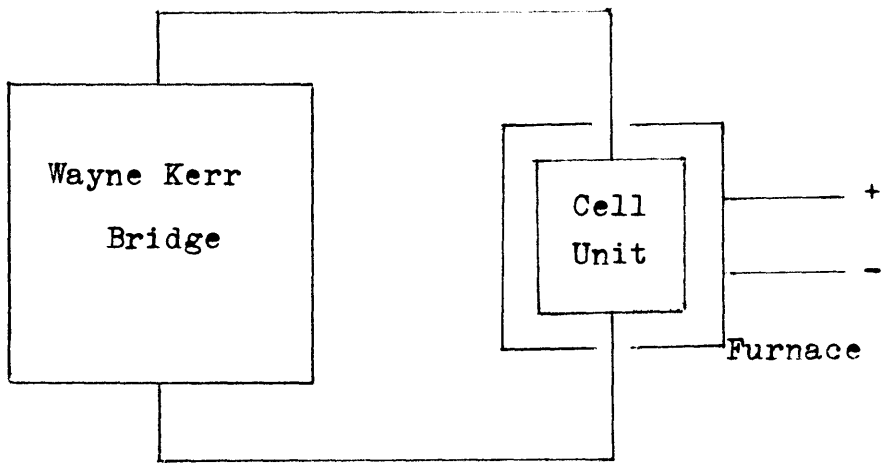

FIGURE 2 The Electrodes

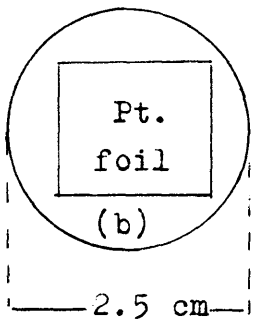

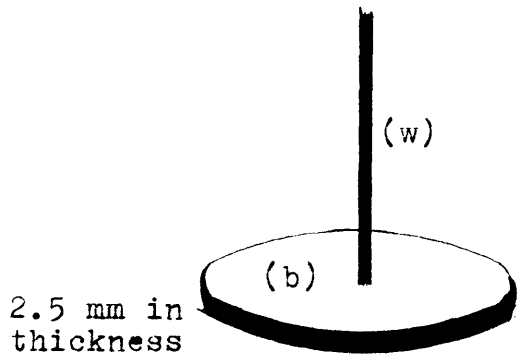

EXPERIMENTAL. CHAPTER 3.

CONDUCTIVITY.

3.1 AIM OF CONDUCTIVITY STUDIES.

Unlike the other alkali halides, in which only the cation is relatively mobile, the caesium halides present a more difficult system to study due to both the anion and the cation possessing a significant mobility under the influence of an applied electric field.

It was decided to carry out conductivity measurements on pure and impurity-doped single crystal specimens of caesium chloride first in an attempt to understand better the nature of the ionic processes taking place, and second to determine the effect of aliovalent impurity ion on the crystallographic transition in caesium chloride.

3.2 THE CIRCUIT.

The most elementary circuit, Fig.1, was used comprising a Wayne Kerr Universal Bridge B.221. The bridge operated at 1592 cycles per second and measured directly the reciprocal resistance of the crystal which was clamped between two electrodes.

3.3 THE CRYSTAL UNIT.

The upper and lower crystal faces were coated with 'dag', a colloidal suspension of graphite in alcohol, using a small camel-hair brush. The function of the 'dag' was to ensure better electrical contact with the electrodes and it was used in preference to silver electrode paint

FIGURE 1. The Cell Unit

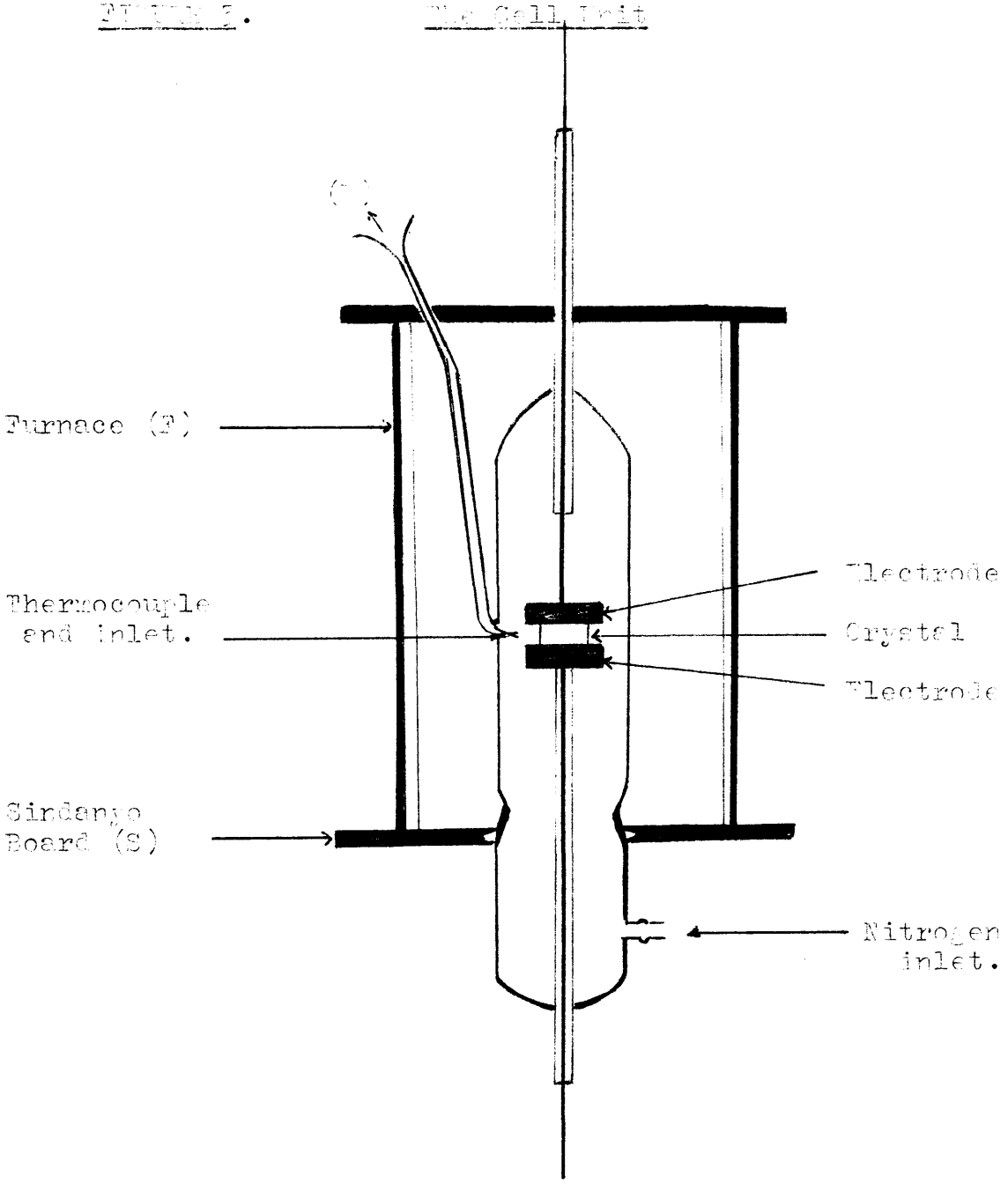

which produced certain anomalous results due possibly to diffusion of silver into the crystal. The crystal was then clamped between two electrodes.

The electrodes were cylindrical in design (Fig.2) and consisted of platinum face platessilver soldered to the brass disc (b). Copper wires (w) silver soldered through the brass disc to the platinum provided the connection with the Wayne Kerr bridge.

The whole was then enclosed in a silica vessel (Fig.3) comprising a B.29 Quickfit cone and socket with two capillary bore tubes acting as electrode supports to minimise electrode movement during measurements. The vessel was fitted with a side-arm acting as an inlet for the supply of nitrogen. The nitrogen was dried by bubbling it through concentrated sulphuric acid, and was constantly passed through the apparatus. An inlet for a thermocouple was situated directly level with the crystal. The silica vessel was surrounded by a furnace (F) capable of producing temperatures of over 500^{o} centigrade.

The furnace consisted of a cylindrical copper core 4" in height and 3" in diameter supported on $\frac{1}{2}$" thick Sindanyo board (S) which had a central hole to allow access of the silica vessel. The core was covered with a layer of asbestos paper and Nichrome wire, of

FIGURE 4

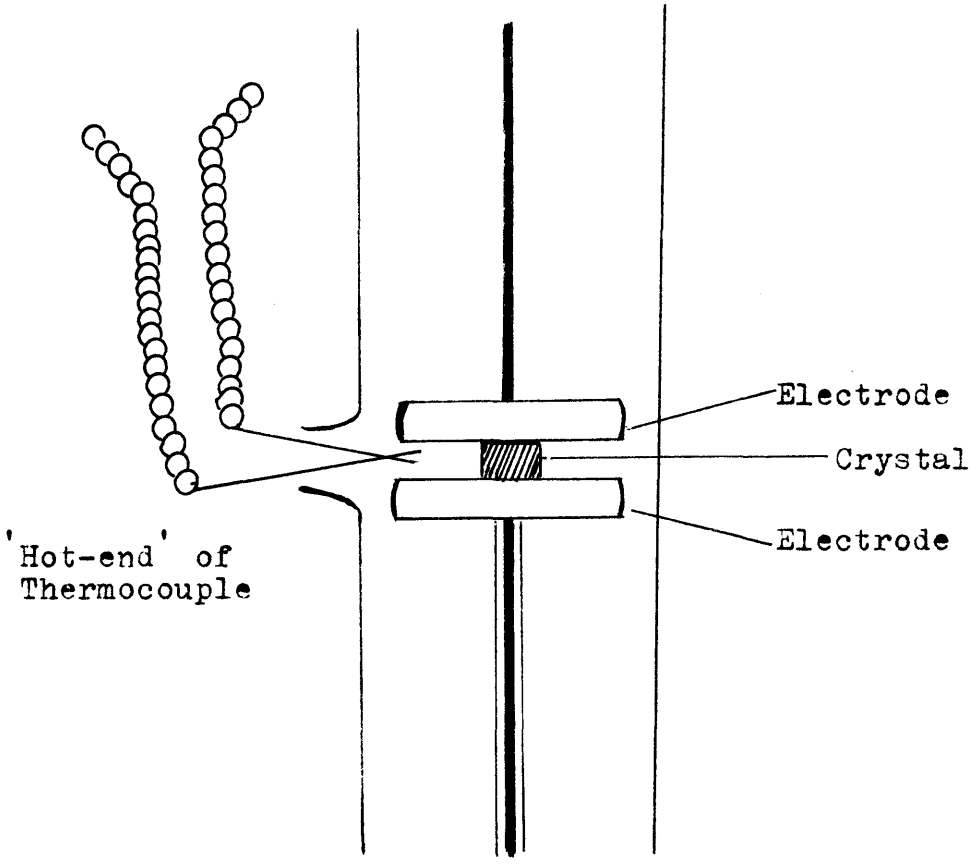

resistance 10 ohms per yard, wound thereon giving a total resistance of 90 ohms at room temperature. The windings were well lagged with asbestos tape and asbestos string. The power was fed to the furnace through a variac from the mains.

The crystal temperature was measured by means of a Platinum--Platinum-13% Rhodium spot-welded thermocouple in conjunction with a Doran Instrument Ltd. thermocouple potentiometer, (E). The thermocouple potentiometer reading produced from the potential difference between the 'hot' and 'cold' ends of the thermocouple was converted from millivolts to degrees centigrade by means of calibrated charts[85]. The 'hot' end of the thermocouple was inserted through the small hole in the side of the silica vessel (Fig.4) and was positioned as close as possible to the crystal. The actual crystal temperature was thus $\pm 2^{o}$centigrade of that of the measured temperature since the thermal gradient between the two was minimal. The 'cold' end of the thermocouple was immersed in an ice-bath in a Dewar flask.

In order to reduce temperature fluctuations due to external draughts, the top of the furnace was carefully lagged with asbestos sheeting.

3.4 EXPERIMENTAL PROCEDURE.

Each crystal was weighed and its thickness measured by means of a micrometer screw gauge calibrated to a thousandth of an inch. The crystal faces were coated with 'dag', as were the platinum electrodes. The crystal was placed in position, the furnace switched on, and the variac adjusted. After the temperature had attained a steady value, the reciprocal resistance of the crystal was measured directly on the Wayne Kerr Universal Bridge. At the same time the capacitance of the crystal in microfarads was measured on the bridge. Thus three readings, (a) reciprocal resistance, (b) capacitance and (c) temperature in degrees centigrade were measured and noted. The furnace temperature was increased by 10-15° centigrade and after stabilization of temperature, usually 20 minutes, another set of readings were taken. This was repeated within the temperature range 200 -530° centigrade.

3.5 CALCULATION OF CONDUCTIVITY FROM RESULTS.

It is a well known physical law that the resistance of any conductor varies directly as its length (l cm) and inversely as its cross-sectional area (A sq. cm), that is

$$R = \frac{S.l}{A} \qquad \ldots.(19)$$

where S is a constant and is known as specific resistance.

It is the resistance of a specimen 1 cm in length and 1 sq. cm in cross section.

Now σ the specific conductivity measured in $ohm^{-1} cm^{-1}$ is defined as the reciprocal of the specific resistance, that is

$$\sigma = \frac{1}{S} \qquad \ldots.(20)$$

Therefore,

$$\sigma = \frac{1}{R} \cdot \frac{l}{A} \qquad \ldots.(21)$$

(l/A) is known as the cell constant. l was measured directly with a micrometer screw gauge. A, the area, was obtained by dividing the weight of the crystal by its density, 3.98 $gm\ cc^{-1}$ for caesium chloride, thus obtaining the volume which, when divided by 1, the thickness, gives A the cross-sectional area. Thus, by multiplying the reciprocal resistance (ohm^{-1}) by l/A, the cell constant, (cm^{-1}), the specific conductivity in $ohm^{-1} cm^{-1}$ was calculated.

EXPERIMENTAL. CHAPTER 4

DIFFUSION.

4.1 INTRODUCTION.

In this work it was proposed to study the ionic self-diffusion in single crystals of caesium chloride using the radioactive isotopes caesium-137 and chlorine-36.

4.2 AVAILABLE METHODS FOR DETERMINING DIFFUSION COEFFICENTS.

There are three principal methods for the determination of diffusion coefficients using radioactive tracers,

(a) Sectioning techniques

(b) Isotope exchange techniques

and (c) Surface decrease technique.

(a) SECTIONING TECHNIQUE.

In this method a thin layer of the compound, containing the radioactive isotope, is placed on one face of the crystal. After allowing diffusion to take place some of the radioactive isotope will have penetrated some depth into the crystal. The solution of Fick's[86] second diffusion law for this particular case is given by

$$C = (C_o/(Dt)^{\frac{1}{2}}).\exp(-x^2/4Dt) \qquad \ldots(22)$$

where C represents the activity at a penetration depth x after time t, D is the diffusion coefficient.

The concentration of the radioactive isotope as a function of penetration into the crystal is determined by

removing thin layers of the crystal.

Removal of thin sections by microtoming has been used by various workers, Laurent and Bénard[48], Mapother, Crooks and Maurer[18], and Chemla[20]. Mapother et al have been able to remove sections of 5×10^{-6} cm in their studies of the self diffusion of Na-24 ion in sodium bromide and sodium chloride.

Alternatively, a grinding method can be employed, and this involves grinding away of layers of material on a ground glass plate. This method was employed by Schamp and Katz[87], in their investigation of bromide self-diffusion in single crystals of sodium bromide.

These methods, however, are likely to give rise to considerable errors in the determination of the self-diffusion coefficient, D, especially in the low temperature range where penetration depths are small. The mounting of the crystals seems extremely critical and slight misalignment would give rise to serious errors in the measurement of the penetration depth. However, a correction can be applied for the misalignment.[88] It also seems likely that there will be a loss of radioactive material from the knife blade on the Scotch tape which is used for collection. Furthermore, some of the material from each slice tends to adhere to the sides of the crystal. Schamp and Katz have estimated 80 per cent error in the low temperature region while Mapother,

Crooks and Maurer [18] estimated the error at 10-20 per cent.

(b) ISOTOPIC EXCHANGE.

The isotope exchange technique differs considerably from the sectioning technique. In this method advantage is taken of isotopic exchange between a crystal and a surrounding gas. The method was used by Harrison, Morrison and Rudham [47]. The system consisted of the radio-isotope chlorine-36 incorporation in sodium chloride crystals and its appearance in surrounding chlorine gas was followed. The counting rate in the gas-phase is given by [89]

$$R = 2\,(\rho R_o/m).A.(Dt/\pi)^{\frac{1}{2}} \qquad .....(23)$$

where A is the surface area of the crystal and D is the diffusion coefficient. The term $(R_o\rho/m)$ is a constant.

A significant feature of the isotope exchange method is that rates at a number of successively higher temperatures can be obtained with a single specimen. In this way an activation energy may be derived from one experiment in which all conditions except temperature are fixed.

(c) SURFACE DECREASE TECHNIQUE.

The surface decrease technique depends on the decrease in surface activity of a radioactive tracer with time. A thin film of the compound containing the radioactive material is evaporated onto a crystal face

[illegible] 2.

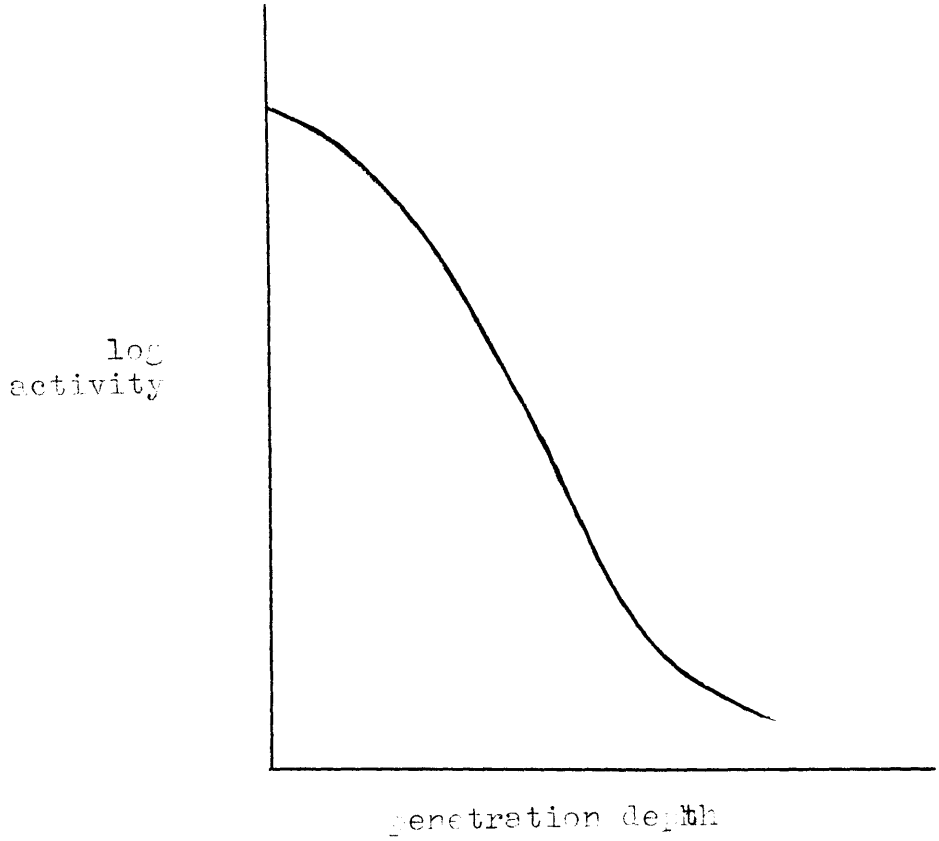

and the activity counted. After allowing diffusion to proceed at a known temperature for a given period of time, the activity is recounted. During diffusion the active material will have penetrated into the crystal, so there will be a variation of the activity with depth of penetration as depicted in Fig 5. If the β-particles emitted by the radioactive material are of a low energy, some which originate in the inner layers will be absorbed by the intervening layers before they reach the outside face. Consequently the count rate will be found to have diminished after diffusion. The diffusion coefficient can be calculated from the following equation.-

$$\log(A_t/A_o) = \log(1 - \mathrm{erf}(\mu^2 Dt)^{\frac{1}{2}}) + \mu^2 Dt/2.303 \quad \cdot(24)$$

where A_o = surface activity before diffusion

A_t = surface activity after diffusion

μ = absorption coefficient

D = diffusion coefficient

t = time for which diffusion took place

erf = error function (Tables- Jost Diffusion, Academic Press, 1952)

This method is particularly suited to the study of low energy β-particles where there is a sharp 'fall-off' in activity at the surface with penetration depth due to their ease of absorption. This method was previously used by Hoodless and Thomson[35] in the study of sodium

ion self diffusion in sodium chloride and first designed by Steigmann, Shockley and Nix[90] for a metallic system.

In the present work the surface decrease method was used, although a few results were obtained by the sectioning technique for comparison purposes.

The isotope exchange method, probably the best of the three, was not employed because it was desired to obtain diffusion coefficients for caesium-137 and chlorine-36 by the same technique. Although admirably suited to the study of chlorine-36 diffusion[60], it is difficult to envisage the study of caesium-137 diffusion being undertaken by the isotope exchange technique.

4.3 PROCESSING OF RADIOACTIVE MATERIAL.

The chlorine-36 isotope was obtained from the Radiochemical Centre at Amersham as HCl-36. Chlorine-36 is a Beta-emitter (0.714 MeV) with a half-life of 3.2×10^5 years.

The HCl^{36} was neutralised with NaOH and the specific activity reduced by addition of inactive caesium chloride. The aqueous solution was carefully evaporated to dryness on an electric hotplate at 50-55° centigrade, and the chloride-36 cooled in a desiccator over silica gel and stored there until required.

The radioactive Cs-137 was also obtained from the Radiochemical Centre at Amersham contained in 1N.HCl. Cs-137 has a 30 year half-life and it is a beta and gamma-emitter. Ninety two per cent of the beta radiation has an energy of 0.52 Mev, the other eight per cent 1.17 MeV. The gamma radiation has an energy of 0.662 MeV. Similar treatment to that described for the Cl-36 was employed for the Cs-137.

A third radioactive isotope sulphur-35, as sodium sulphate, was used in the earlier stages of the research, and was obtained from the same source as Cl-36 and Cs-137. Sulphur-35 is a weak beta-emitter (0.167 MeV) with a half-life of 87 days.

4.4 DEPOSITION OF ACTIVITY ON TO THE CRYSTALS.

Initially in the research the radioactive Cl-36 was deposited on to a warm crystal face from an alcoholic solution, which was evaporated under an infra-red lamp, taking care not to overheat the crystal in the process. The drawbacks, however, to this procedure proved quite serious. It was impossible to obtain an evenly distributed deposit. This led to errors of self absorption and geometric reproducibility. Furthermore, the deposit tended tobe rather easily knocked off of the crystal during the course of the

FIGURE 6. The Evaporator.

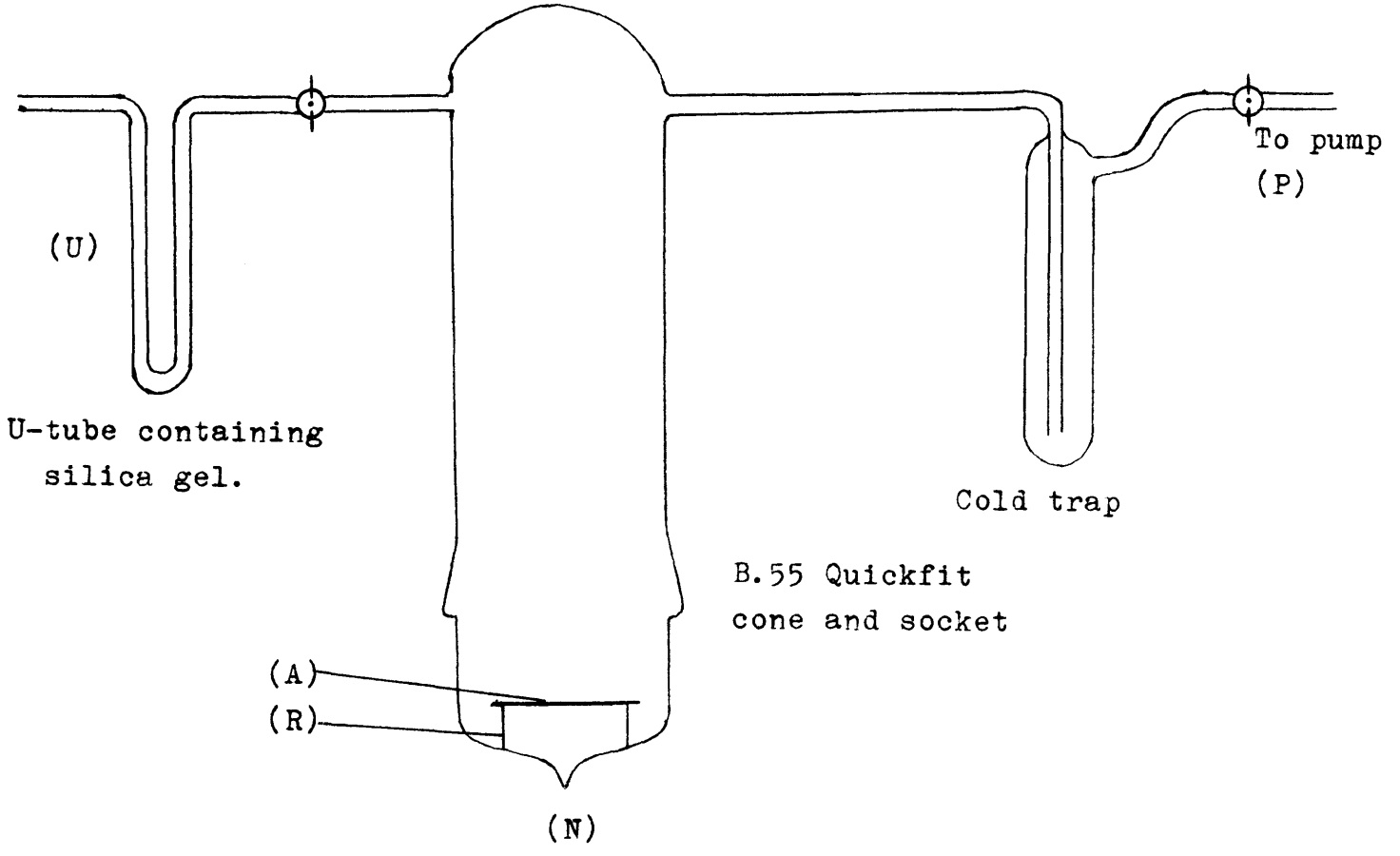

experiment.

To overcome these difficulties a system was devised whereby the caesium chloride was evaporated directly on to the crystal face in vacuum.

4.5 THE EVAPORATOR.

The system consisted of a B.55 Quickfit cone and socket (Fig.6) with a nipple (N) introduced into the base of the cone to hold the radioactive material. Above this rested a cylindrical glass ring (R) 3/4" in height. Placed on top of the glass ring was a thin aluminium disc (A)with a series of small holes (0.3 cm in diameter) bored in it. The crystals were placed over the holes. A side arm led, via a cold trap in liquid air, to a rotary pump (P). As it was found that, owing to the deliquescent nature of caesium chloride, contact with moisture had to be avoided, a second side-arm fitted with a U-tube containing silica gel (U), which acted as a drying agent to the incoming air after evaporation had taken place.

When the active material and crystals were in position, the system was pumped for 30 minutes. The radioactive material was then evaporated, under vacuum, by applying a small flame below the nipple. Care had to be taken at this point to prevent overheating. Taking his precaution, a nice even deposit was obtained in a matter of seconds.

FIGURE 7.

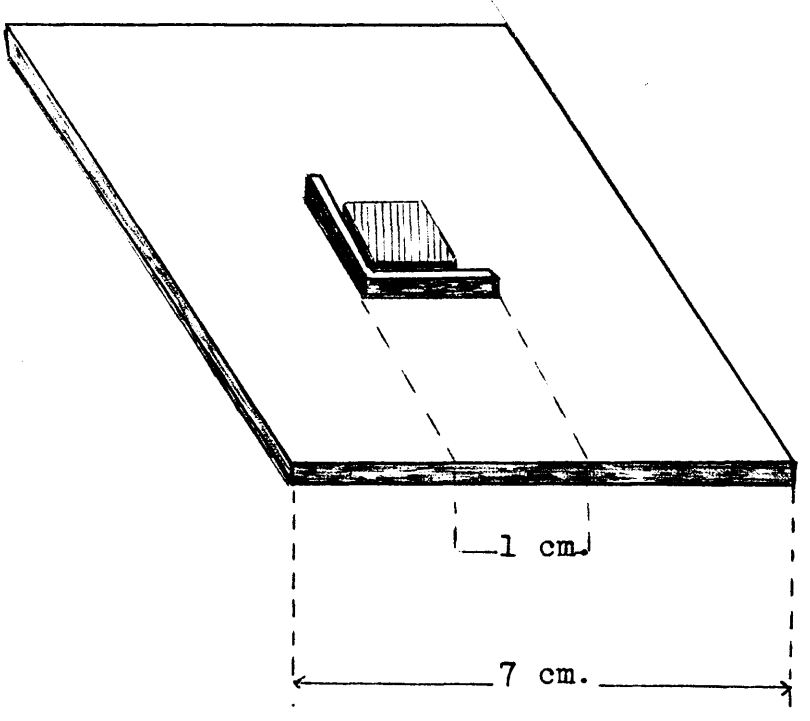

After allowing the system to cool, dry air was admitted, the crystals removed and immediately transferred to a desiccator prior to counting.

4.6 COUNTING PROCEDURE FOR ^{36}Cl.

All counting was determined using a Geiger-Müller thin end window counter of window thickness 3.75 mg cm^{-2}. The working voltage of the counter was determined with a carbon-14 source. This was found to be 687.5 volts and the counter was pre-set to this voltage for all countings.

In order that the same geometry was maintained throughout the experiment, the crystals were counted within an L-shaped bracket mounted on a metal plate (Fig.7). Each crystal was marked so as to make possible positional reproducibility within the bracket.

It was found that rotation of the crystal in the counting position had little effect on the observed count rate in cases where the activity had been evaporated on by the method described in 4.4, indicating an even distribution of activity. In the case of the deposit put on by evaporation under the infra-red lamp, there was a significant difference in count rates depending on crystal position.

Counting was carried out in this manner before and after diffusion. Each count was corrected for background radiation, the value of this being determined

FIGURE 8. The Counting Set-up.

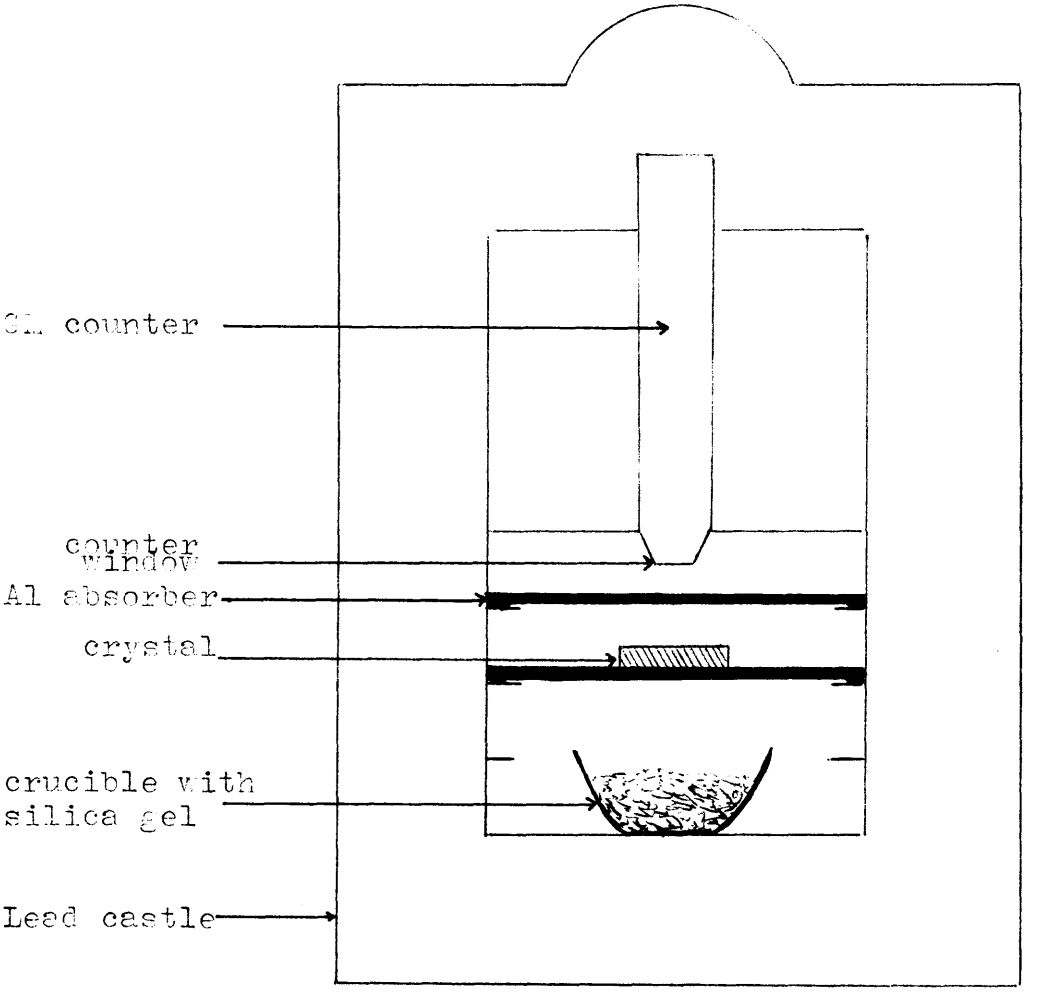

by counting an inactive crystal of similar dimensions under the same conditions. Corrections were also made for dead-time losses, self-absorption and radioactive decay. A further source of error occassionally arose due to counter voltage fluctuations before and after diffusion. A standard cobalt-60 source was therefore counted both before and after diffusion and the count rates were corrected to this standard.

To ensure a statistical accuracy of one per cent 10,000 counts were taken for each measurement.

4.7 DETERMINATION OF THE ABSORPTION COEFFICIENT FOR Cl^{36} IN CsCl.

In order to calculate the diffusion coefficient it was necessary to know the extent of the absorption of the Cl^{36} in CsCl. As it was not possible to prepare thin enough sections of caesium chloride for this purpose, measurements were made with standard aluminium absorbers and the corresponding absorption in caesium chloride calculated from a comparison of densities. The chloride-36 was evaporated on to a caesium chloride crystal of similar dimensions to that of the crystals used in the diffusion experiments thus ensuring a reasonable equality of back scattering.

A series of counts were made with the apparatus described in Fig.8 using aluminium absorbers of varying thickness. A number of counts were made with each

absorber and their average taken. A graph was then drawn of the logarithm of the activity in counts per minute against absorber thickness in mg cm^{-2} corrected for window thickness of 3.75 mg cm^{-2} and absorption by air (1.27 mg cm^{-2} under these conditions). The results are shown in Table A.

As with all counting, a small crucible containing silica gel was placed in the base of the counting chamber to maintain as dry an atmosphere as possible.

From the graph of these results, Graph A, $d_{\frac{1}{2}}$, the thickness required for the count rate to drop from A_o the value without absorber, to $A_o/2$ was calculated. Now the absorption coefficient u is given by

$$\mu = (2.303/d_{\frac{1}{2}})\log(A_t/A_o) \qquad \ldots(25)$$

$$= (2.303/d_{\frac{1}{2}})\log 2$$

$$\therefore \mu = 0.693/d_{\frac{1}{2}}$$

From the graph, $d_{\frac{1}{2}}$ = 46 mg cm^{-2}, and $d_{\frac{1}{2}}$(mg cm^{-2}) was converted to $d_{\frac{1}{2}}$(cm) by multiplying by 10^3 and dividing by the density of caesium chloride, 3.98 g cm^3.

Solving the above equation, a value of 60.3 cm^{-1} was arrived at for the absorption coefficient of Cl^{36} in caesium chloride.

4.8 DETERMINATION OF THE ABSORPTION COEFFICIENT FOR Cs-137 IN CAESIUM CHLORIDE.

Cs-137 being a beta and gamma emitter necessitates

GRAPH A

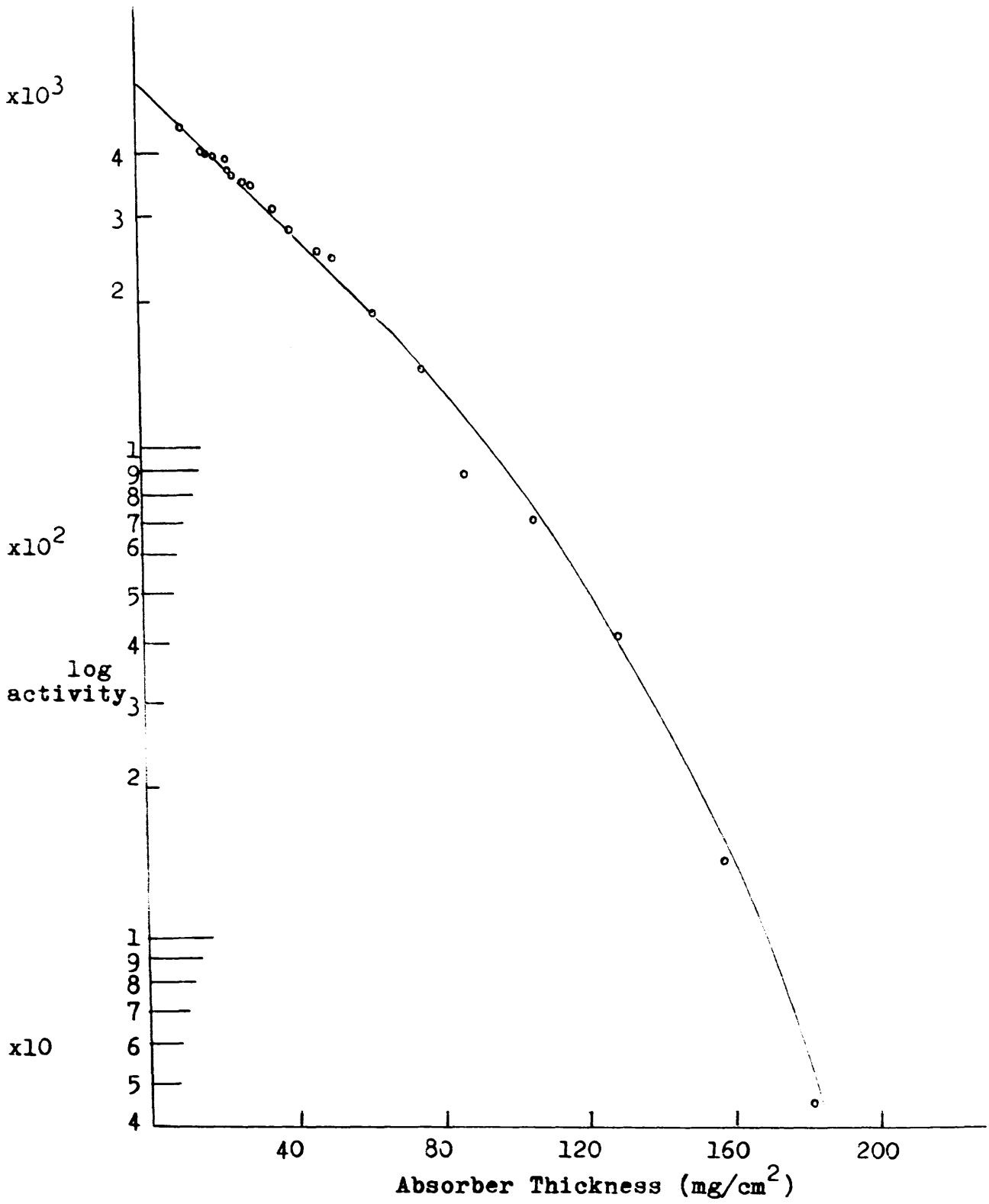
x10^3
4
3
2
1
9
8
7
x10^2
6
5
4
log activity
3
2
1
9
8
7
x10
6
5
4
40
80
120
160
200
Absorber Thickness (mg/cm^2)

TABLE A

Thickness of Absorber (mg cm^{-2})	Counts per minute
5.04	4,467
10.14	3,921
11.70	3,882
14.14	3,807
17.54	3,747
19.04	3,566
20.34	3,521
23.04	3,382
25.14	3,296
31.94	3,006
36.59	2,762
43.74	2,396
46.99	2,352
57.84	1.774
74.14	1,405
84.34	851
103.04	686
126.04	392
155.04	134
180.04	44

a slightly different counting technique from that adopted with Cl^{36} and $S^{35}O_4^{2-}$.

As the gamma contribution will remain almost unaltered during diffusion, the diffusion coefficient must be claculated from the decrease in the count rate of the beta component only, and hence the absorption coefficient for the beta component must be evaluated.

As with Cl^{36} absorption a series of count rates were made with varying thickness of aluminium absorber.

Absorber thickness	Total c.p.m.	γ count	β count
5.04	5,022	2,310	2,712
10.14	4,297	2,150	2.147
11.70	4,013	2,110	1,903
14.14	3,731	2,020	1,721
17.54	3,372	1,960	1,412
19.04	3,253	1,900	1,353
20.98	3,124	1,850	1,274
23.04	2,898	1,800	1,098
25.14	2,742	1,750	992
31.94	2,313	1,590	723
36.59	2,080	1,480	600
43.74	1,766	1,360	406
46.99	1,660	1,290	370
57.84	1,353	1,110	243
74.14	990	890	100
84.34	830	760	70

GRAPH B.

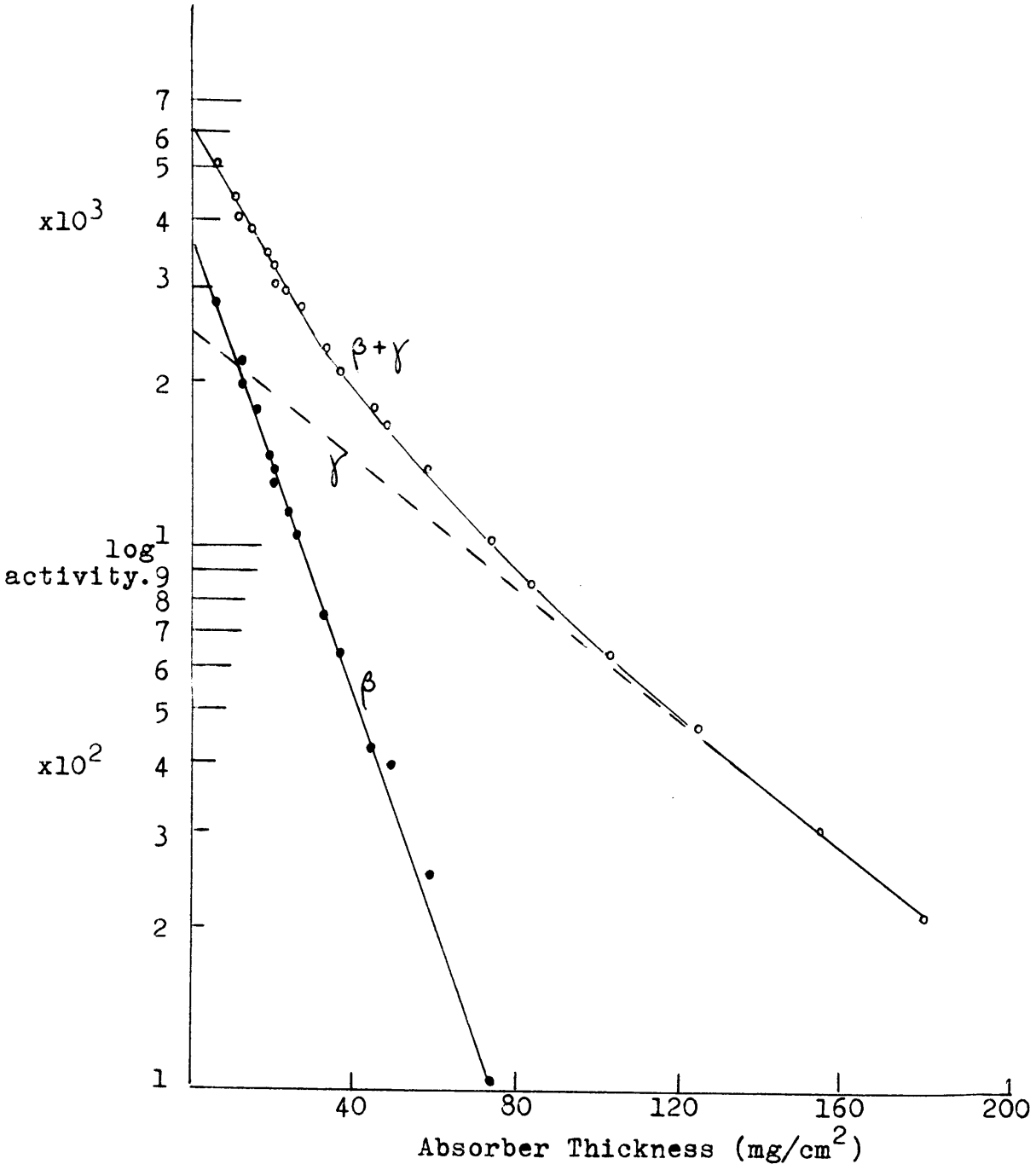
7
6
5
x10^3
4
3
β+γ
2
γ
log
activity.
1
9
8
7
6
5
β
x10^2
4
3
2
1
40
80
120
160
200
Absorber Thickness (mg/cm^2)

Absorber thickness	Total c.p.m.	γ-count	β-count
103.04	630	600	30
126.04	439	438	1
155.04	294	294	--
180.04	203	203	--

A plot of log count rate against aluminium absorber thickness, Graph B, was made. It is seen that the graph is in two parts, one corresponding to the fall off of total beta plus gamma activity with increasing absorber thickness, and the other due only to a reduction in the gamma count. Extrapolation of the latter region to zero thickness represents the gamma contribution to the total count rate and by subtraction the beta contribution was found and plotted. From this line the half-thickness was determined to be 14.8 mg cm^{-2}.

$$\mu = (2.303/d_{\frac{1}{2}})\log(A_o/\tfrac{1}{2}A_o)$$
$$= (2.303/d_{\frac{1}{2}})\log 2$$
$$= 0.693/d_{\frac{1}{2}}$$
$$= \frac{(0.693 \times 3.98 \times 10^3)}{14.8} = \underline{\underline{187.1\ cm^{-1}}}.$$

4.9 COUNTING OF CAESIUM-137.

The fact that caesium-137 is a beta and gamma emitter necessitates a different technique for determining the initial and final activity of the caesium-137 beta count from that used to determine the beta of the

chloride-36.

The procedure adopted was as follows:-

1) The crystal to be counted was placed on the metal tray and inserted into the second shelf of the lead castle below the counter window.

2) A count rate was taken, which, when corrected for background radiation, self-absorption and dead-time losses represented T_o, the initial total count rate due to the combined beta and gamma radiation.

3) An aluminium absorber of sufficient thickness to completely remove all the beta radiation was inserted into the top shelf, thus allowing only γ-radiation to enter the counter. The count rate of the crystal was then determined and this count rate was corrected for background radiation. From the slope of the absorption of gamma radiation from Graph B, the initial gamma activity, γ_o , could be calculated.

4) Subtracting the γ_o value from the T_o value gave A_o, the initial count rate due only to the beta radiation.

This procedure was repeated after diffusion and A_t the final count rate due to the beta radiation was similarly calculated.

FIGURE 2.

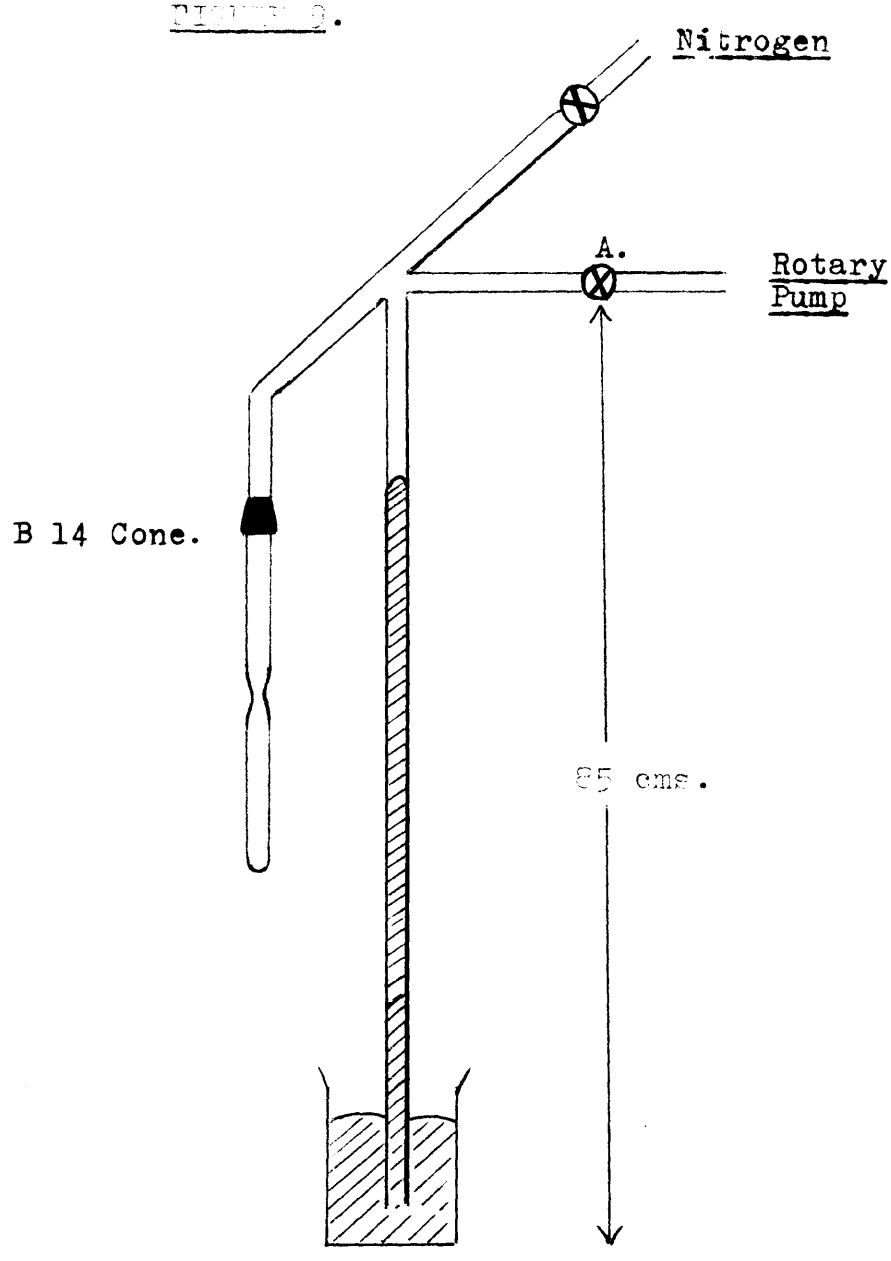

FIGURE 10. Diffusion Tube Holder.

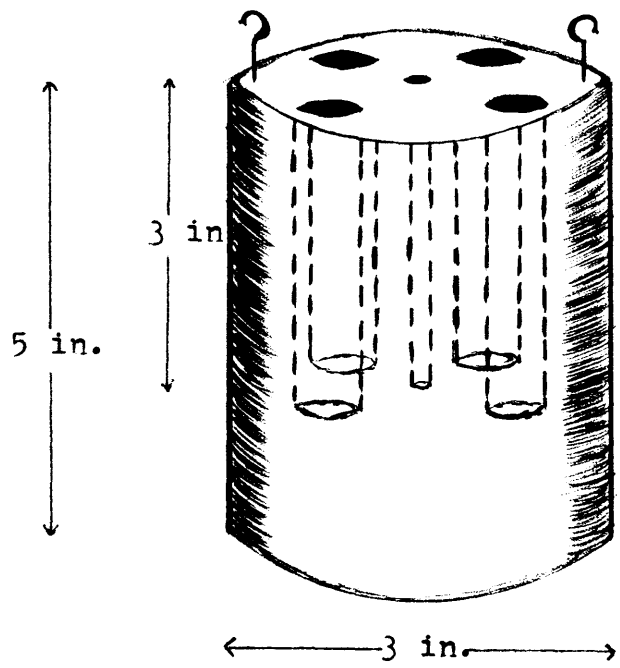

4.10 DIFFUSION TUBES AND PREPARATION.

The diffusion tubes consisted of Pyrex tubing approximately 20cm in length. For diffusion in vacuum and nitrogen they were fitted with a B.14 cone at one end and sealed at the other. The length of the tube minimised evaporation during the sealing of the tubes.

The crystal was slid gently down the tube until it rested at the sealed end. A constriction was made about 5cm from the end of the cone and the tube sealed with black wax to the B.14 socket of the apparatus shown in Fig.9. The apparatus was evacuated by means of a rotary pump and the mercury in the manometer rose. The stopcock A was closed and the tube sealed at the constriction. If desired in an atmosphere of nitrogen, nitrogen was allowed to enter, after evacuation, until the pressure was approximately 68cm of mercury and the tube sealed. A straightforward seal was made if the diffusion was done in air. Each tube had a groove cut in it with a glass knife to facilitate opening after diffusion. Once sealed the tubes were inserted in a holder.

4.11 DIFFUSION TUBE HOLDER.

This consisted of a cylindrical brass block 5" in height and 3" in diameter with five holes bored in it as shown in Fig. 10. The central hole was used as the

FIGURE 11. The Furnace.

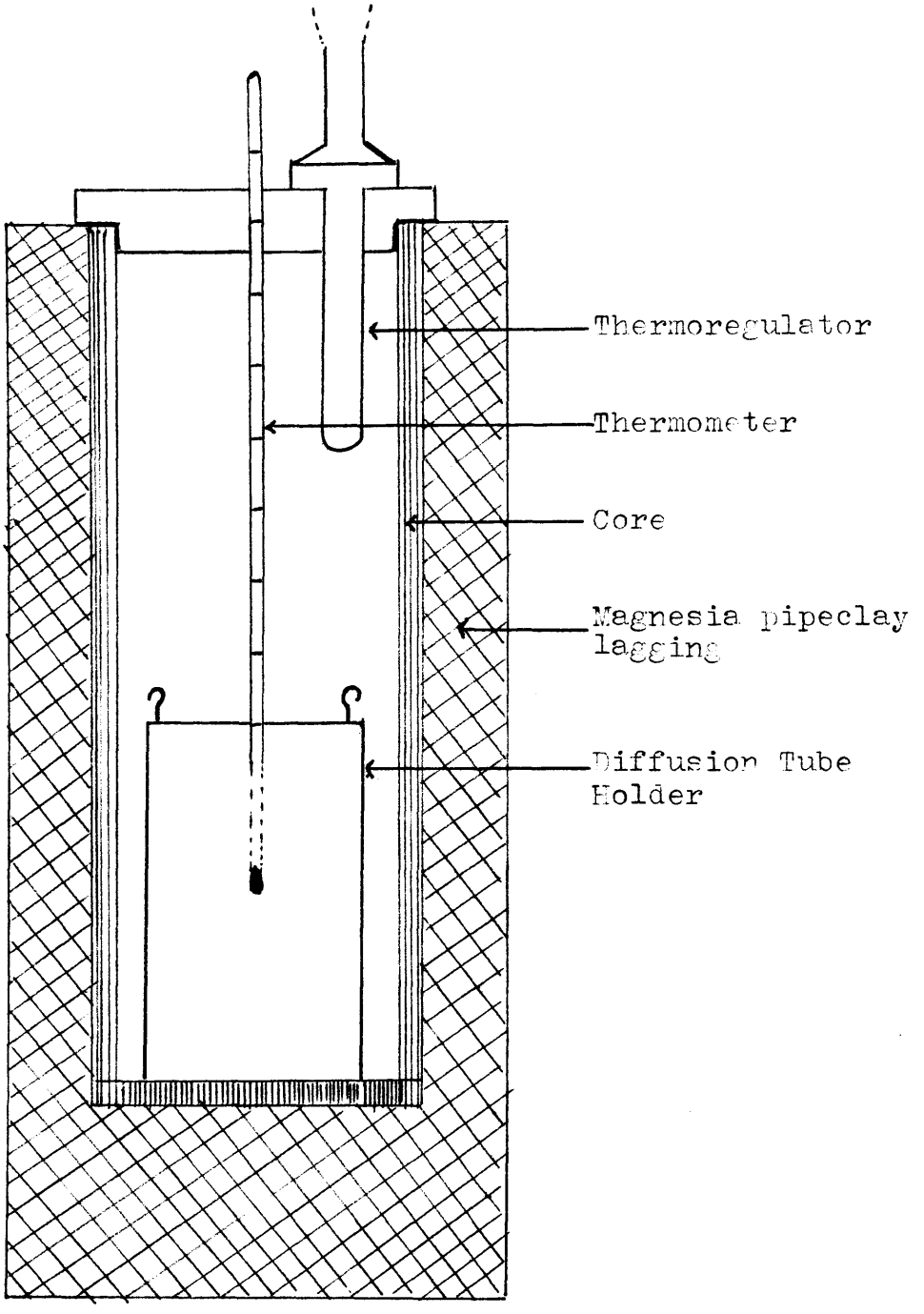

DIFFUSION FURNACE

thermometer holder. The block was raised and lowered from the furnace by means of two brass rods and the two hooks on the holder top.

4.12 THE FURNACE.

Due to certain difficulties of voltage fluctuations it proved difficult in the early stages of this work to obtain sufficiently accurate temperature control. Later, a furnace was designed which overcame this problem.

The furnace, Fig.11, consisted of a cylindrical fireclay core 3/8" thick, 12" in length and having an internal diameter of 4". Around the core a length of 'Nichrome' wire (10 ohms per yard) was wound to give a total resistance of about 100 ohms. A layer of asbestos paper covered the internal coil, and a second coil was wound on top. The resistance of the second coil was 300 ohms. The whole was then enwrapped in asbestos string.

The core was placed in the centre of a large metal drum, 15½" in height and 11" in diameter, and the surrounding volume tightly packed with magnesia-pipeclay lagging. A tightly fitting covering lid of 3/4" thick Sindanyo board, made in two sections, was provided with two holes, the larger being used to accomodate a Jumo GKT 15-0 thermoregulator. The thermoregulator was wired to the external coil (300 ohms) and a Jumo M.S.6.62 mercury relay switch. The power to the internal coil

FIGURE 10.

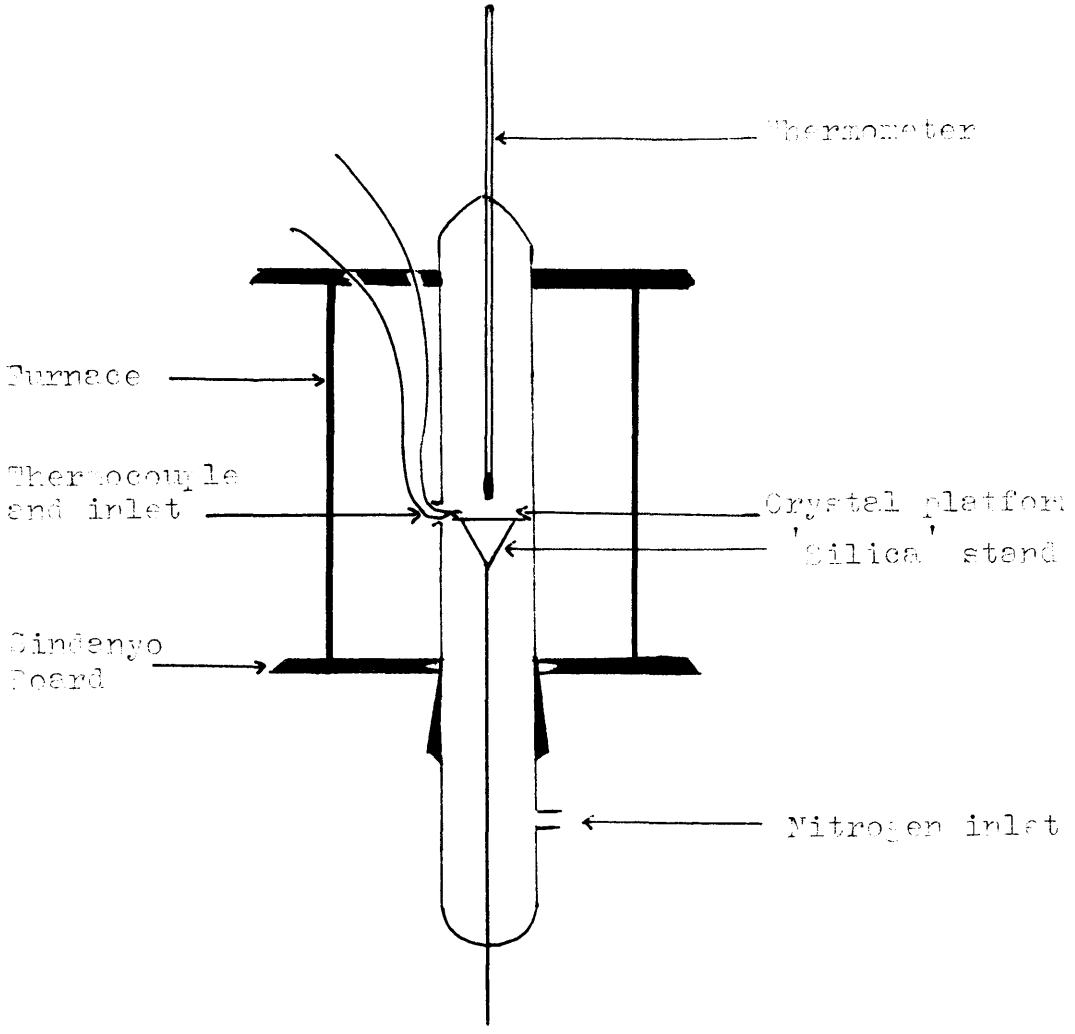
Thermometer
Furnace
Thermocouple and inlet
Crystal platform
'Silica' stand
Cindenyo Board
Nitrogen inlet

was supplied from the mains via a variac - this variac was adjusted to give a reading 20-25° centigrade below the temperature desired. The external coil, in conjunction with the thermoregulator provided the additional heating. The actual temperature was recorded on a 540° mercury in glass thermometer, previously calibrated against a standard Platinum--Platinum-13% Rhodium spot-welded thermocouple. Using this design a temperature control of ±3° centigrade was achieved over aperiod of days.

The most serious disadvantage of this arrangement was the error introduced due to the time necessary for the crystals to attain the desired temperature. It required about 20 minutes for stabilization which, for long diffusion periods of over two days, was not too serious, but for shorter diffusion periods, embedding the tubes in a vessel of preheated fine copper turnings reduced the stabilization time to about 10-12 minutes. In this set-up the thermometer was embedded in the copper turnings to the same depth as the diffusion tubes. In experiments where the diffusion time was less than 14 hours, thus allowing a constant watch to be maintained, a system similar to that used for conductivity measurements was employed (Fig 12). Here all diffusions were carried out in an atmosphere of dry nitrogen. The stabilization time was 5-7 minutes and a temperature control of ±2°centigrade was achieved.

After diffusion the diffusion tubes were hot-pointed and the crystals immediately transferred to desiccators to cool before counting. The inside of the tube was wiped with a piece of moist tissue which was counted to see if there had been any evaporation of activity during diffusion.

4.13 CALCULATION OF THE DIFFUSION COEFFICIENT D.

The diffusion equation is,

$$\log(A_t/A_o) = \log(1 - \mathrm{erf}(\mu^2 Dt)^{\frac{1}{2}}) + \mu^2 Dt/2.303$$

where A_o = initial surface activity

A_t = surface activity after time t

μ = absorption coefficient

t = time of diffusion in seconds

erf = error function (Tables - Jost p.62 Diffusion 1952)

D = diffusion coefficient

Having determined μ and knowing A_t, A_o, and t we calculate D in the following manner.

Crystal from Cs-137 diffusion No.8.

$A_t = 290$ time (secs) = 1.08×10^4

$A_o = 434$ $\mu = 187.1\ \mathrm{cm}^{-1}$

$\log(A_t/A_o) = -0.1751$

Let $D = 8 \times 10^{-11}\ \mathrm{cm}^2\ \mathrm{sec}^{-1}$

$$\mu^2 Dt/2.303 = (187.1)^2 \times 8 \times 10^{-11} \times 1.08 \times 10^4 / 2.303$$

$$= 0.0131$$

$$(\mu^2 Dt)^{\frac{1}{2}} = 0.1738$$

$$\text{erf}(\mu^2 Dt)^{\frac{1}{2}} = 0.1941$$

$$1 - \text{erf}(\mu^2 Dt)^{\frac{1}{2}} = 0.8059$$

$$\log(1-\text{erf}(\mu^2 Dt)^{\frac{1}{2}}) = \bar{1}.9063 = -0.0937 + 0.0131$$

$$\therefore \log(A_t/A_o) = -0.0806 \qquad \text{(a)}$$

Let $D = 1.6 \times 10^{-10}\ cm^2\ sec^{-1}$

$$\mu^2 Dt/2.303 = 0.0264$$

$$(\mu^2 Dt)^{\frac{1}{2}} = 0.2460$$

$$\text{erf}(\mu^2 Dt)^{\frac{1}{2}} = 0.2720$$

$$1 - \text{erf}(\mu^2 Dt)^{\frac{1}{2}} = 0.7280$$

$$\log(1 - \text{erf}(\mu^2 Dt)^{\frac{1}{2}}) = \bar{1}.8621 = -0.1379$$

$$\mu^2 Dt/2.303 = 0.0264$$

$$\therefore \log(A_t/A_o) = -0.115 \qquad \text{(b)}$$

Let $D = 3.2 \times 10^{-10}\ cm^2\ sec^{-1}$

$$\mu^2 Dt/2.303 = 0.0528$$

$$(\mu^2 Dt)^{\frac{1}{2}} = 0.3476$$

$$\text{erf}(\mu^2 Dt)^{\frac{1}{2}} = 0.3770$$

$$(1 - \text{erf}(\mu^2 Dt)^{\frac{1}{2}}) = 0.6230$$

$$\log(1 - \text{erf}(\mu^2 Dt)^{\frac{1}{2}}) = \bar{1}.7940$$

$$\mu^2 Dt/2.303 = 0.0528$$

$$\therefore \log(A_t/A_o) = -0.2074 \qquad \text{(c)}$$

Let $D = 6.4 \times 10^{-10}\ cm^2\ sec^{-1}$

$$\mu^2 Dt/2.303 = 0.1056$$

$$(\mu^2 Dt)^{\frac{1}{2}} = 0.4920$$

$$\text{erf}(u^2Dt)^{\frac{1}{2}} = 0.5135$$

$$1-\text{erf}(u^2Dt)^{\frac{1}{2}} = 0.4865$$

$$\log(1-\text{erf}(u^2Dt)^{\frac{1}{2}}) = \bar{1}.6870 = -0.3130$$

$$u^2Dt/2.303 = 0.1056$$

$$\therefore \log(A_t/A_o) = -0.2074 \qquad \text{(d)}$$

Having determined a series of values (a), (b), (c), (d) etc., for $\log(A_t/A_o)$ at various values of D, a graph is drawn of $\log(A_t/A_o)$ against D and the value of D corresponding to the actual $\log(A_t/A_o)$ in question is read off. In this particular case,

$$D = 4.5 \times 10^{-10} \text{ cm}^2\text{sec}^{-1}$$

Repeating this process for each set of results, the corresponding diffusion coefficients were evaluated.

4.14 MICROTOMING TECHNIQUE.

Some diffusion coefficients were determined by the sectioning or microtoming technique. The microtome used was a 3880/A 165 model supplied by Beck, London. The crystal was fixed to a wooden microtome block with 'Araldite' adhesive. The wooden block was then clamped in position above the fixed stainless steel microtome blade. The active material on the surface was removed and individual sections collected on Scotch tape and counted. The microtome could be adjusted to produce sections of 1-15 microns in thickness.

FIGURE 13.

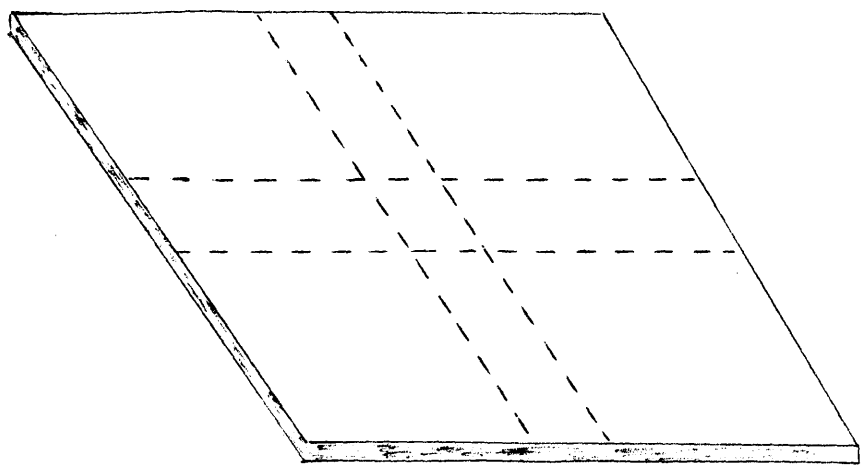

Marked Plate.

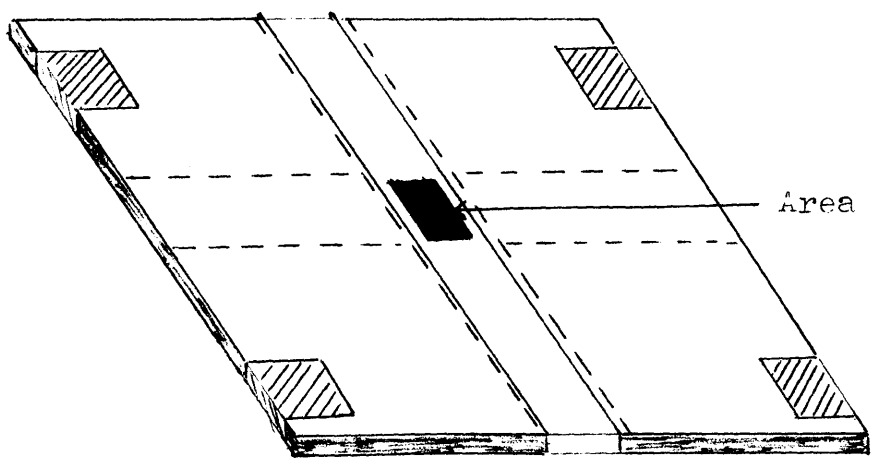

The removed slice was collected by pressing a strip of Scotch tape against the knife blade and allowing the slice to fall against it. By trial and error a technique was developed whereby a reproducibly even deposit could be collected.

The tape was laid across a marked metal plate so that the deposit was always in the same position with respect to the counter Fig.13. The tape was rigidly held in position by means of two further strips of tape which held it taught from the underside. The activity of each slice was determined as in Section 4.9.

A series of slices were prepared and counted in this manner and plots made for each crystal of logarithm of activity against the square of the penetration depth.

4.15 CALCULATION OF DIFFUSION COEFFICIENT.

The equation used is

$$C(x,t) = (C_o/(\pi Dt)^{\frac{1}{2}})\exp(-x^2/4Dt) \quad \ldots.(26)$$

where C(x,t) represents the activity at a penetration depth of x, after time t. D is the diffusion coefficient. A plot, therefore, of logC against x^2 should produce a straight line of slope -(1/4Dt) from which the diffusion coefficient can be calculated.

FIGURE 14.

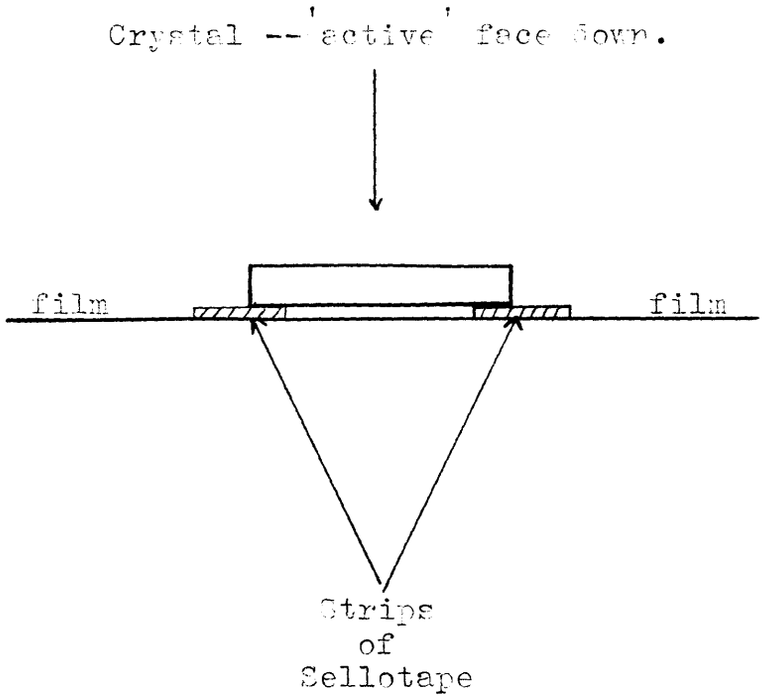

EXPERIMENTAL. CHAPTER 5

AUTORADIOGRAPHY

5.1 INTRODUCTION.

The autoradiographic technique provides a very useful means of determining the extent of any contribution by grain boundaries to diffusion since this type of diffusion is usually more rapid than that of simple bulk diffusion. The method was previously used successfully by Hoodless and Thomson [35] in the study of sodium-22 diffusion in sodium chloride.

5.2 OUTLINE OF THE METHOD.

A circular deposit of activity was evaporated on to the crystal face. After diffusion had been allowed to proceed for a given period, the active surface was counted to determine the length of exposure on the photographic film. A total of about 5-7 million beta particles per sq.cm. require to strike the film to produce blackening. Allowing for the fact that the crystals were much nearer the film than the counter window, the necessary exposure time was calculated. The active face was then exposed to the film as in Fig. 14. After development the film was examined under a 40× magnification. Sections of 10 micron thickness were removed from the active surface, the surface counted and exposed. This process was repeated until all activity removed from the crystal.

If grain boundary diffusion was taking place and if it was faster than bulk diffusion, a point would be reached in the removal of thin sections, where the penetration depth due to simple bulk diffusion would be passed and only activity in grain boundary regions would be left. On exposure and development thegrain boundaries would be expected to show up as regions of dark spots on the film.

5.3 FILMS, EXPOSURE AND DEVELOPMENT.

The films used were Ilford Industrial G X-ray film and to avoid pressure markings by the crystal, the crystal edges rested on narrow strips of sellotape. The crystal was exposed for the calculated time in a darkened desiccator. After exposure the films were developed using PQX-1 high contrast developer supplied by Ilford Ltd, for 4-7 minutes at room temperature 68°F, washed and left in the Hypam fixer for twice the clearing time.

5.4 RESULTS.

In all cases, both for Cs-137 and Cl-36, no evidence was found for the grain boundary diffusion, an even shading, indicative of simple bulk diffusion, being found.

5.5 EFFECT OF MOISTURE ON RADIOACTIVE MATERIAL.

The autoradiographic technique was used to study the effect of moisture on the radioactive deposit during

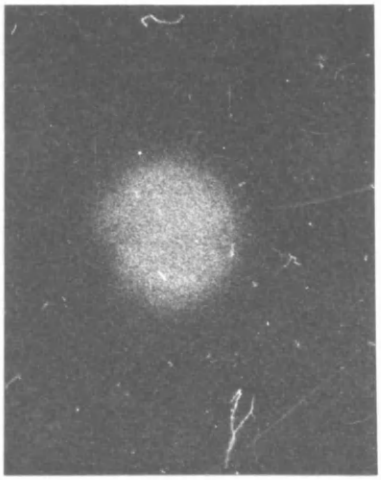

PLATE A.

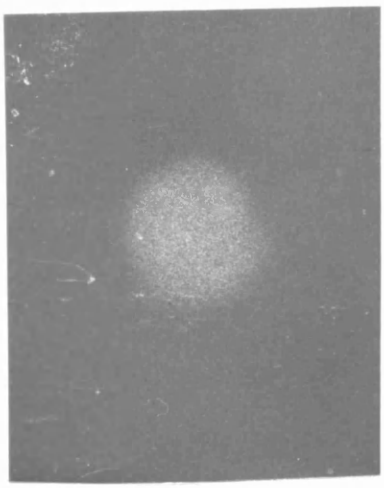

PLATE B.

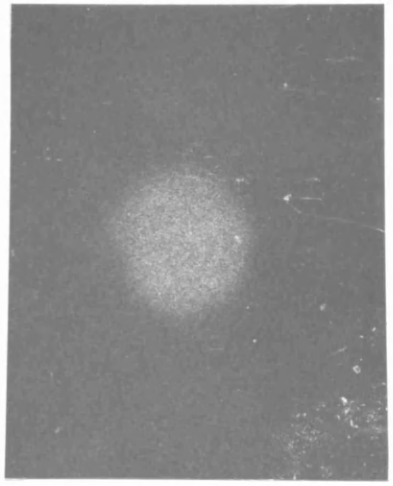

PLATE A.2

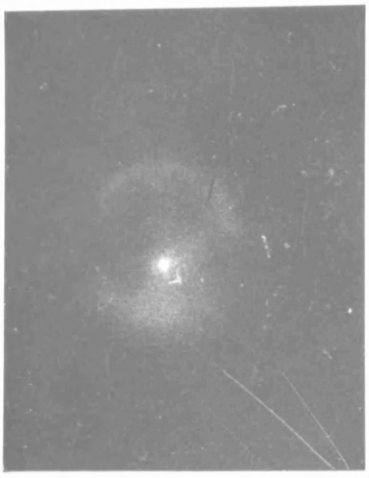

PLATE B2.

diffusion.

Two crystals, A and B, had a radioactive deposit evaporated onto them simultaneously by the method described previously in Chapter 4.4. Both crystals were then exposed to a photographic film for the same length of time, and the films subsequently developed. Plates A and B.

Diffusion was allowed to proceed on both crystals. Crystal A was subjected to all precautions previously described to prevent contact with moisture. Crystal B was not so treated and was at no stage prevented from contact with air, diffusion being carried out in unsealed tubes. After diffusion the crystals were again exposed on photographic films. Plates A.2 and B.2.

In plate B.2 there has been a surface spread of activity which would tend to produce slower diffusion and therefore a lower diffusion coefficient than the correct value.

EXPERIMENTAL. CHAPTER 6

ANALYSIS OF CRYSTALS

6.1 INTRODUCTION.

In order that any significance could be attached to the difference conductivity results and different diffusion results obtained from different crystals containing divalent cation impurities and sulphate as an anion impurity, it was essential that an accurate method of analysis be employed.

After unsuccessful attempts to utilize flame photometry owing to caesium interference, and precipitation with radioactive sulphate, which proved insufficiently accurate for serious consideration, the method finally employed was that of a spectrophotometric estimation using ethylene diamine tetraacetic acid. This method was developed by Parry and Dollman[91].

6.2 THEORY.

Ethylene diamine tetraacetic acid (EDTA) complexes readily with alkaline earth ions in the presence of alkali metal ions. Free ethylene diamine tetraacetic acid absorbs at 222mμ in the ultraviolet, whereas the EDTA complex does not absorb to any appreciable extent. Hence, once sufficient EDTA has been added to complex all the alkaline earth material present, the absorbance will rise significantly with increasing EDTA concentration. By plotting the volume of EDTA added against the

FIGURE 15

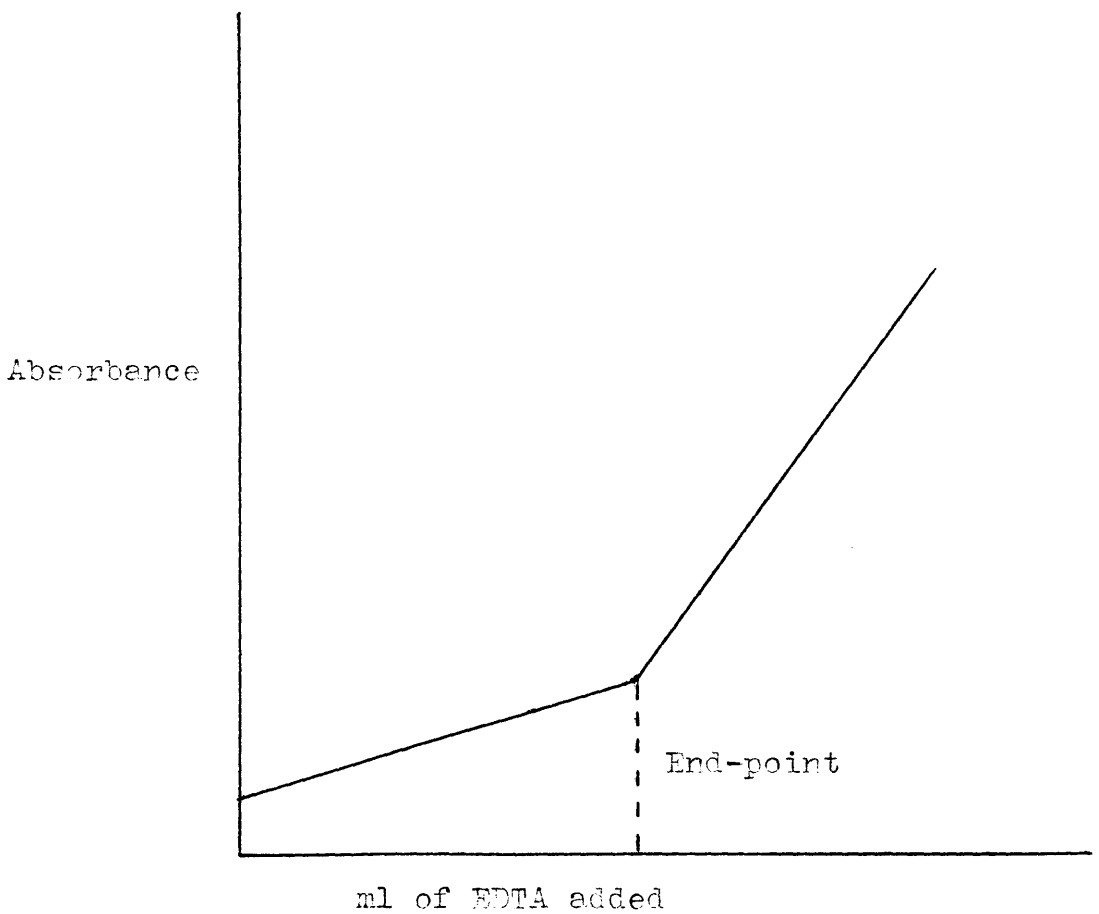

resulting absorbance, a two part graph (Fig.15) is produced, the break point indicating the end-point of the titration. Knowing the molarity of the EDTA, the end-point volume, the volume of unknown solution and the weight of sample used, the impurity concentration can be calculated.

6.3 REAGENTS.

Approximately 1 mM EDTA solution was prepared by dissolving 0.375g dihydrogen disodium ethylene diamine tetraacetate in distilled water and diluting to 1 litre.

1 Molar ammonium chloride-ammonia buffer of pH=10 was prepared by diluting 5.4g ammonium chloride and 75ml of ammonia (specific gravity 0.88) to 100 ml.

6.4 PROCEDURE FOR BARIUM ANALYSIS.

The crystal to be analysed was weighed and dissolved in a minimum of distilled water, 10 drops of buffer were added and the solution made up to 5ml in a standard flask. Using a calibrated pipette 2ml of this solution was transferred to a 1cm quartz cuvet and placed in the cell compartment of a Perkin-Elmer UV spectrophotometer A blank was prepared and 2ml of this solution placed in a similar quartz cuvet in the adjoining cell compartment. The absorbance of the blank was adjusted to zero and the absorbance of the crystal solution at 222mμ read and noted. A small amount of EDTA was added from a 2ml burtte, and an equal volume of water was added to

the blank. The contents of both cells were stirred by a fine stream of air bubbles. The blank was adjusted to zero and the absorbance of the unknown solution again noted. The process was repeated until the end-point had been well passed. A plot was made of ml EDTA added against absorbance.

6.5 STANDARDIZATION OF EDTA.

The EDTA was standardized against a standard magnesium sulphate solution at pH = 10 and a temperature of 60°C using Eriochrome Black T as indicator. The magnesium solution was first neutralized with sodium hydroxide using methyl red as indicator. The methyl red also acted as a screening dye producing a somewhat sharper end-point. The colour change was from a dark red to a greenish blue. The strength of the EDTA was calculated from the equation.-

1ml 0.001 M EDTA = 0.0243mg Mg.

Before each series of analysis, a standard solution of CsCl containing $BaCl_2$ was prepared and a check made to determine the accuracy of the method.

6.6 STORAGE.

Glass vessels, which yield cations and anions, are unsuitable for storage. Each batch of freshly prepared EDTA solution was immediately transferred to polythene bottles and stored there until used. No change can be

observed in the strength of even 1 mM EDTA over a period of several months.

6.7 ESTIMATION OF SULPHATE IMPURITY.

The sulphate concentration was not determined directly but by using a back titration with a standard barium solution.

The theory was that the sulphate in the crystal would be precipitated as barium sulphate, and by titrating the excess barium with EDTA the sulphate concentration could be estimated. This method, however, presumes the complete insolubility of barium sulphate. This is not so. Barium sulphate is soluble to the extent of 0.22mg per 100ml water at 18°C and 0.246mg per 100ml water at 25°C. These quantities are by no means negligible when trying to estimate low impurity concentrations.

It was therefore necessary to use a saturated solution of barium sulphate in distilled water as the solvent mixture, and the following procedure was adopted.

a) 2ml of the standard barium chloride solution was added to 2ml of the solvent mixture and 2ml of the resultant solution titrated against standard EDTA solution to give an end-point (V_1)

b) The crystal containing sulphate was weighed and dissolved in 2ml of the solvent mixture. To this was added 2ml of standard barium chloride solution. After centrifuging at 3000 r.p.m.

for 5 minutes, 2ml of the resultant solution was titrated against the standard EDTA solution giving an end-point (V_2).

c) The difference (V_1-V_2) was equivalent to the amount of sulphate present in the crystal. Hence the sulphate impurity content in ppm could be calculated.

RESULTS

CHAPTERS 7-9

RESULTS

CHAPTER 7

CONDUCTIVITY

7.1 Introduction.

The conductivity equation,

$$\sigma T = \sigma_o \exp(-E/kT) \qquad \ldots.(27)$$

where

σ = specific conductivity ($ohm^{-1}cm^{-1}$)

σ_o = specific conductivity for an ideal crystal ($ohm^{-1}cm^{-1}$)

E = activation energy for process (ev)

T = absolute temperature

and k = Boltzmann constant,

is such that a graph of log σT as a function of reciprocal temperature is a straight line of slope equal to (E) the activation energy.

7.2 Method of Presentation.

In this section we have included log σT as a function of reciprocal temperature graphs, together with tables summarising the important features of each graph. The results in detail are listed in Appendix A.

The graphs included in this section are as follows:-

Graphs 1a,1b,1c	Typical graphs for untreated single crystals of 'pure' solution-grown Caesium chloride.
Graphs 2-6a	Treated crystals of above type.
Graphs 7-8	Melt-grown single crystals of 'pure' Caesium chloride.

Graphs 9-29	Divalent cation (mainly Ba^{2+}) impurity-doped single crystals of Caesium chloride.
Graphs 30-37	SO_4^{2-}-doped single crystals of Caesium chloride.
*Graphs 38-39	Mixed crystals.

*It should be pointed out that these crystals were studied at an early stage in the research. Later results were obtained under different experimental conditions,and,as a result,we have plotted log 1/R (R=specific resistance), rather than log σT,as a function of reciprocal temperature in Graphs 38 and 39.

7.3 <u>The results</u>

GRAPH 1a. Pure CsCl.

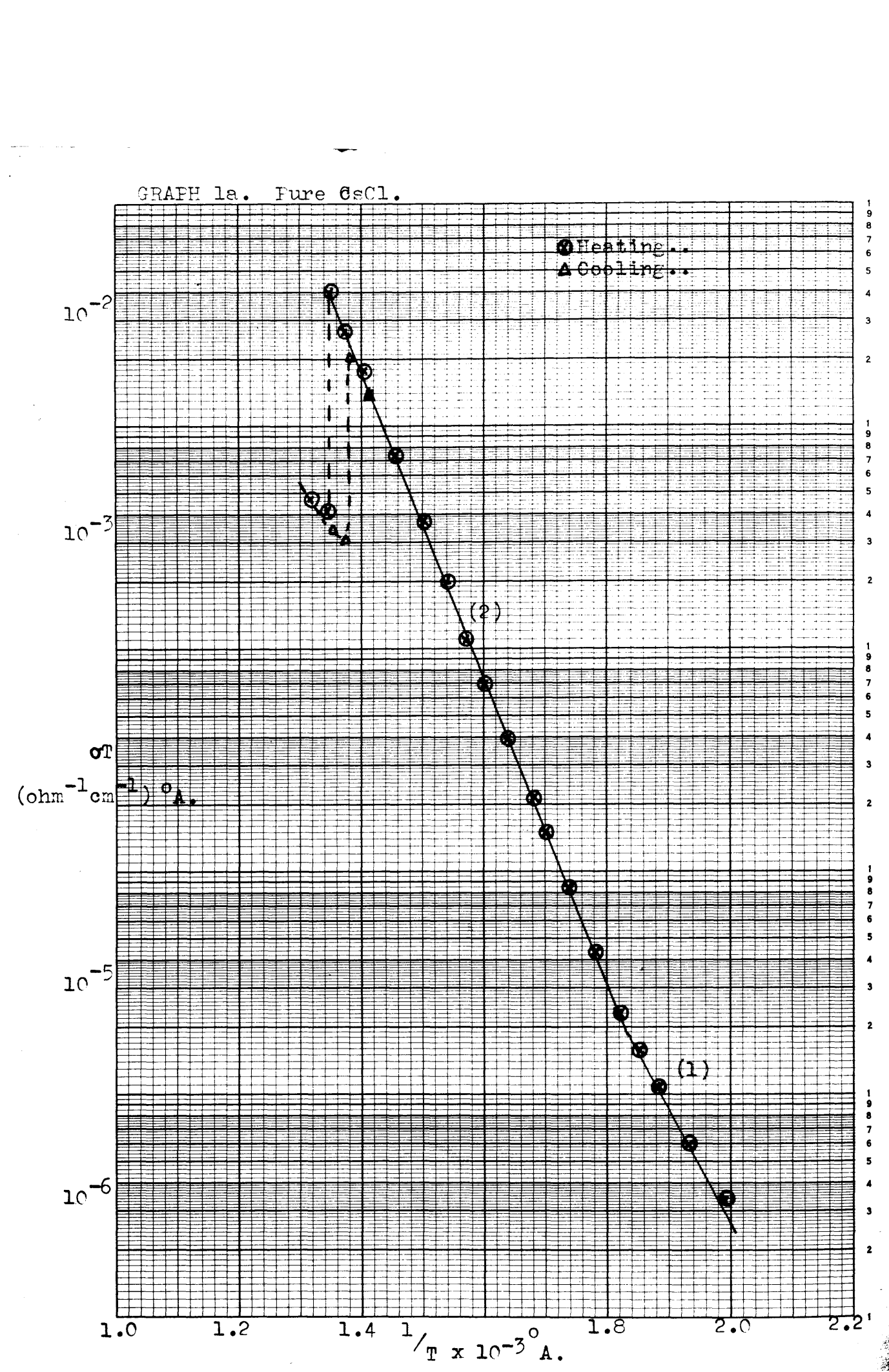

TABLE 1a.

Graph 1[a] Pure CsCl.

	Heating	Cooling
Activation energy below knee (ev)	0.96[(1)]	---
Activation energy above knee (ev)	1.37[(2)]	---
Knee (r.t.u.)	1.83	---
Temperature at which transition starts (^{o}C)	469^{o}	455^{o}
σT at start of transition (ohm^{-1} cm^{-1} ^{o}A)	3.93×10^{-2}	3.00×10^{-3}
Temperature at which transition is complete (^{o}C)	472^{o}	451^{o}
σT at completion of transition (ohm^{-1} cm^{-1} ^{o}A.	4.17×10^{-3}	2.00×10^{-2}

GRAPH 1b. Pure CsCl. Impurity undetectable.

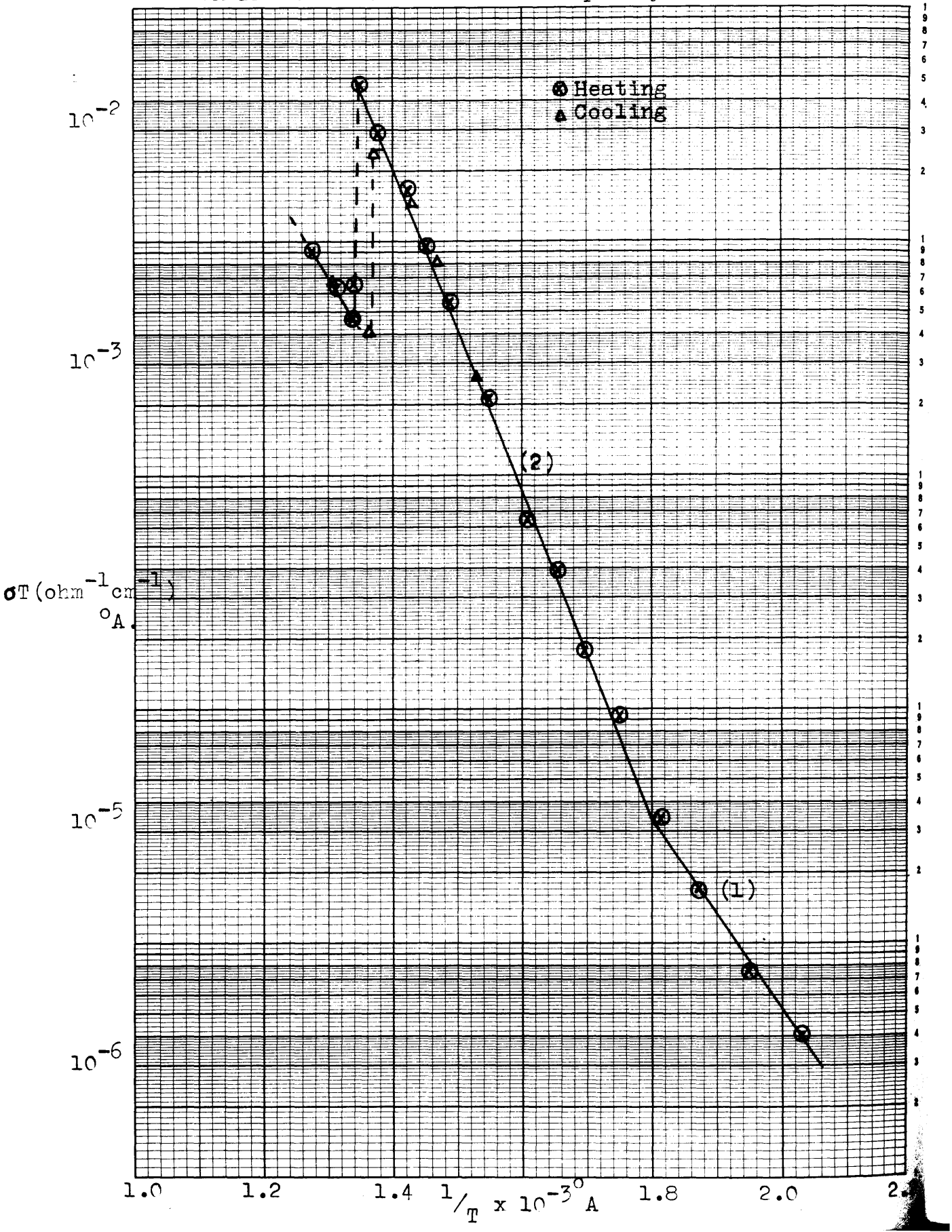

LOG 5 CYCLES X 10ths, ½ & 1 INCH

GRAPH SHEET No. 5555

TABLE 1b.

Graph 16 Pure CsCl

	Heating	Cooling
Activation energy below knee (ev)	0.80 (1)	---
Knee (r.t.u.)	1.80	---
Activation energy above knee (ev)	1.38 (2)	---
Temperature at which transition starts (^{o}C)	469^{o}	461^{o}
σT at start of transition (ohm^{-1} cm^{-1})^{o}A.	4.74×10^{-2}	4.10×10^{-3}
Temperature at which transition is complete (^{o}C)	474^{o}	457^{o}
σT at completion of transition (ohm^{-1} cm^{-1})^{o}A.	4.67×10^{-3}	2.41×10^{-2}
Activation energy after transition (ev)	0.97	---

GRAPH 1c. Pure CsCl

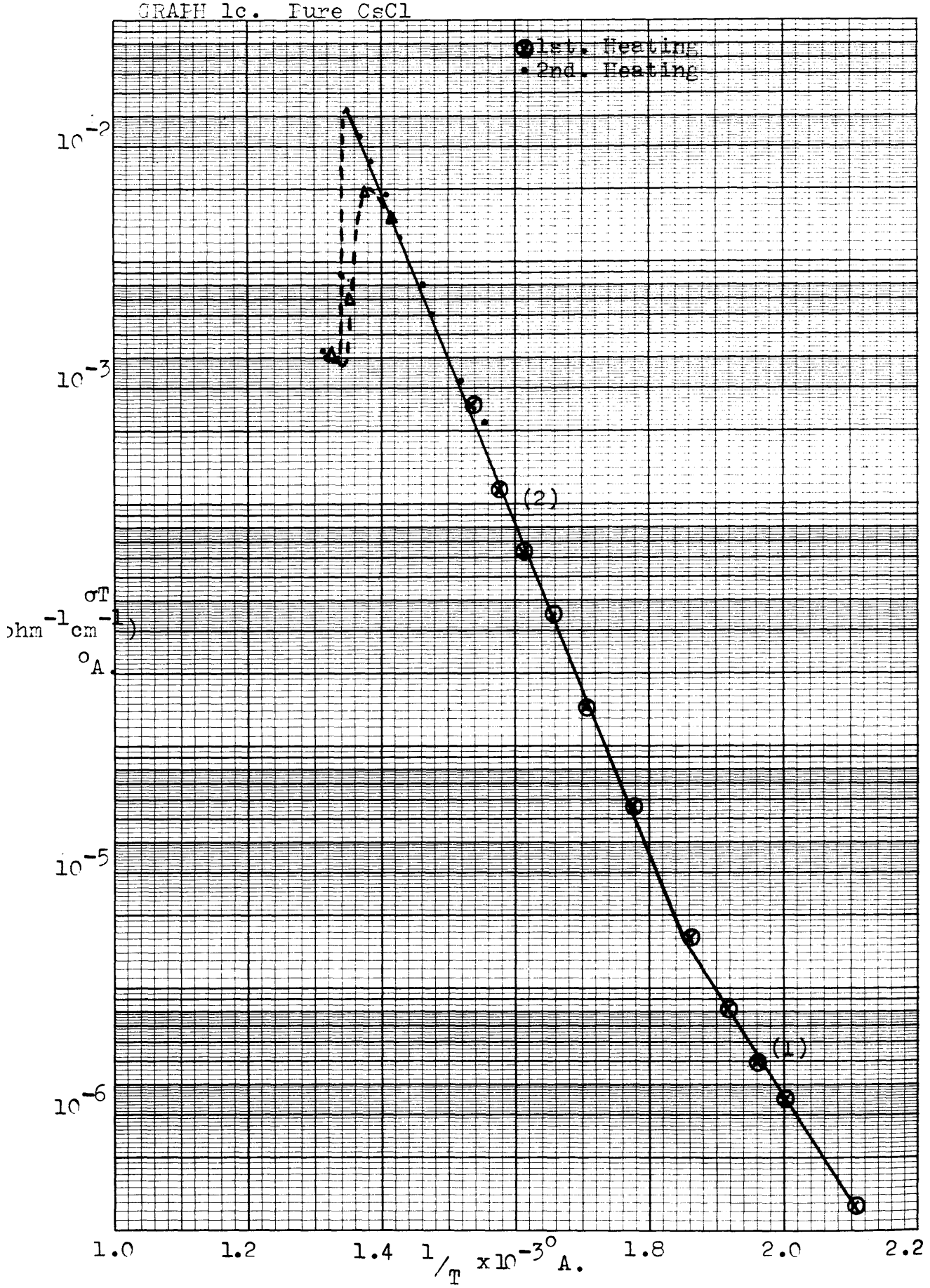

TABLE 1c

Graph 1c Pure CsCl

	1st heating	2nd heating	Cooling
Activation energy below knee (ev)	0.93 (1)	---	---
Knee (r.t.u.)	1.86	---	---
Activation energy above knee (ev)	1.37 (2)	1.37 (2)	---
Temperature at which transition starts (^{o}C)	---	467^{o}	468^{o}
σT at start of transition (ohm^{-1} cm^{-1} ^{o}K.)	---	4.20×10^{-2}	3.69×10^{-3}
Temperature at which transition is complete (^{o}C)	---	475^{o}	455^{o}
σT at completion of transition (ohm^{-1} cm^{-1} ^{o}K.)	---	3.93×10^{-3}	1.90×10^{-2}

GRAPH 2. Pure CsCl.

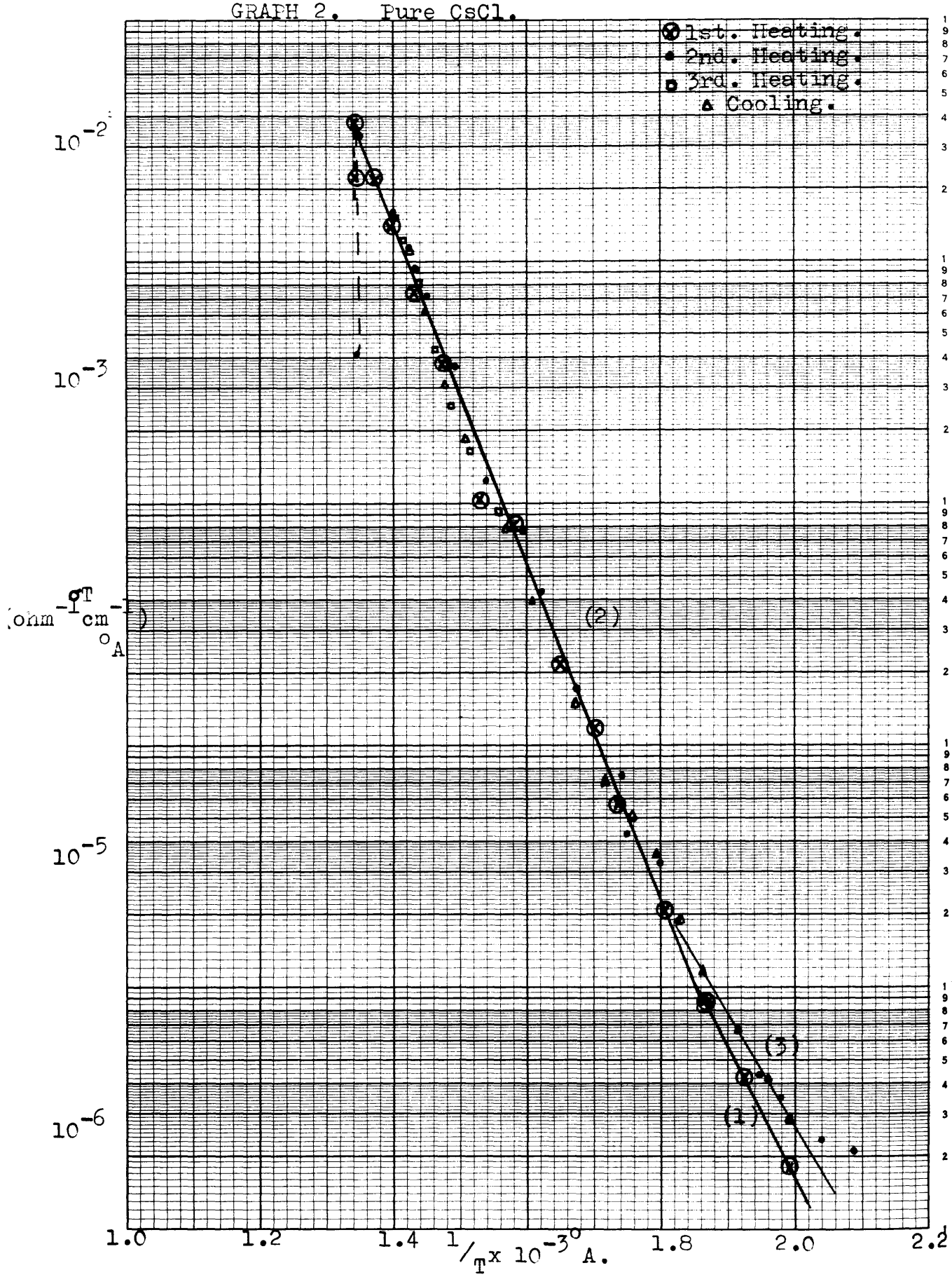

σT (ohm^{-1} cm^{-1} °A)

TABLE 2

Graph 2 Pure CsCl

	1st heat	2nd heat	3rd heat	cooling
Activation energy below knee (ev)	1.68(1)	---	---	0.94(3)
Knee (r.t.u.)	1.86	---	---	1.82
Activation energy above knee (ev)	1.39(2)	1.39(2)	1.39(2)	1.39(2)
Temperature at which transition starts °C	472°	468°	---	---
σT at start of transition ($ohm^{-1}cm^{-1}$)	3.72×10^{-2}	3.40×10^{-2}	---	---
Temperature at which transition is complete °C	---	472°	---	---
σT at completion of transition ($ohm^{-1}cm^{-1}$) °A.	---	4.11×10^{-3}	---	---

Impurity content less than 4 ppm divalent cation

GRAPH 3. Pure CsCl. (From Cs^{137} diffusion No. 2.)

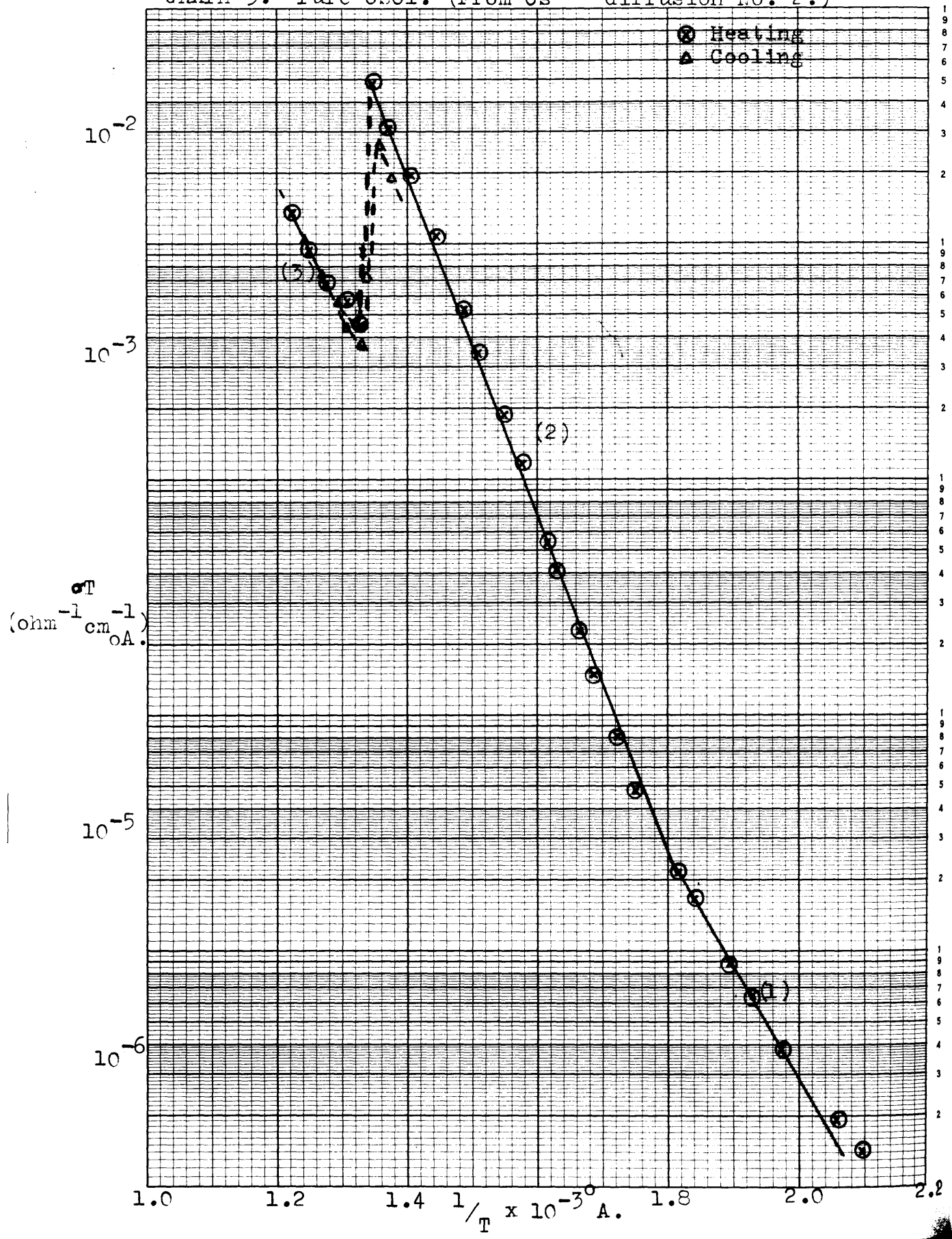

TABLE /3

Graph 3 'Pure' CsCl (from Cs^{137} diffusion No. 2)

	Heating	Cooling
Activation energy below knee (ev)	0.95 (1)	---
Knee (r.t.u.)	1.81	---
Activation energy above knee (ev)	1.42 (2)	---
Temperature at which transition starts ^{o}C	471^{o}	477^{o}
σT at start of transition ($ohm^{-1}cm^{-1}$) $^{o}A.$	4.76×10^{-2}	3.75×10^{-3}
Temperature at which transition is complete ^{o}C	480^{o}	464^{o}
σT at completion of transition ($ohm^{-1}{}_{o}^{}{}_{A.}^{}cm^{-1}$)	4.40×10^{-3}	2.66×10^{-2}

GRAPH 4. Pure CsCl

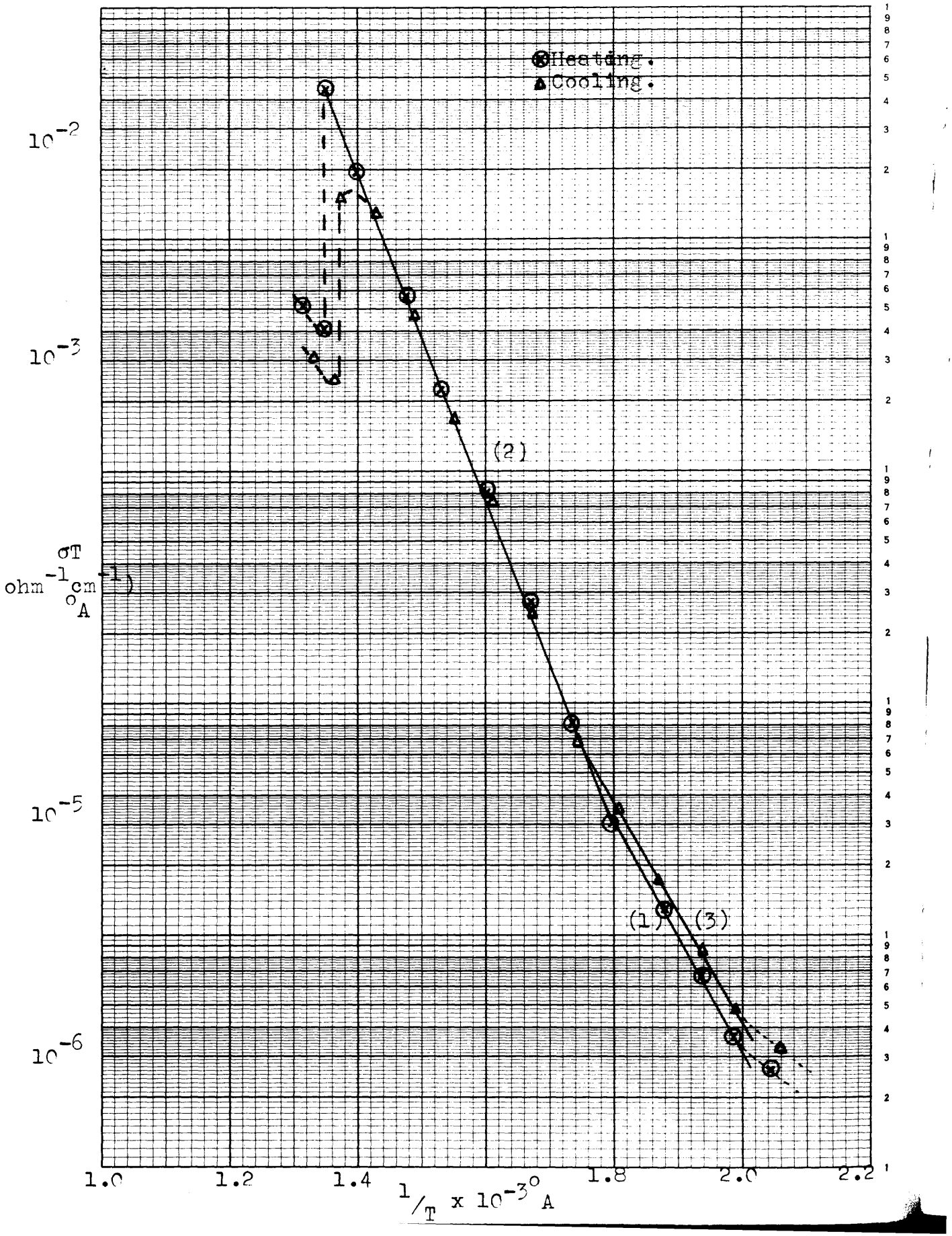

TABLE 4

Graph 4 Pure CsCl

	Heating	Cooling
Activation energy below knee (ev)	0.93(1)	0.88(3)
Knee (r.t.u.)	1.80	1.78
Activation energy above knee (ev)	1.40(2)	1.40(2)
Temperature at which transition starts °C	469°	461°
σT at start of transition ($ohm^{-1}cm^{-1}$)°A.	4.40×10^{-2}	2.48×10^{-3}
Temperature at which transition is complete	475°	454°
σT at completion of transition ($ohm^{-1}cm^{-1}$)°A.	4.04×10^{-3}	1.61×10^{-2}

Impurity content less than 4 ppm divalent cation

GRAPH 4[a]. Pure CsCl. (Run 4, four days later).

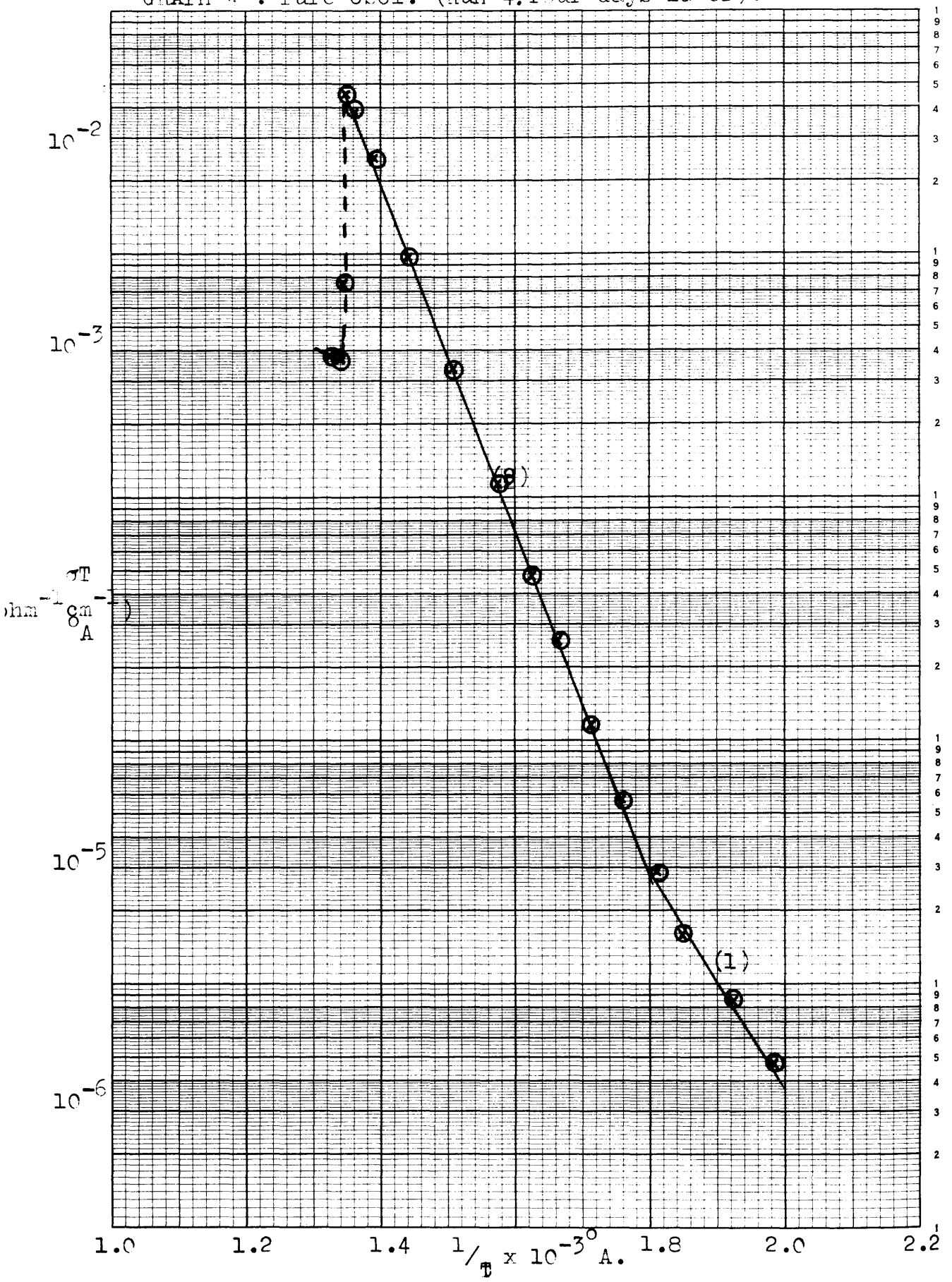

TABLE 4a.

Graph 4[a] Pure CsCl (Run 4, four days later)

Activation energy below knee (ev)	0.88[(1)]
Knee (r.t.u.)	1.80
Activation energy above knee (ev)	1.41[(2)]
Temperature at which transition starts ^{o}C	469^{o}
σT at start of transition ($ohm^{-1}cm^{-1}$) ^{o}A.	4.57×10^{-2}
Temperature at which transition is complete ^{o}C	473^{o}
σT at completion of transition ($ohm^{-1}cm^{-1}$)^{o}A.	3.66×10^{-3}

Impurity content less than 4 ppm divalent cation

GRAPH 5. Pure CsCl. Annealed in vacuo 192 hrs. @ 400°C.

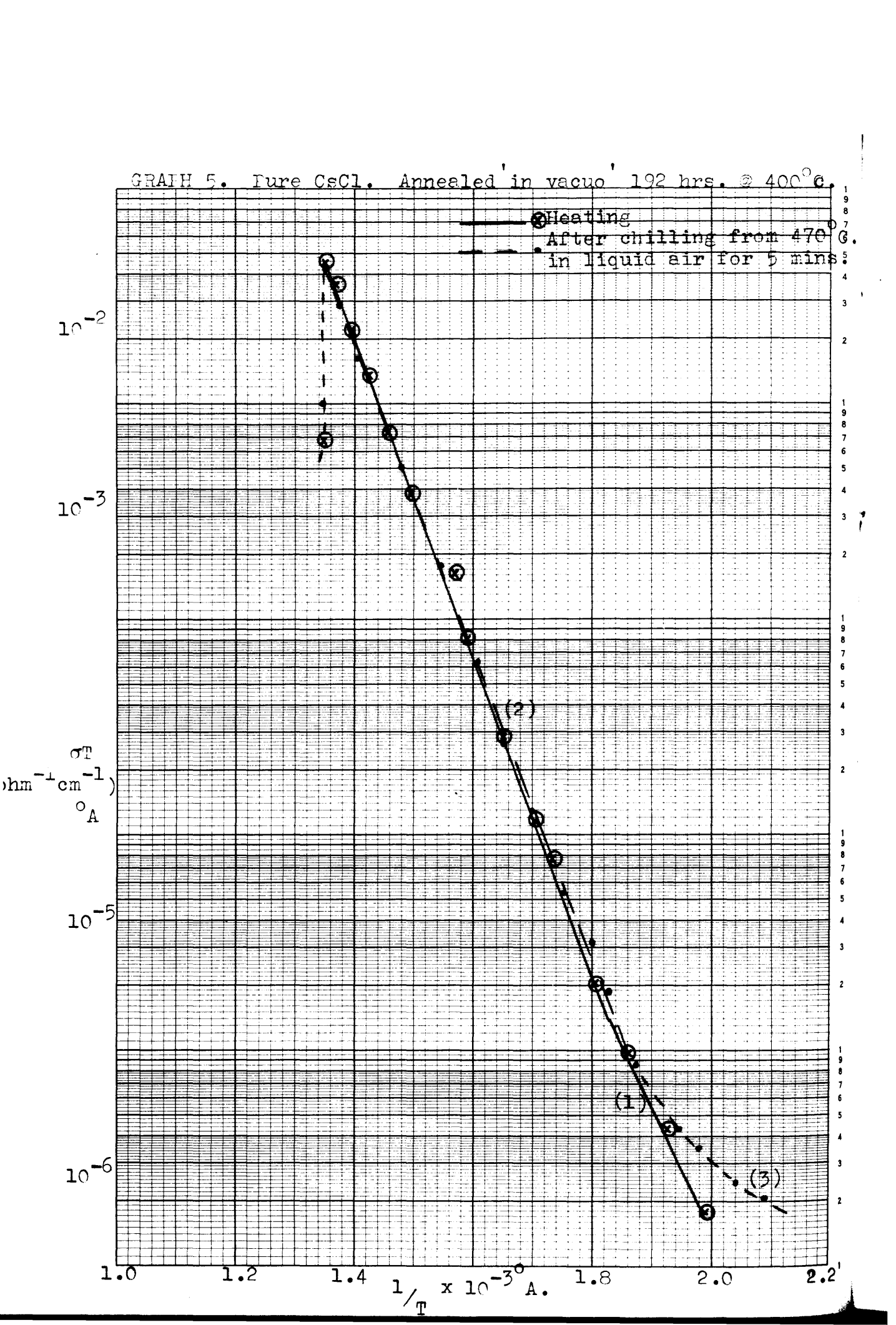

TABLE 5

Graph 5 Pure CsCl Annealed in vacuo 192 hrs at 400°C

	1st heating	2nd heating (after chilling from 470°in liquid air)
Activation energy below knee (ev)	1.13(1)	curved(3)
Knee (r.t.u.)	1.83	---
Activation energy above knee (ev)	1.47(2)	1.41
Temperature at which transition starts °C	468°	467°
σT at start of transition ($ohm^{-1}cm^{-1}$)	4.53×10^{-2}	4.29×10^{-2}

GRAPH 6. Pure CsCl.

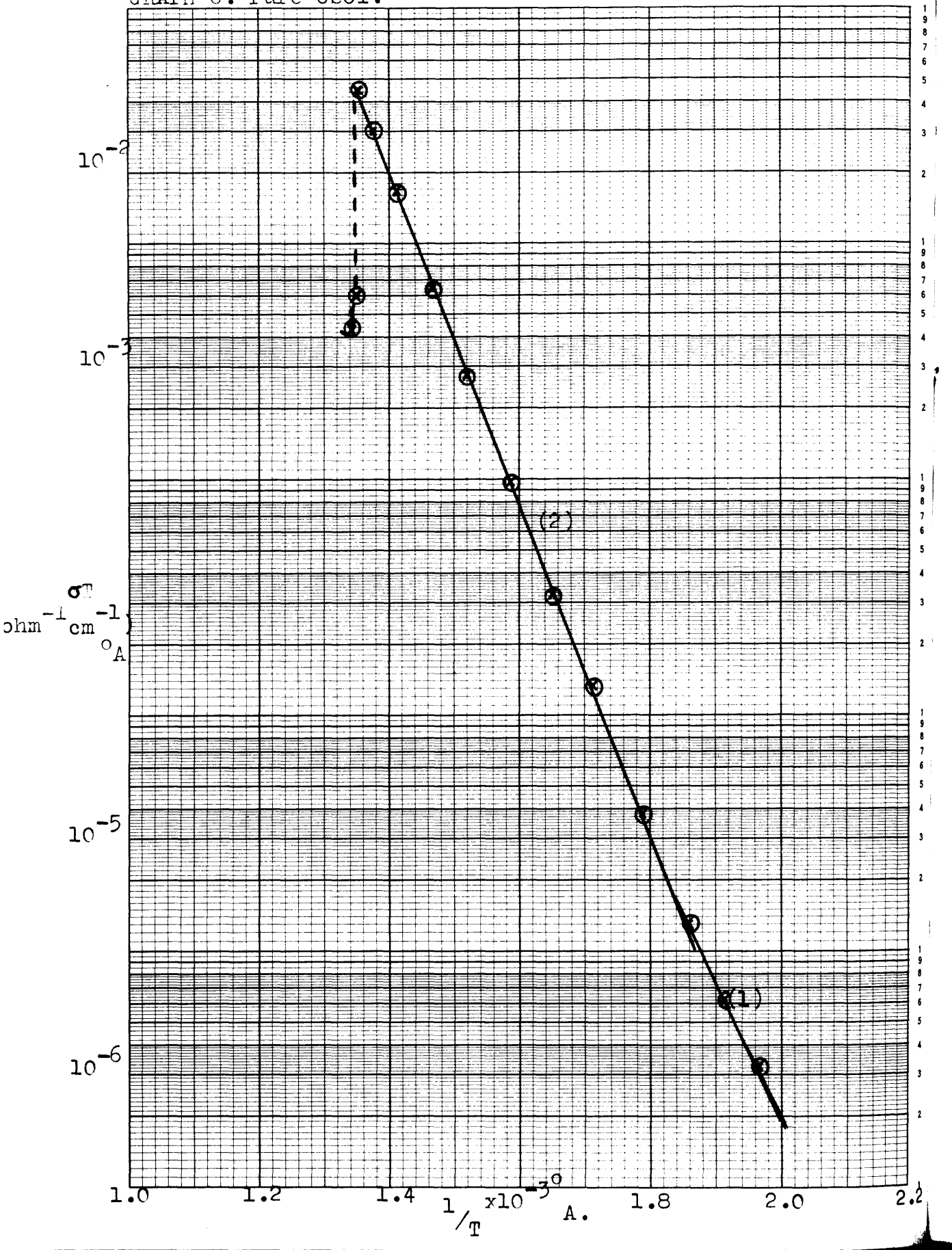

TABLE 6

Graph 6 Pure CsCl

Activation energy below knee (ev)	1.15[1]
Knee (r.t.u.)	1.85
Activation energy above knee (ev)	1.40[2]
Temperature at which transition starts (^{o}C)	467^{o}
σT at start of transition (ohm^{-1}cm^{-1}) ^{o}A.	4.39 x 10^{-2}
Temperature at which transition is complete (^{o}C)	472^{o}
σT at completion of transition (ohm^{-1}cm^{-1}) ^{o}A.	4.31 x 10^{-3}

GRAPH 6[a]. Pure CsCl. (Run 6. after γ-irradiation

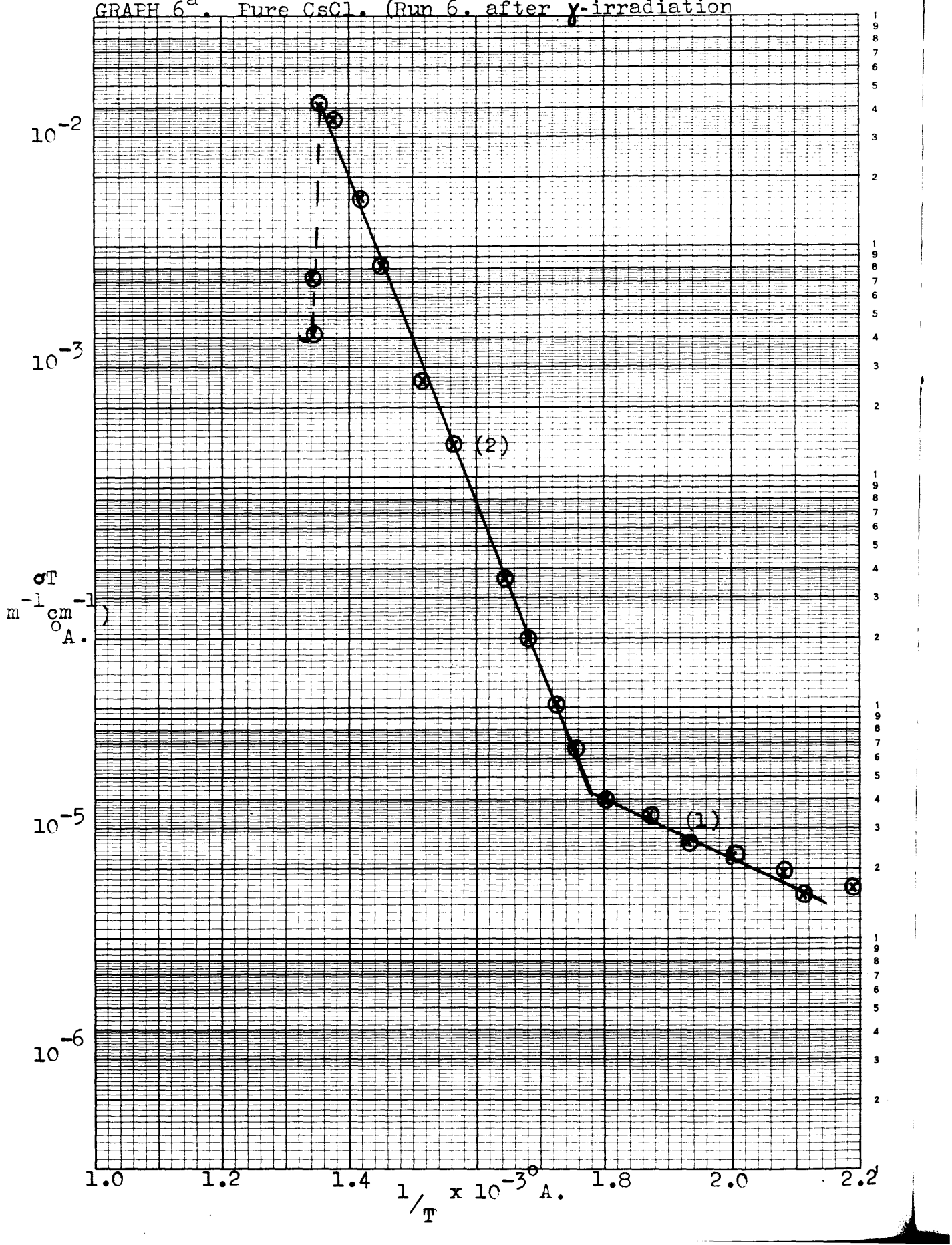

TABLE 6a.

Graph 6^a Pure CsCl (Run 6 after γ -irradiation)

Activation energy below knee (ev)	$0.25^{(1)}$
Knee (r.t.u.)	1.77
Activation energy above knee (ev)	$1.40^{(2)}$
Temperature at which transition starts (^oC)	466^o
σT at start of transition ($ohm^{-1}cm^{-1}$) ^oA.	4.11×10^{-2}
Temperature at which transition is complete (^oC)	474^o
σT at completion of transition ($ohm^{-1}cm^{-1}$) ^oA.	4.18×10^{-3}

Graph 7. Pure CsCl-Melt grown.

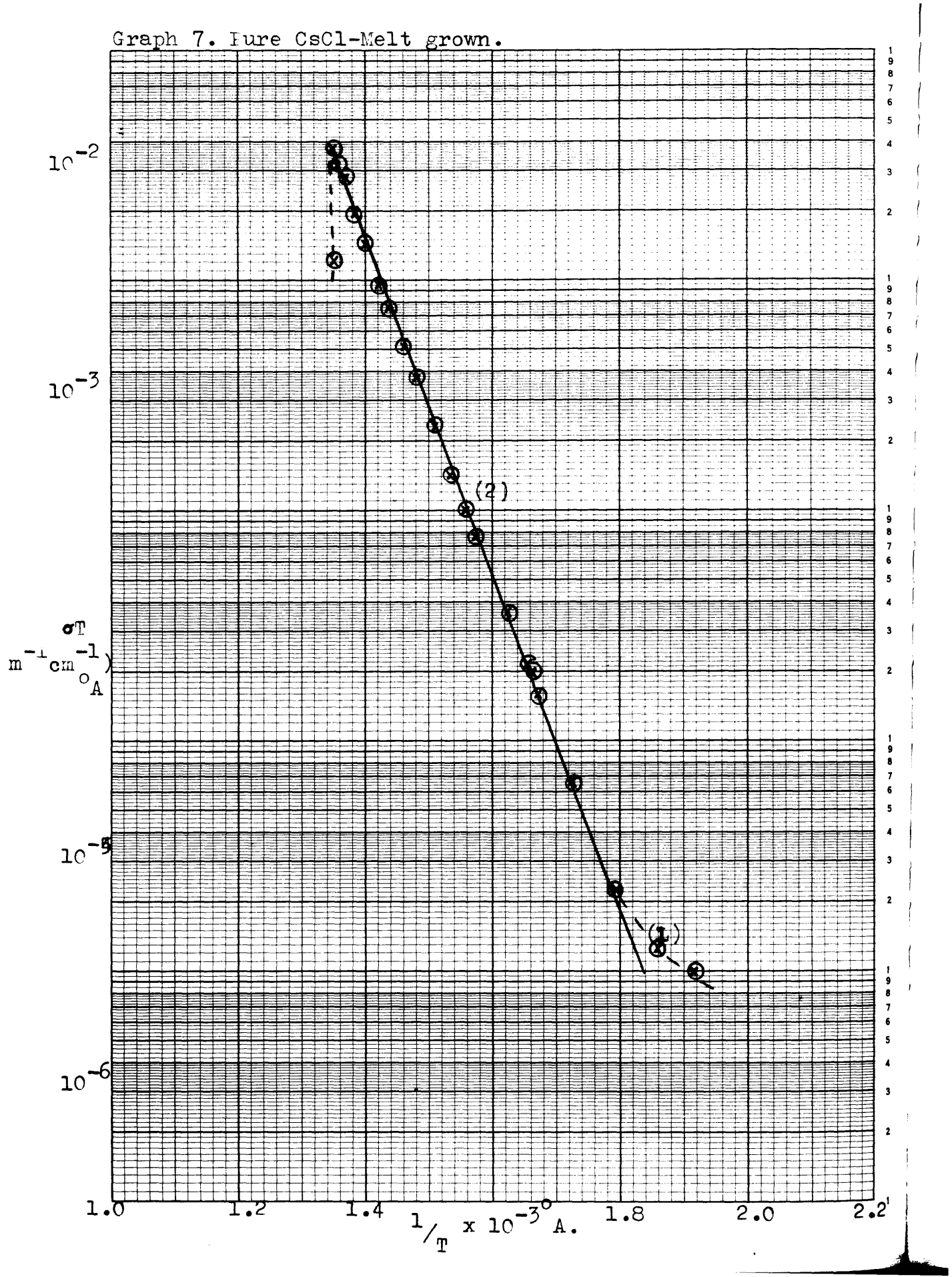

TABLE 7

Graph 7 Pure CsCl (melt-grown)

Activation energy below knee (ev)	curve(1)
Knee (r.t.u.)	1.79
Activation energy above knee (ev)	1.47
Temperature at which transition starts (^{o}C)	470^{o}
σT at start of transition ($ohm^{-1}cm^{-1}$) ^{o}A.	3.60×10^{-2}

GRAPH 7[a]. Pure CsCl Melt-grown, (from Run 7 after γ-irradiation

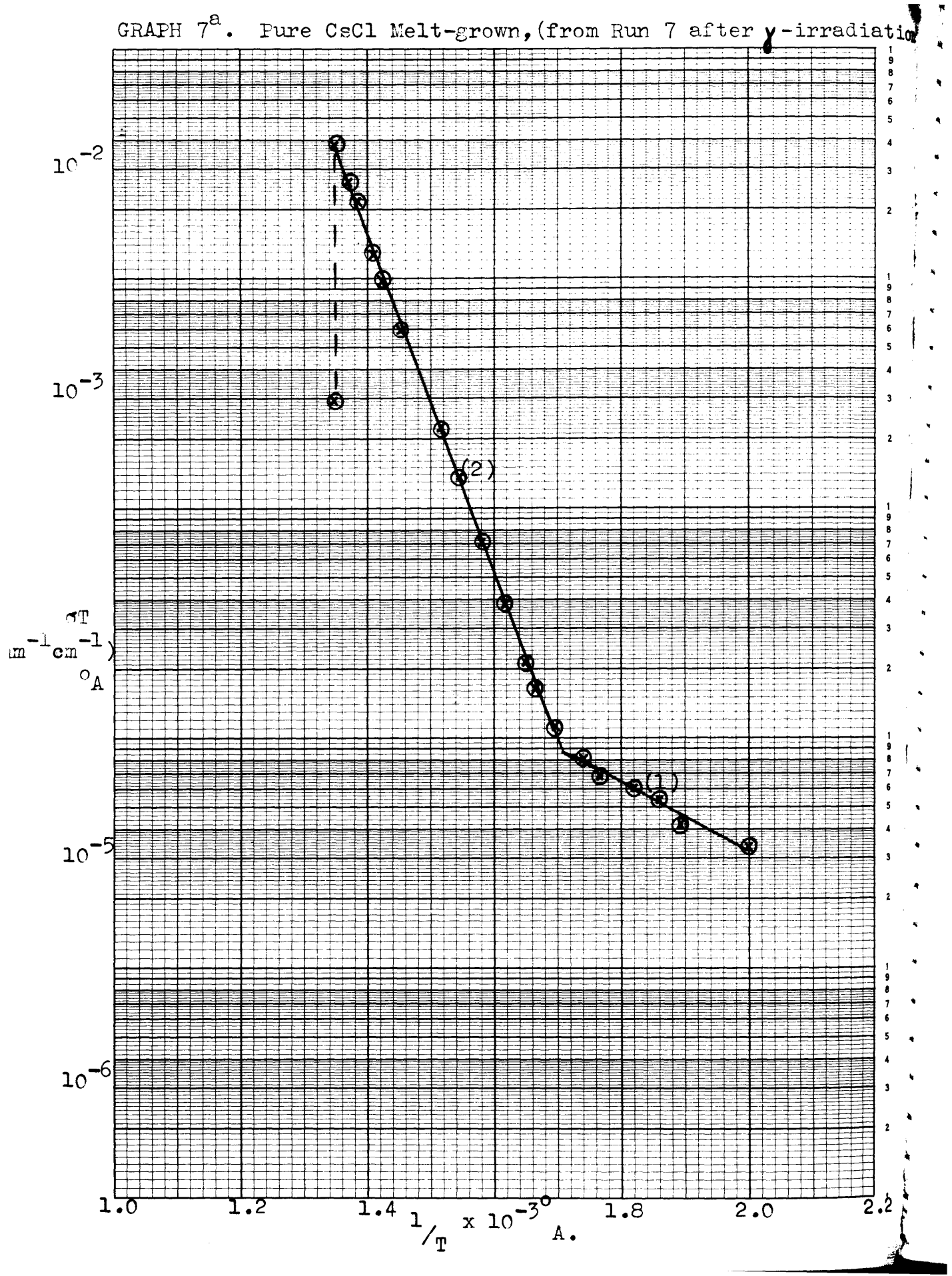

TABLE 7a.

Graph 7[a] Pure Melt-grown CsCl (from Run 7 after γ-irradiation)

Activation energy below knee (ev)	0.28[(1)]
Knee (r.t.u.)	1.71
Activation energy above knee (ev)	1.46[(2)]
Temperature at which transition starts (^{o}C)	470^{o}
σT at start of transition (ohm^{-1}cm^{-1}) ^{o}A.	3.80 x 10^{-2}
Temperature at which transition is complete (^{o}C)	471^{o}
σT at completion of transition (ohm^{-1}cm^{-1}) ^{o}A.	2.97 x 10^{-3}

GRAPH 8. Pure CsCl melt-grown after 196hrs. @ 400°C between pellets of $BaCl_2$

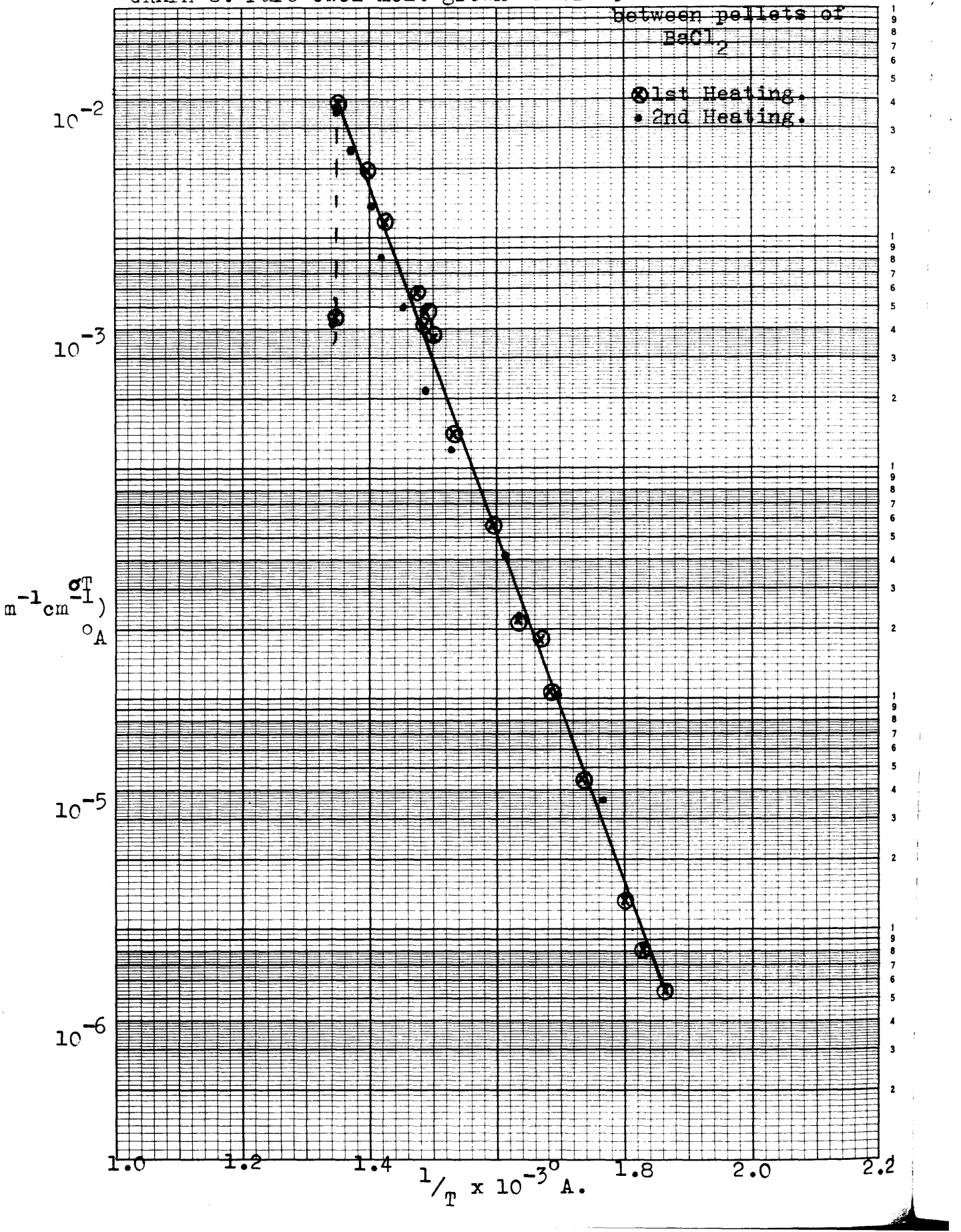

TABLE 8

Graph 8 Pure CsCl Melt-grown (after 196 hrs at 400°C between pellets of $BaCl_2$)

	1st heating	2nd heating
Activation energy	1.48	1.48
Temperature at which transition starts (°C)	467°	467°
σT at start of transition ($ohm^{-1}cm^{-1}$)°A.	3.79×10^{-2}	3.66×10^{-2}
Temperature at which transition is complete (°C)	471°	470°
σT at completion of transition ($ohm^{-1}cm^{-1}$)	4.51×10^{-3}	4.20×10^{-3}

GRAPH 9. Ba^{2+}-doped CsCl.

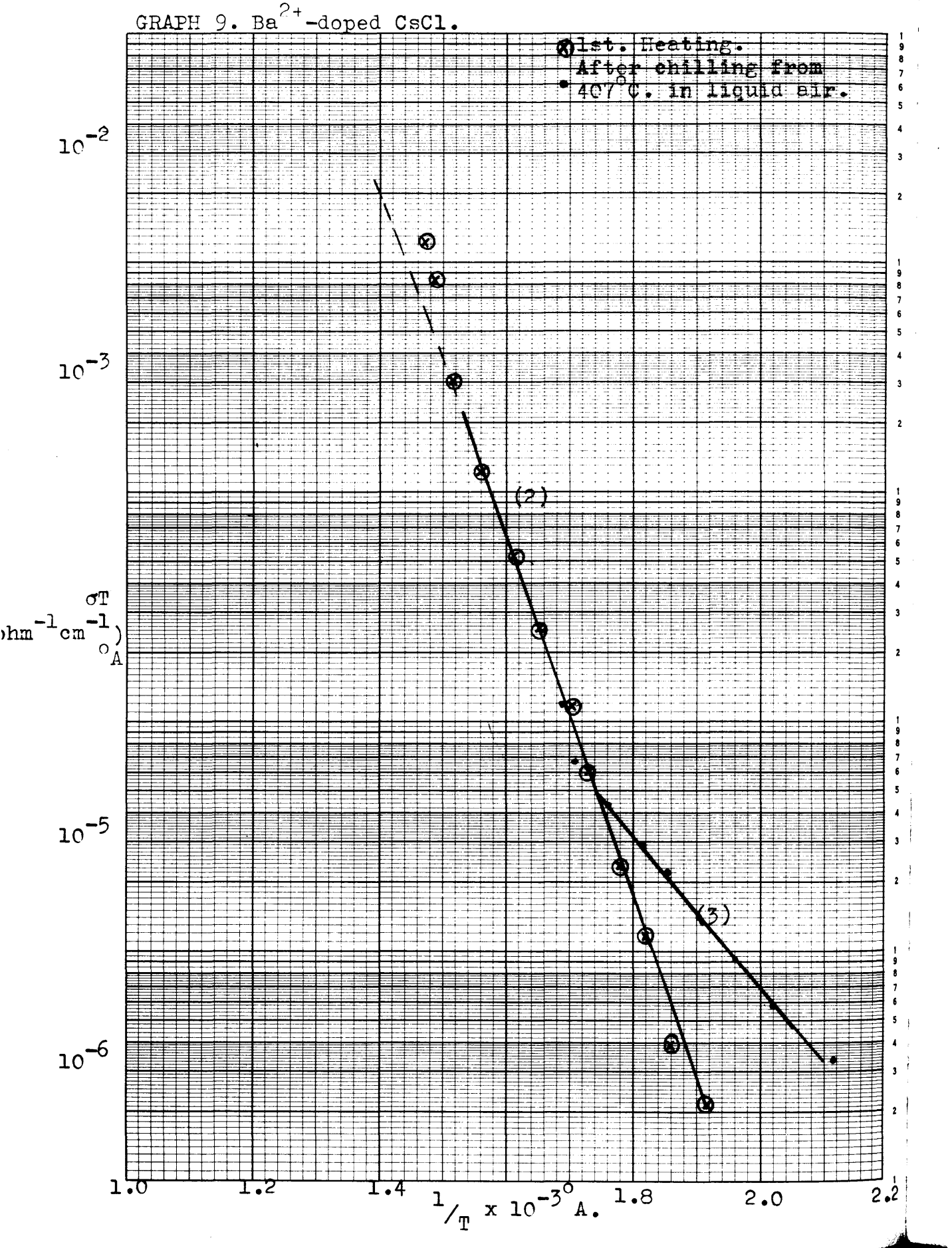

TABLE 9

Graph 9 Ba^{2+}-doped CsCl

	1st heating	2nd heating (after chilling from 407° in liquid air
Activation energy below knee (ev)	---	0.70[3]
Knee (r.t.u.)	---	1.75
Activation energy above knee (ev)	1.42[2]	

GRAPH 10. Ba^{2+}-doped CsCl.

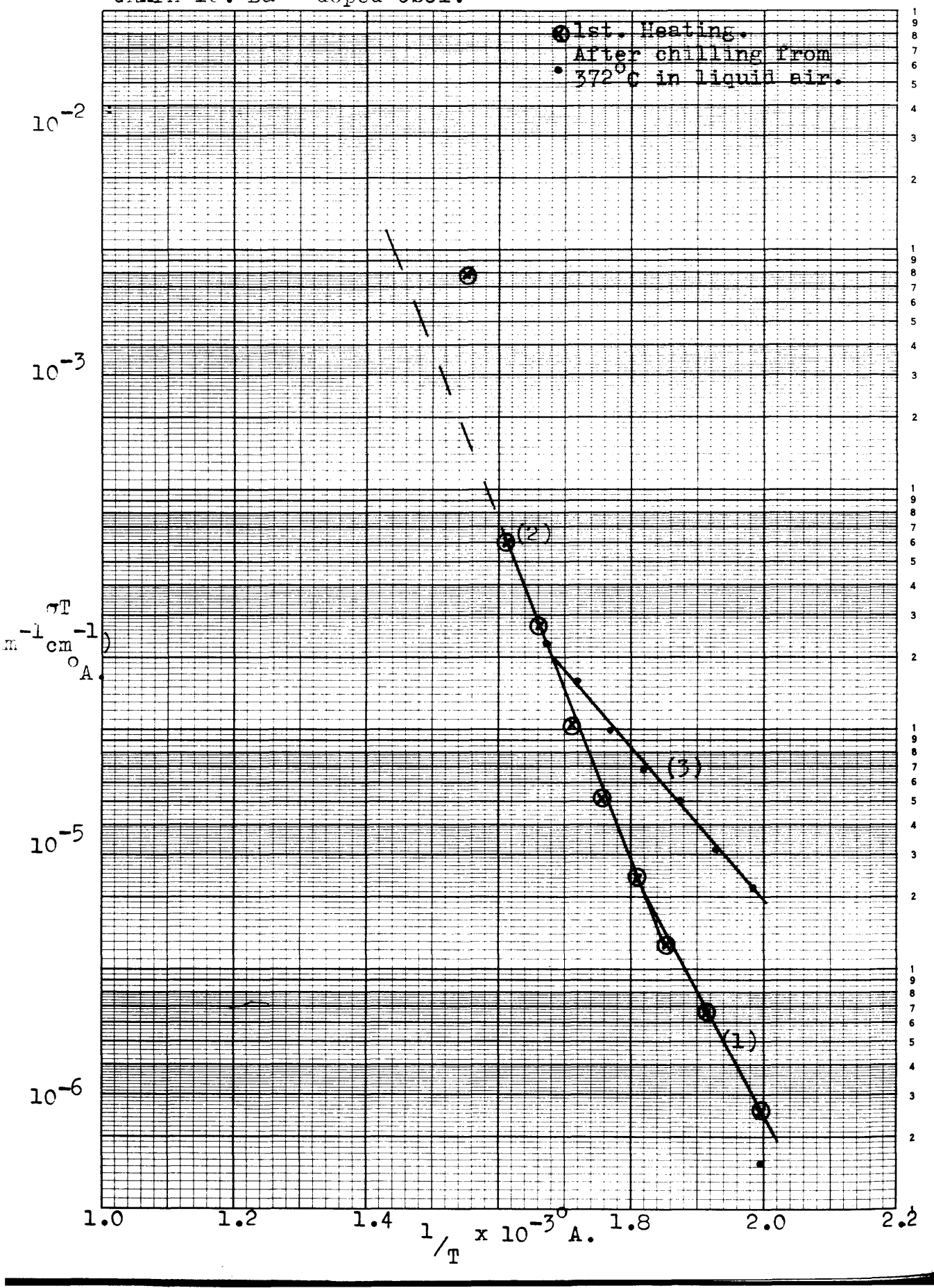

TABLE 10

Graph 10. Ba^{2+}-doped CsCl

	1st heating	2nd heating (after chilling from 372° in liquid air)
Activation energy below knee (eV)	1.02(1)	0.63(3)
Knee (r.t.u.)	1.83	1.68
Activation energy above knee (eV)	1.40	---

GRAPH 11. Ba^{2+}-doped CsCl. Impurity Content 57 ppm.

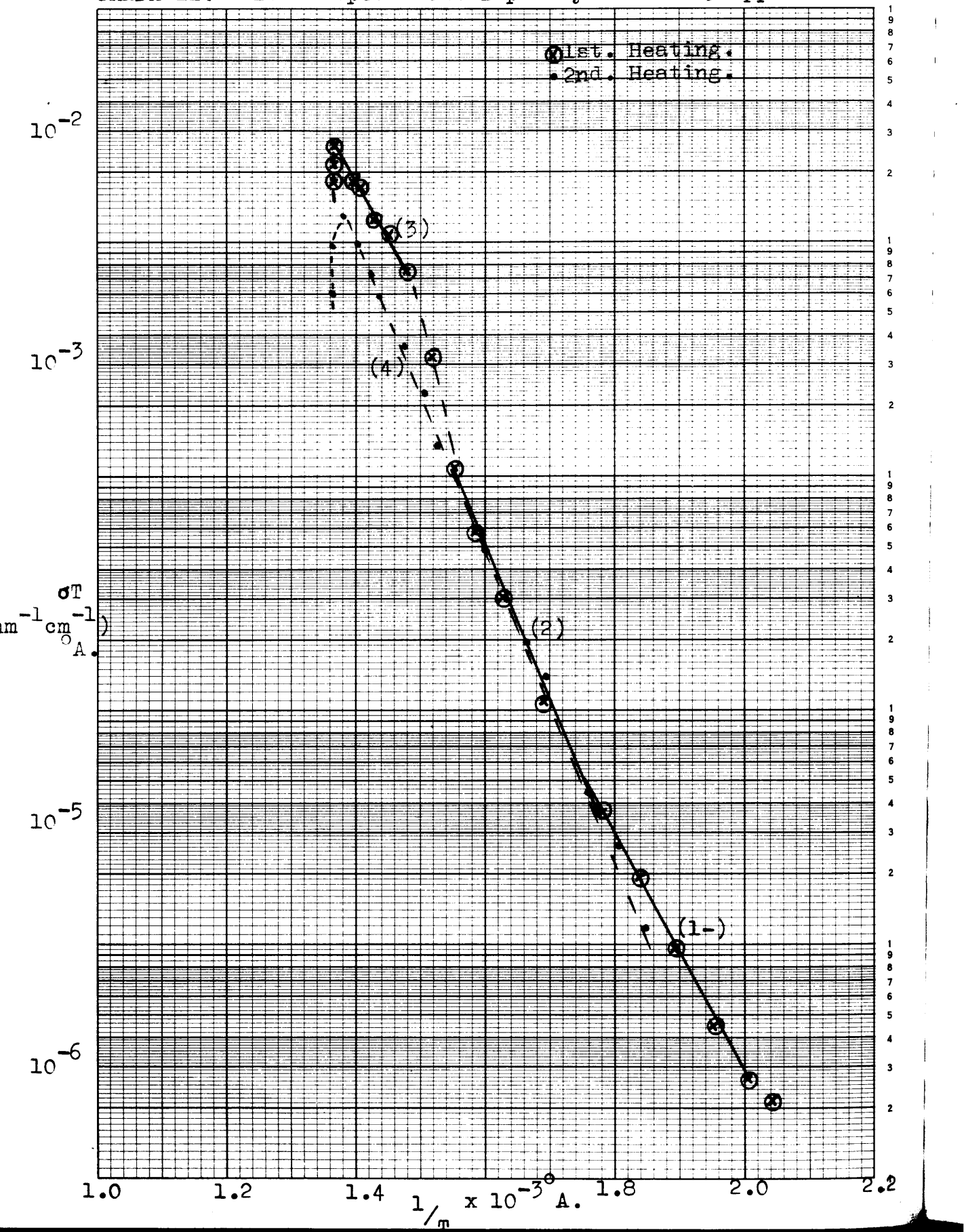

TABLE 11

Graph 11 Ba^{2+}-doped CsCl. Impurity content 57ppm

	1st heating	2nd heating
Activation energy below knee (ev)	1.03(1)	---
Knee (r.t.u.)	1.75	---
Activation energy above knee (ev)	1.38(2)	1.32(4)
Rise temperature range (r.t.u.)	1.55-1.48	---
Amount of rise	2.7 (times)	---
Activation energy above rise (ev)	1.00(3)	---
Temperature at which transition starts (°C)	458°	451°
σT at start of transition ($ohm^{-1}cm^{-1}_{o}{}_{A.}$)	2.61×10^{-2}	1.27×10^{-2}

GRAPH 12. Ba^{2+}-doped CsCl. Impurity Content 62 ppm.

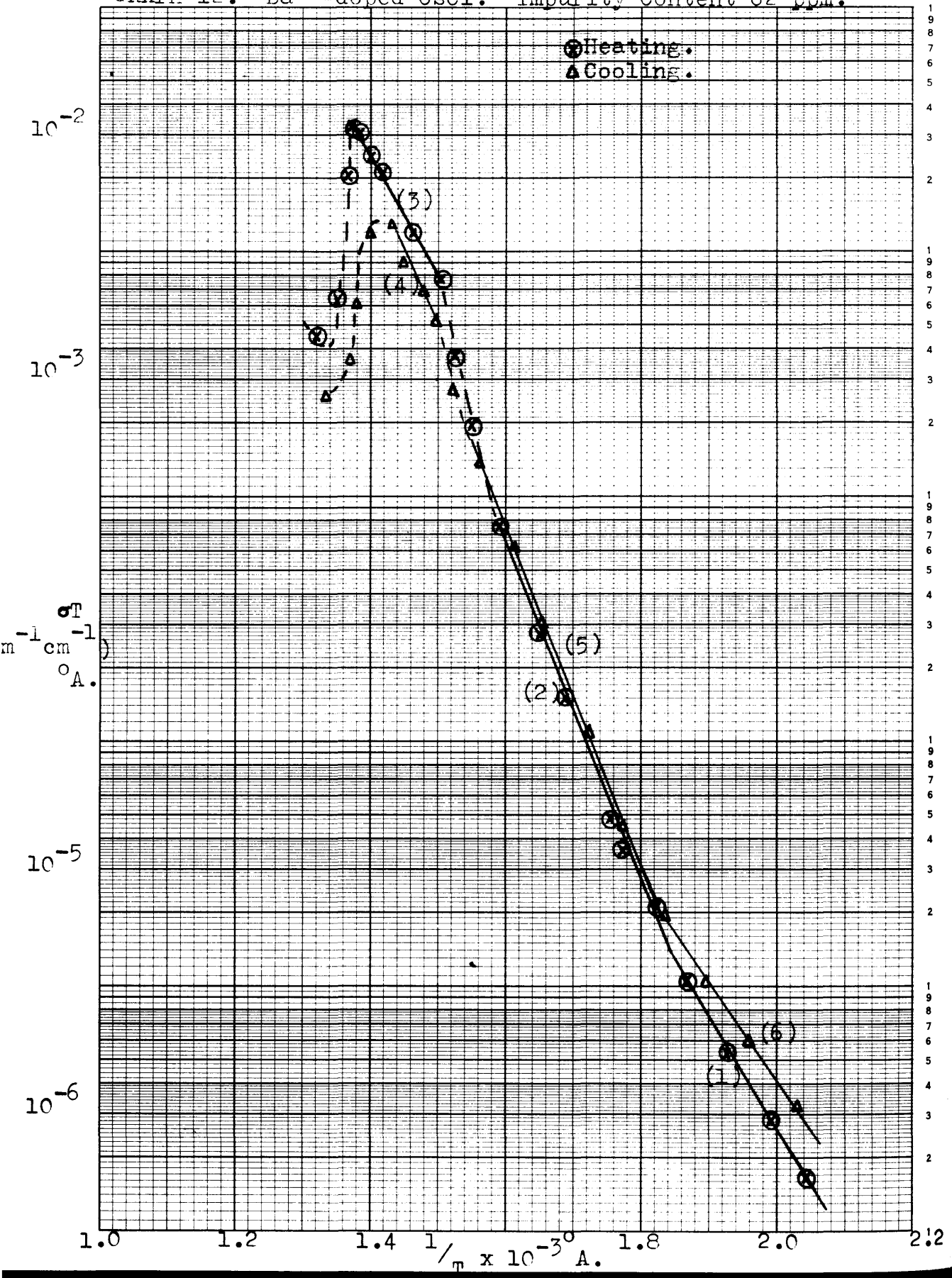

TABLE 12

Graph 12 Ba^{2+}-doped CsCl. 62ppm

	Heating	Cooling
Activation energy below knee (ev)	0.91 (1)	0.82 (6)
Knee (r.t.u.)	1.85	1.82
Activation energy above knee (ev)	1.37 (2)	1.37 (5)
Rise temperature range (r.t.u.)	1.59-1.50	---
Amount of rise	2.9 (times)	1.5 (times)
Activation energy above rise (ev)	0.97 (3)	1.17 (4)
Temperature at which transition starts (°C)	456°	477-458°
σT at start of transition ($ohm^{-1}cm^{-1}$)$_A$	3.27×10^{-2}	---
Temperature at which transition is complete (°C)	469-484°	442-426°
σT at completion of transition ($ohm^{-1}cm^{-1}$)$_{o_A}$	app.4.00×10^{-3}	app.1.30×10^{-2}

GRAPH 13. Ba^{2+}-doped CsCl. Impurity Content 71 ppm.

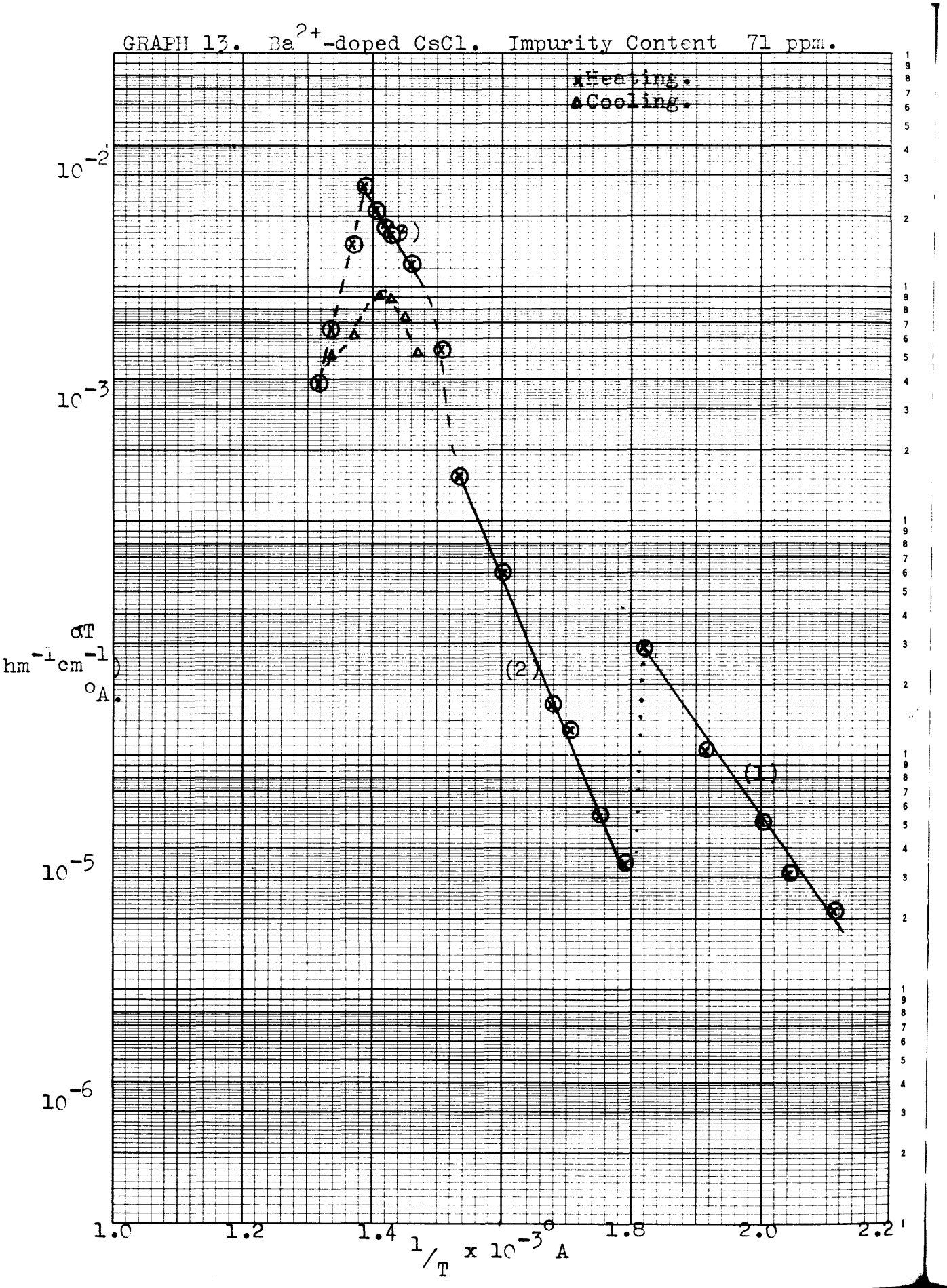

TABLE 13

Graph 13. Ba^{2+} - doped CsCl. 71ppm.

	Heating	Cooling
Activation energy below knee (ev)	0.78 (1)	---
Knee (r.t.u.)	conductivity falls by a factor of 10 times 1.82-1.79	---
Activation energy above knee (ev)	1.35 (2)	---
Rise temperature range (r.t.u.)	1.53-1.48	---
Amount of rise	3.2 (times)	---
Activation energy above rise (ev)	0.91 (3)	---
Temperature at which transition starts (^{o}C)	448^{o}	475^{o}
σT at start of transition ($ohm^{-1}cm^{-1}$ $^{o}_{A.}$)	2.70×10^{-2}	5.91×10^{-3}
Temperature at which transition is complete (^{o}C)	487^{o}	438-427^{o}
σT at completion of transition ($ohm^{-1}cm^{-1}$ $^{o}_{A.}$)	3.78×10^{-3}	9.00×10^{-3}

GRAPH 14. Ba^{2+}-doped CsCl. Impurity Content 85ppm.

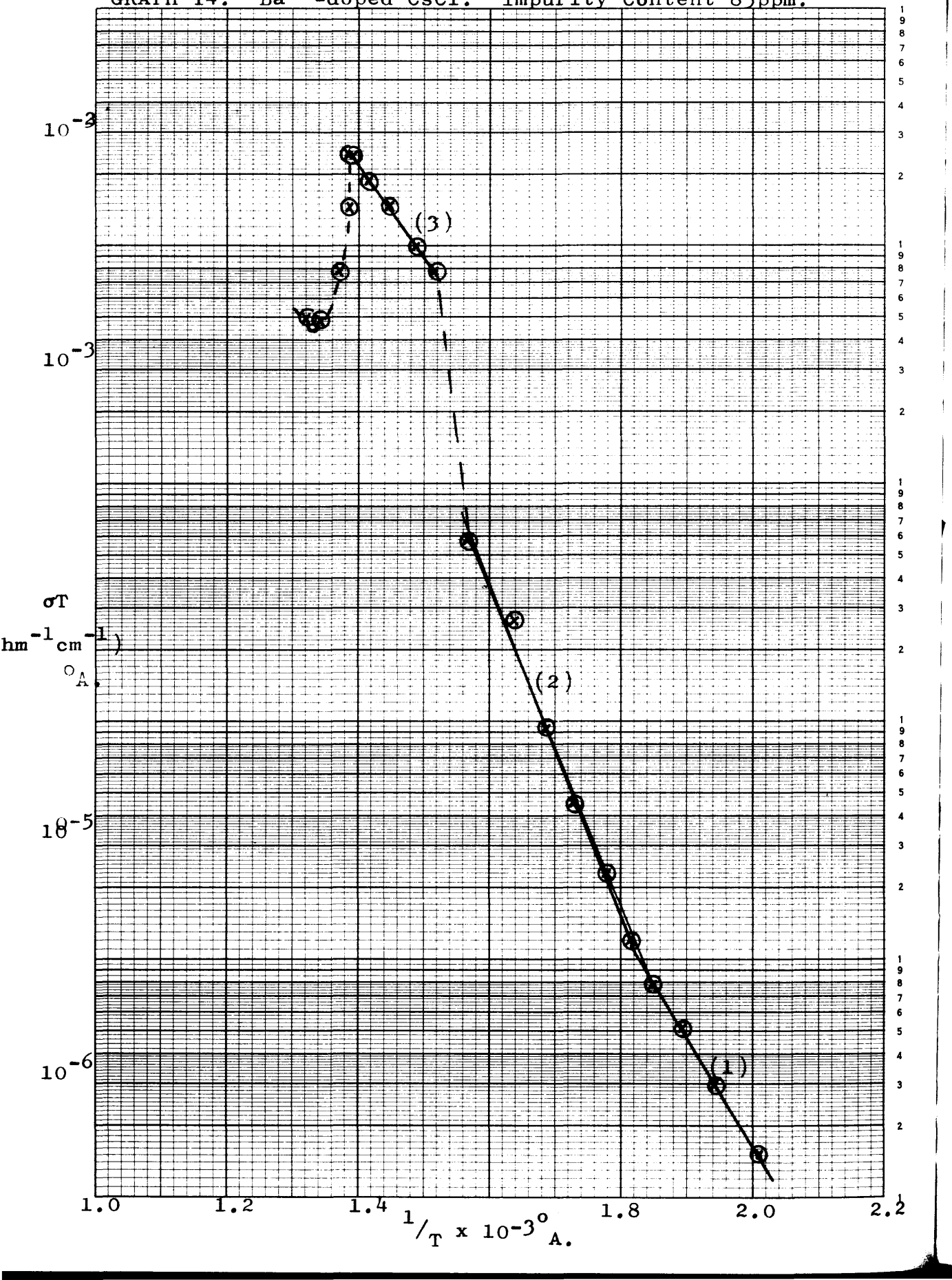

TABLE 14

Graph 14. Ba^{2+} - doped CsCl. 85ppm

Activation energy below knee (ev)	0.93 (1)
Knee (r.t.u.)	1.82
Activation energy above knee (ev)	1.40 (2)
Rise temperature range (r.t.u.)	1.57-1.52
Amount or rise	5.5 (times)
Activation energy above rise (ev)	0.79 (3)
Temperature at which transition starts (^{o}C)	445^{o}
σT at start of transition ($ohm^{-1} cm^{-1}_{o}$) $A.$	2.41×10^{-2}
Temperature at which transition is complete (^{o}C)	473^{o}
σT at completion of transition ($ohm^{-1} cm^{-1}_{o}$) $A.$	4.78×10^{-3}

GRAPH 15. Ba^{2+}-doped CsCl. Impurity Content 97 ppm.

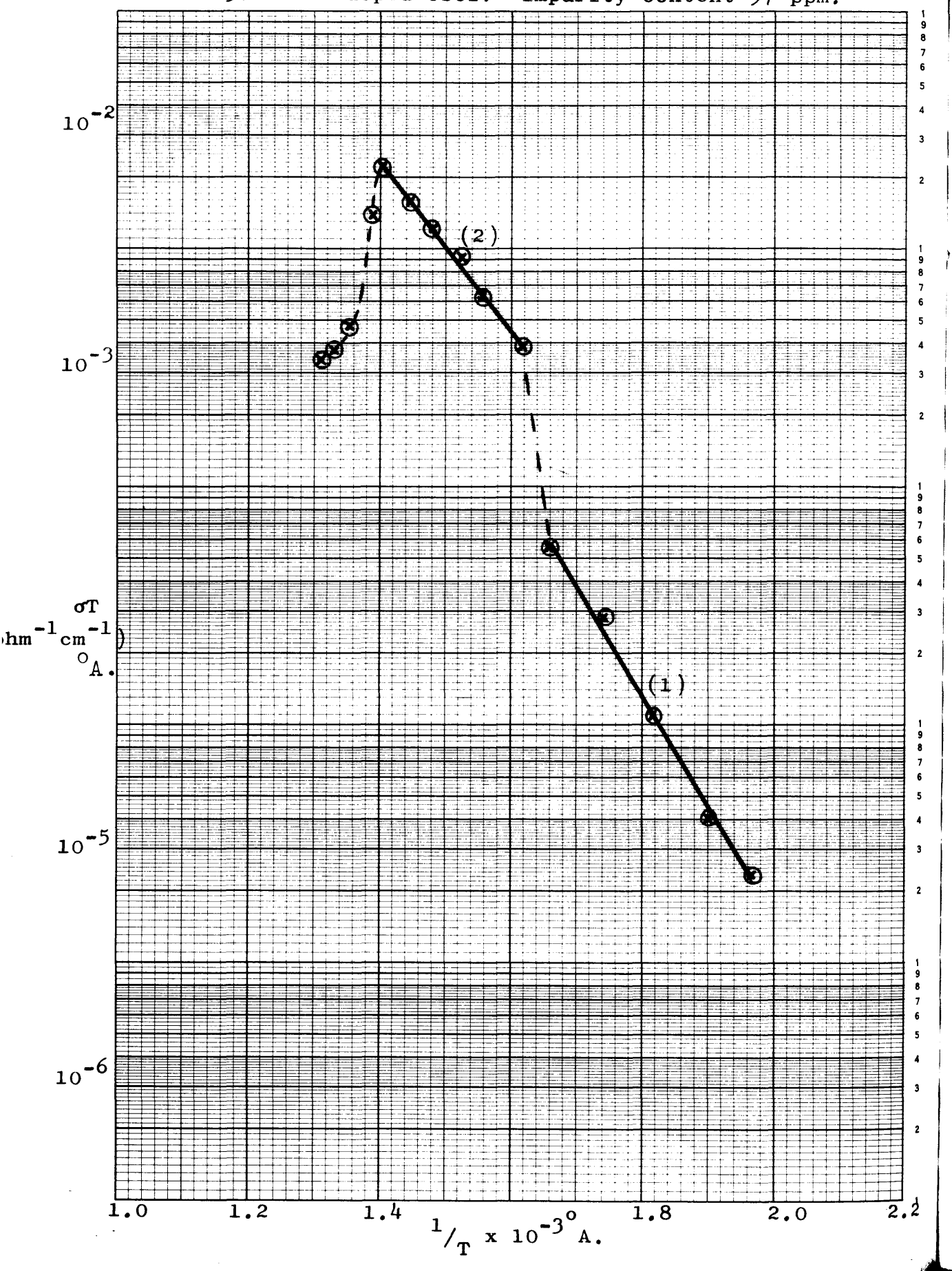

TABLE 15

Graph 15 Ba^{2+}-doped CsCl 97ppm

Activation energy (ev)	0.95 (1)
Range of rise (r.t.u.)	1.66-1.62
Amount of rise	4.4 (times)
Activation energy above rise (ev)	0.70 (2)
Temperature at which transition starts (°C)	440°
σT at start of transition $(ohm^{-1}cm^{-1})^{\circ}A.$	2.20×10^{-2}
Temperature at which transition is complete (°C)	490°
σT at completion of transition $(ohm^{-1}cm^{-1})^{\circ}A.$	3.40×10^{-3}

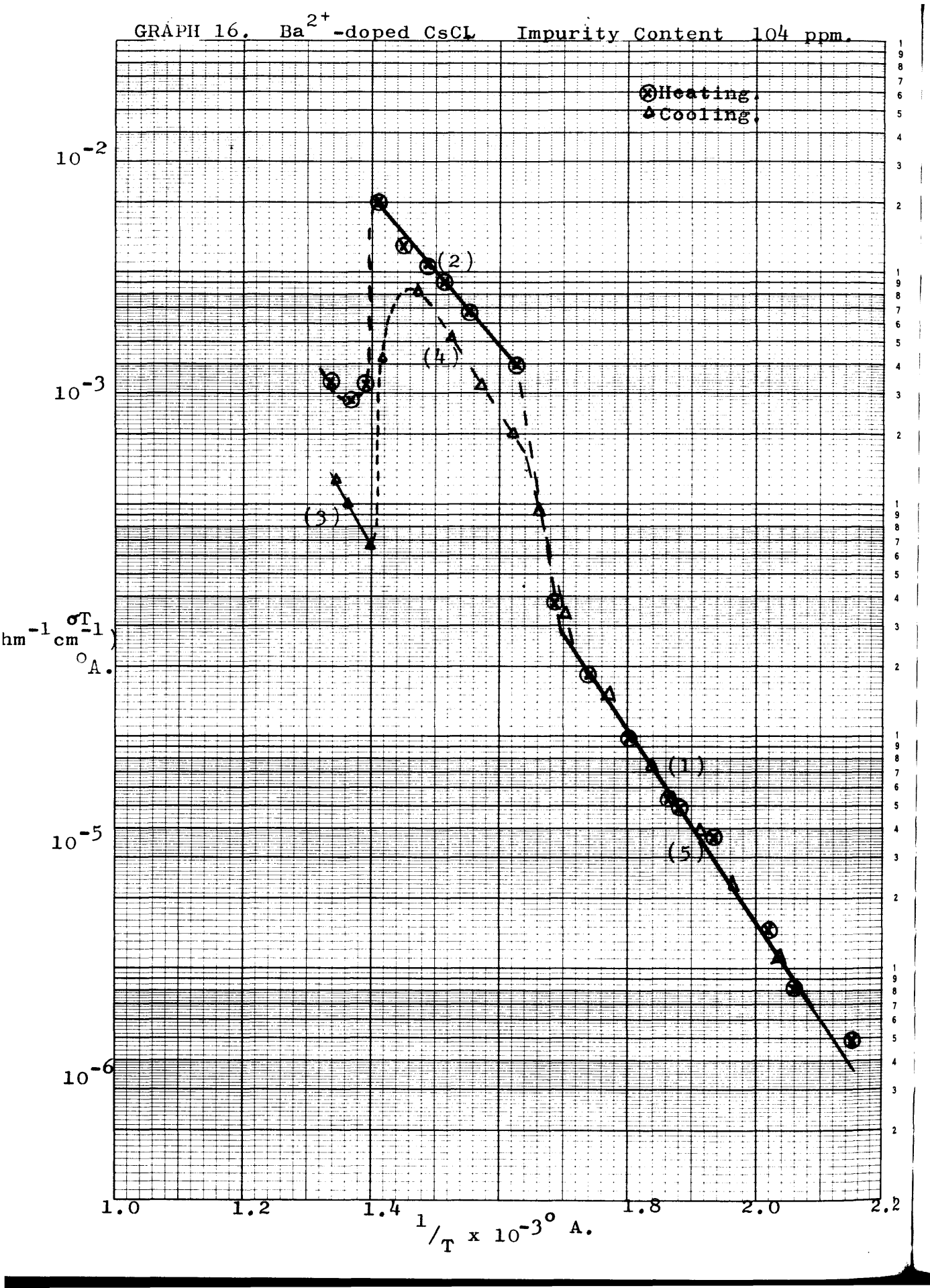
GRAPH 16. Ba^{2+}-doped CsCL Impurity Content 104 ppm.
⊗Heating.
△Cooling.
10^{-2}
10^{-3}
10^{-5}
10^{-6}
(1)
(2)
(3)
(4)
(5)
σT ohm^{-1} cm^{-1} °A.
1.0
1.2
1.4
1.8
2.0
2.2
$1/T \times 10^{-3}$ ° A.

TABLE 16

Graph 16. Ba^{2+}-doped CsCl. 104ppm

	Heating	Cooling
Activation energy (ev)	0.84 (1)	0.84 (5)
Rise temperature range (r.t.u.)	1.70-1.62	1.65-1.72
Amount of rise	7.7 (times)	3.2 (times)
Activation energy above rise (ev)	0.65 (2)	0.86 (4)
Temperature at which transition starts (^{o}C)	437^{o}	442^{o}
σT at start of transition ($ohm^{-1}cm^{-1}$) ^{o}A.	2.04×10^{-2}	6.64×10^{-4}
Temperature at which transition is complete (^{o}C)	460^{o}	433-408^{o}
σT at completion of transition ($ohm^{-1}cm^{-1}$) $_{o}$A.	2.80×10^{-3}	9.00×10^{-3} approx.

GRAPH 17. Ba^{2+}-doped CsCl. Impurity content. 133ppm.

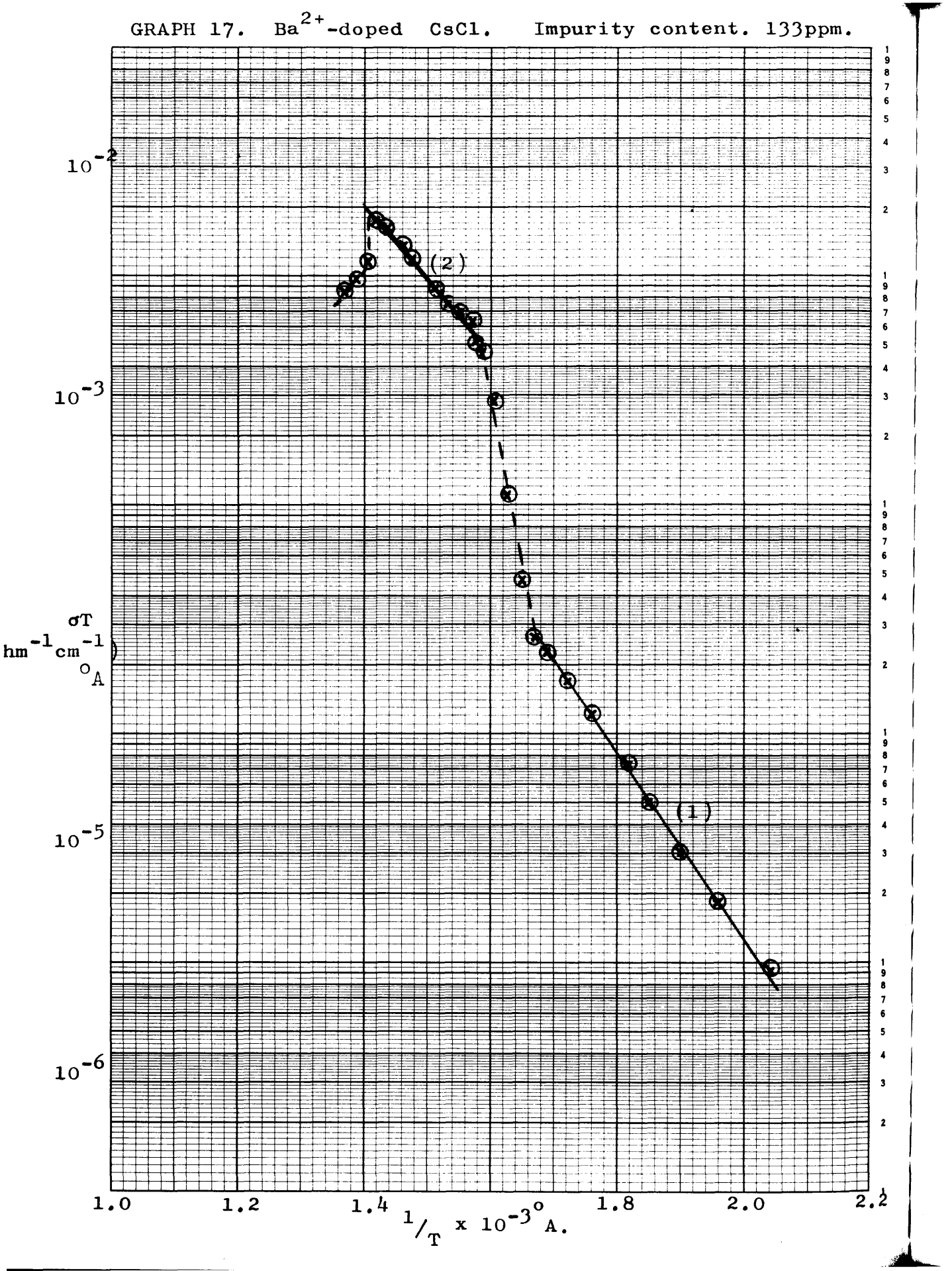

TABLE 17

Graph 17 Ba^{2+} - doped CsCl 133 ppm

Activation energy (ev)	0.82 (1)
Rise temperature range (r.t.u.)	1.66-1.58
Amount of rise	8.0 (times)
Activation energy above rise (ev)	0.64 (2)
Temperature at which transition starts (^{o}C)	432^{o}
σT at start of transition ($ohm^{-1}cm^{-1}$) ^{o}A.	1.76×10^{-2}

Graph 18. Ba^{2+}-doped CsCl. Impurity content ppm.

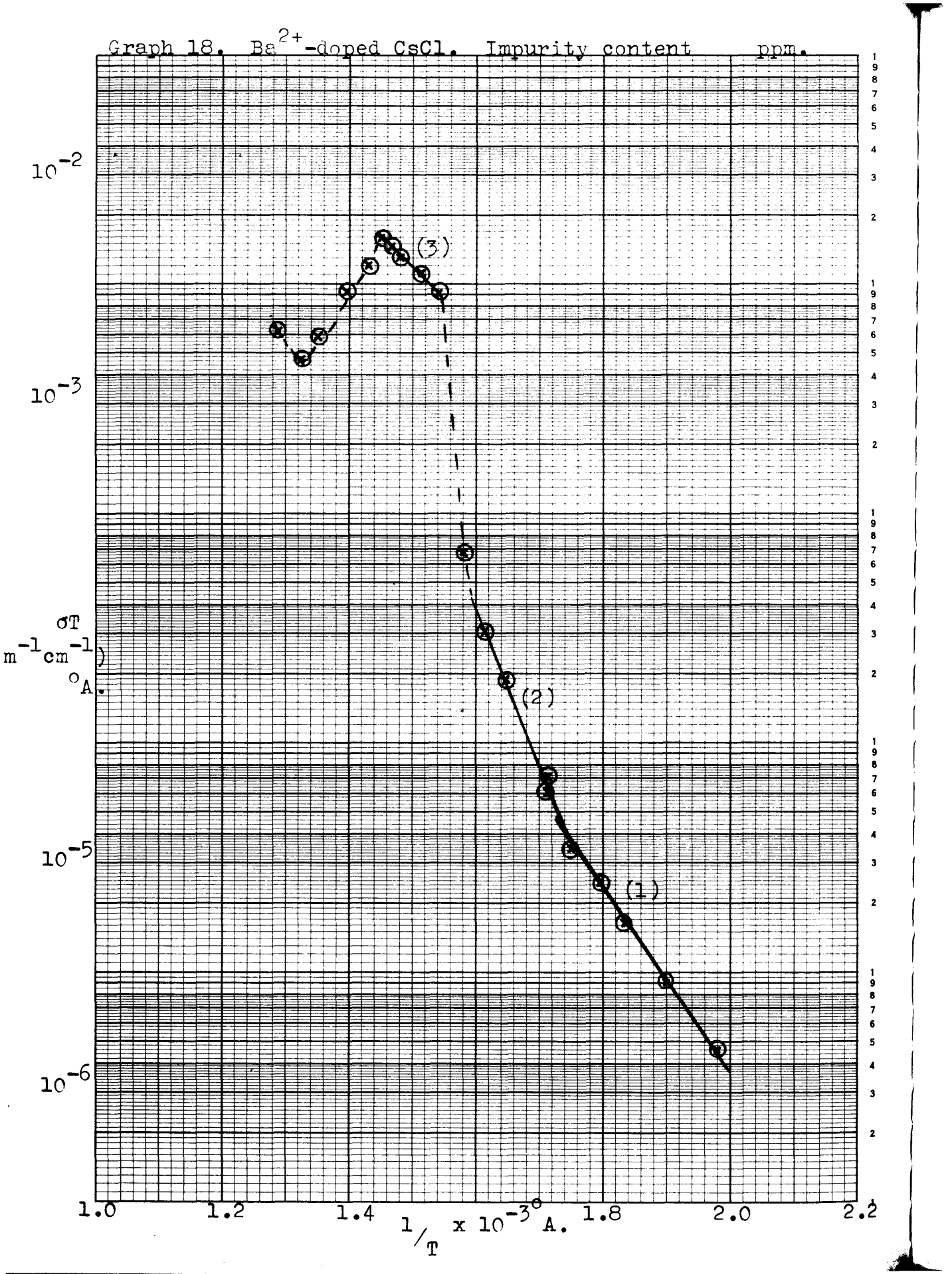

TABLE 18

Graph 18 Ba^{2+}-doped CsCl

Activation energy below knee (ev)	$0.81^{(1)}$
Knee (r.t.u.)	1.73
Activation energy above knee (ev)	$1.39^{(2)}$
Rise temperature range (r.t.u.)	1.60 - 1.54
Amount of rise	11.4 (times)
Activation energy above rise (ev)	$0.60^{(3)}$
Temperature at which transition starts (^{o}C)	418^{o}
σT at start of transition ($ohm^{-1}\ cm^{-1}$) ^{o}A.	1.59×10^{-2}
Temperature at which transition is complete (^{o}C)	482^{o}
σT at completion of transition ($ohm^{-1}\ cm^{-1}$) ^{o}A.	4.62×10^{-3}

GRAPH 19. Ba^{2+}-doped CsCl. Impurity content 153 ppm.

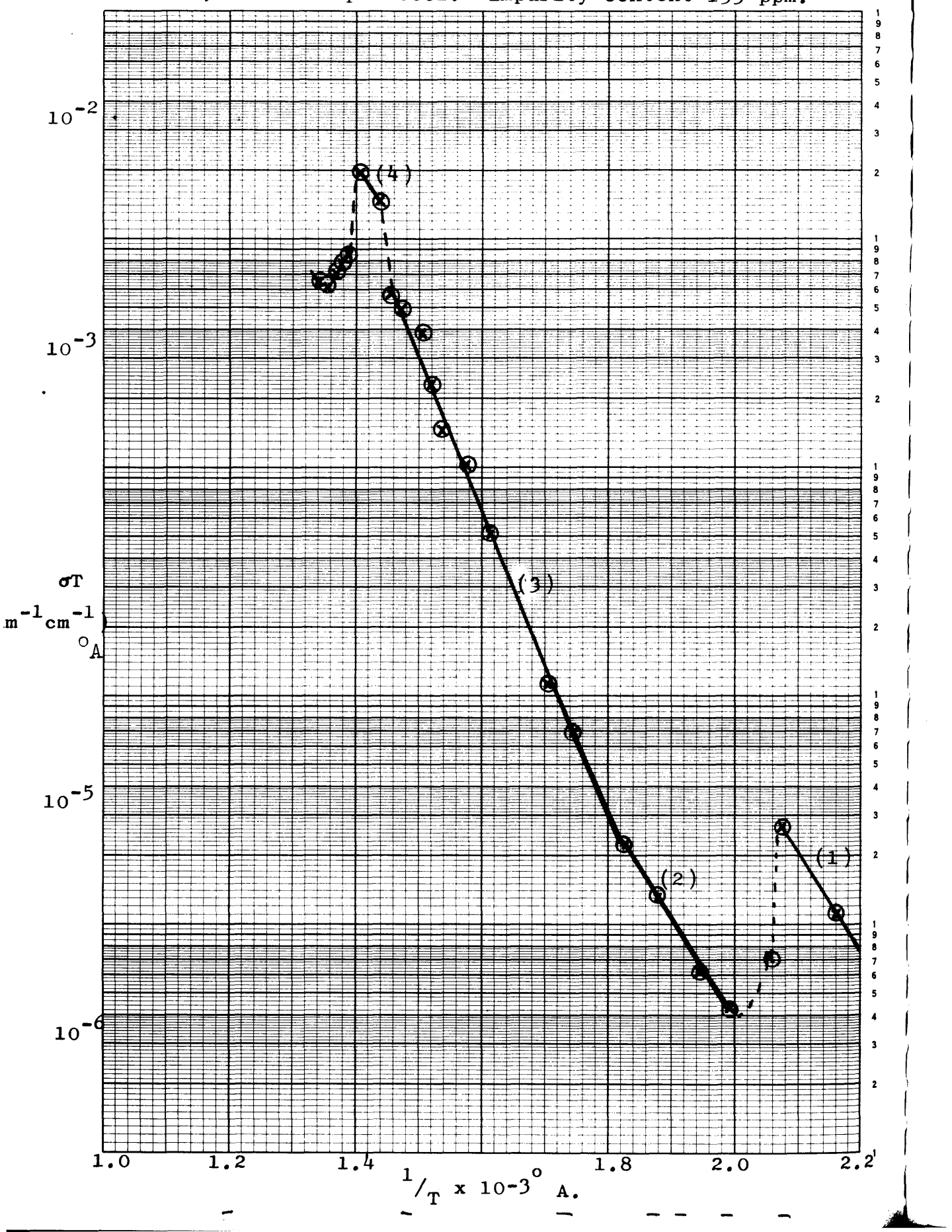

TABLE 19

Graph 19 Ba^{2+} - doped CsCl 153 ppm

Activation energy below knee (ev)	0.85 (1)
Conductivity drops 7 times between 2.08 and 2.00 r.t.u.	
Activation energy below knee (ev)	0.88 (2)
Knee (r.t.u.)	1.82
Activation energy above Knee (e.v.)	1.35
Rise temperature range (r.t.u.)	1.46-1.44
Amount of rise	2.0 (times)
Activation energy above rise (ev)	0.74 (4)
Temperature at which transition starts (^{o}C)	439^{o}
σT at start of transition $(ohm^{-1} cm^{-1})^{o}$ A.	1.96×10^{-2}
Temperature at which transition is complete (^{o}C)	464^{o}
σT at completion of transition $(ohm^{-1} cm^{-1})^{o}$ A.	6.12×10^{-3}

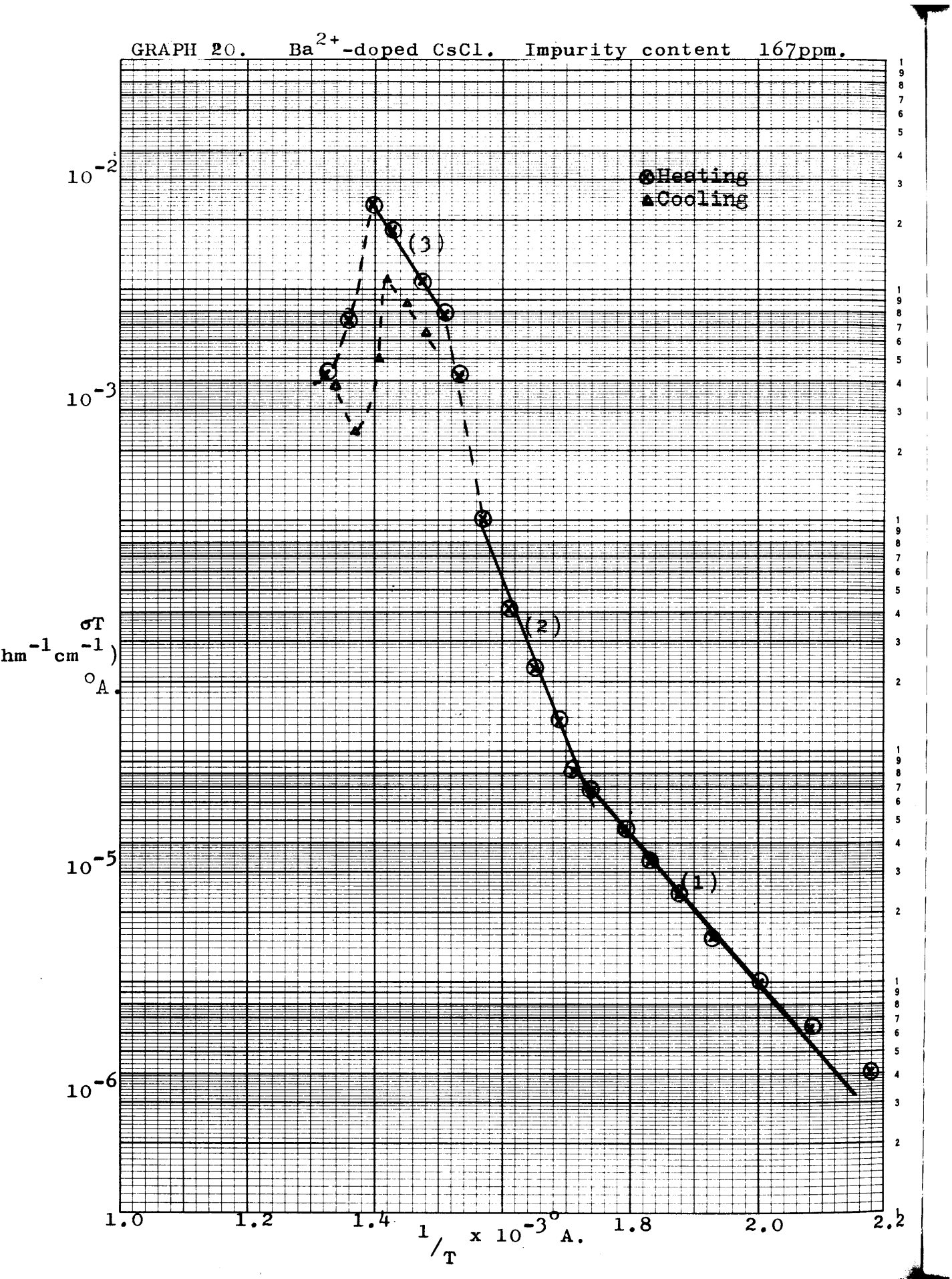
GRAPH 20. Ba2+-doped CsCl. Impurity content 167ppm.
Heating
Cooling
(1)
(2)
(3)
10-2
10-3
10-5
10-6
σT (ohm-1cm-1) °A.
1.0
1.2
1.4
1.8
2.0
2.2
1/T x 10-3 °A.

TABLE 20

Graph 20. Ba^{2+} -doped CsCl. 167 ppm from Cs^{137} diffusion No.8.

	Heating	Cooling
Activation energy below knee (ev)	0.65 (1)	---
Knee (r.t.u.)	1.73	---
Activation energy above knee (ev)	1.33 (2)	---
Rise temperature range (r.t.u.)	1.57-1.51	---
Amount of rise	4.7 (times)	---
Activation energy above rise (ev)	0.88	---
Temperature at which transition starts (^{o}C)	443^{o}	457^{o}
σT at start of transition (ohm^{-1} cm^{-1} ^{o}A.)	2.30×10^{-2}	2.38×10^{-3}
Temperature at which transition is complete (^{o}C)	483^{o}	431^{o}
σT at completion of transition (ohm^{-1} cm^{-1} ^{o}A.)	4.23×10^{-3}	1.09×10^{-2}

GRAPH 21. Ba^{2+}-doped CsCl. Impurity content 196 ppm.

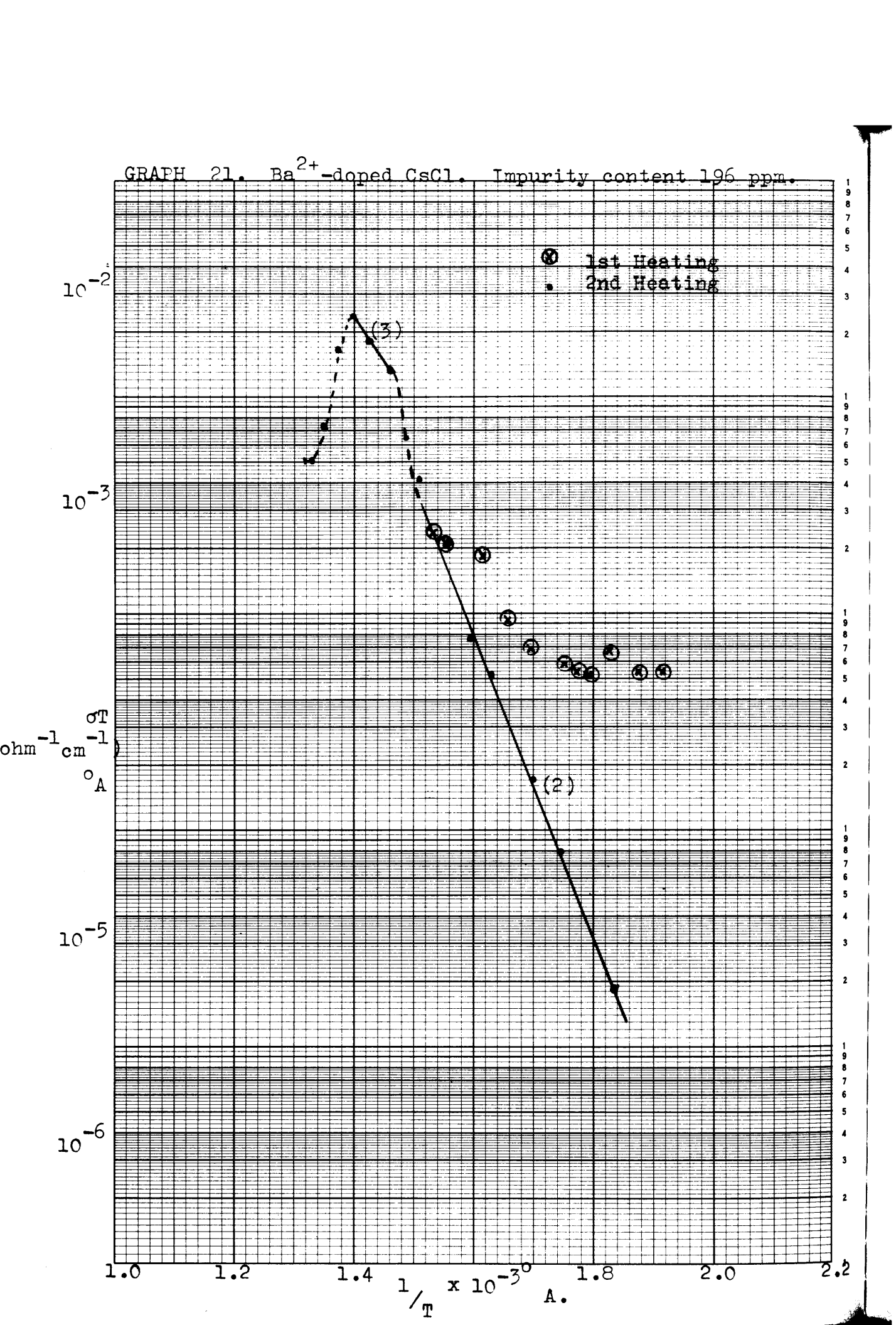

TABLE 21

Graph 21 Ba^{2+}-doped CsCl. 196 ppm

	1st heating	2nd heating
Activation energy (ev)	low activation energy up to 1.54 (r.t.u.)	1.40 (2)
Rise temperature range (r.t.u.)		1.52-1.46
Amount of rise		2.0 (times)
Activation energy above rise (ev)		0.84 (3)
Temperature at which transition starts (^{o}C)		442^{o}
σT at start of transition (ohm^{-1} cm^{-1} ^{o}A.		2.38×10^{-2}
Temperature at which transition is complete (^{o}C)		479^{o}
σT at completion of transition (ohm^{-1} cm^{-1} ^{o}A.		5.00×10^{-3}

GRAPH 22. Ba^{2+}-doped CsCl. Impurity content 234 ppm.

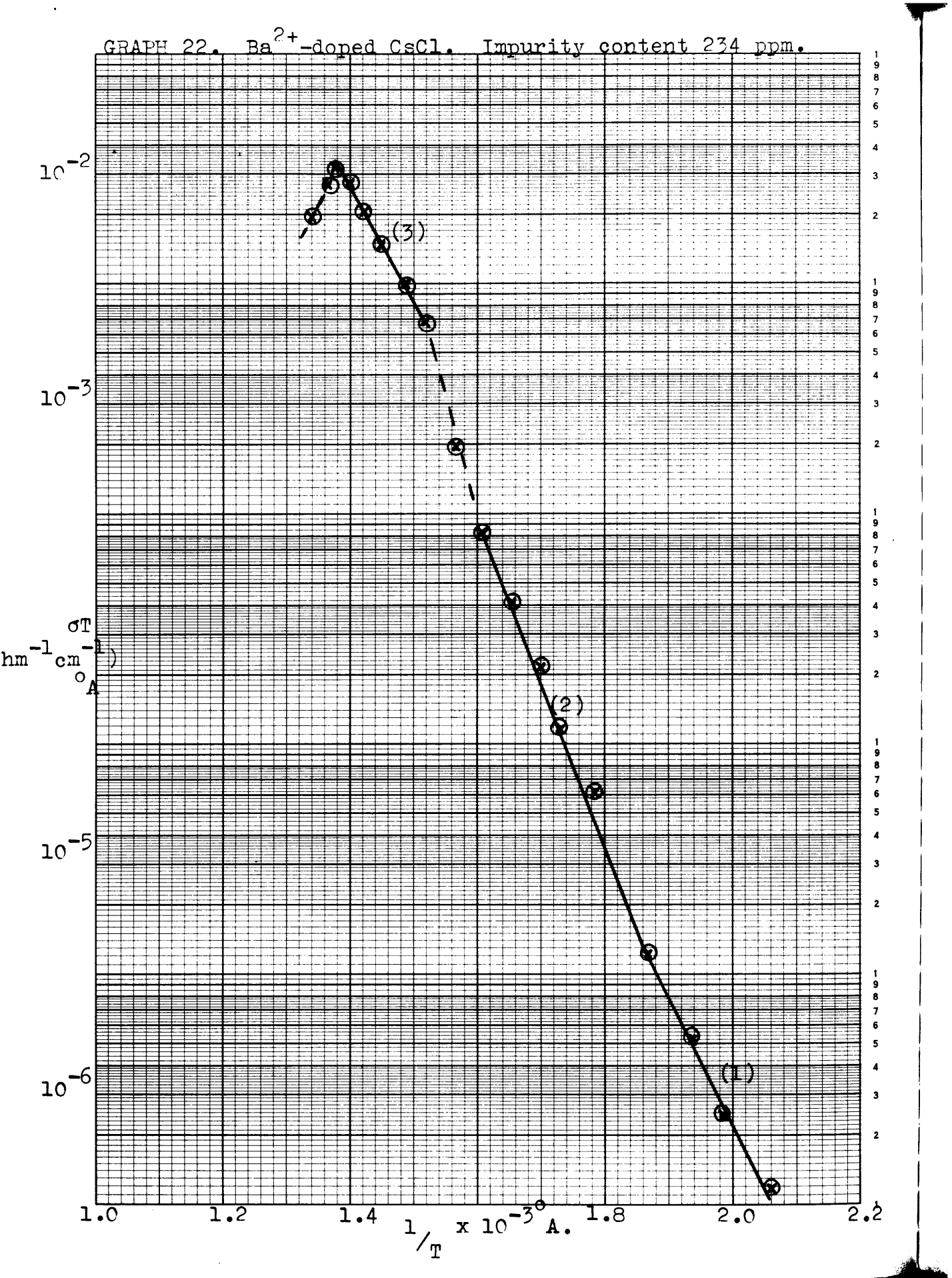

TABLE 22

Graph 22. Ba^{2+}-doped CsCl. 234 ppm.

Activation energy	1.12 (1)
Knee (r.t.u.)	1.87
Activation energy above knee (ev)	1.39 (2)
Rise temperature range (r.t.u.)	1.59-1.52
Amount of rise	3 (times)
Activation energy above rise (ev)	1.00 ev
Temperature at which transition starts (^{o}C)	450^{o}
σT at start of transition ($ohm^{-1}\ cm^{-1}$)^{o}A.	3.16×10^{-2}

GRAPH 23. Ba^{2+}-doped CsCl. Impurity Content 260 ppm.

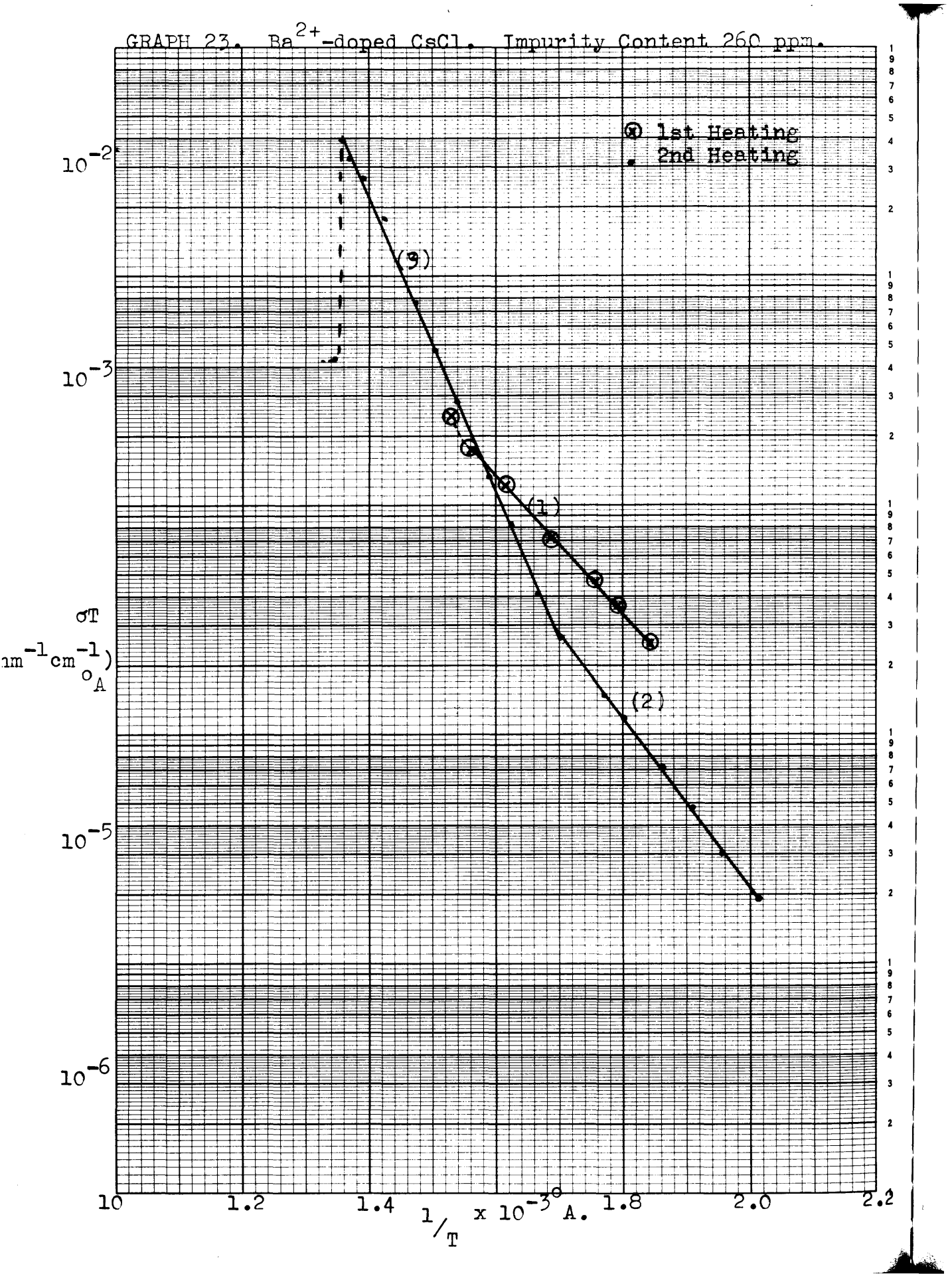

TABLE 23

Graph 23 Ba^{2+} - doped CsCl. 260 ppm

From Cs^{137} Diffusion No. 3.

	1st heating	2nd heating
Activation energy below knee (ev)	0.60 (1)	0.76 (2)
Knee (r.t.u.)	1.58	1.70
Activation energy above knee (ev)	1.50	1.29 (3)
Temperature at which transition starts (^{o}C)	---	463^{o}
σT at start of transition (ohm^{-1} cm^{-1} ^{o}A)	---	3.97×10^{-2}
Temperature at which transition is complete (^{o}C)	---	471^{o}
σT at completion of transition (ohm^{-1} cm^{-1} ^{o}A.		4.34×10^{-2}

GRAPH 24. Ba^{2+}-doped CsCl. Impurity Content 280ppm.

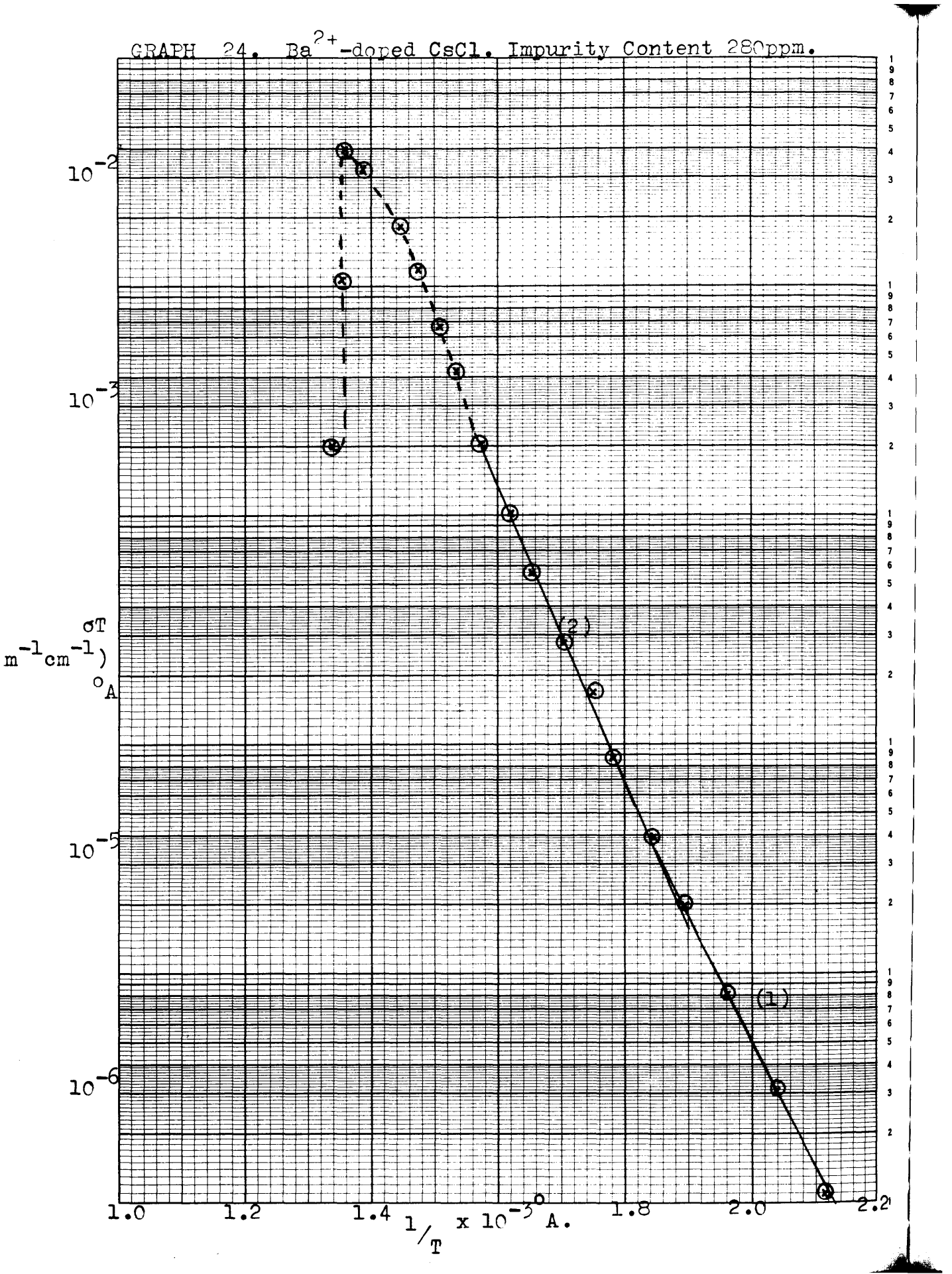

TABLE 24

Graph 24. Ba^{2+} -doped CsCl. 280 ppm Cs^{137} -diffusion No. 7

Activation energy below knee (ev)	1.08 (1)
Knee (r.t.u.)	1.86
Activation energy above knee (ev)	1.30 (2)
Higher temperature region curved	
temperature at which transition starts (^{o}C)	465 ^{o}
σT at start of transition ($ohm^{-1}\ cm^{-1}\ ^{o}$) A.	3.95×10^{-2}
Temperature at which transition complete (^{o}C)	475 ^{o}
σT at completion of transition ($ohm^{-1}\ cm^{-1}\ ^{o}$) A.	1.99×10^{-3}

GRAPH 25. Ba^{2+}-doped CsCl. Impurity content 1000ppm.
(estimated using radioactive SO_4^{2-} sulphur-35.)

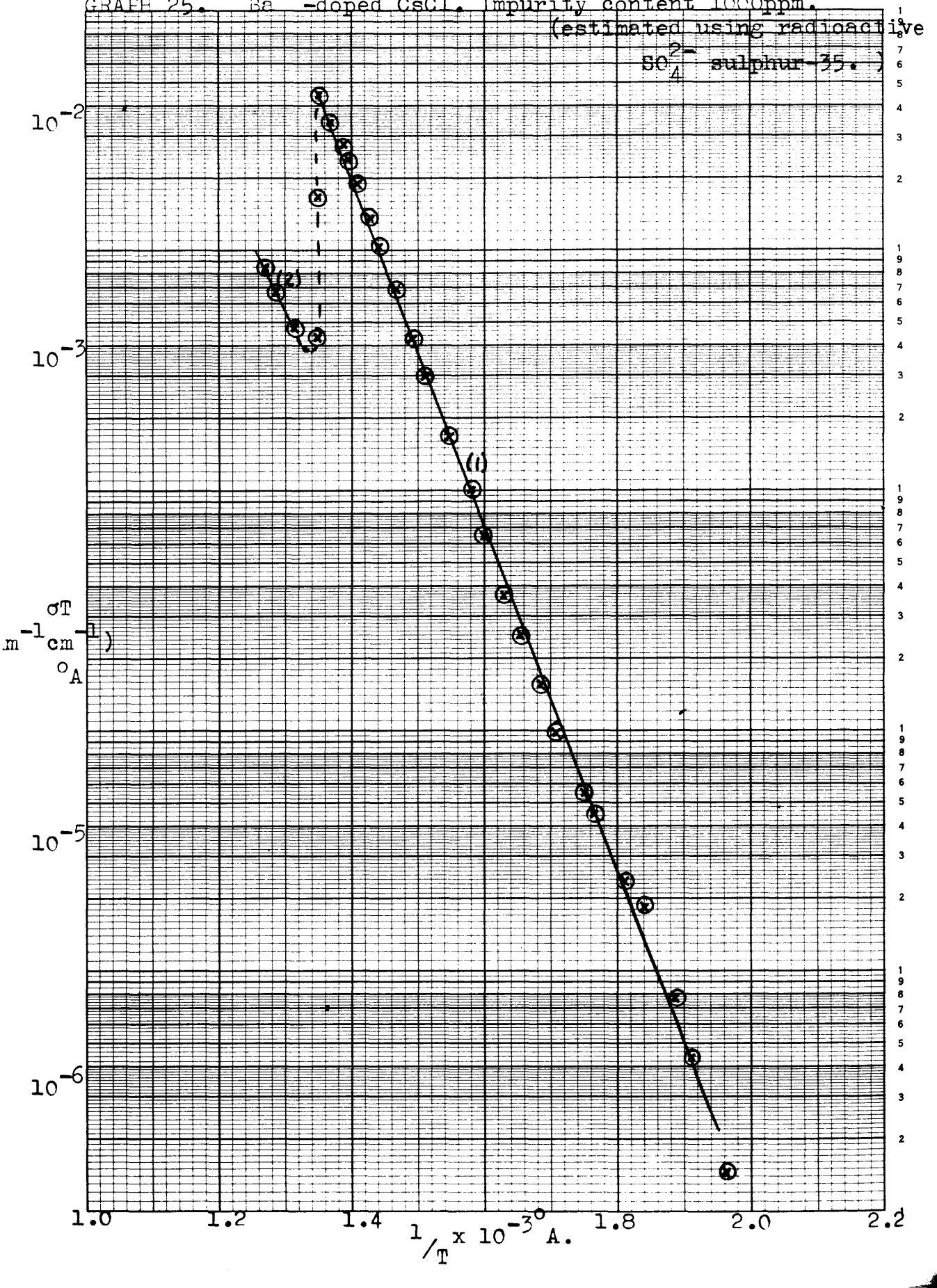

TABLE 25

Graph 25. Ba^{2+}-doped CsCl. 1000 ppm (estimated using $S^{35}O_4^{2-}$)

Activation energy (ev)	1.43 (1)
Temperature at which transition starts (^{o}C)	466 ^{o}
σT at start of transition ($ohm^{-1}\ cm^{-1}$) $^{o}A.$	4.40×10^{-2}
Temperature at which transition is complete (^{o}C)	472 ^{o}
σT at completion of transition ($ohm^{-1}\ cm^{-1}$) $^{o}A.$	4.38×10^{-3}
Activation energy after the transition (ev)	1.13 (2)

GRAPH 26. Ba^{2+}-doped CsCl. Impurity content less than 5ppm.

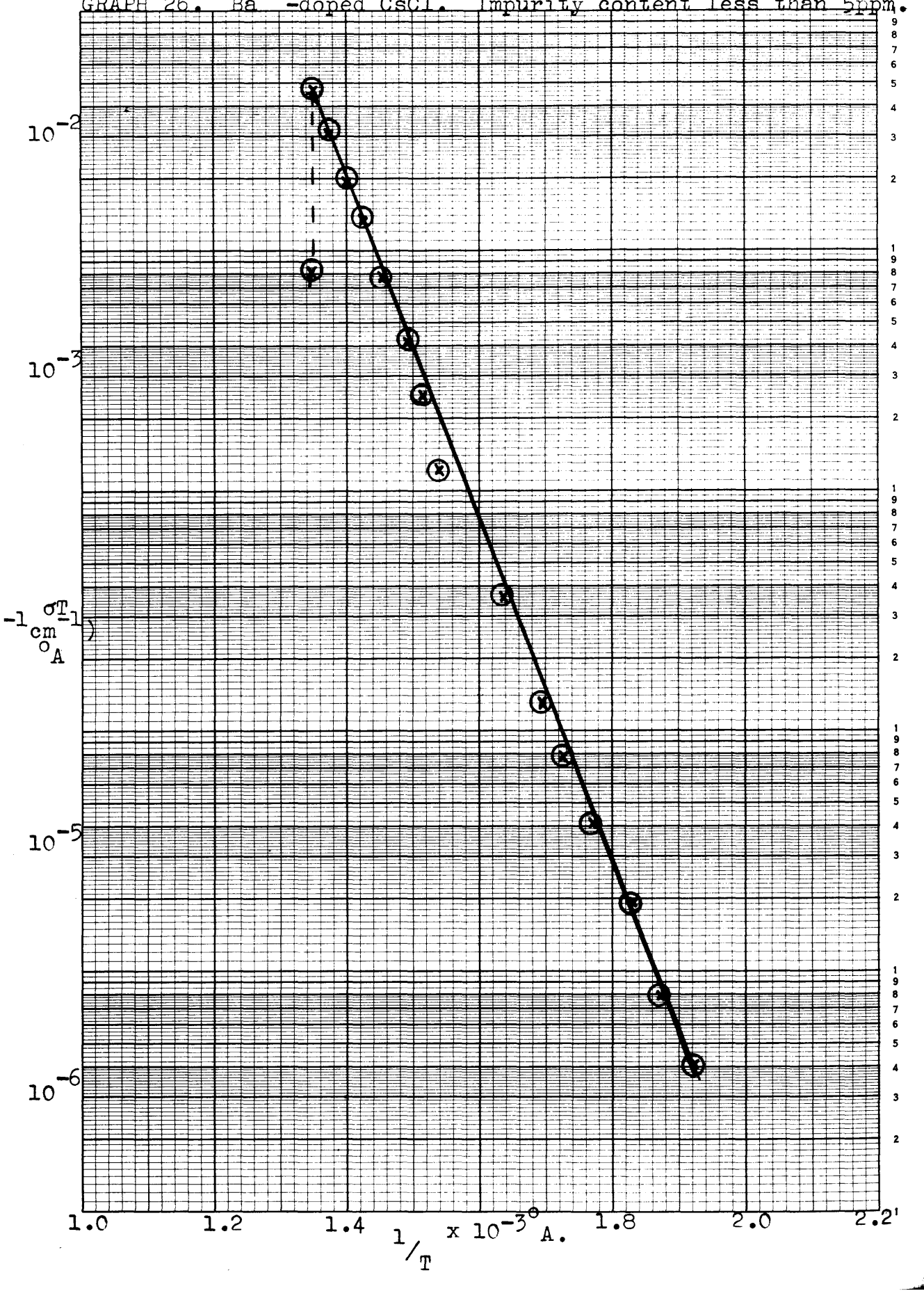

TABLE 26

Graph 26 Ba^{2+}-doped CsCl less than 5 ppm
From Cs^{137} diffusion No.10

Activation energy (ev)	1.41
Temperature at which transition starts (^{o}C)	467^{o}
σT at start of transition ($ohm^{-1}\ cm^{-1}\ ^{o}A.$)	4.66×10^{-2}

GRAPH 27. Ba^{2+}-doped CsCl. Impurity content undetectable.

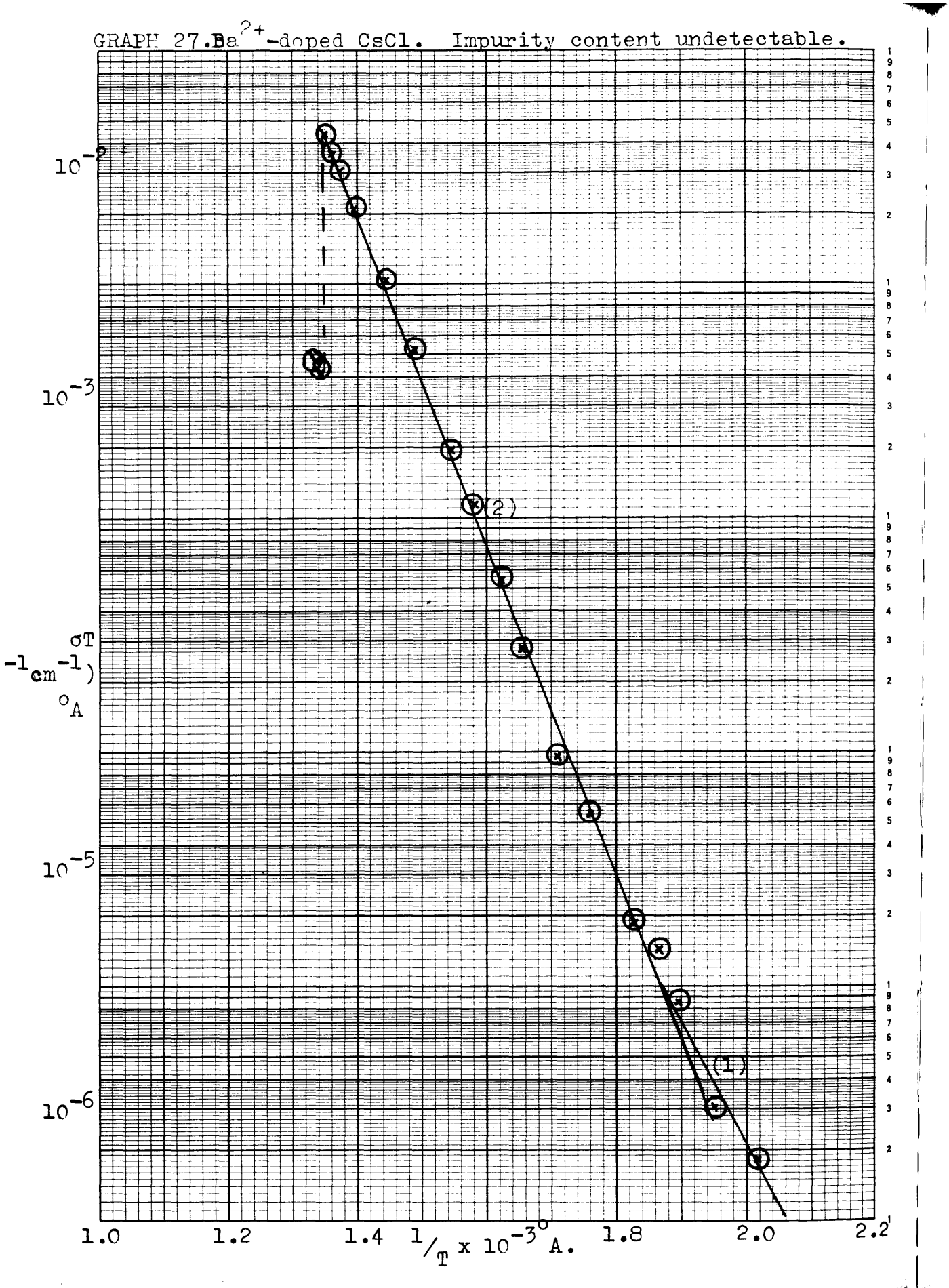

TABLE 27

Graph 27 Ba^{2+}-doped CsCl, No Ba^{2+} detected from Cs^{137} diffusion No. 7

Activation energy below knee (ev)	1.02 (1)
Knee (r.t.u.)	1.87
Activation energy above knee (ev)	1.39 (2)
Temperature at which transition starts ^{o}C	468^{o}
σT at start of transition (ohm^{-1} cm^{-1}) ^{o}A.	4.44×10^{-2}
Temperature at which transition is complete ^{o}C	471^{o}
σT at completion of transition (ohm^{-1} cm^{-1}) ^{o}A.	4.16×10^{-3}

GRAPH. 28 Sr^{2+}-doped CsCl. Impurity content less than 5ppm.

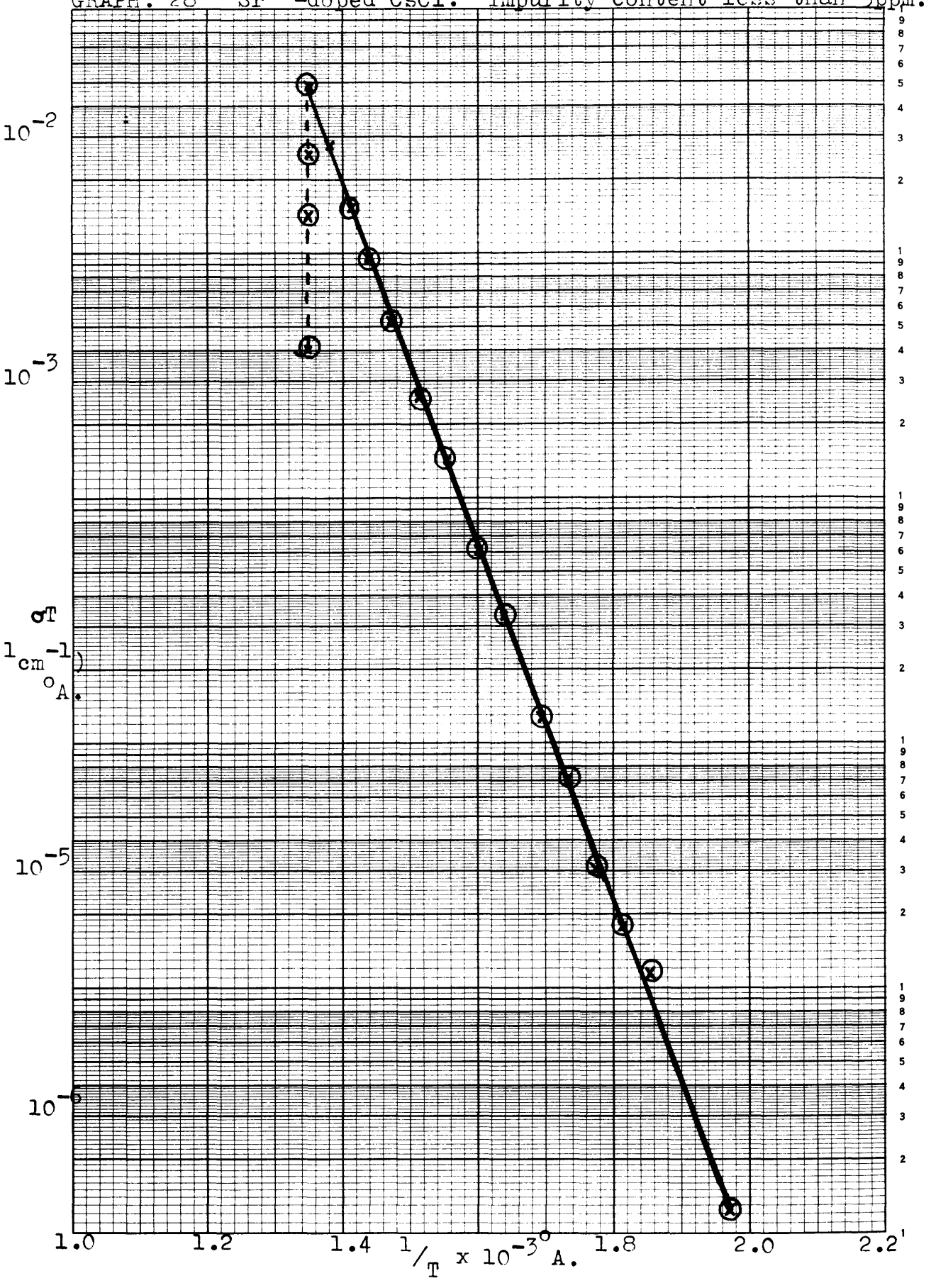

TABLE 28

Graph 28 Sr^{2+} -doped CsCl Less than 5 ppm from Cs^{137} diffusion No. 4.

Activation energy (ev)	1.45
Temperature at which transition starts ^{o}C	468^{o}
σT at start of transition $(ohm^{-1}\ cm^{-1})^{o}A.$	4.84×10^{-2}
Temperature at which transition is complete ^{o}C	469^{o}
σT at completion of transition $(ohm^{-1}\ cm^{-1})^{o}A.$	4.00×10^{-3}

GRAPH 29. Ca^{2+}-doped CsCl. Impurity content 125ppm.

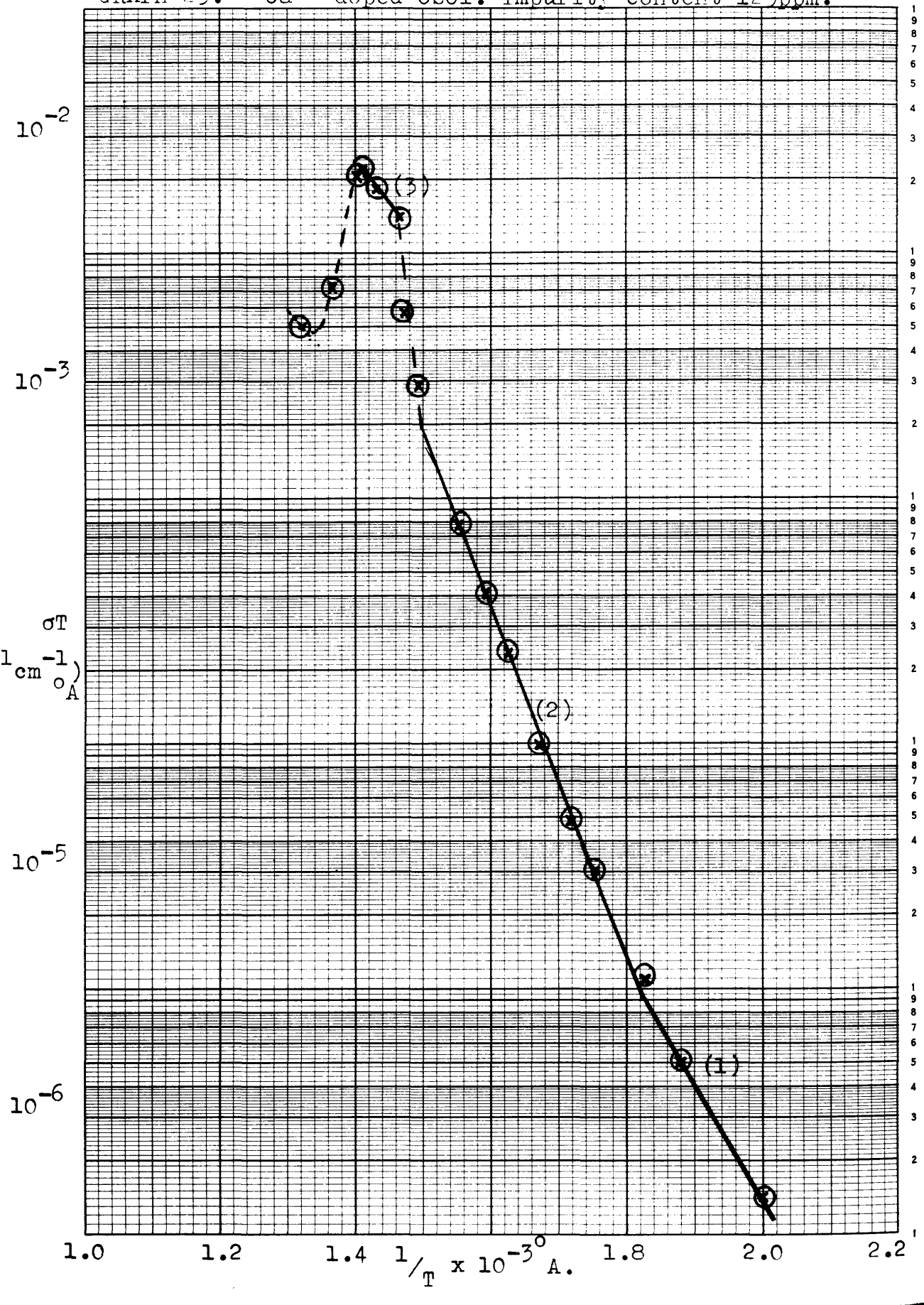

TABLE 29

Graph 29 Ca^{2+} - doped CsCl 125 ppm

from Cs^{137} diffusion No. 5

Activation energy below knee (ev)	0.97 (1)
Knee (r.t.u.)	1.82
Activation energy above knee (ev)	1.42 (2)
Rise temperature range (r.t.u.)	1.49 - 1.47
Amount of rise	5.0 (times)
Activation energy above rise (ev)	0.72 (3)
Temperature at which transition starts ^{o}C	436^{o}
σT at start of transition (ohm $^{-1}$ cm $^{-1}$) ^{o}A.	2.21×10^{-2}
Temperature at which transition is complete ^{o}C	484^{o}
σT at completion of transition (ohm $^{-1}$ cm $^{-1}$) ^{o}A.	5.00×10^{-3}

GRAPH 30. SO_4^{2-}-doped CsCl. Impurity content 83 ppm.

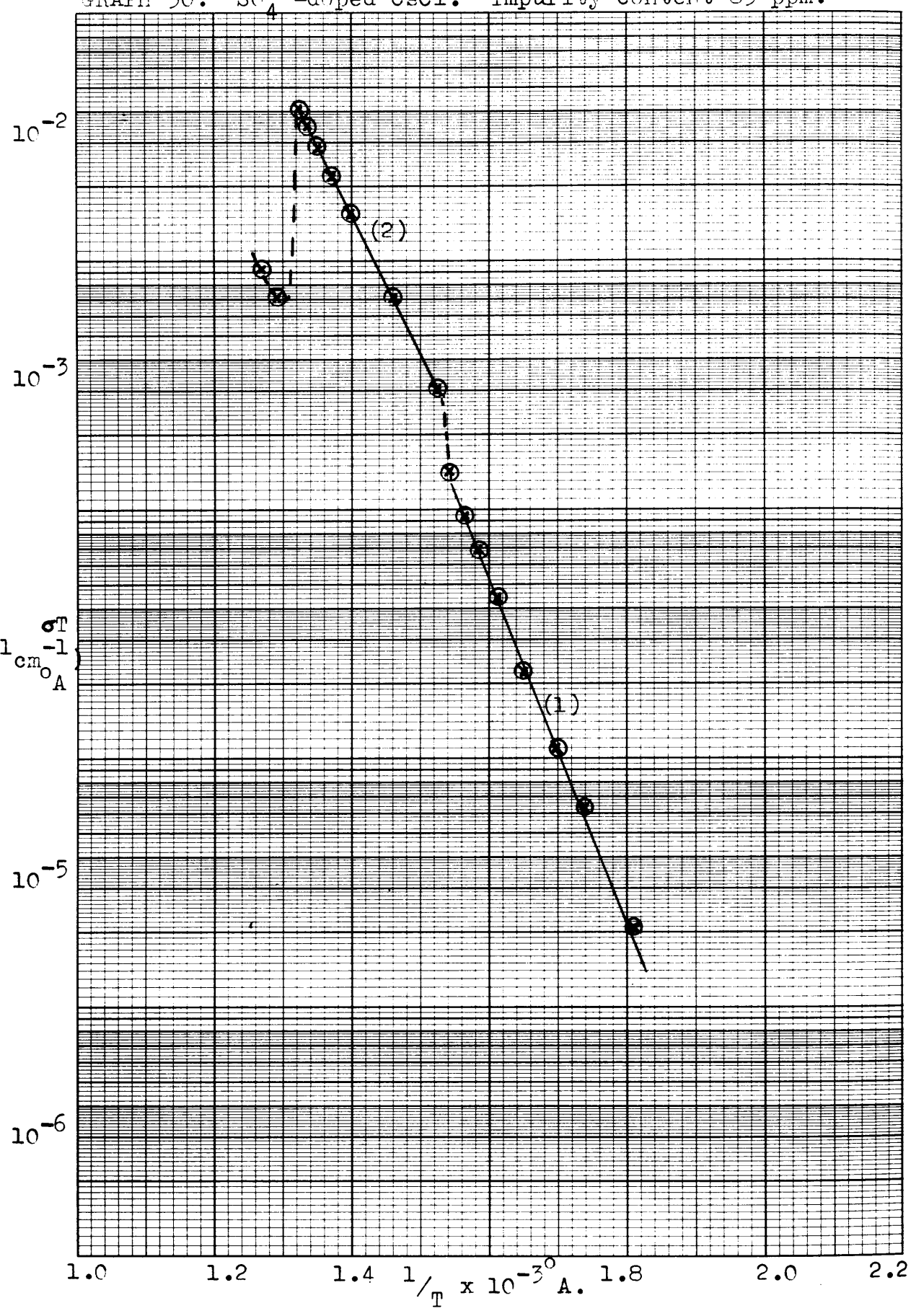

TABLE 30

Graph 30 SO_4^{2-}-doped CsCl 83 ppm

Activation energy (ev)	1.40ev (1)
Rise temperature range (r.t.u.)	1.54 - 1.52
Amount of rise	1.8 (times)
Activation energy above rise (ev)	1.09 (2)
Temperature at which transition starts (^{o}C)	484^{o}
σT at start of transition (ohm^{-1} cm^{-1} ^{o}A.	4.03×10^{-2}
Temperature at which transition is complete (^{o}C)	502
σT at completion of transition (ohm^{-1} cm^{-1} ^{o}A.	7.02×10^{-3}

Graph 31. SO_4^{2-}-doped CsCl. Impurity content 100 ppm.

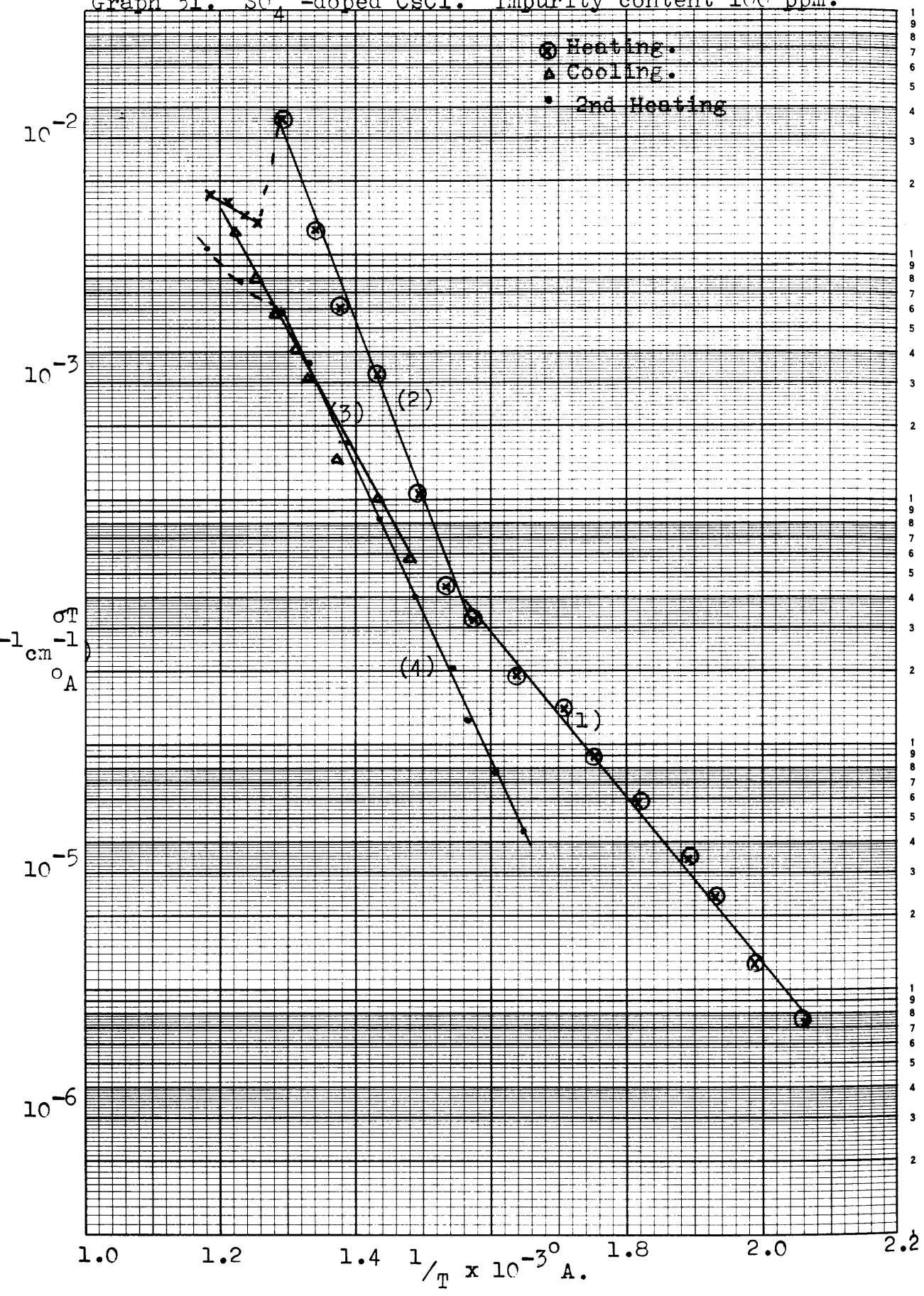

TABLE 31

Graph 31 SO_4^{2-}-doped CsCl 100 ppm

	1st heating	cooling	2nd heating
Activation energy below knee (ev)	0.66 (1)	---	---
Knee (r.t.u.)	1.56	---	---
Activation energy above knee (ev)	1.43 (2)	1.00 (3)	1.19 (4)
Temperature at which transition starts ^{o}C	502 ^{o}	No reverse transition	no transition
σT at start of transition $(ohm^{-1} cm^{-1})\ ^{o}A.$	3.56×10^{-2}	---	---
Temperature at which transition is complete ^{o}C	523 ^{o}	---	---
σT at completion of transition $(ohm^{-1}cm^{-1})\ ^{o}A.$	1.36×10^{-2}	---	---

GRAPH 32. SO_4^{2-}-doped CsCl. Impurity content 120 ppm.

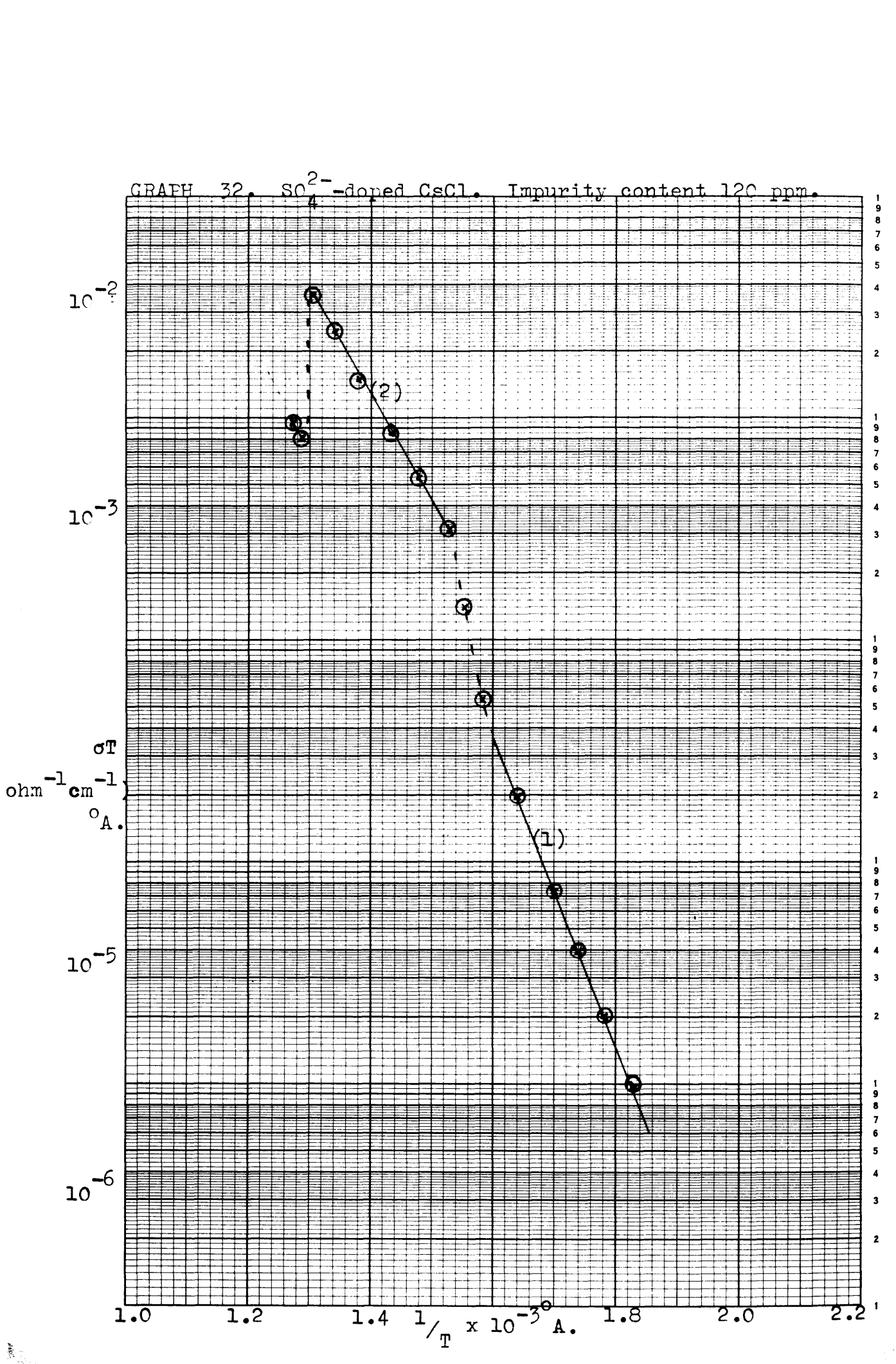

TABLE 32

Graph 32 SO_4^{2-}-doped CsCl 120 ppm

Activation energy (ev)	$1.39^{(1)}$
Rise temperature range (r.t.u.)	1.60 - 1.53
Amount of rise	4.0 (times)
Activation energy above rise (ev)	$0.96^{(2)}$
Temperature at which transition starts ^{o}C	492^{o}
σT at start of transition $(ohm^{-1}\ cm^{-1})^{o}$ A.	3.51×10^{-2}
Temperature at which transition is complete	504^{o}
σT at completion of transition $(ohm^{-1}\ cm^{-1})^{o}$ A.	8.00×10^{-3}

GRAPH 33. SO_4^{2-}-doped CsCl. Impurity content 137 ppm.

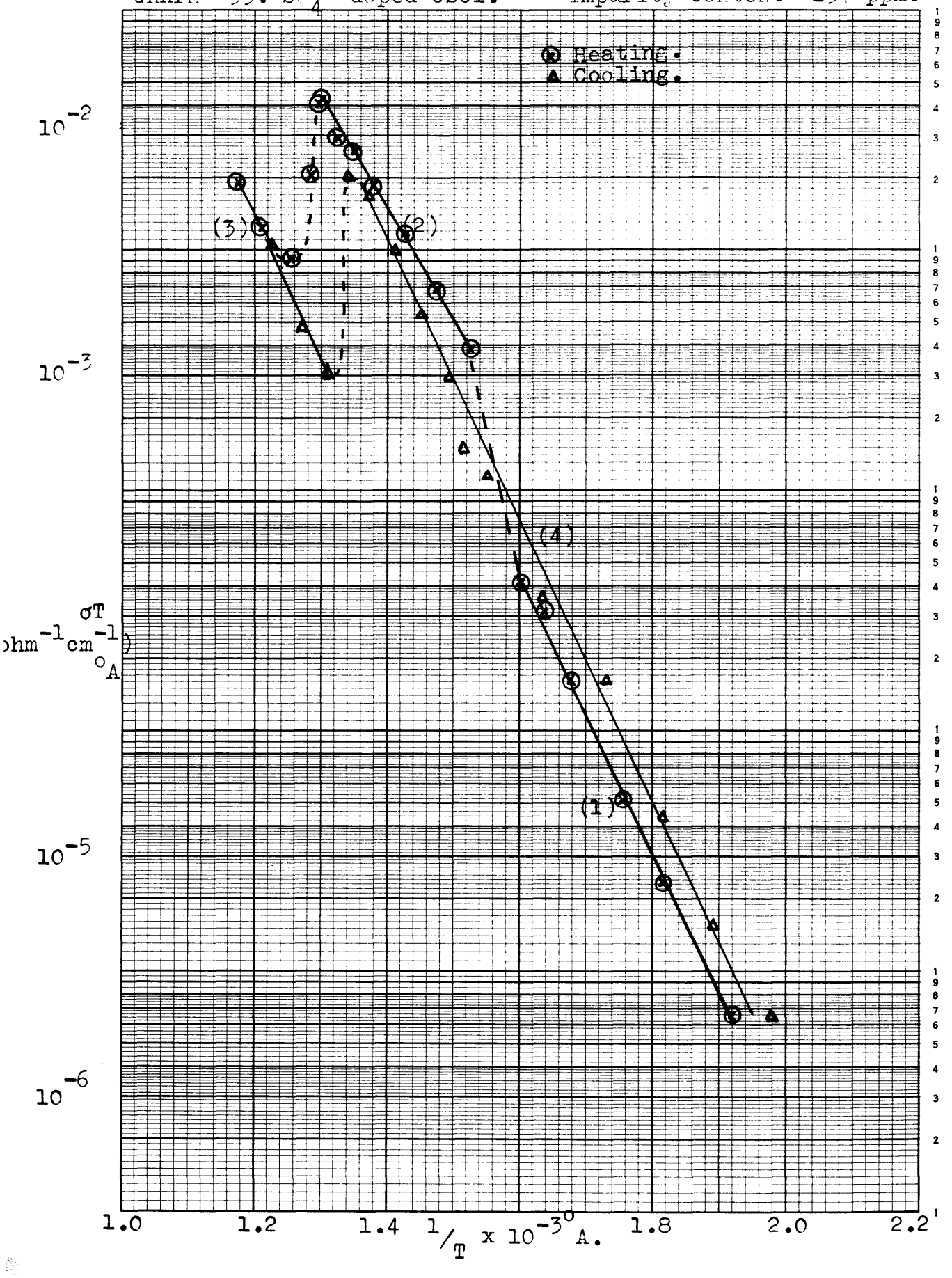

TABLE 33

Graph 33 SO_4^{2-}-doped CsCl 157 ppm

	Heating	Cooling
Activation energy (ev)	1.15 (1)	1.18 (4)
Rise temperature range (r.t.u.)	1.60-1.52	---
Amount of rise	3.6 (times)	---
Activation energy above rise	0.92 (2)	---
Temperature at which transition starts ^{o}C	^{o} 495	^{o} 491
σT at start of transition ($ohm^{-1}\ cm^{-1}\ ^{o}A.$)	4.32×10^{-2}	3.19×10^{-3}
Temperature at which transition is complete ^{o}C	^{o} 528	^{o} 473
σT at completion of transition ($Ohm^{-1}\ cm^{-1}\ ^{o}A.$)	9.29×10^{-3}	2.10×10^{-2}
Activation energy after transition (ev)	1.15 (3)	

GRAPH 34. SO_4^{2-}-doped CsCl. Impurity content 150 ppm.

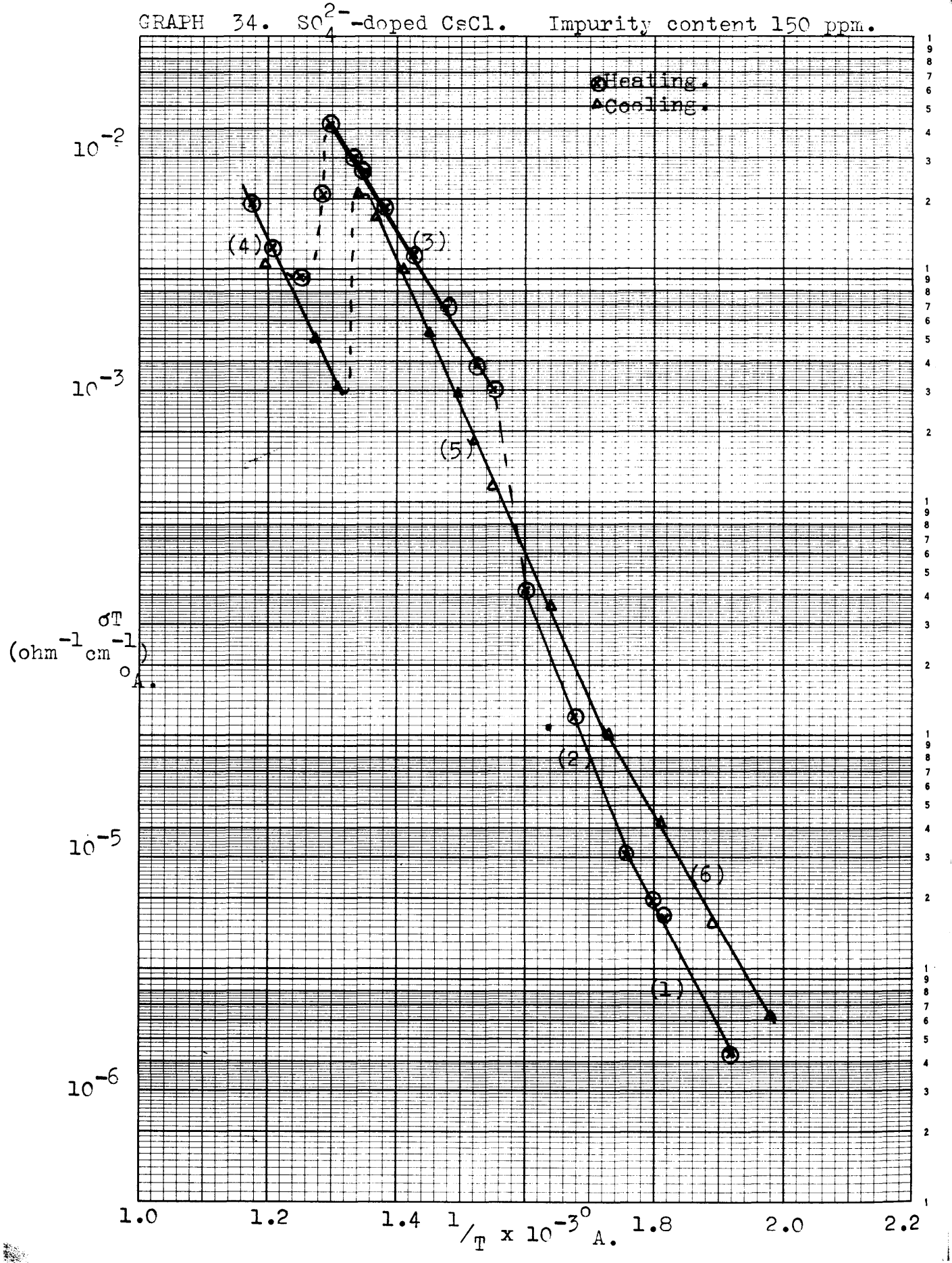

TABLE 34

Graph 34 SO_4^{2-}-doped CsCl 150 ppm

	Heating	Cooling
Activation energy below knee (ev)	1.03 (1)	0.95 (6)
Knee (r.t.u.)	1.76	1.73
Activation energy above knee (ev)	1.38 (2)	1.26 (5)
Rise temperature range (r.t.u.)	1.60-1.55	---
Amount of rise	3.8 (times)	---
Activation energy above rise (ev)	0.87 (3)	---
Temperature at which transition starts ^{o}C	^{o} 498	^{o} 491
σT at start of transition (ohm^{-1} cm^{-1} ^{o}A.	4.16×10^{-2}	3.18×10^{-3}
Temperature at which transition is complete ^{o}C	^{o} 527	^{o} 473
σT at completion of transition (ohm^{-1} cm^{-1} ^{o}A.	9.04×10^{-3}	2.10×10^{-2}
Activation energy after transition.	1.14 (4)	---

GRAPH 35. SO_4^{2-}-doped CsCl. Impurity content. 212ppm.

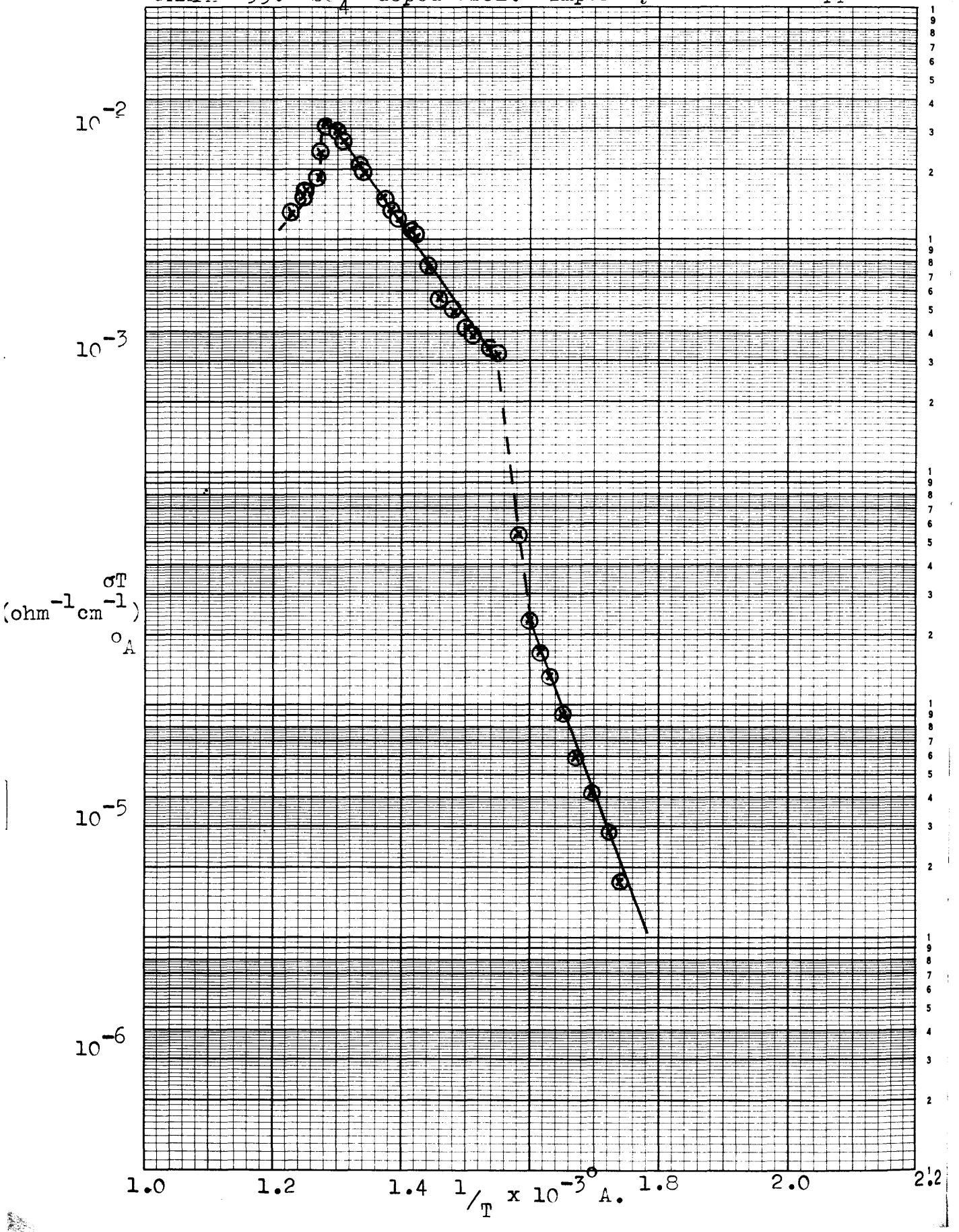

TABLE 35

Graph 35 SO_4^{2-}-doped CsCl 212 ppm

Activation energy (ev)	1.44 (1)
Rise temperature range (r.t.u.)	1.60-1.54
Amount of rise	6.3 (times)
Activation energy above rise (ev)	0.78 (2)
Temperature at which transition starts ^{o}C	508^{o}
σT at start of transition ($ohm^{-1}\ cm^{-1}\ ^{o}A.$)	3.12×10^{-2}
Temperature at which transition is complete ^{o}C	546
σT at completion of transition ($ohm^{-1}\ cm^{-1}\ ^{o}A.$)	1.28×10^{-2}

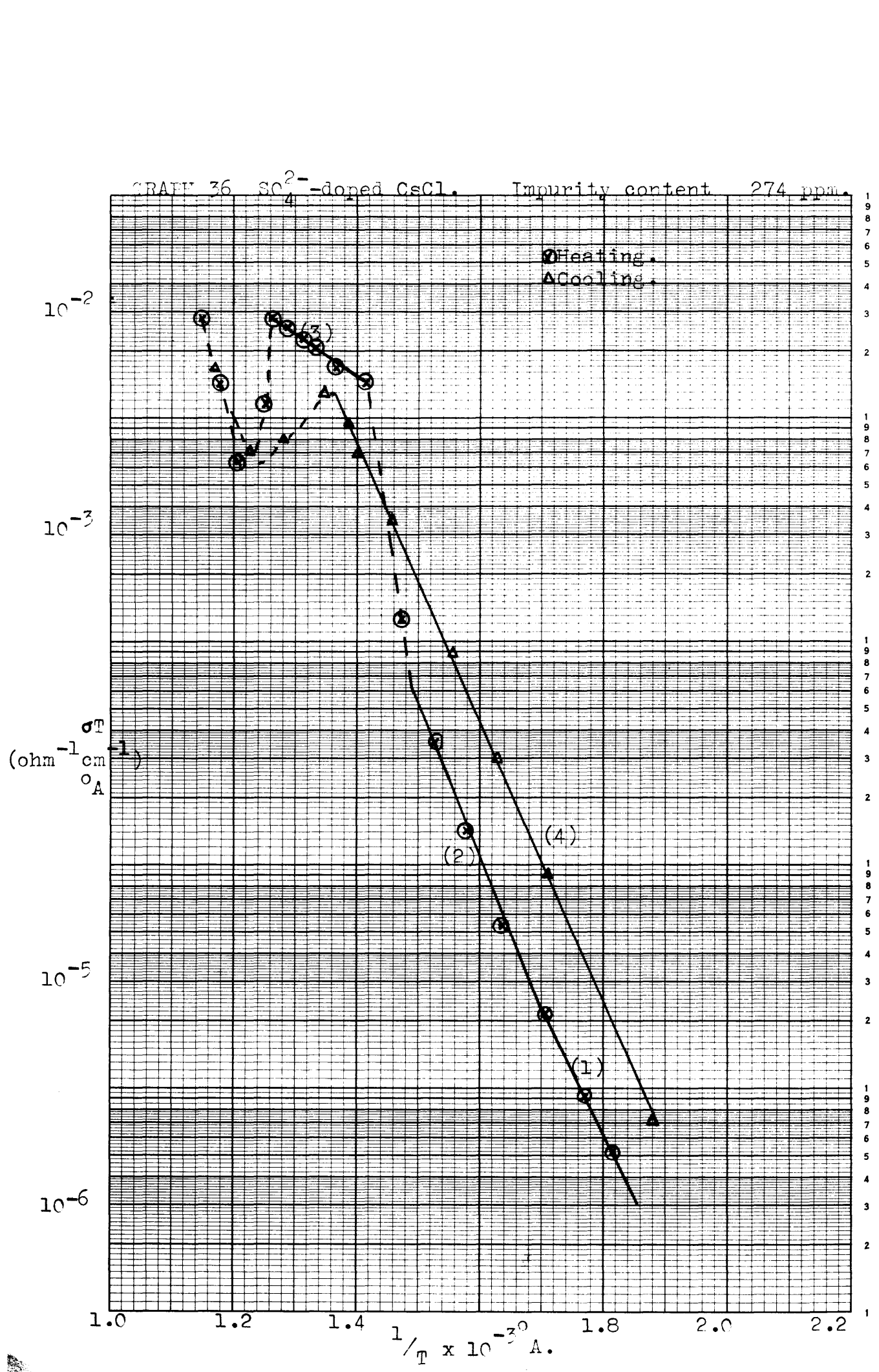
GRAPH 36 SO_4^{2-}-doped CsCl. Impurity content 274 ppm.
Heating.
Cooling.
(1)
(2)
(3)
(4)
10^{-2}
10^{-3}
10^{-5}
10^{-6}
σT (ohm^{-1}cm^{-1}) ^{o}A
1.0
1.2
1.4
1.8
2.0
2.2
$1/T \times 10^{-3}$ A.

TABLE 36

Graph 36 SO_4^{2-}-doped CsCl 274 ppm

	Heating	Cooling
Activation energy below knee (ev)	1.13 (1)	---
Knee (r.t.u.)	1.71	---
Activation energy above knee (ev)	1.40 (2)	1.25 (4)
Rise temperature range (r.t.u.)	1.49-1.42	---
Amount of rise	10 (times)	---
Activation energy above rise (ev)	0.40 (3)	---
Temperature at which transition starts °C	526°	543°
σT at start of transition (ohm^{-1} cm^{-1}) °A.	2.81×10^{-2}	7.14×10^{-3}
Temperature at which transition is complete (°C)	554°	470°
σT at completion of transition (ohm^{-1} cm^{-1}) °A.	6.29×10^{-3}	1.30×10^{-2}

GRAPH 37. SO_4^{2-}-doped CsCl. Impurity content 437 ppm.

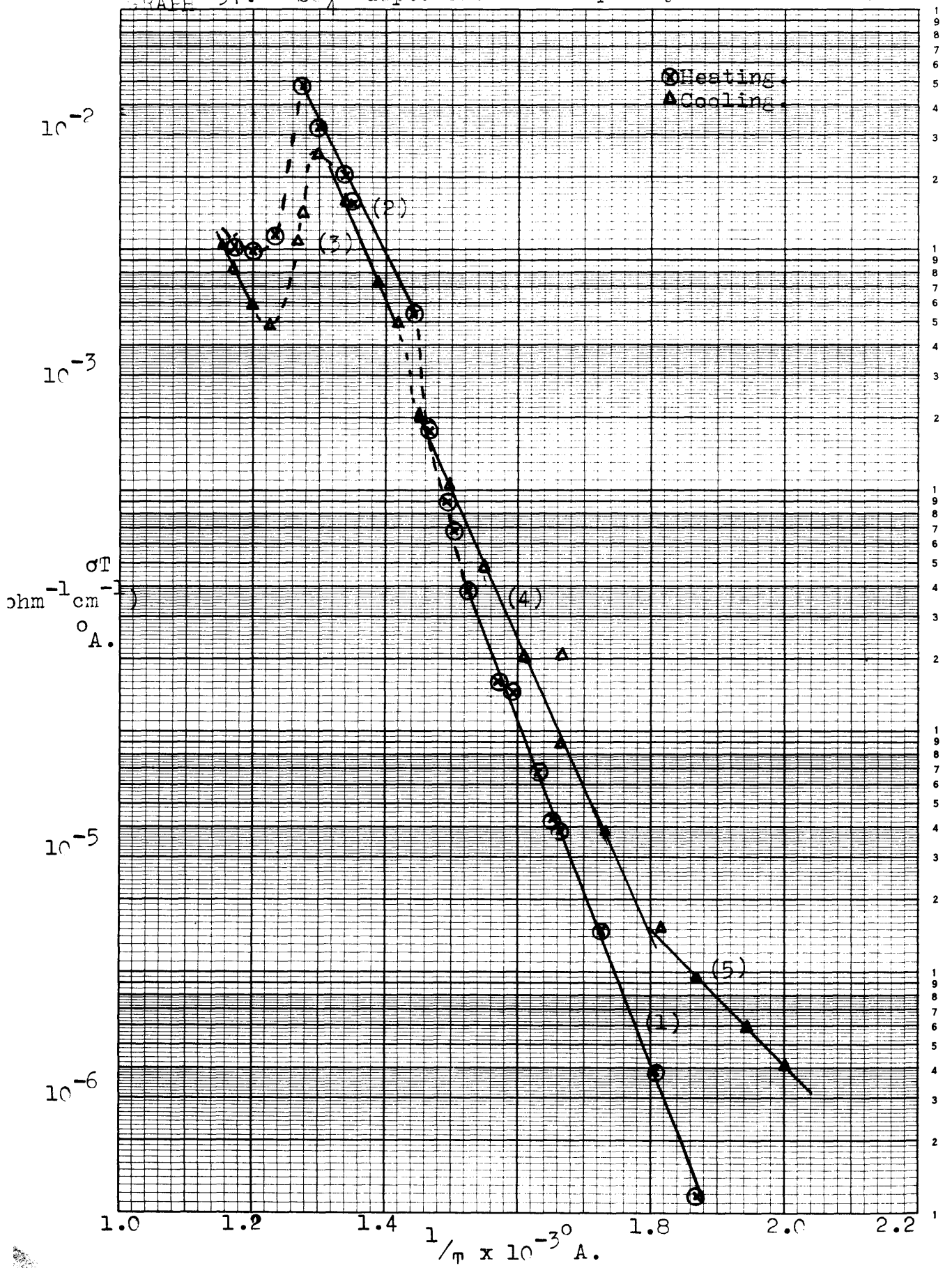

TABLE 37

Graph 37 SO_4^{2-}-doped CsCl 437 ppm

	Heating	Cooling
Activation energy below knee (ev)	---	0.57 (5)
Knee (r.t.u.)	---	1.80
Activation energy above knee (ev)	1.37 (1)	1.25 (4)
Rise temperature range (r.t.u.)	1.62-1.54	1.53-1.55
Amount of rise	4.0(times)	1.6 (times)
Activation energy above rise (ev)	1.10 (2)	1.25 (3)
Temperature at which transition starts (^{o}C)	510^{o}	551^{o}
σT at start of transition (ohm^{-1} cm^{-1} ^{o}) A.	4.70×10^{-2}	4.78×10^{-3}
Temperature at which transition is complete (^{o}C)	560^{o}	498^{o}
σT at completion of transition (ohm^{-1} cm^{-1} ^{o}) A.	1.00×10^{-2}	2.46×10^{-2}

GRAPH 38. KCl-CsCl 'mixed' crystal.

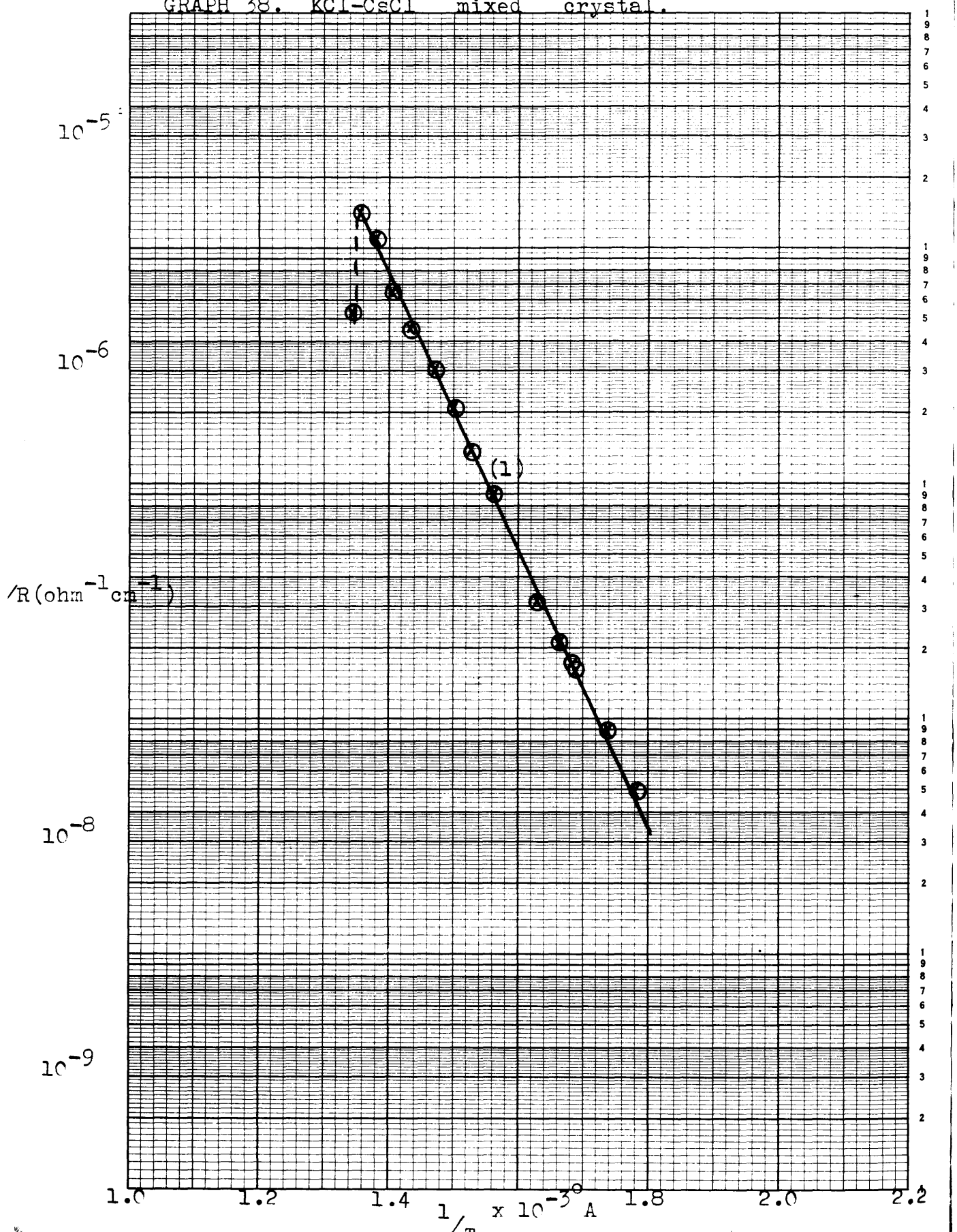

TABLE 38

KCl-CsCl mixed crystal from Graph 38.

Activation energy (eV)	1.19
Temperature at which transition starts (^{o}C)	467^{o}
1/R at start of transition ($ohm^{-1}cm^{-1}$)	1.33×10^{-5}
Temperature at which transition is complete (^{o}C)	473^{o}

GRAPH 39. CsI-CsCl 'mixed' crystal

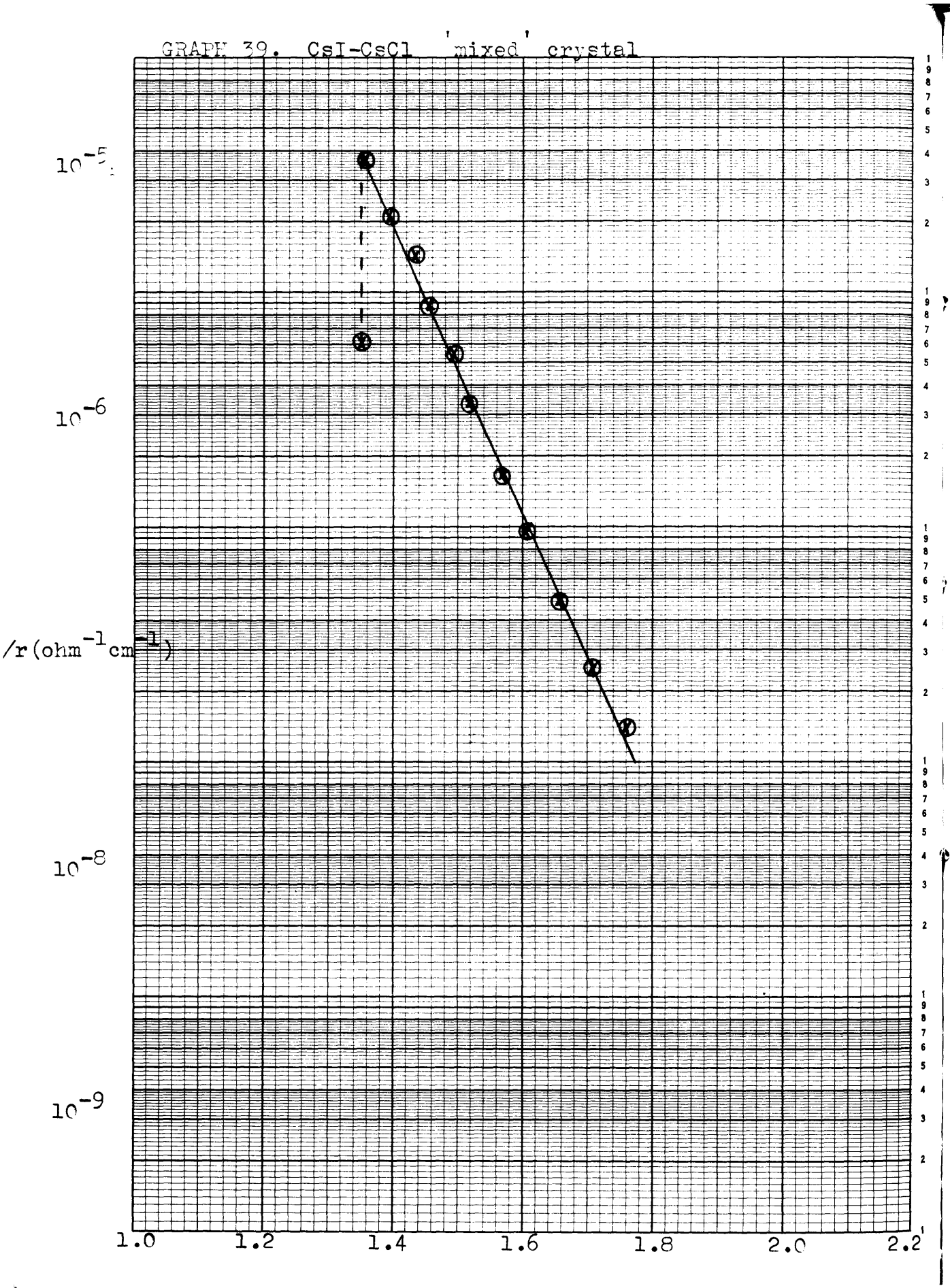

TABLE 39

CsI-CsCl mixed crystal from Graph 39.

Activation energy (eV)	1.24
Temperature at which transition starts (^{o}C)	466^{o}
1/R at start of transition ($ohm^{-1}cm^{-1}$)	3.62×10^{-5}
Temperature at which transition is complete (^{o}C)	469^{o}
1/R at completion of transition ($ohm^{-1}cm^{-1}$)	6.00×10^{-6}

RESULTS

CHAPTER 8

DIFFUSION

8.1 Introduction.

The diffusion equation,

$$D = D_o \exp(-E/kT) \qquad \ldots.(28)$$

where

D = diffusion coefficient (cm^2/sec)

D_o = diffusion coefficient of an ideal crystal

and E,k,T have same significance as in 7.1 ,

is such that a graph of log D as a function of reciprocal temperature is a straight line of slope equal to (E) the activation energy for diffusion.

8.2 Method of Presentation.

In this section we have included graphs of log D as a function of reciprocal temperature for Cl-36 and Cs-137 diffusion in 'pure' and impurity-doped single crystals of caesium chloride. We have also included those tables of results from which the graphs have been compiled. The individual counting measurements for each crystal are listed in Appendix B for Cl-36 diffusion and in Appendix C for Cs-137 diffusion.

The graphs included in this section are as follows:-

Graph 40	Cl-36 diffusion in 'pure' single crystals of caesium chloride.
Graph 41	Cl-36 diffusion in Ba^{2+}-doped single crystals of caesium chloride.

Graph 42 Cl-36 diffusion in SO_4^{2-}-doped single crystals of caesium chloride.

Graph 43 Cs-137 diffusion in 'pure' single crystals of caesium chloride.

Graph 44 Cs-137 diffusion in aliovalent impurity-doped single crystals of caesium chloride.

Graph 45 Comparison of measured and calculated diffusion coefficients.

8.3 The results

GRAPH 40. Cl^{36}-diffusion in 'pure' CsCl.

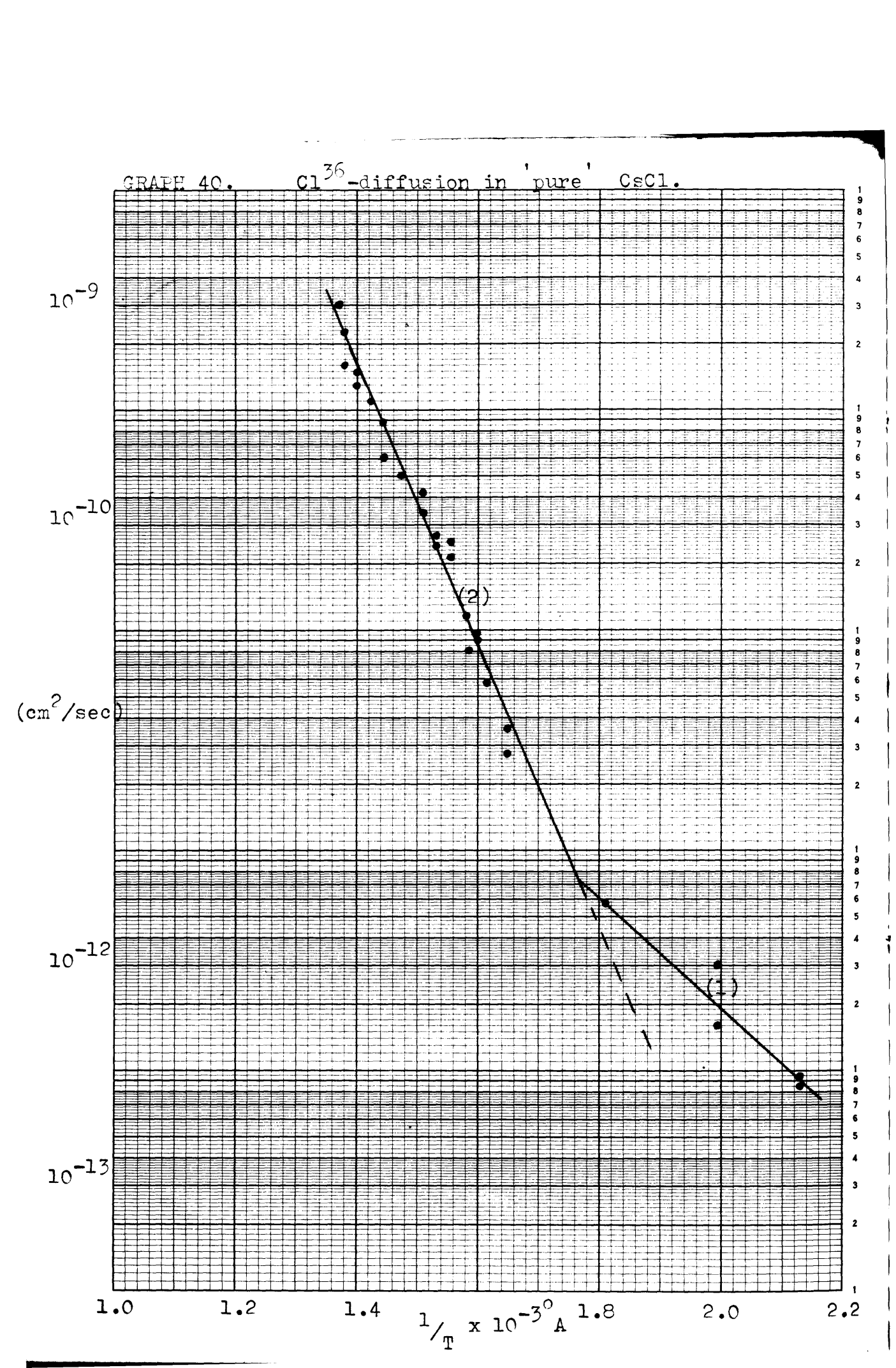

TABLE 40

Graph 40 Cl^{36}-diffusion in 'pure' CsCl

Temp(°C)	1/T x 10^{-3}(°A)	D(cm^2/sec)
195	2.137	8.6×10^{-13}
195	2.137	9.4×10^{-13}
228	1.996	3.0×10^{-12}
228	1.996	1.6×10^{-12}
280	1.808	5.6×10^{-12}
333	1.650	2.8×10^{-11}
333	1.650	3.6×10^{-11}
345	1.618	5.8×10^{-11}
352	1.600	9.2×10^{-11}
352	1.600	9.6×10^{-11}
358	1.585	8.2×10^{-11}
358	1.585	1.2×10^{-10}
358	1.585	1.2×10^{-10}
358	1.585	1.2×10^{-10}
370	1.555	2.2×10^{-10}
370	1.555	2.5×10^{-10}
380	1.531	2.4×10^{-10}
380	1.531	2.7×10^{-10}
388	1.513	3.4×10^{-10}
388	1.513	4.3×10^{-10}
404	1.477	4.9×10^{-10}
404	1.477	5.0×10^{-10}
420	1.443	6.0×10^{-10}
420	1.443	8.8×10^{-10}

TABLE 4C (continued)

Temp (^{o}C)	1/T x 10^{-3} (^{o}A)	D (cm^2/sec)
429	1.425	1.1×10^{-9}
440	1.403	1.3×10^{-9}
440	1.403	1.5×10^{-9}
450	1.383	1.6×10^{-9}
450	1.383	2.3×10^{-9}
456	1.372	3.0×10^{-9}

.o.o.o.o.o.o.o.o.o.o.o.o.o.o.

	Activation Energy (ev)	D_o (cm^2/sec)
Low temperature range below knee.	0.50	1.95×10^{-7}
High temperature range above knee.	1.30	2.1

.o.o.o.o.o.o.o.o.o.o.o.o.o.o.

GRAPH 41. Cl^{36}-diffusion in Ba^{2+}-doped CsCl

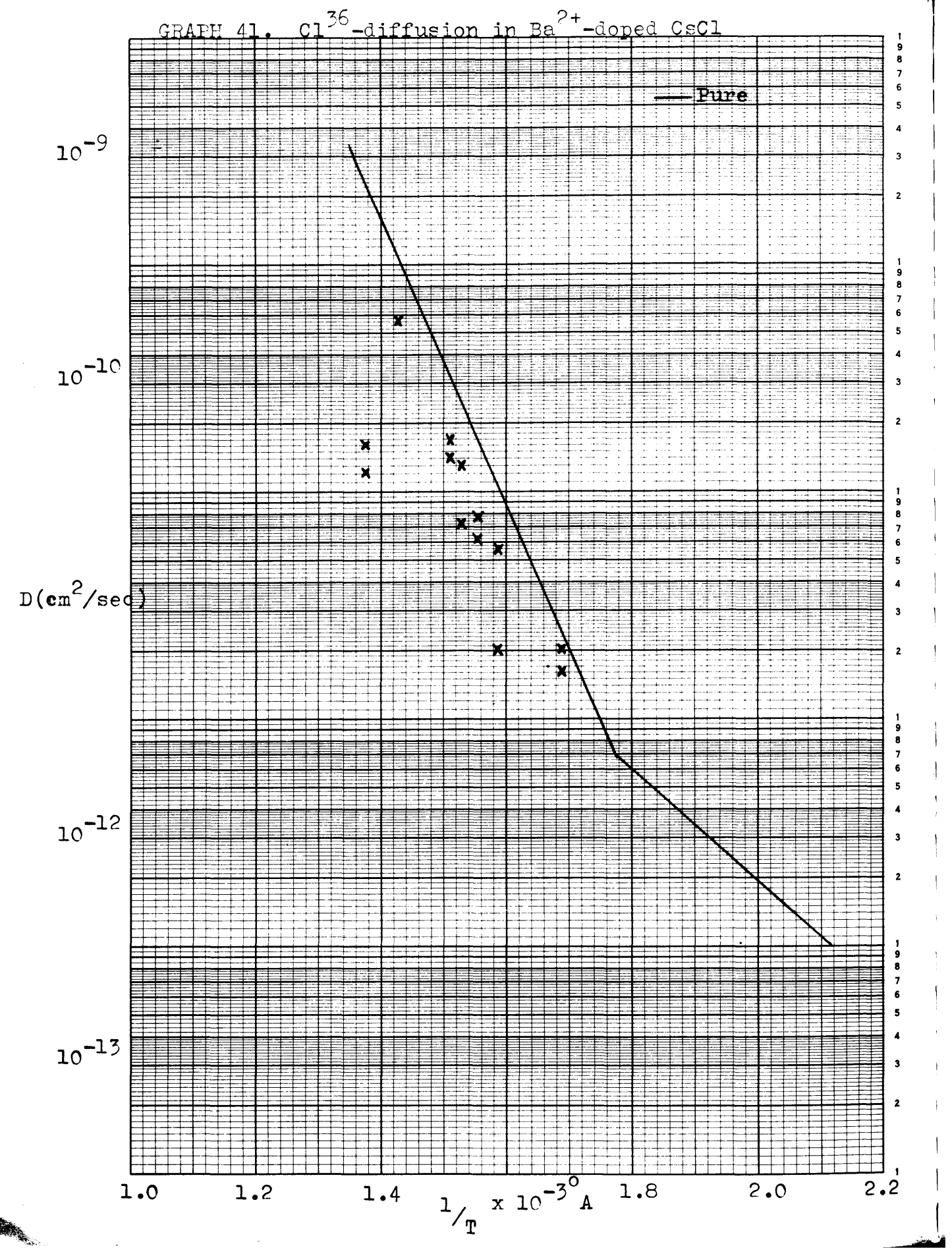

TABLE 41

Cl^{36}-diffusion in Ba^{2+}-doped CsCl from Graph 41

Impurity content (ppm)	Temp (^{o}C)	$Y/T \times 10^{-3}$ ^{o}A	$D(cm^2/sec)$
211	320	1.686	1.6×10^{-11}
49	320	1.686	2.0×10^{-11}
162	358	1.585	2.0×10^{-11}
77	358	1.585	5.7×10^{-11}
128	370	1.555	6.3×10^{-11}
?	370	1.555	7.7×10^{-11}
97	380	1.531	7.2×10^{-11}
?	380	1.531	1.3×10^{-10}
116	388	1.513	1.7×10^{-10}
?	388	1.513	1.4×10^{-10}
88	429	1.425	5.8×10^{-10}
?	456	1.372	1.6×10^{-10}
?	456	1.372	1.2×10^{-10}

.....

GRAPH 42. Cl^{36}-diffusion in SO_4^{2-}-doped CsCl

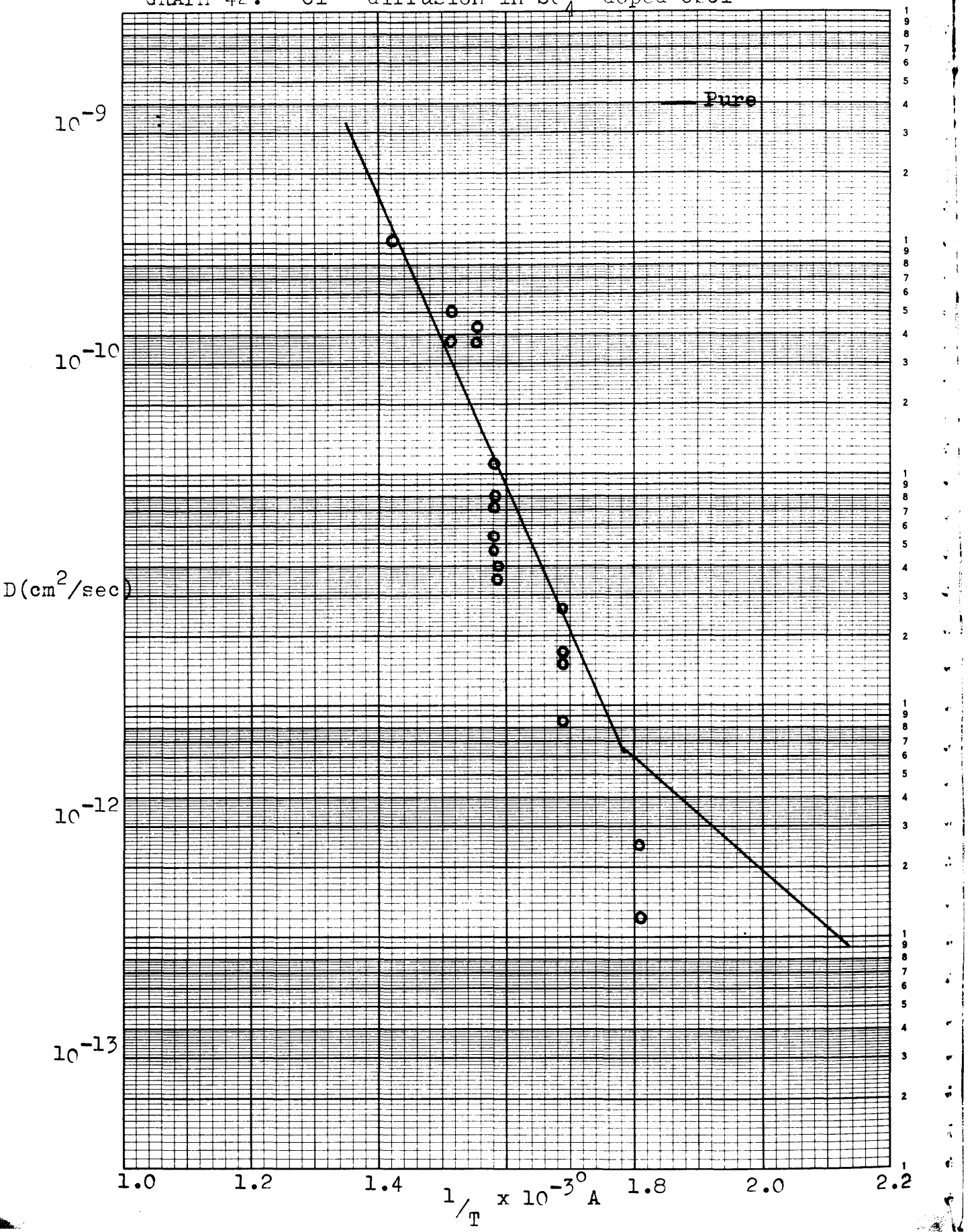

TABLE 42

Cl^{36} diffusion in SO_4^{2-}-doped CsCl from Graph 42.

Impurity content (ppm)	Temp (°C)	1/T x 10^{-3} (°A)	D (cm^2/sec)
	280	1.808	1.2 x 10^{-12}
	280	1.808	2.5 x 10^{-12}
	280	1.808	2.5 x 10^{-12}
	320	1.686	8.5 x 10^{-12}
	320	1.686	1.5 x 10^{-11}
	320	1.686	1.7 x 10^{-11}
	320	1.686	2.6 x 10^{-11}
	358	1.585	3.5 x 10^{-11}
	358	1.585	4.0 x 10^{-11}
	360	1.580	4.7 x 10^{-11}
162	360	1.580	5.4 x 10^{-11}
	360	1.580	8.0 x 10^{-11}
123	360	1.580	7.4 x 10^{-11}
	360	1.580	7.5 x 10^{-11}
	360	1.580	1.1 x 10^{-10}
180	370	1.555	3.7 x 10^{-10}
	370	1.555	4.4 x 10^{-10}
	388	1.513	3.7 x 10^{-10}
	388	1.513	5.0 x 10^{-10}
	429	1.425	1.0 x 10^{-9}

.....

GRAPH 43. Cs^{137} diffusion in 'pure' CsCl

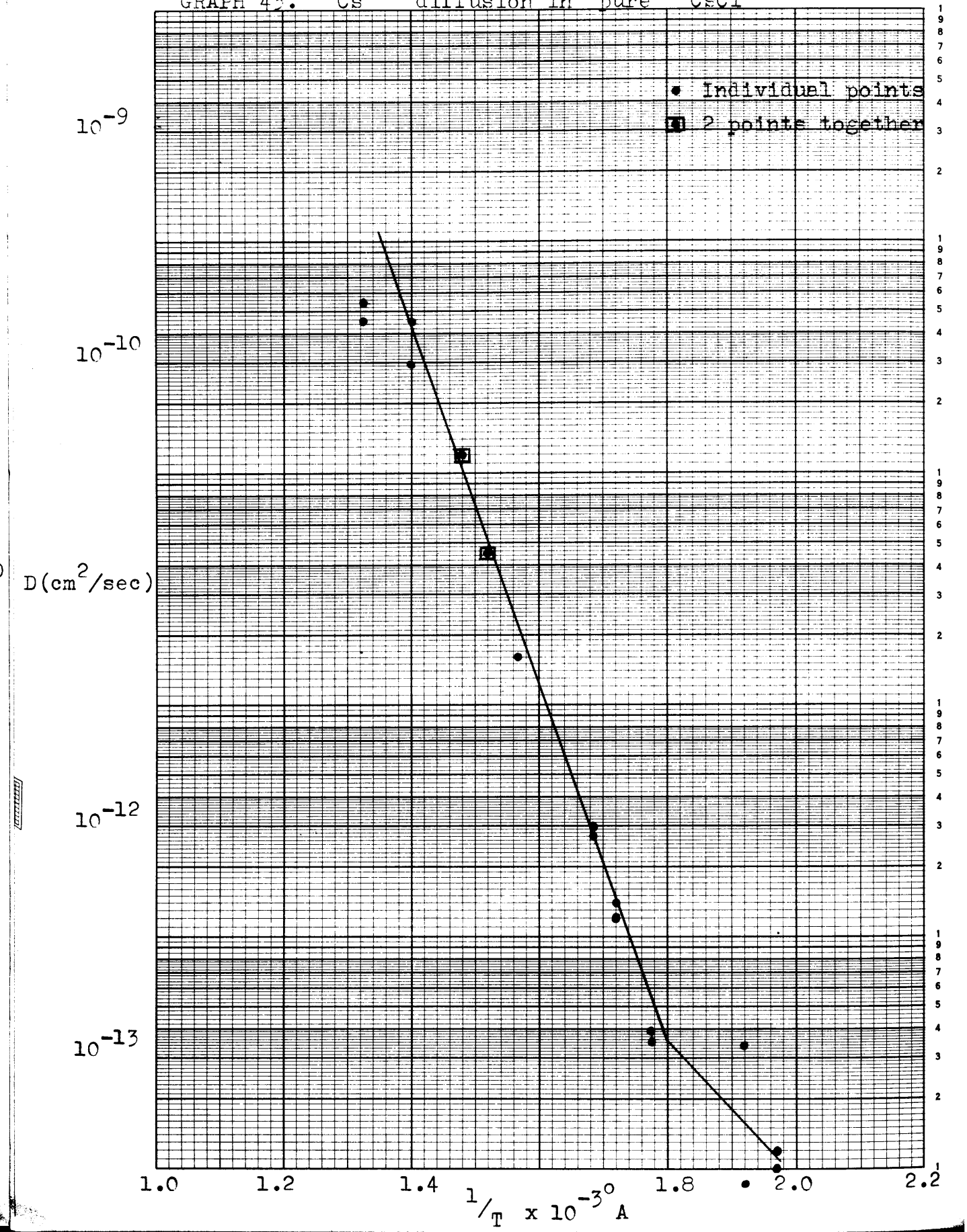

TABLE 43

Cs-137 diffusion in 'pure' CsCl from Graph 43

Temp (°C)	$1/T \times 10^{-3}$ °A.	D(cm^2/sec)
233	1.972	1.0×10^{-13}
233	1.972	1.2×10^{-13}
248	1.919	8.2×10^{-14}
248	1.919	3.4×10^{-13}
290	1.776	3.4×10^{-13}
290	1.776	3.8×10^{-13}
307	1.724	1.4×10^{-12}
307	1.724	1.2×10^{-12}
320	1.686	2.7×10^{-12}
320	1.686	3.0×10^{-12}
364	1.570	1.6×10^{-11}
383	1.524	4.5×10^{-11}
383	1.524	4.6×10^{-11}
402	1.481	1.2×10^{-10}
402	1.481	1.2×10^{-10}
449	1.385	2.9×10^{-10}
449	1.385	4.5×10^{-10}
481	1.326	4.6×10^{-10}
481	1.326	5.5×10^{-10}

.....

	Activation Energy (ev)	D_o (cm^2/sec)
Low temperature range below knee	0.60	9.04×10^{-8}
High temperature range above knee	1.54	25.3

.....

GRAPH 44 Cs^{137} diffusion in aliovalent impurity-doped CsCl

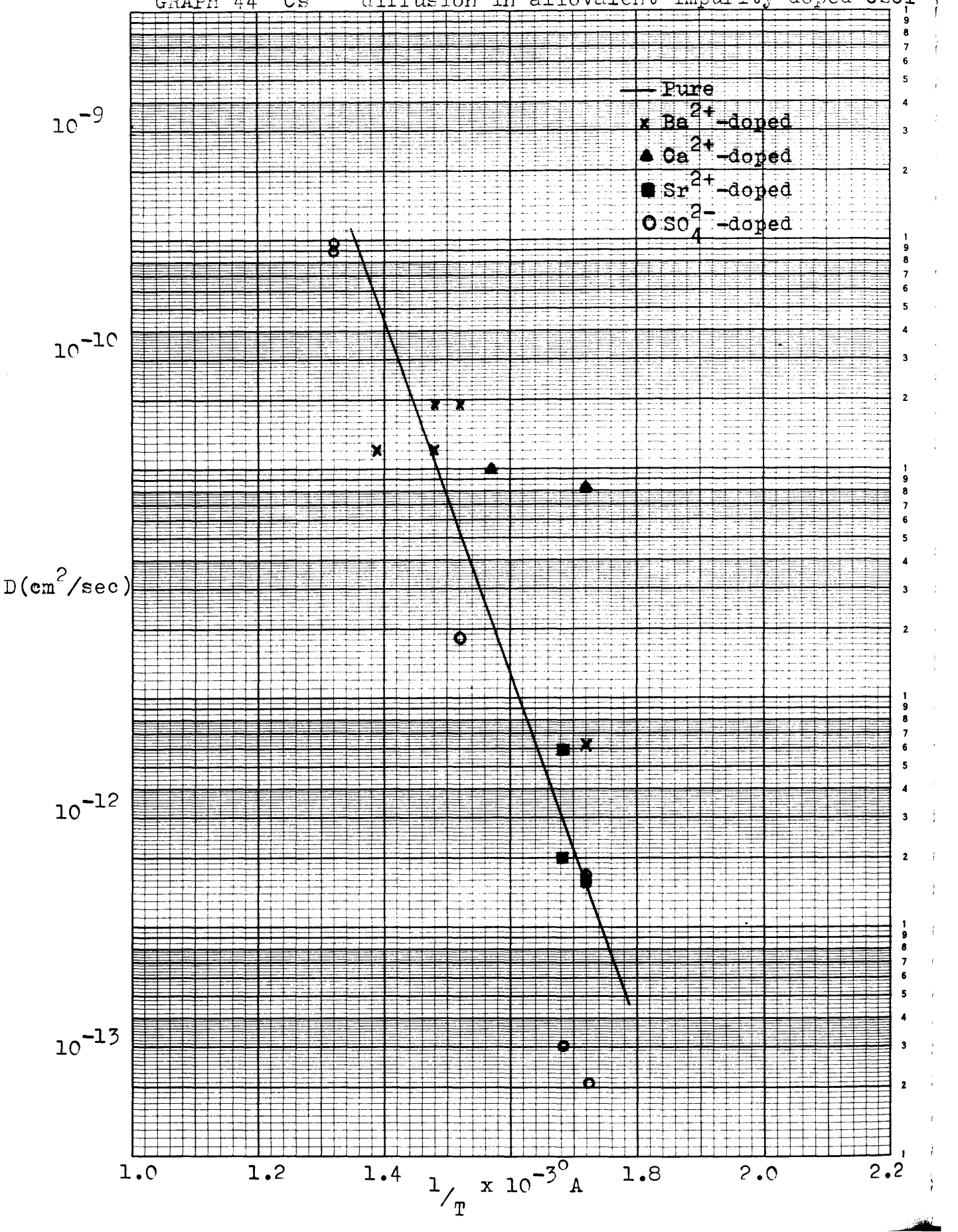

TABLE 44

Cs^{137} diffusion in aliovalent impurity doped CsCl.

Impurity (ppm)	Temp.(°C)	$1/T \times 10^{-3}$ °A	$D(cm^2/sec)$	Graph**
Barium (260)	307	1.724	6.5×10^{-12}	(23)
Strontium (<5)	307	1.724	1.6×10^{-12}	
Calcium	307	1.724	8.4×10^{-11}	
Sulphate	307	1.724	1.6×10^{-12}	
Sulphate	307	1.724	2.1×10^{-13}	
Strontium (<5)	320	1.686	2.0×10^{-12}	(28)
Strontium	320	1.686	5.8×10^{-12}	
Sulphate	320	1.686	3.1×10^{-13}	
Calcium (125)	364	1.570	1.0×10^{-10}	(29)
Barium	383	1.524	1.9×10^{-10}	
Sulphate	383	1.524	1.9×10^{-11}	
Barium (<5)	402	1.481	1.2×10^{-10}	(27)
Barium (280)	402	1.481	1.9×10^{-10}	(24)
Barium (167)	449	1.385	5.3×10^{-11}	(20)
Barium	449	1.385	1.2×10^{-10}	
Sulphate	481	1.326	9.4×10^{-10}	
Sulphate	481	1.326	9.7×10^{-10}	

.....

** Numbers in this column correspond to the conductivity graphs which were measured after diffusion.

.....

GRAPH 45 Comparison of diffusion coefficients.

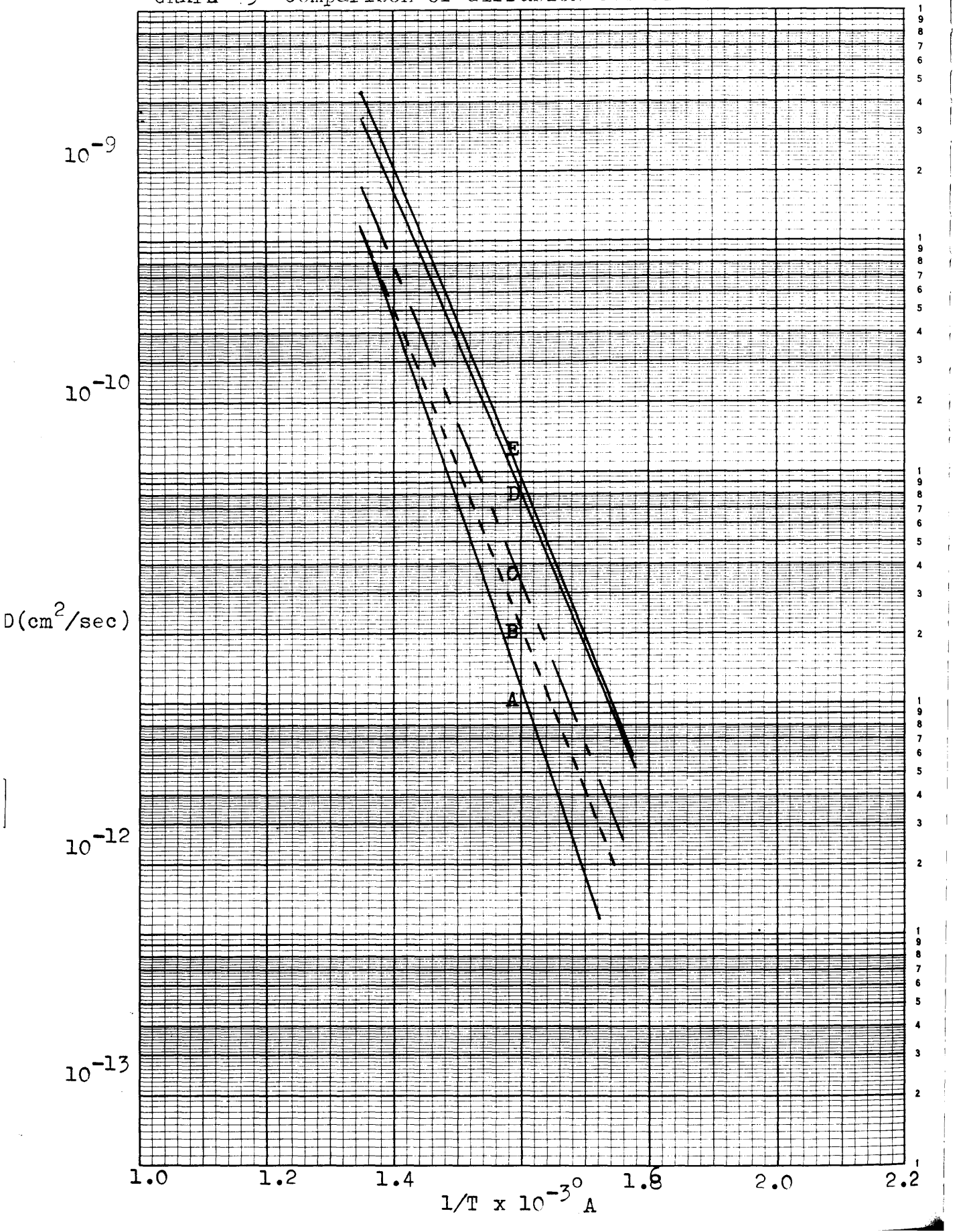

TABLE 45

Comparison of diffusion coefficients from Graph 45

Line	Origin	Activation Energy (ev)	D (cm^2/sec) at 1.4 r.t.u.
A	Cs-137 diffusion	1.54	4.3×10^{-10}
*B	Calculated from conductivity and correlation factor correction (f) introduced	1.395	5.0×10^{-10}
C	Calculated from conductivity	1.395	7.8×10^{-10}
D	Cl-36 diffusion	1.30	1.6×10^{-9}
E	Total diffusion (A + D)	1.34	2.0×10^{-9}

*Correlation factor (f) = 0.653 for simple interpenetrating cubic lattice.[92]

If the Nernst-Einstein relationship is obeyed

$$D^* = D_o(f) \quad \text{or} \quad D^*/D_o = (f)$$

where

D^* = total diffusion coefficient using radioactive tracers. i.e. Line E

D_o = diffusion coefficient calculated from conductivity measurements. i.e. Line C

(f)= correlation factor for tracer diffusion

Our results indicate $D^*/D_o = 2.5 = (f)$

GRAPH 46

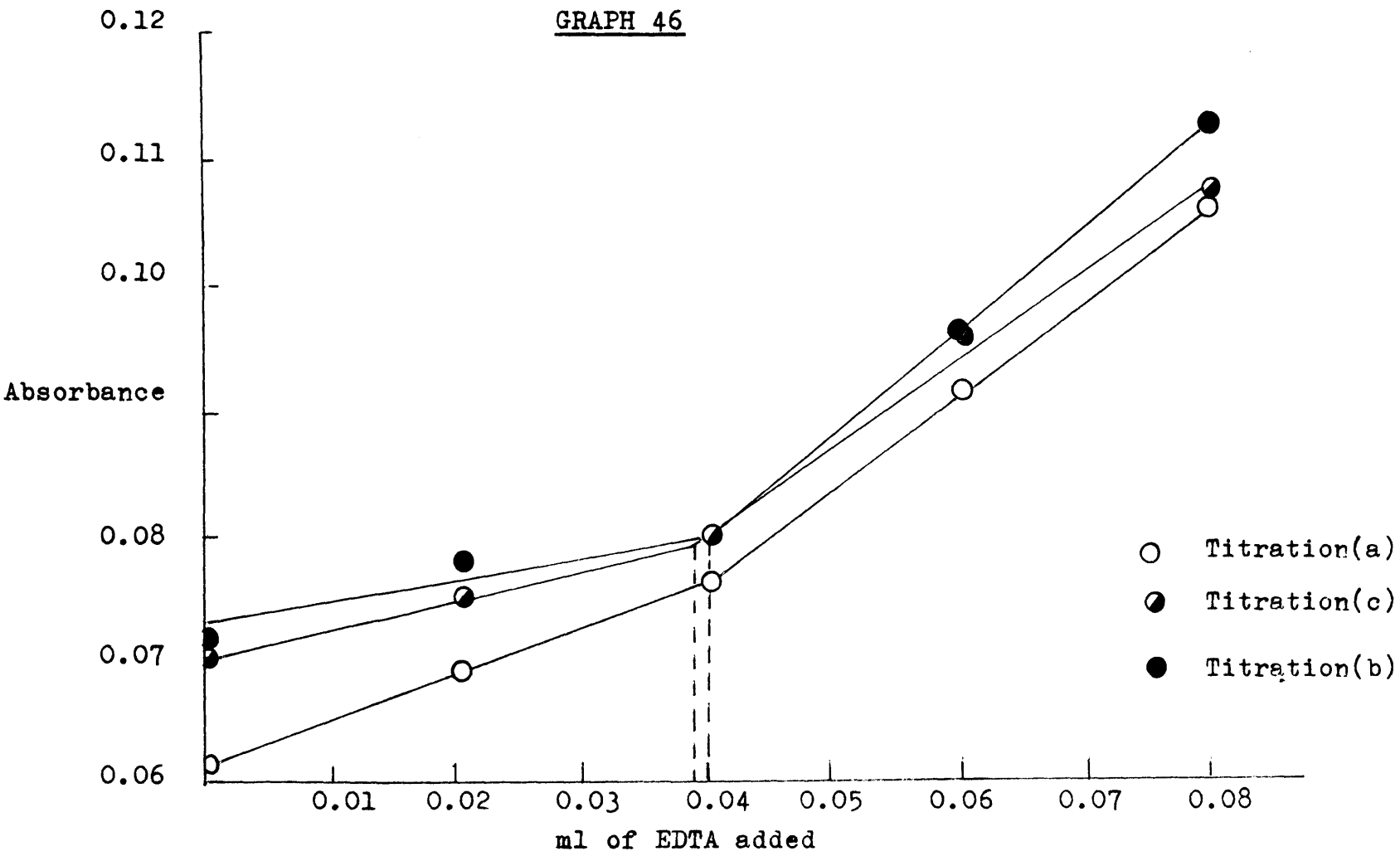
0.12
0.11
0.10
0.08
0.07
0.06
Absorbance
0.01
0.02
0.03
0.04
0.05
0.06
0.07
0.08
ml of EDTA added
Titration(a)
Titration(c)
Titration(b)

RESULTS

CHAPTER 9

ANALYSIS

9.1 Method of Presentation.

Included in this section are sample results for

a) a typical standard calibration

b) a typical Ba^{2+} determination

c) a typical SO_4^{2-} determination

d) a 'pure' estimation

Figures for all other analyses are listed in Appendix D.

9.2 Standard Calibration.

Wt. of $BaCl_2$ = 0.0020 g

Wt. of CsCl = 20.00 g

These quantities were dissolved in 500 ml of distilled water. Three 2ml portions, (a),(b) and(c), were titrated against 1.03 mM EDTA in the presence of ammonia buffer.

Results.

(a)		(b)		(c)	
ml EDTA	Absorbance	ml EDTA	Absorbance	ml EDTA	Absorbance.
0.00	0.061	0.00	0.072	0.00	0.070
0.02	0.069	0.02	0.077	0.02	0.074
0.04	0.076	0.04	0.079	0.04	0.079
0.06	0.091	0.06	0.096	0.06	0.094
0.08	0.108	0.08	0.113	0.08	0.107

The corresponding end-points are

(a) at 0.040 ml (b) at 0.040 ml (c) at 0.038 ml.

The results are plotted in Graph 46.

Calculations.

(a) and (b)

1 ml of 1 mM EDTA = 0.137 mg Ba^{2+}

$\therefore$ 0.040 ml of 1.03 mM = 0.00564 mg Ba^{2+}

$$\therefore \frac{Ba^{2+}}{Cs^{+}} = \frac{0.00564 \times 168.4 . 10^{6}}{137.4 \times 0.08 . 10^{3}}$$

$$= \underline{86 \text{ ppm}}$$

(c)

0.038 ml of 1.03 mM = 0.00536 mg Ba^{2+}

$$\therefore \frac{Ba^{2+}}{Cs^{+}} = \frac{0.00536 \times 168.4 \times 10^{6}}{137.4 \times 0.08 \times 10^{3}}$$

$$= \underline{82 \text{ ppm}}.$$

Amount of Ba^{2+} theoretically present = 81ppm

$\therefore$ Percentage accuracy = 95.5%

.....

GRAPH 47

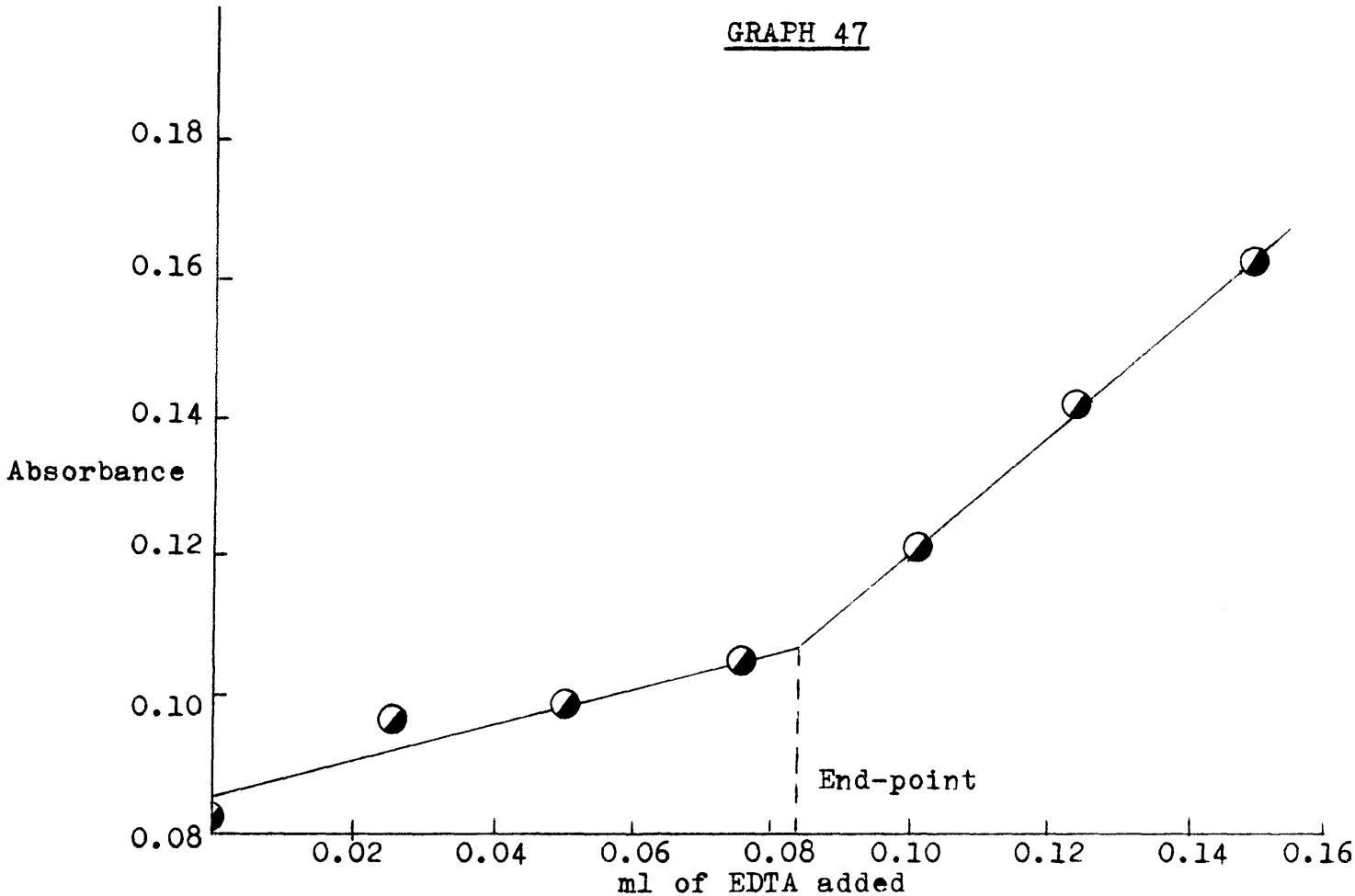
0.18
0.16
0.14
Absorbance
0.12
0.10
0.08
End-point
0.02
0.04
0.06
0.08
0.10
0.12
0.14
0.16
ml of EDTA added

3.3 Typical Ba^{2+} determination (from Graph 19)

Wt. of crystal = 0.2350 g.

Dissolved in distilled water, 10 drops of ammonia buffer added and solution made up to 5 ml. 2 ml titrated against 1.03 mM EDTA.

Results

ml EDTA added	Absorbance
0.00	0.083
0.025	0.095
0.050	0.097
0.075	0.105
0.100	0.120
0.125	0.142
0.150	0.162

The results are plotted in Graph 47.

End point occurs at 0.084 ml.

Now, 1 ml of 1 mM EDTA = 0.137 mg Ba^{2+}

$\therefore$ 0.084 ml of 1.03 mM = 0.0119 mg Ba^{2+} in 2 ml

= 0.0298 mg Ba^{2+} in 5 ml

$$\therefore \quad Ba^{2+}/\,Cs^{+} = \frac{0.0298 \times 168.4 \times 10^{6}}{0.0350 \times 137.4 \times 10^{3}}$$

= 153 ppm.

.....

GRAPH 48

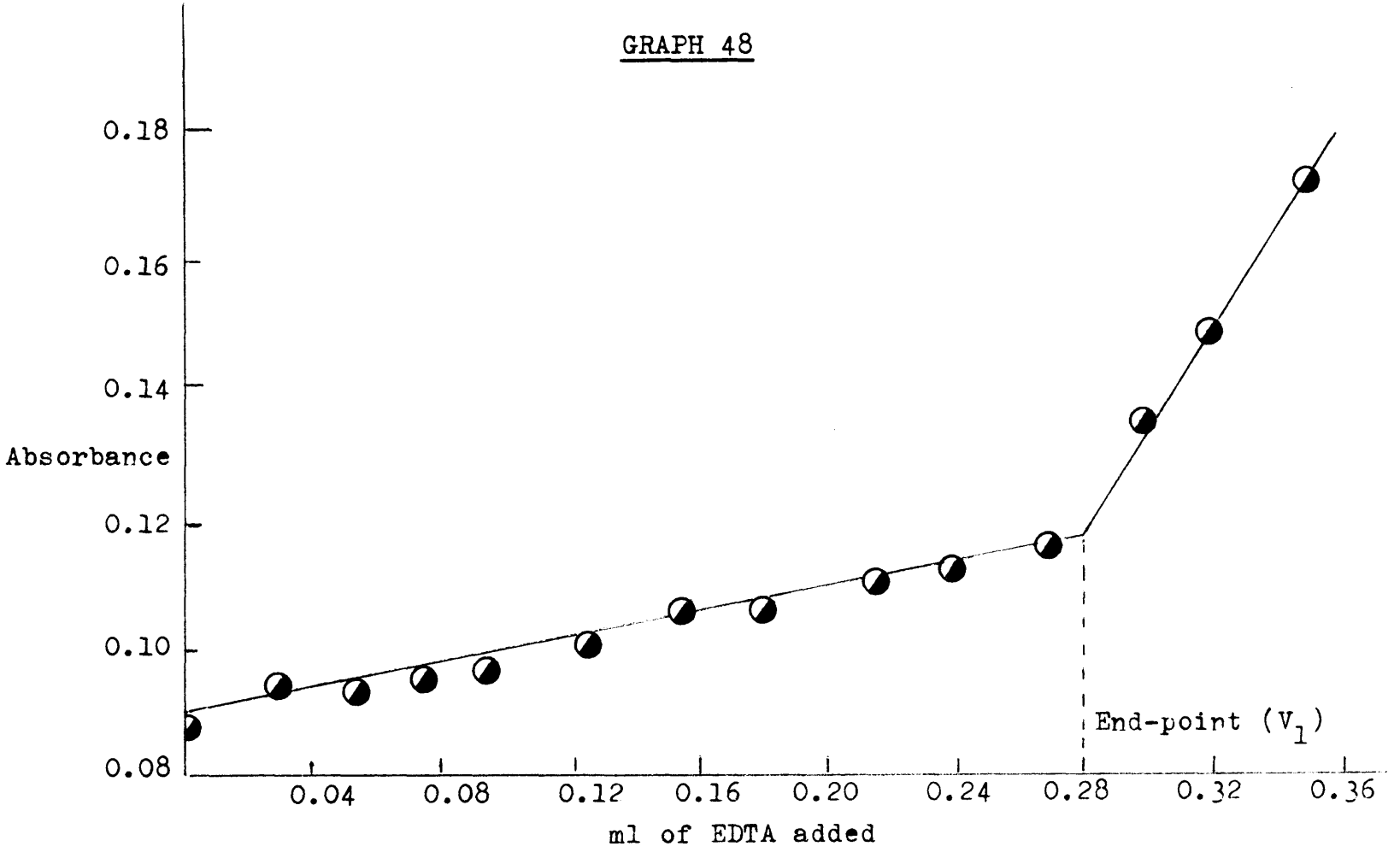
0.18
0.16
0.14
Absorbance
0.12
0.10
0.08
End-point (V_1)
0.04
0.08
0.12
0.16
0.20
0.24
0.28
0.32
0.36
ml of EDTA added

3.4 Typical SO_4^{2-}-determination

(1) Calibration of Ba^{2+} standard.

0.0300 g $BaCl_2$ were dissolved in $BaSO_4$ solution and the solution made up to 500 ml. 2 ml of the resulting solution was centrifuged with 2ml of $BaSO_4$ solution and 2 ml of the resulting solution titrated against 1.03 mM EDTA in the presence of ammonia buffer.

Results	ml EDTA added	Absorbance
	0.000	0.086
	0.030	0.094
	0.055	0.093
	0.075	0.095
	0.095	0.095
	0.125	0.100
	0.155	0.106
	0.180	0.106
	0.215	0.109
	0.240	0.112
	0.270	0.115
	0.295	0.135
	0.320	0.149
	0.350	0.172

The results are plotted in Graph 48

The end point occurs at 0.280 ml (V_1)

(2) SO_4^{2-} determination from Graph 31

Wt. of crystal = 0.2073 g

Crystal dissolved in 2 ml of $BaSO_4$ solution and this solution centrifuged with 2 ml of Ba^{2+} standard solution. 2 ml of the resulting solution titrated against 1.03 mM EDTA in the presence of ammonia buffer.

GRAPH 49

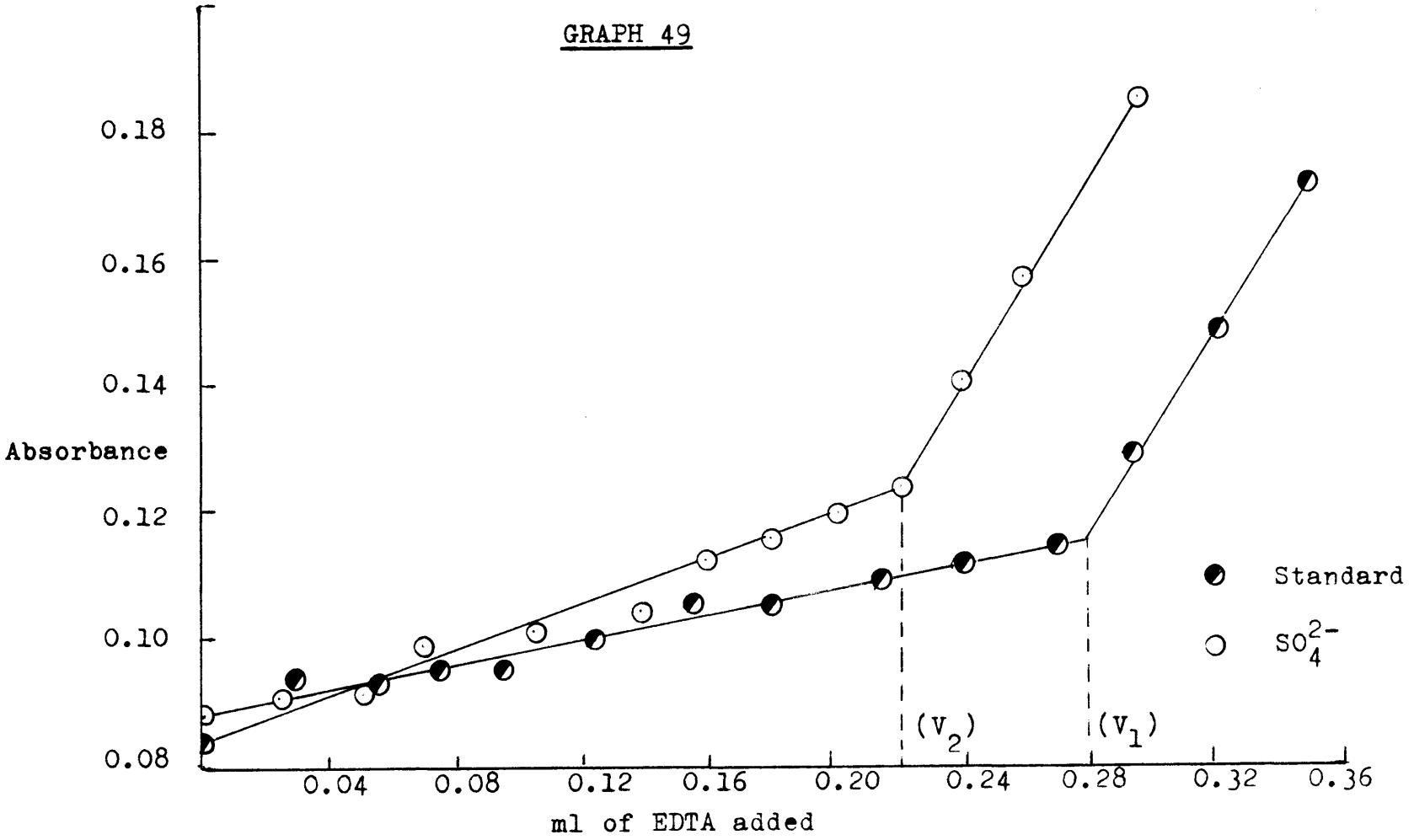
0.18
0.16
0.14
Absorbance
0.12
0.10
0.08
0.04
0.08
0.12
0.16
0.20
0.24
0.28
0.32
0.36
ml of EDTA added
(V2)
(V1)
Standard
SO4 2-

Results	ml EDTA added	Absorbance
	0.000	0.083
	0.025	0.091
	0.050	0.092
	0.070	0.099
	0.105	0.102
	0.140	0.106
	0.160	0.113
	0.180	0.116
	0.200	0.120
	0.220	0.125
	0.240	0.142
	0.260	0.158
	0.295	0.186

The results are plotted in Graph 49 together with those obtained in part (1).

The end point occurs at 0.220 ml (V_2)

In the absence of SO_4^{2-} the end point occurs at 0.280 (V_1)

$\therefore$ Amount of Ba^{2+} reacting with SO_4^{2-} = $(V_1) - (V_2)$

= 0.060 ml EDTA

Now, 1 ml of 1 mM EDTA = 0.137 mg Ba^{2+} = 0.096 mg SO_4^{2-}

$\therefore$ 0.060 ml of 1.03 = 0.00593 mg SO_4^{2-} in 2 ml

= 0.01186 mg SO_4^{2-} in 4 ml

$$\therefore SO_4^{2-}/Cl^- = \frac{0.01186 \times 168.4 \times 10^6}{0.2073 \times 96.07 \times 10^3}$$

= 100 ppm.

GRAPH 50

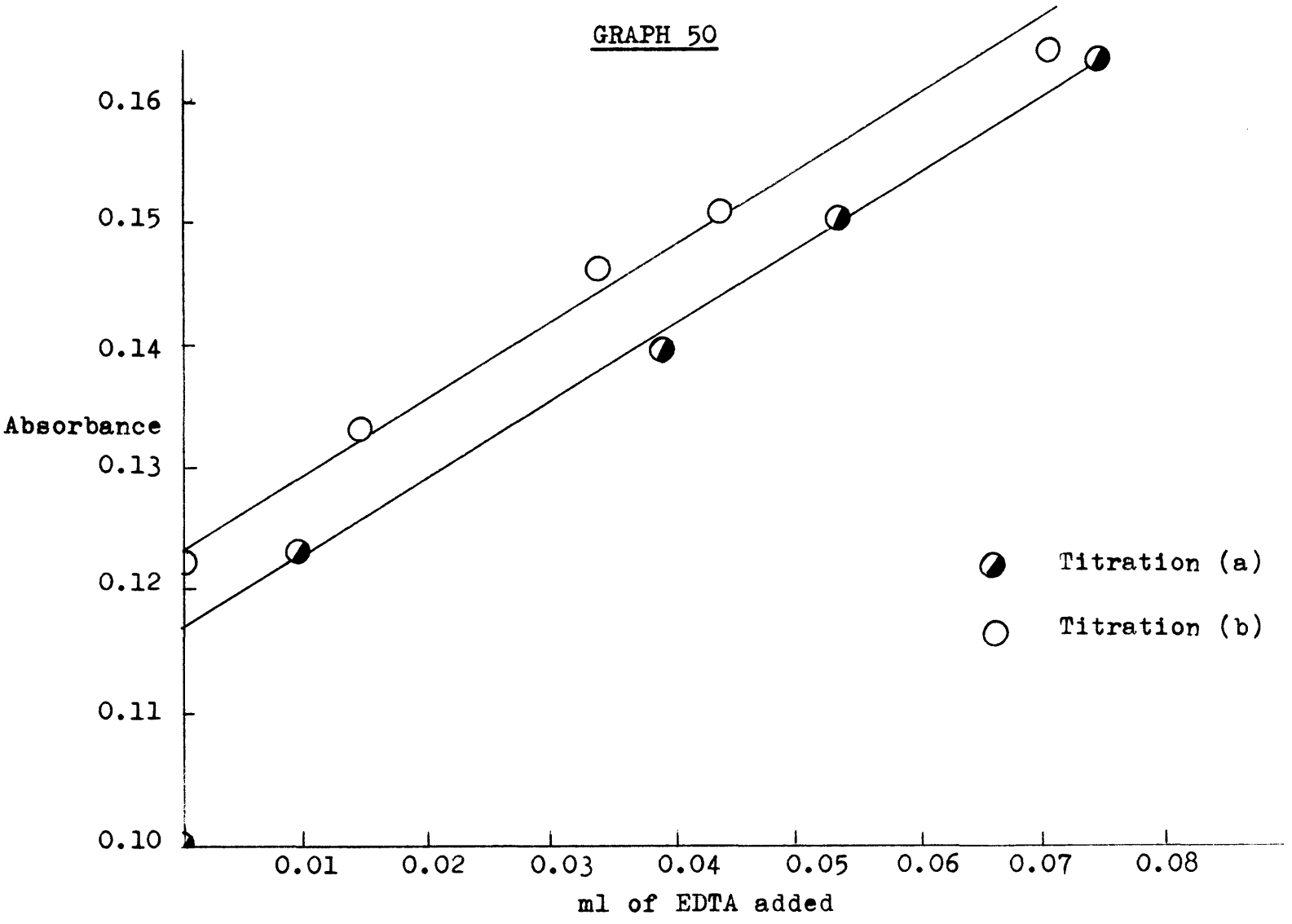
0.16
0.15
0.14
Absorbance
0.13
0.12
0.11
0.10
0.01
0.02
0.03
0.04
0.05
0.06
0.07
0.08
ml of EDTA added
Titration (a)
Titration (b)

9.5 Typical 'pure' estimation.

Wt. of crystal = 0.3254 g

Dissolved in distilled water and 10 drops ammonia buffer added. Solution made up to 5 ml and two 2 ml portions titrated against 1.03 mM EDTA.

Results

(a)		(b)	
ml EDTA	Absorbance	ml EDTA	Absorbance
0.000	0.100	0.000	0.123
0.010	0.123	0.015	0.133
0.040	0.136	0.035	0.146
0.055	0.150	0.045	0.151
0.075	0.165	0.070	0.166

The results are plotted on Graph 50.

In neither case is there evidence of an end point and the divalent cation impurity content is therefore undetectable.

TABLE 46

Experimental Parameters for Self-Diffusion in the Caesium Halides.

Material	Tracer	Temp. Range (°C)	D_o (cm^2/sec)	Activation Energy (ev)	Author and Reference
CsCl (compacts)	Cl-36	below 465	1.3×10^{-3}	0.87	Laurant & Bénard(48)
CsCl (")	Cs-137	below 465	10^{-5}	0.70	Laurant & Bénard(48)
CsCl (single crystals)	Cl-36	280-470		1.30....1.00	Hoodless & Morrison(60)
CsCl (")	Cl-36	below 290	1.95×10^{-7}	0.50	Present work
CsCl (")	Cl-36	290-470	2.1	1.30	Present work
CsCl (")	Cs-137	below 290	9.04×10^{-8}	0.60	Present work
CsCl (")	Cs-137	290-470	25.3	1.54	Present work
CsBr (melt-grown)	Br-82	330-415	0.441	1.29	Lynch(55)
CsBr (")	Br-82	415-530	3.92	1.42	Lynch(55)
CsBr (")	Cs-134	320-550	15.1	1.54	Lynch(55)
CsI (")	I-131	410-540	2.05	1.37	Lynch(55)
CsI (")	I-131	300-410	0.487	1.28	Lynch(55)
CsI (")	Cs-134	320-550	14.24	1.53	Lynch(55)

DISCUSSION

CHAPTER 10.

IONIC MOBILITY IN PURE CAESIUM CHLORIDE.

10.1 Self-Diffusion.

The diffusion graph, (Graph 40) ,for Cl-36 self-diffusion in 'pure' single crystals of caesium chloride shows the existence of two regions separated by a 'knee' at 290°C.

The region above the knee, 290-470°C, is a good straight line with an activation energy of 1.30ev. In the low temperature region there are insufficient measurements to obtain an accurate activation energy, but the apparent activation energy is 0.50ev.

A similar situation is observed for Cs-137 diffusion in 'pure' single crystals of caesium chloride, (Graph 43). The region above the knee has an activation energy of 1.54ev., while below the knee the apparent activation energy is 0.50.ev.

A comparison of our results, with those of previous workers is given in Table 46.

The results of Laurant & Bénard seem to be relatively low. Their measurements, however, were made on compacts, not on single crystals. Furthermore, they observe that although less mobile than the chloride ion, the caesium ion migrates with a lower activation energy. This is contradictory.

Hoodless and Morrison[60] obtained an activation energy of 1.30ev.,falling off to 1.00ev. at higher temperatures, for Cl-36 diffusion. This decrease in activation energy is probably due to sintering, as they were using very small crystals.

Our results are in very good agreement with those of Lynch[55], which were obtained for self-diffusion in caesium bromide and caesium iodide. We do not, however, observe the higher temperature region for anion self-diffusion. Lynch has shown, from a comparison of conductivity and diffusion studies, that ion migration in caesium bromide and caesium iodide takes place via Schottky vacancies. If such is the case in caesium chloride, we can express the results for anion and cation self-diffusion in the following manner:-

$$E_{anion} = U_{anion} + W/2_{anion}$$

and

$$E_{cation} = U_{cation} + W/2_{cation}$$

where E = measured activation energy for self-diffusion

U = energy required for ion to migrate

and W = energy to create a pair of Schottky defects.

Conductivity results (to be discussed later) and values obtained by Lynch enable us to substitute values of 0.58 and 0.30ev. for U_{cation} and U_{anion} respectively in the equations. This leads to values of 2.00ev and 1.92 ev. for (W). These are in good agreement and we can, therefore, state that the energy required to create a pair of Schottky defects in caesium chloride is 1.96 ± 0.04ev.

The diffusion studies also provide information about the respective ionic mobilities. Over the complete temperature range studied the anion is the more mobile species, in agreement with the findings of previous workers. We can express the ratio of the mobilities as,

$$\frac{\text{mobility of anion}}{\text{mobility of cation}} = u_-/u_+ = \phi = D_{Cl^-}/D_{Cs^+}$$

At 290°C., $\phi = 12$ and at 470°C., $\phi = 3$.

As we have previously stated, both the Cl-36 and Cs-137 diffusion plots show low temperature regions of low activation energy. Two possible explanations for the existence of these low temperature regions are:-

(a). There may be significant grain boundary diffusion at these temperatures.

(b). They may arise due to accidental incorporation of aliovalent impurities.

Anion diffusion in the alkali halides is known to be grain boundary dependent at lower temperatures[35]. In the present investigation, however, it has been found that annealing does not produce the changes in diffusion coefficient one would expect if diffusion was proceeding via these boundaries. Furthermore, autoradiographic studies fail to indicate the presence of grain boundaries. It should be remembered, however, that in the alkali halides the anion is the least mobile species, whereas the reverse is true in the caesium halides.

On the other hand, annealing studies and autoradiography seem to indicate that the diffusion of the slower moving caesium ion is also independent of grain boundaries.

We cannot, however, satisfactorily explain the experimental observations simply on a basis of their being due to impurity effects. While the accidental incorporation of aliovalent impurities in the lattice may give rise to the low temperature region in one of the self-diffusion plots, it cannot give rise to this phenomenon for both anion and cation self-diffusion. Lidiard[5] has pointed out that only one type of impurity ion, either anion or cation, can be effective in any one crystal. The species which is in excess "salts out" impurity ions of opposite charge. In general, the alkali halides are more likely to contain trace amounts

of cation, rather than anion, impurities. So, while the Cs-137 diffusion results may be explicable on the basis of impurity effects, the Cl-36 diffusion results at low temperatures cannot be so explained.

We shall return to this problem later in the discussion. Suffice to say at present that a more detailed investigation of self-diffusion in caesium chloride at temperatures below 290°C. is warranted.

10.2 Conductivity.

The conductivity graphs (Graphs 1a-6) for 'pure' solution grown single crystals of caesium chloride exhibit, like the self-diffusion plots, two regions separated by a knee. The activation energy above the knee is reproducible from crystal to crystal as is illustrated in Table 47.

TABLE 47

Graph Number	Treatment	Activation Energy(ev)
1a	Untreated	1.37
1b	"	1.38
1c	"	1.37
2	Thermal Cycling	1.39
3	After Diffusion	1.42
4	Untreated	1.40
4a	(4) 96 hrs. later	1.41
5	After Chilling from 470°C.	1.40
6	Untreated	1.41
6a	Irradiated	1.39

The mean value of activation energy is 1.395ev.

TABLE 48

Experimental Parameters for Conductivity in the Caesium Halides.

Material	Temp. Range(^{o}C)	σ_o(ohm^{-1}cm^{-1})	E_A(ev)	Author & Reference
CsCl	330-460		1.04	Harpur, Moss and Ubbelohde(53)
CsCl	280-470	2.3×10^4	1.22	Hoodless & Morrison(60)
CsCl	280-470	1.64×10^5	1.395	Present work
CsBr	475-590	2.48×10^5	1.435	Lynch(55)
CsBr	Impurity range-475	2.51×10^4	1.285	Lynch(55)
CsI	480-595	2.21×10^5	1.43	Lynch(55)
CsI	Impurity range-480	1.38×10^4	1.25	Lynch(55)
CsI	below 420		1.00	Besson, Chauvy and Rossel(61)
CsI	above 420	1×10^6	1.49	Besson, Chauvy and Rossel(61)
CsI	below 560		1.33	Ecklin, Nadler and Rossel(62)

This reproducibility in activation energy in the temperature range 290-470°C., which is not destroyed by the treatments listed, is indicative of ion migration via thermally created Schottky vacancies.

A comparison of our results with those of other workers is given in Table 48.

The results of Harpur, Moss and Ubbelohde are thought to be low because of their method of preparation. However, a more interesting explanation will be discussed later.

At first sight it would appear that our results are in better agreement with those obtained by Lynch at higher temperatures. However, we have plotted log (σT) as a function of reciprocal temperature, and not, as other workers have done, simply log (σ) as a function of reciprocal temperature. Our value of 1.395ev. would become 1.34ev. had we plotted log (σ) as a function of reciprocal temperature and this brings it into line with the activation energies obtained by Lynch for caesium bromide and caesium iodide in the same temperature range.

Although our conductivity results are reproducible at temperatures above the knee, below the knee reproducibility ceases. The activation energy in this region varies from crystal to crystal but there is a relationship between the 'knee temperature' and the activation energy below the knee. This is illustrated in Table 49.

TABLE 49

Knee Temperature (r.t.u.)	Activation Energy below knee (ev)
1.87	1.02
1.86	1.08
1.86	0.93
1.85	1.15
1.83	1.13
1.83	0.96
1.82	0.94
1.81	0.95
1.80	0.93
1.80	0.88
1.80	0.80
1.76	0.88

There is a very general tendency for the knee (^{o}C) temperature to increase as the activation energy decreases.

The reason for the variable activation energy at low temperatures is possibly due to slightly different amounts of aliovalent impurity ions in different crystals. More will be said about this region when considering impurity-doped crystals. It should be noted that the results of Ubbelohde et al[53,54] record the same activation energy as we have observed in this low temperature region. The presence of large grain boundaries in their polycrystalline specimen, although not acting as routes for ion migration, may be affecting the impurity solubility.

10.3 Comparison of Conductivity and Diffusion.

A comparison of the conductivity and diffusion is possible by means of the Nernst-Einstein equation (18).

$$\sigma T(f)/D = Ne^2/k$$

This relationship enables us to compare the measured diffusion coefficient with that calculated from conductivity measurements. Since our diffusion measurements have shown that both the anion and the cation are sufficiently mobile to contribute to the measured conductivity, we must compare the total diffusion coefficient, Danion and D cation, with conductivity.

If the Nernst-Einstein relationship is obeyed, within the limits of experimental error, we can say that both diffusion and conductivity are proceeding by the same mechanism. We have plotted in Graph 45 (page 114) the experimentally determined diffusion coefficients with those calculated from conductivity measurements.

Agreement between calculated and measured values is not good, the measured diffusion coefficient being 3.8 times greater than that value calculated from the conductivity.

There are a number of possible reasons which may explain the failure of the results to obey the desired relationship.

(a) There may be an electronic contribution to the conductivity.

(b) We may be dealing with interstitial movement.

(c) Vacancy pairs, or other neutral entities, may be contributing to the diffusion but not to the conductivity.

We can immediately discount (a) and (b). If the deviation was due to an electronic contribution to the conductivity the calculated diffusion coefficient would be higher than the measured value. Interstitial movement is not favoured in caesium chloride from a consideration of ion sizes, Van der Waals energies and dielectric constant.

Recent studies by Morrison et al[52], and by Laurance[51] have indicated the distinct probability that vacancy pairs play an important role in anion diffusion in the alkali halides. Even more recently, Downing[93] has suggested the possibility that vacancy pairs may also contribute to Na-22 self-diffusion in sodium chloride.

It would appear, therefore, that vacancy pairs may be important in self-diffusion in caesium chloride. However, there are certain other factors which have not yet been considered.

(a) Our results for Cs-137 and Cl-36 diffusion in caesium chloride agree particularly well in activation

energy with the results obtained by Lynch for the self-diffusion in caesium bromide and caesium iodide. Lynch has shown that, within the limits of experimental error, the Nernst-Einstein relationship is approximately obeyed for these crystals.

(b) Although our measured diffusion and diffusion calculated from conductivity differ in magnitude, there is good agreement in the activation energies.

Taking these two factors into account, it now appears doubtful if the failure of our results to obey the Nernst-Einstein equation can be due entirely, if indeed at all, to vacancy pairs.

The possibility that the disagreement is due to experimental technique must now be considered. The temperature factor can be immediately ruled out as the thermometer used in the diffusion measurements was calibrated against the thermocouple used in the conductivity measurements.

Two possible errors may exist in the experimental technique. Firstly, in order to calculate the diffusion coefficients, we have had to measure the absorption coefficients, 4.7 and 4.8. Standard aluminium absorbers were used for this purpose due to the inaccessability of sufficiently thin caesium chloride sections, and the results

so obtained were converted by means of density considerations. Strictly speaking, they should be related not by densities but by atomic numbers. For sodium chloride the atomic numbers are Z_{Na}= 11 and Z_{Cl}= 17. These are similar to that of aluminium, Z = 13. In the case of caesium chloride, however Z_{Cs}= 55. An error in the absorption coefficients may have been introduced.

We may also have an error in the absolute magnitude of the conductivity. In the initial stages of the research a magnitude of conductivity,similar to that obtained by Hoodless and Morrison[60], was obtained. Reproducibility, however, was poor. After modifying the apparatus to give reproducible results, subsequent measurements were always a factor of 2 lower than those obtained earlier.

FIGURE 16.

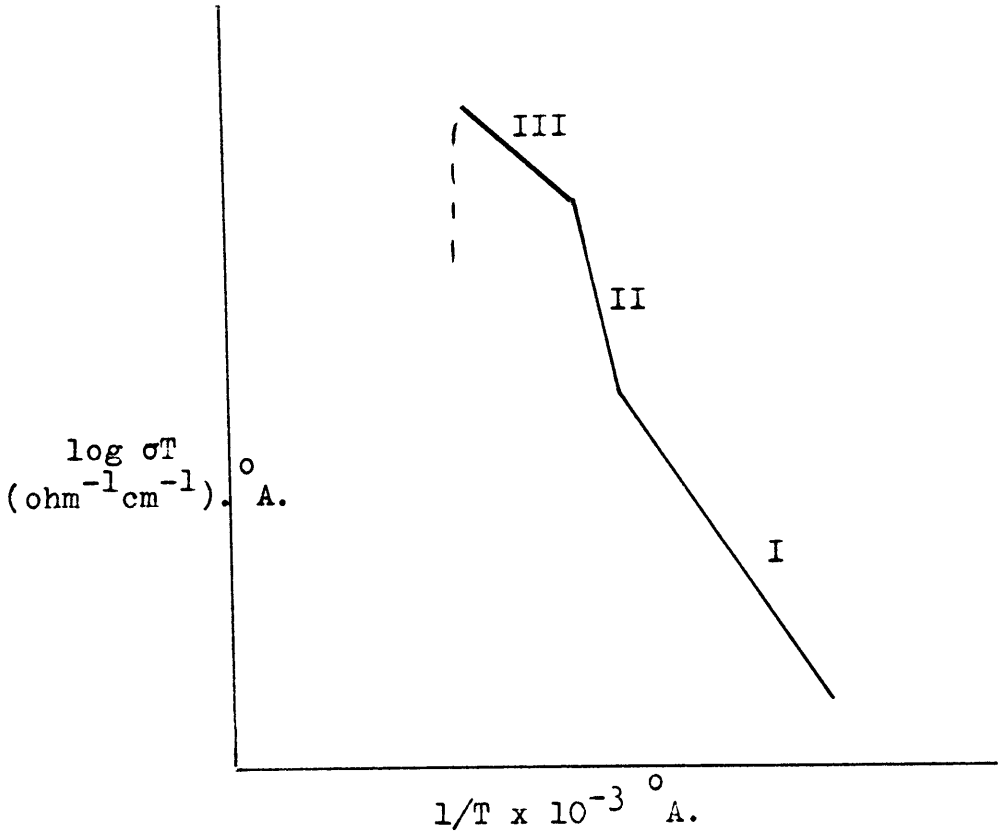

DISCUSSION. CHAPTER 11

THE EFFECT OF ALIOVALENT IMPURITIES ON ION MIGRATION IN CAESIUM CHLORIDE.

11.1 GENERAL SUMMARY AND THEORETICAL TREATMENT.

The general shapes of the conductivity graphs for both Ba^{2+}-doped and SO_4^{2-}-doped crystals are remarkably similar. Above 300°C it is possible to distinguish three regions of conductivity before the transition point, Fig.16. From 300°C to approximately 350°C, the activation energy for conduction is the same as for pure crystals (region I). Above this temperature there is a very rapid increase in conductivity (region II), leading to a region of conduction of low activation energy (region III) above approximately 390°C. In the latter region the activation energy is dependent upon the aliovalent impurity concentration.

Before discussing the results in detail, it will be convenient to consider some theoretical aspects of impurity doping. The concentration of vacancies will be governed by a relationship of the type given in equation (7), i.e.

$$n_1 n_2 = n_o^2 \qquad \text{.....(31)}$$

Since both the anion and cation contribute to the conductivity in this system the effects of both types of impurity should be observable. Addition of Ba^{2+} will increase the cation impurity vacancy concentration but will depress both the thermal anion and thermal cation vacancy concentration. Addition of SO_4^{2-} will have a similar effect on the anion vacancy concentration.

In a pure crystal, at a fixed temperature, the conductivity is given by

$$\sigma = Ne n_o(\mu_1 + \mu_2) \quad \ldots\ldots(32)$$

On addition of a mole fraction (c) of divalent cation impurity, electroneutrality requires that

$$n_1 - c = n_2 \quad \ldots\ldots(33)$$

Hence from equation (31),

$$n_1(n_1 - c) = n_o^2 \quad \ldots\ldots(34)$$

or $$n_1 = \tfrac{1}{2}c(1 + (1 + (4n_o^2/c^2))^{\frac{1}{2}}) \quad \ldots\ldots(35)$$

Using the Lidiard notation[5], the conductivity of the crystal is given by

$$\sigma = Ne n_o(\mu_1 + \mu_2)\left((c/2n_o)^2 + 1\right)^{\frac{1}{2}} - (c/2n_o)(\phi-1)/(\phi+1)) \quad \ldots(36)$$

i.e. $$(\sigma/\sigma_o) = \left((c/2n_o)^2 + 1\right)^{\frac{1}{2}} - (c/2n_o)(\phi-1)/(\phi+1)) \quad \ldots(37)$$

FIGURE 17.

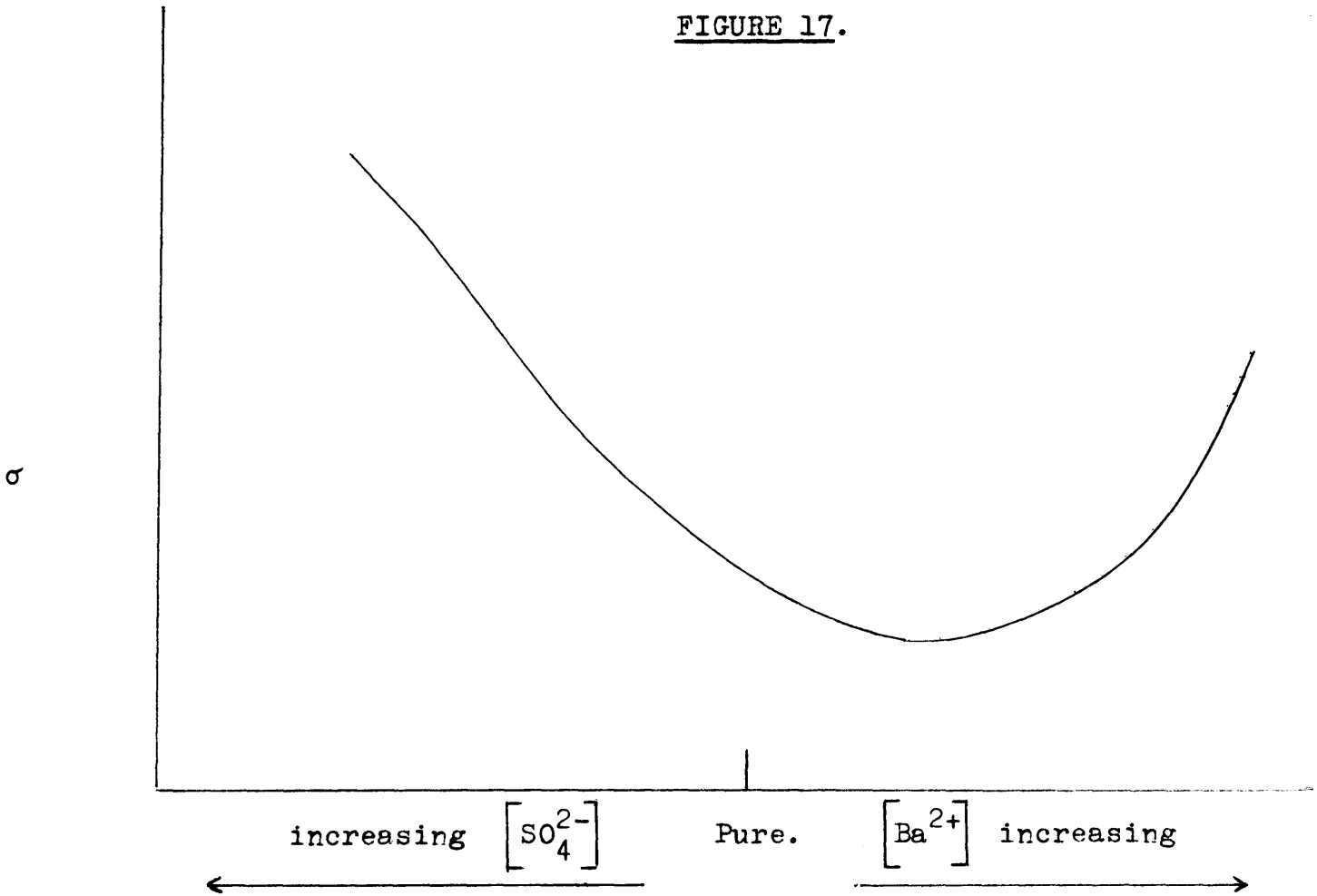

where $\phi = \mu_2/\mu_1$

If ϕ is greater than unity, as in the case of caesium chloride, a plot of (ϕ) against (c) will exhibit a minimum when,

$$(c)_{min} = n_o(\phi - 1)/(\phi)^{\frac{1}{2}} \quad .....(38)$$

and $$(\sigma/\sigma_o)_{min} = 2(\phi)^{\frac{1}{2}}/(\phi + 1) \quad .....(39)$$

The aliovalent impurity additions should therefore affect the conductivity as in Fig.17. Increase in temperature will lead to the minimum moving to higher Ba^{2+} concentrations.

The results of the present work will now be examined on the basis of this theoretical approach.

11.2 Ba^{2+}-doped crystals.

The results of the conductivity measurements in Ba^{2+}-doped crystals, above 300°C, are shown in Table 50.

The theoretical approach, previously discussed, would indicate that plots of conductivity as a function of impurity concentration should exhibit a minimum when equations (38) and (39) are satisfied. Values of n_o, however, are not available, so equation (38) cannot be used initially. On the other hand, equation (39) only requires the value of (ϕ) and this can be deduced from a consideration of the self-diffusion results in pure crystals. (ϕ) should, in fact, be

TABLE 50

Summary table of conductivity results for Ba^{2+}-doped single crystals of CsCl.

ppm Ba^{2+}	E_A in region I (ev)	σT @ 1.7 r.t.u. ($ohm^{-1}cm^{-1}$) A.	Knee temp. (r.t.u.)	Amt. of rise in region II	E_A in region III (ev)	σT @ 1.5 ($ohm^{-1}cm^{-1}$) A.
'Pure'	1.395	1.5×10^{-4}	1.80	none	1.395	3.6×10^{-3}
57	1.38	1.1×10^{-4}	1.75	2.7	1.00	6.0×10^{-3}
62	1.37	1.4×10^{-4}	1.85	2.9	0.97	8.0×10^{-3}
71	1.35	1.25×10^{-4}		3.2	0.91	8.0×10^{-3}
85	1.40	7.8×10^{-5}	1.82	5.5	0.79	8.7×10^{-3}
97	0.95	3.7×10^{-4}	none	4.4	0.70	9.6×10^{-3}
104	0.84	2.7×10^{-4}	none	7.7	0.65	1.0×10^{-2}
133	0.82	2.1×10^{-4}	none	8.0	0.64	9.6×10^{-3}
?	1.39	8.0×10^{-5}	1.74	11.4	0.60	1.2×10^{-2}
153	1.35	1.35×10^{-4}	1.82	2.0	0.74	8.0×10^{-3}
167	1.33	1.1×10^{-4}	1.73	4.7	0.88	8.3×10^{-3}
196	1.40	1.6×10^{-4}	none	2.0	0.84	9.0×10^{-3}
234	1.39	1.8×10^{-4}	1.87	3.0	1.00	8.4×10^{-3}
260	1.30	2.6×10^{-4}	1.70	none	1.30	5.0×10^{-3}
280	1.30	3.0×10^{-4}	1.86	none	1.30	8.0×10^{-3}

given by D_{Cl^-} / D_{Cs^+} and the values of (ϕ), calculated in this way are listed in Table 51.

Table 51

Temperature (r.t.u.)	ϕ	$(\sigma/\sigma_o)_{min}$
1.7	9.3	0.69
1.6	6.4	0.68
1.5	4.6	0.76
1.4	3.4	0.83

In Graphs (51, 52 and 53) plots of (σT) against (c) are given for one temperature region I (1.7 r.t.u.) and two temperatures in region II (1.5 and 1.4 r.t.u.) respectively. The calculated minima values are also shown on these graphs. There is considerable scatter in the results and it is difficult to draw a reasonable curve through the points at any one temperature.

Examination of the (σT) versus (c) plot at 1.7 r.t.u. indicates the existence of more than one minimum. At first sight there is evidence for minima at about 80 and 120 ppm of Ba^{2+}. There is some anomaly in these results as the majority of the crystals give an activation energy for conduction of 1.35eV (cf. pure crystal), but the crystals doped with 97, 104 and 133 ppm Ba^{2+}, marked o in Graph (51), show a much lower activation

GRAPH 51

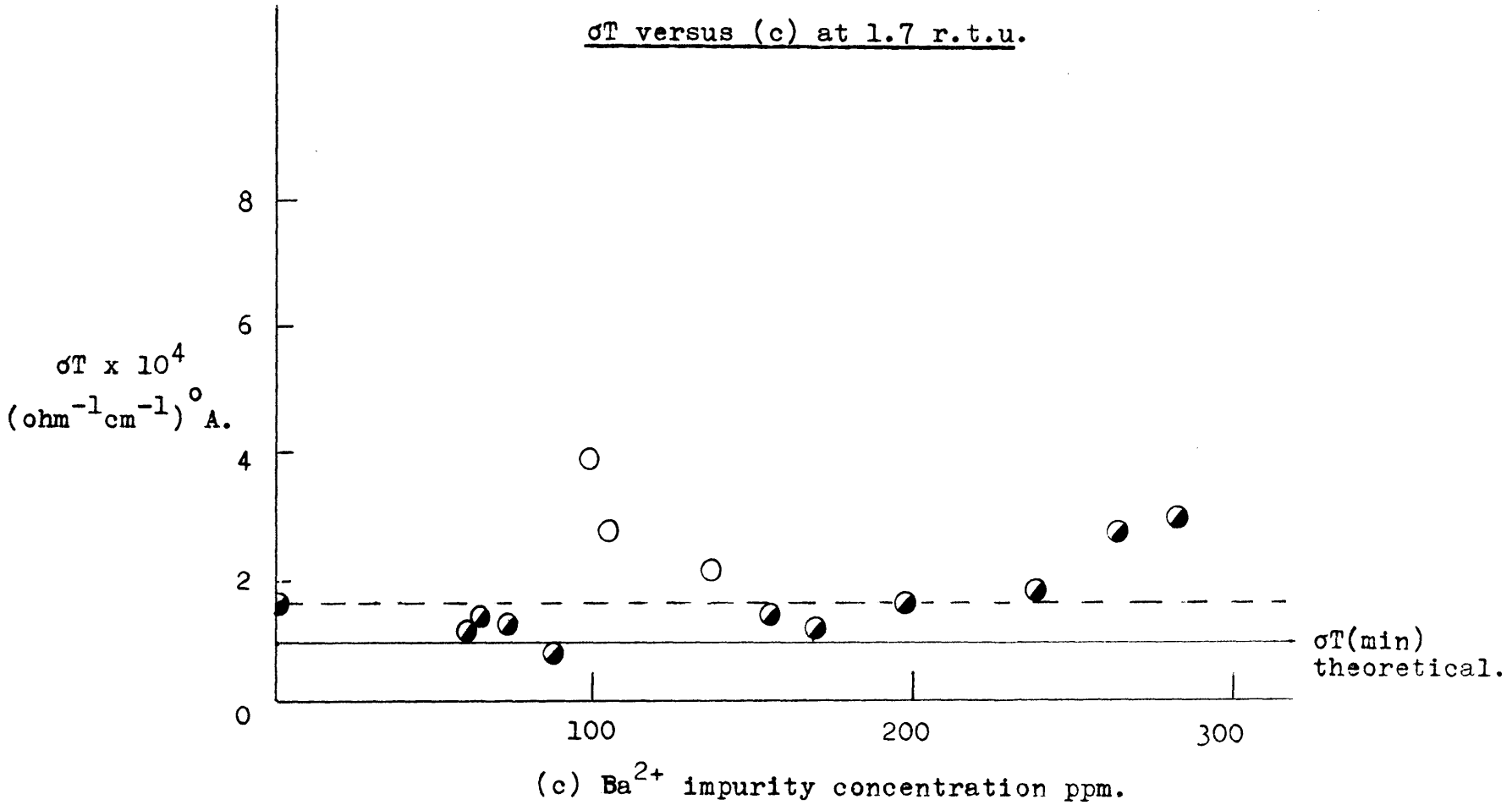
σT versus (c) at 1.7 r.t.u.
σT x 10^4
(ohm^-1 cm^-1) °A.
8
6
4
2
0
100
200
300
σT(min)
theoretical.
(c) Ba2+ impurity concentration ppm.

GRAPH 52.

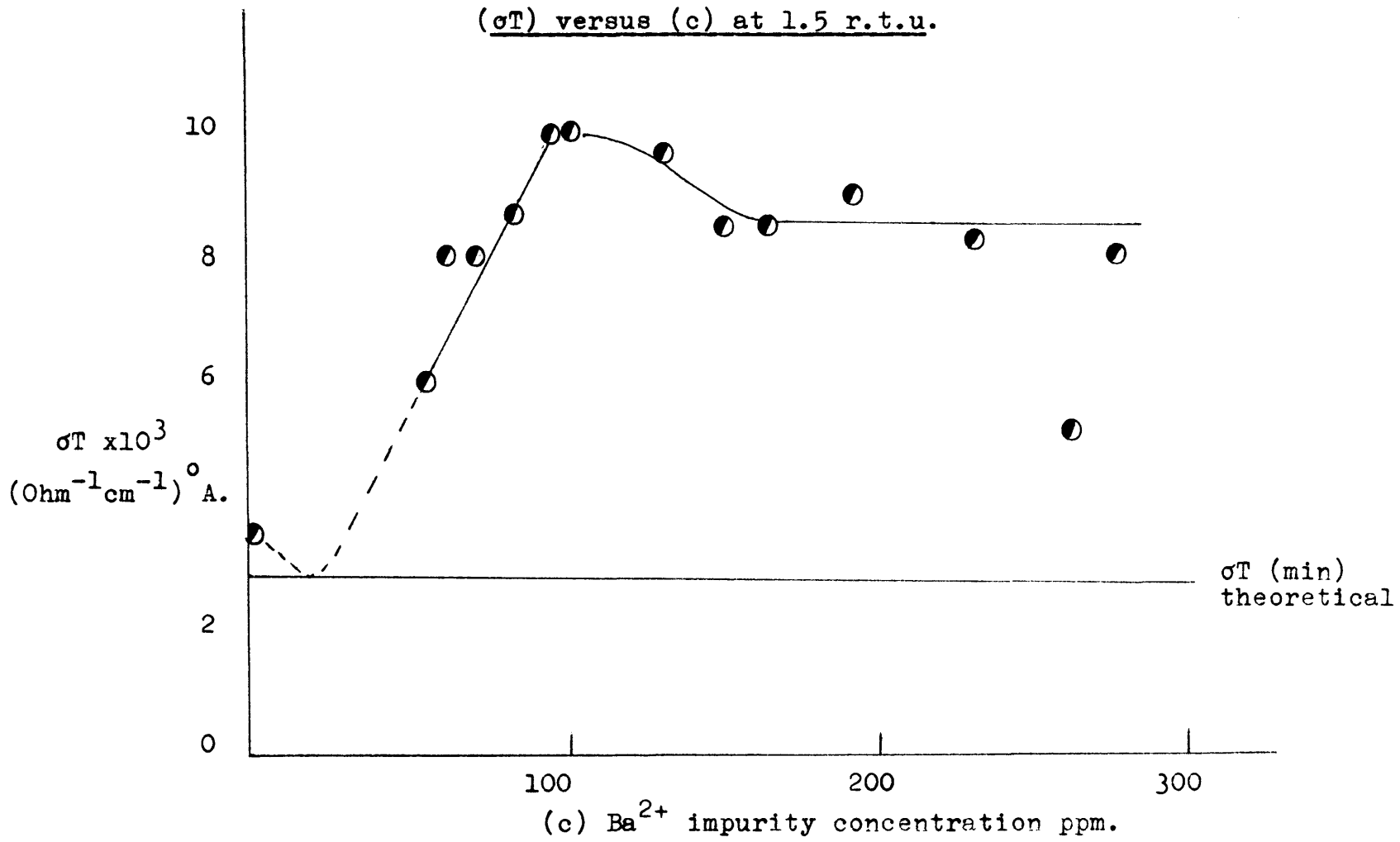
(σT) versus (c) at 1.5 r.t.u.
10
8
6
2
0
σT x10^3
(Ohm^-1 cm^-1) °A.
σT (min)
theoretical
100
200
300
(c) Ba^2+ impurity concentration ppm.

GRAPH 53

(σT) versus (c) at 1.4 r.t.u.

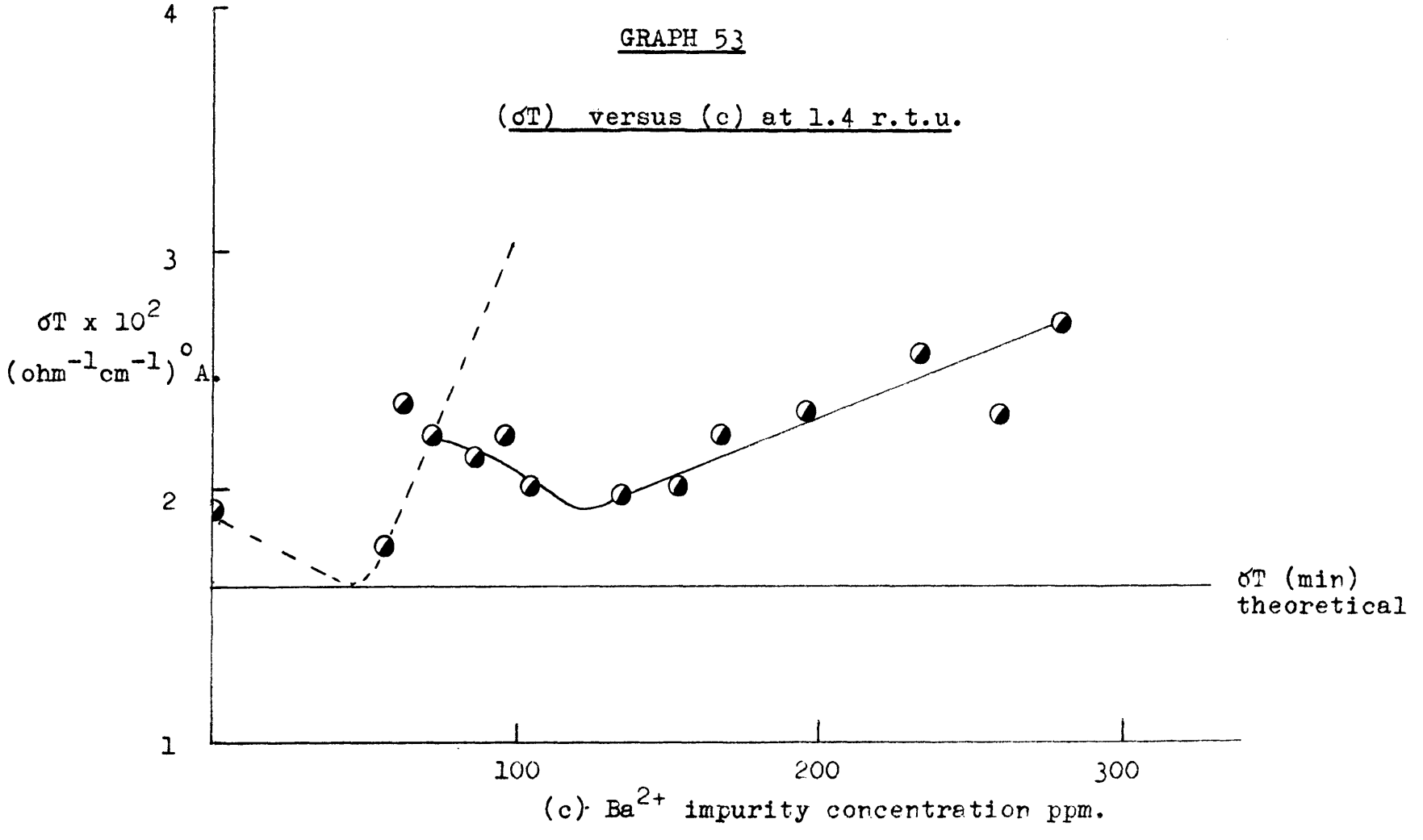

energy and somewhat different conduction characteristics, Table 50. If these three points are ignored, then a minimum in the plot occurs at approximately 100 ppm (1×10^{-4} m.f.). Substitution of this value for (c) in equation (38) gives

$$n_o = 3.7 \times 10^{-5}$$

This is an extremely high value of n_o at this temperature. The self-diffusion results give a value of approximately 2.0 ev for the energy to create a Schottky pair and substitution in equation (6) indicates values of 3.7×10^{-4} and 1.15×10^{-5} for n_o at 1.5 and 1.4 r.t.u. respectively. The effect of impurities therefore, within the concentrations used in the experiments and at these higher temperatures, should be extremely small. The observed results (Table 50) do not agree with this prediction. It must be concluded, therefore, that the minimum is not due to equilibrium behaviour associated with the creation of impurity vacancies.

It is significant that the activation energy for conduction in region I is approximately the same as for pure crystals. If the Ba^{2+} was completely soluble the activation energy would be expected to approach 0.60 ev., (the suggested value for the energy of mobility of cation vacancies). The difference between the predicted and the observed activation energies

could be accounted for if the Ba^{2+} was forming neutral impurity-vacancy complexes. This should, however, result in a decrease in the magnitude of conduction since the production of free or complex vacancies by the Ba^{2+} will depress the thermal vacancy concentration.

The results suggest that at these temperatures the Ba^{2+} is essentially insoluble in the lattice. It should be noted that there is a significant difference in ionic volume between the host and impurity ion.

$$\frac{\text{Ionic volume of } Ba^{2+}}{\text{Ionic volume of } Cs^{+}} = \left(\frac{1.35}{1.69}\right)^{3} = 0.51$$

The substitution of Ba^{2+} for Cs^{+} could lead to instability in the lattice. It would appear that the system, under equilibrium conditions, would be more stable with the impurity present as a second phase in aggregates. The disparity in ion size raises the possibility of the impurity being in interstitial positions in the lattice. Under these conditions, each Ba^{2+} ion would create two cation vacancies to retain electroneutrality in the system. The predicted effects of Ba^{2+}-doping should have been readily observed in this case.

If the assumption that the impurity is insoluble at this temperature is correct, the conductivity

should be independent of impurity concentration. The results shown in Graph (51) do indicate that this is approximately observed for those crystals having the same conduction activation energy as the pure crystal (marked ● in Graph (51)). It is believed that in the crystals which exhibit much lower activation energies, (marked o in Graph (51)), the observed conductivity is due to non-equilibrium phenomena. This will be discussed in more detail when considering the region below 300°C.

Increase of temperature will cause lattice expansion and, as a result, the disparity in ion size will be of less significance. It is suggested that the rapid increase in conductivity above 300°C (region II) is associated with impurity dissolving in the lattice, thus producing an increase in the cation vacancy concentration. It should be noted that in region III the activation energies do indicate a substantial contribution from impurity created cation vacancies. This would appear to confirm that region II is associated with impurity dissolution. Although the rapid increase in conductivity is much greater than is generally observed for this process[37], dissolution is usually accompanied by the formation of associated-vacancy complexes. If these complexes are not formed with Ba^{2+} then this would lead to a greater increase in conductivity.

This could not account entirely for the magnitude of the increase and it is suggested that further experimental investigation of this region is required.

The results in region III support the proposal that region II is associated with the production of impurity induced vacancies, probably by dissolution of Ba^{2+} in the lattice. The activation energy in region III indicates that these vacancies contribute significantly to the conductivity. It should be possible to apply the theoretical treatment of Lidiard[5] in this region.

Extrapolation of the (σ) versus (c) curve at 1.5 r.t.u. (for concentrations below 100 ppm) indicates that the theoretical minimum conductivity should be observed at about 10-20 ppm. of Ba^{2+}. If we base our calculation on the smaller value of concentration, (the reason for this will be obvious later in the discussion), then by applying equation (38)

$$n_o = 6 \times 10^{-6} \text{ m.f.}$$

Knowing the value of n_o and ϕ (from the self-diffusion measurements at this temperature) it is possible to calculate the conductivity as a function of impurity concentration using equation (37).

$$\sigma = \sigma_o \sqrt{(c/2n_o)^2 + 1} - (c/2n_o)(\phi - 1)/(\phi + 1)$$

The theoretical conductivities, calculated in this

GRAPH 54.

A comparison of σT(measured) and σT(calculated) at 1.5 r.t.u.

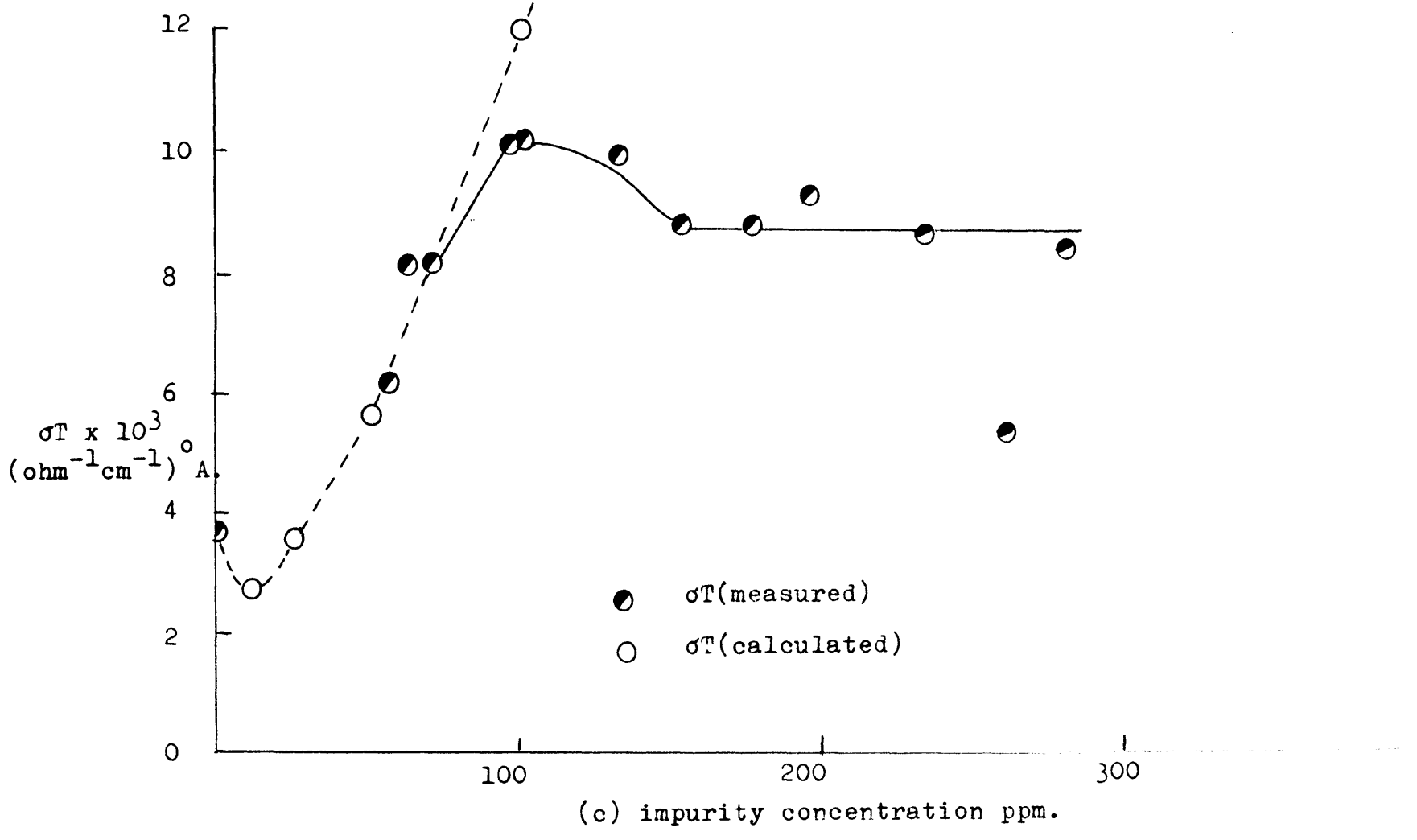

way are compared with the observed results in Graph (54).

There is reasonable agreement between the calculated and the few observed conductivities at lower impurity concentrations. The results indicate that the maximum impurity solubility at this temperature is about 100 ppm. It has frequently been observed that vacancy-impurity complexes and even larger more complex aggregates are precursors to precipitation[94,95]. The formation of these complexes will reduce the free vacancy concentration and so the conductivity would be expected to fall below the calculated value[96] near the solubility limit. If we assume that our conductivity measurements are accurate enough to ascribe some significance to the small decrease in conductivity above 100 ppm of impurity, then it would seem that the larger impurity aggregate complexes are trapping some free vacancies[97].

The measurements of self-diffusion give a value of approximately 2.0eV for the formation energy of Schottky defects. Using this value and the value of n_o at 1.5 r.t.u., the corresponding value of n_o at 1.4 r.t.u. can be calculated from equation (6). Solution of this equation gives

$$n_o = 1.9 \times 10^{-5}$$

Similar calculations to those described for the results at 1.5 r.t.u. can now be applied. The predicted

GRAPH 55

A comparison of σT(measured) with σT(calculated) at 1.4 r.t.u.

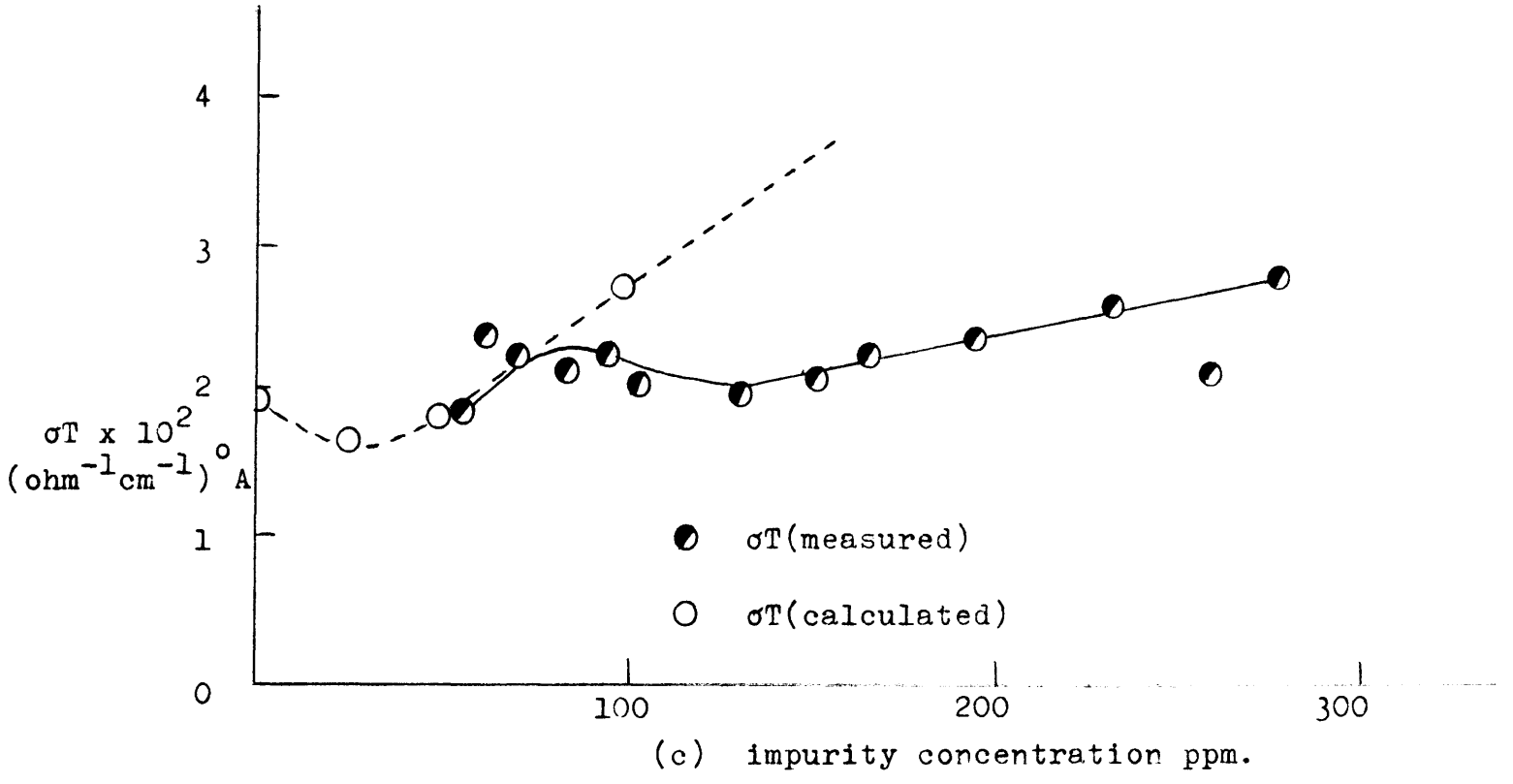

minimum in the conductivity graph should be 26 ppm of impurity. The calculated and observed conductivity results are compared in Graph (55). Again there is some agreement at lower impurity concentrations but there is evidence of a second minimum at higher concentrations. It is possibly significant that in the crystals whose conductivities fall in this second minimum region, (impurity concentrations 97-167 ppm), the phase transition occurs at or below 1.4 r.t.u.. There is some hysteresis in this region of the phase transition[53,54] and this phenomenon is associated with the co-existence of the two phases. Ionic mobility in the face-centred cubic form of caesium chloride is considerably smaller than in the simple interpenetrating cubic form. There is also evidence that at still higher concentrations, above 200 ppm, the Ba^{2+} is still soluble in the lattice but the slope of the (σ) versus (c) plot in this region suggests that the Ba^{2+} is forming large impurity-vacancy complexes.

The activation energies observed in this region do, in fact, correspond to the mode of conduction proposed above. In this high temperature region the thermal vacancy concentration, at the impurity concentration used in the experiments, is by no means negligible. For example, at the impurity concentration of 100 ppm,

the average contribution of thermal vacancies to the conductivity is approximately 20 per cent. The activation energy decreases with increasing impurity concentration indicating an increase in impurity-vacancy concantration and a corresponding decrease in the thermal vacancy contribution. The minimum activation energy is observed in the region 150 ppm. Since the activation energy averages the results in this region, the value of 150 ppm is in good agreement with the previously suggested values for the solubility limits. It was previously suggested that more impurity dissolution takes place at these higher temperatures with the formation of impurity-vacancy aggregates. Under these circumstances the conductivity is given by

$$\sigma = \underbrace{\sigma_1 \exp(-U/kT)}_{\text{free vacancies}} + \underbrace{\sigma_2 \exp((-U+\tfrac{1}{2}W_s)/kT)}_{\text{impurity dissolution}}$$

where W_s is the solubility energy for Ba^{2+}. The activation energy would therefore be expected to increase as the second term increases in importance. The crystal containing 280 ppm Ba^{2+}, the maximum concentration, does exhibit a decrease in activation energy above 1.4 r.t.u. which may indicate that all the impurity has dissolved in the lattice at this temperature (Graph 24).

The self-diffusion results in Ba^{2+}-doped crystals are in general agreement with the proposed mechanism. In region I both cation and anion self-diffusion are apparently unaffected by impurity-doping. At higher temperatures, (regions II and III), the chloride ion diffusion is decreased and the caesium ion diffusion increased by the presence of Ba^{2+}, Graphs (41) and (44). (It should be noted that the result for 167 ppm in the latter graph is above the transition point). This is in accord with the impurity dissolving in the lattice at these higher temperatures, thus increasing the cation vacancy concentration and decreasing the anion vacancy concentration.

The results from the Ba^{2+}-doped crystals are also of interest in that they provide information about the nature of the intrinsic defects in caesium chloride. The theoretical treatment of the minimum in the conductivity curve is equally applicable to vacancy or interstitial migration. However, a decision between the two mechanisms can be made on the basis of equation (7)

$$n_1 n_2 = n_o^2$$

which can be rewritten for a pure crystal as

$$n_1 = n_2 = n_o = \text{const.}\exp(-W/2kT) \quad \ldots(40)$$

Differentiation between the two types of intrinsic defects can usually be made by consideration of the value of the pre-exponential factor[98]. Theoretical estimates[99] indicate that values of the constant will be in the order of 10^2-10^4 for Schottky defects, while for Frenkel defects the constant is much smaller. Pre-exponential factors of 10^2 to 10^3 have been calculated for the sodium and potassium halides on the basis of the observed conductivities[100]. Self-diffusion results for CsCl indicate that W - 2.0ev and from the doped crystals' conductivity measurements, a value of 6×10^{-6} at 1.5 r.t.u. has been calculated for n_o. Substitution in equation (40) gives

$$\text{constant} = 1.9 \times 10^2$$

The result confirms that Schottky defects are the predominant intrinsic point defects, as indicated by the self-diffusion studies. The previous discussion on Ba^{2+}-doped crystals made this assumption.

11.3 SO_4^{2-}-doped Crystals.

The general shape of the conductivity graphs for SO_4^{2-}-doped crystals is very similar to that for the Ba^{2+}-doped crystals. Above 300°C., three regions of conductivity are observable and these have been designated by analogy with the Ba^{2+}-doped crystal results. The results for

TABLE 52

Summary table of conductivity results for SO_4^{2-}-doped single crystals of CsCl.

ppm. SO_4^{2-}	E_A in region I (ev)	σT @ 1.7 ^oA. ($ohm^{-1}cm^{-1}$)	Amt. of rise in region II	E_A in region III (ev)	σT @ 1.5 ($ohm^{-1}cm^{-1}$)	σT @ 1.4 ^oA.
'Pure'	1.395	1.5×10^{-4}	none	1.395	3.6×10^{-3}	1.9×10^{-2}
83	1.40	1.1×10^{-4}	1.8	1.09	4.2×10^{-3}	1.5×10^{-2}
100	0.66	1.3×10^{-4}	none	1.43	1.0×10^{-3}	5.3×10^{-3}
120	1.39	7.4×10^{-5}	4.0	0.96	4.2×10^{-3}	1.3×10^{-2}
137	1.15	1.2×10^{-4}	3.6	0.92	5.1×10^{-3}	1.5×10^{-2}
150	1.38	8.4×10^{-5}	3.8	0.87	5.1×10^{-3}	1.4×10^{-2}
212	1.44	4.2×10^{-5}	6.3	0.78	4.7×10^{-3}	1.1×10^{-2}
274	1.40	2.2×10^{-5}	10.0	0.40	5.4×10^{-4}	1.5×10^{-2}
437	1.37	2.1×10^{-5}	4.0	1.10	2.8×10^{-3}	1.0×10^{-2}

the sulphate-doped crystals are summarized in Table 52.

In region I, the activation energy is the same as for the pure crystals, but there is a general decrease in conductivity as the sulphate concentration is increased, Graph (56). The conductivity decreases to one third that of a pure crystal and the magnitude of this decrease is such that it could not be accounted for by experimental error.

The addition of sulphate, therefore, must be reducing the thermal vacancy concentration without changing the mode of conduction. The radius of the SO_4^{2-} ion, based on thermochemical data[101], has been estimated to be approximately 2.3Å. The SO_4^{2-} ion will, therefore, require a much larger volume in the crystal lattice than the Cl^- ion (radius 1.81Å) which it is replacing. A comparison of the ionic volumes gives

$$\frac{\text{sulphate volume}}{\text{chloride volume}} = \left(\frac{2.3}{1.81}\right)^3 = 2.05$$

The substitution of SO_4^{2-} for Cl^- in the lattice will increase the concentration of anion vacancies in order to satisfy electroneutrality requirements, but the SO_4^{2-} will probably occupy two Cl^- ion lattice sites, i.e. the sulphate ion will occupy both the chloride ion site and the vacancy it has created. This

GRAPH 56

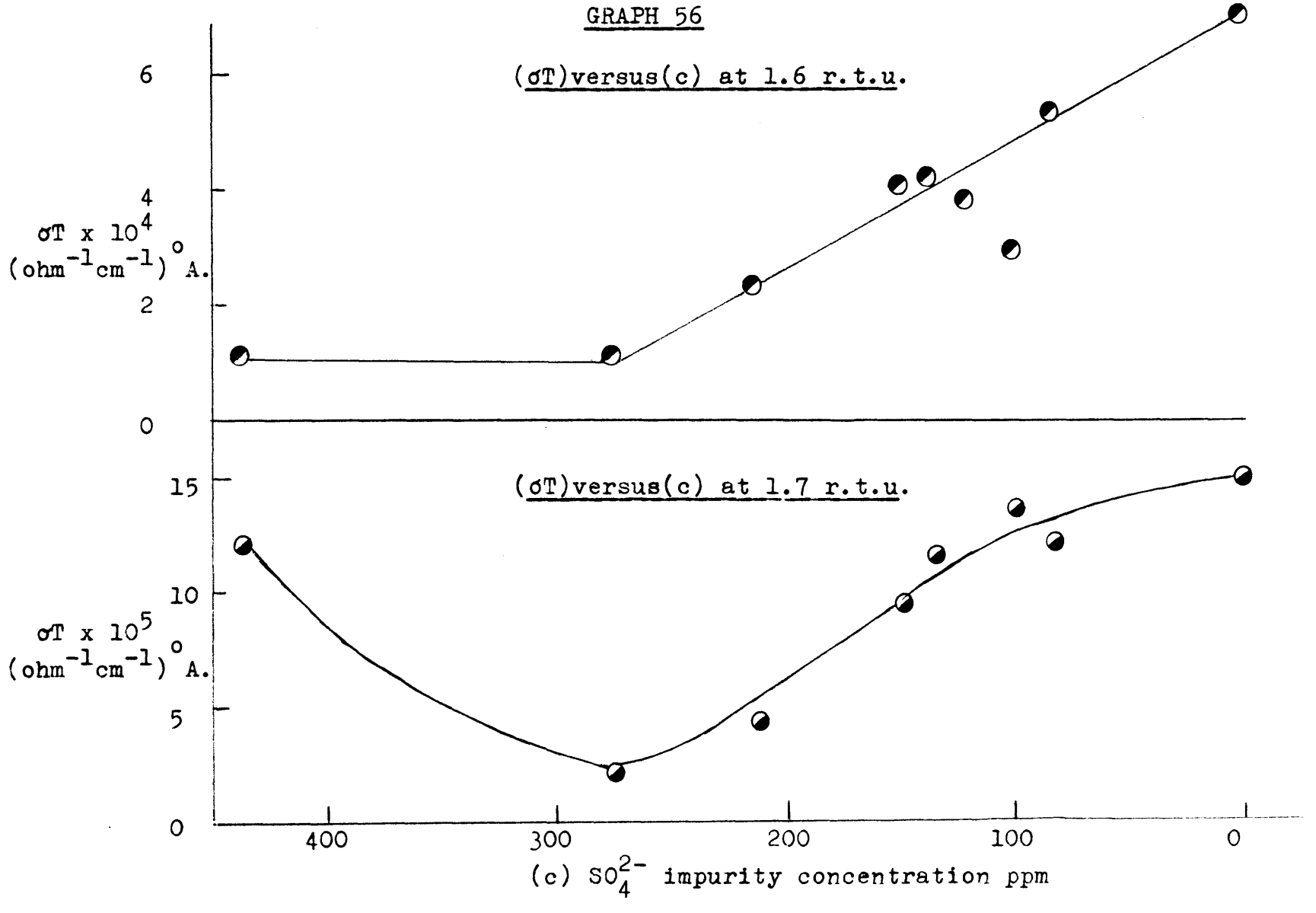
(σT)versus(c) at 1.6 r.t.u.
6
4
2
0
σT x 10^4
(ohm^-1cm^-1)°A.
(σT)versus(c) at 1.7 r.t.u.
15
10
5
0
σT x 10^5
(ohm^-1cm^-1)°A.
400
300
200
100
0
(c) SO4^2- impurity concentration ppm

has also been suggested by Gruzensky and Scott[102] to account for the effects of sulphate-doping on the conductivity of KCl. Thus the impurity induced vacancies will not be available for conduction, but the concentration of thermal vacancies will be depressed.

If we examine the quantitative aspect of sulphate-doping in region I, then from equation (31),

$$n_1 n_2 = n_o^2$$

Addition of mole fraction c_2 of sulphate will increase n_2 but decrease n_1. However, in order to retain electroneutrality, the thermal cation and thermal anion vacancy concentration will be depressed to the same extent. Equation (31) can be written in the form

$$n_t(n_t + c_2) = n_o^2$$

where n_t is the thermal vacancy (anion or cation) concentration in the presence of c_2 mole fraction of sulphate. When $c_2 \gg n_t$ (this should be true in region I),

$$n_t c_2 = n_o^2 \quad \text{or} \quad n_t \propto (1/c_2)$$

In region I the conductivity is essentially anionic. From our self-diffusion results D_{Cl^-} / D_{Cs^+} =9.3 and 6.4 at 1.7 and 1.6 r.t.u. respectively. If the proposal that sulphate ion requires the induced vacancy and, therefore, this does not contribute to the conductivity,

GRAPH 57

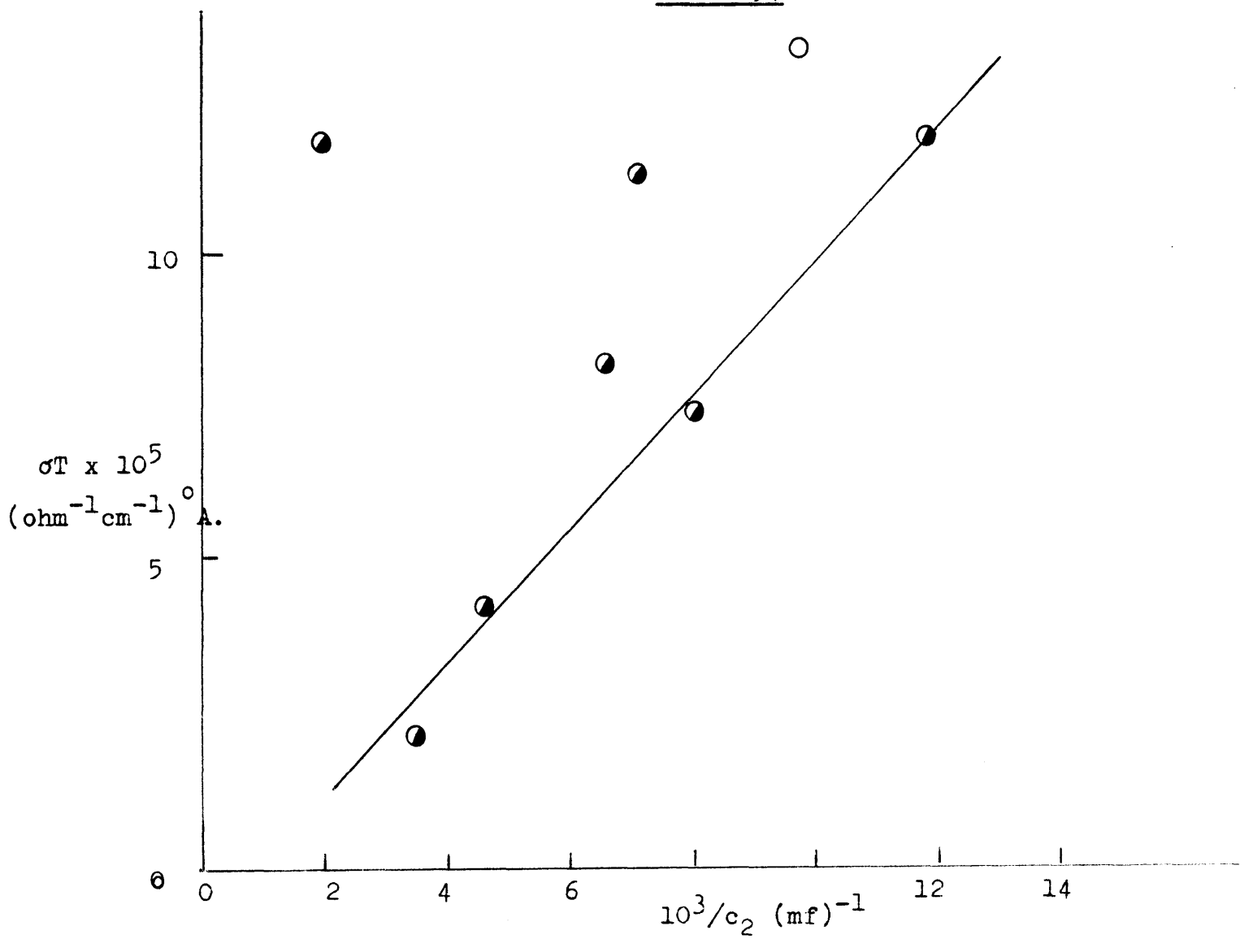

GRAPH 58

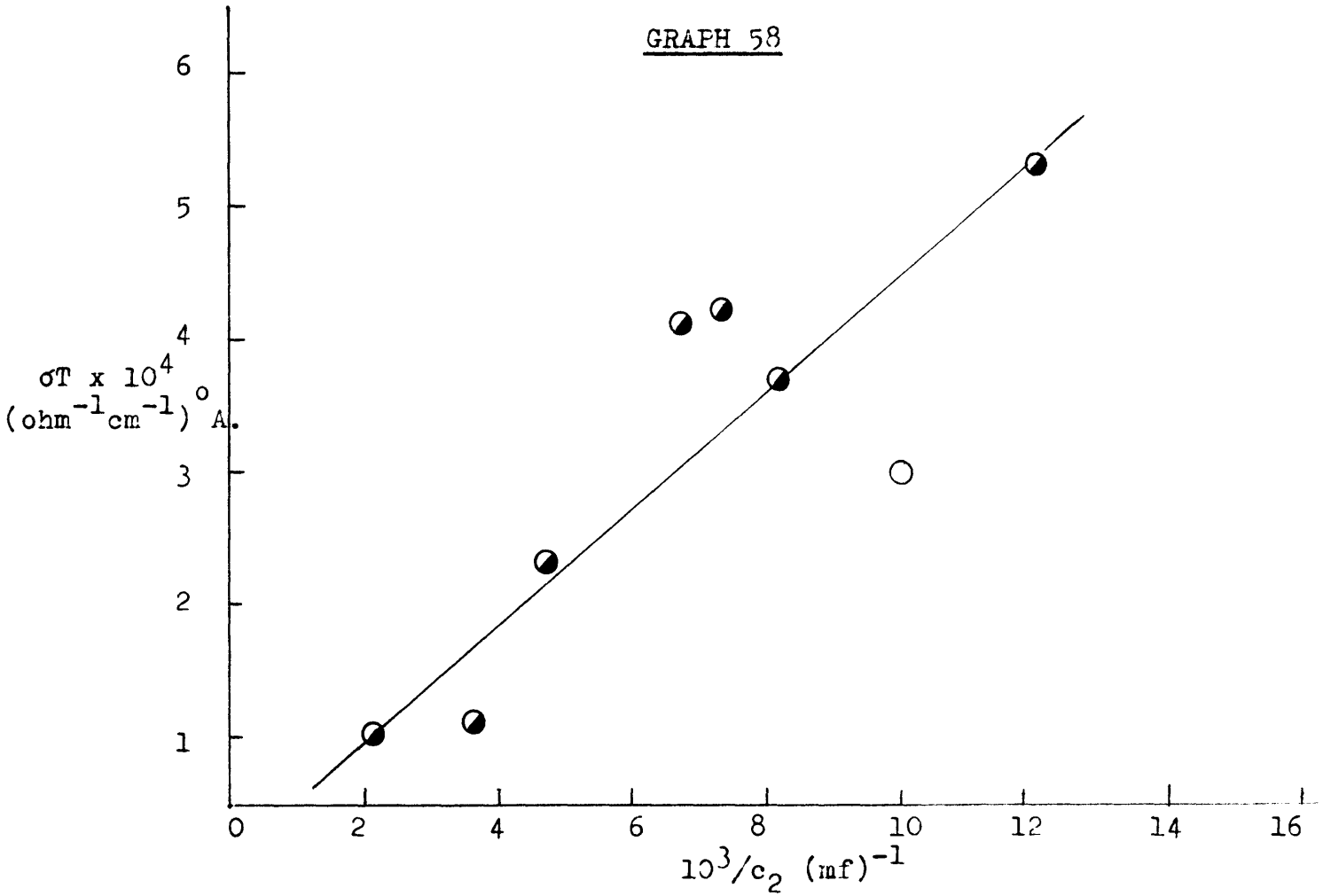

is correct, then

$$\sigma \propto n_t \propto (1/c_2)$$

Plots of(σT) against $(1/c_2)$ at 1.7 and 1.6 r.t.u. are shown in Graphs (57) and (58). The above relationship appears to be approximately true in this region with the exception of the crystal containing 100 ppm (marked o in the graphs). This crystal does not show any conduction behaviour typical of sulphate-doping. The results of the highest SO_4^{2-}-doping (437 ppm) are also anomalous.

It would appear, therefore, that a substantial amount of the impurity in this case is present as a second phase. If this is present as large second phase aggregates, then the general solubility relationships may not be valid. The impurity may be less soluble with these large aggregates present than it would be if the second phase was more uniformly distributed. The results indicate that at higher temperatures (1.6 r.t.u.) thesulphate ion is more soluble as would be expected.

The conductivity results in this region can, therefore, be interpreted in terms of the sulphate ion creating impurity-induced vacancies, which are not available for ion migration, and depressing the thermal vacancy

concentration. It would be expected, therefore, that SO_4^{2-}-doping would depress both the anion and the cation self-diffusion in this region. The present diffusion results are in agreement with this proposal. Cl-36 diffusion is usually less in doped than in pure crystals in this region, (Graph (42)), and although very few results have been obtained for Cs-137 diffusion, the diffusion coefficents are generally smaller than for pure crystals (Graph (44)).

In region II a very rapid increase in conductivity is observed. This increase usually occurs at approximately the same temperature with the exception of the crystal containing 274 ppm; the increase in this case occurs at approximately 50° higher temperature. The crystal containing 100 ppm of SO_4^{2-} is again anomalous in that no rapid increase is observed.

It is of interest to note that the extent of the sharp increase appears to be correlated to the value of conductivity of the pure crystal at that particular temperature. In Table 53 the values of conductivity at the temperature marking the end of the increase are compared with the values for the pure crystal at the corresponding temperature.

TABLE 53

ppm SO_4^{2-}	final (σT) in region II	$10^3/T^oA$	(σT) for pure crystal at this temperature.
83	3.0×10^{-3}	1.53	2.5×10^{-3}
100	----	----	----
120	3.0×10^{-3}	1.53	2.5×10^{-3}
137	4.0×10^{-3}	1.52	3.0×10^{-3}
150	3.0×10^{-3}	1.55	2.0×10^{-3}
212	3.0×10^{-3}	1.55	2.0×10^{-3}
274	1.4×10^{-2}	1.42	1.4×10^{-2}
437	6.0×10^{-2}	1.44	1.0×10^{-2}

The extent of the rapid increase usually brings the conductivity to a value slightly greater than the conductivity of the pure crystal. The reason for this may be that the thermal vacancy concentration at this temperature is greatly in excess of the concentration of impurity induced vacancies and, consequently, the crystal is behaving as a pure crystal, i.e. intrinsic conduction. The activation energies, however, observed in region III, and the results of the Ba^{2+}-doped crystals do not support this view.

The rapid increase in conductivity probably arises because in this region the lattice expansion may be sufficient to accomodate some of the SO_4^{2-} ions in single lattice positions, the release of the associated

vacancies producing the observed increase in conductivity. As with the Ba^{2+}-doped crystals, the rate of increase is somewhat unexpected.

Since anion mobility is appreciably greater than cation mobility, ($D_{Cl^-} / D_{Cs^+} \simeq 5$), one would expect the release of anion vacancies to raise the conductivity above that of the pure crystal. The observed activation energies in region III (Table 52) indicate that the majority of the sulphate is still present as impurity complexes. Consequently, the increase in region II is due to dissociation of only a small fraction of the impurity-vacancy complexes. In region III, the activation energy decreases with increasing sulphate concentration as would be expected. The calculations for the Ba^{2+}-doped crystals indicate that the thermal vacancy contribution in this region is by no means negligible and so the conductivity in this region can be written as,

$$\sigma = \underset{\substack{\text{sulphate impurity-}\\\text{created vacancies}}}{\sigma_1 \exp(-0.3/kT)} + \underset{\substack{\text{thermal}\\\text{vacancies}}}{\sigma_2 \exp(-1.39/kT)}$$

As the impurity concentration increases the first term should become increasingly important and, therefore, a decrease in activation energy would be expected and is observed. The fact that the increase in conductivity

TABLE 54

	Impurity content (ppm)	Low temperature activation energy (ev)	σT @ 1.9 r.t.u. $(ohm^{-1}cm^{-1})^{o}A$.
($\underline{Ba^{2+}}$)	57	1.03	9.3×10^{-6}
	62	0.91	7.6×10^{-6}
	71	0.78	1.4×10^{-4}
	85	0.93	4.7×10^{-6}
	97	0.95	4.5×10^{-5}
	104	0.84	4.0×10^{-5}
	133	0.82	3.2×10^{-5}
	?	0.81	9.3×10^{-6}
	153	0.88	1.1×10^{-5}
	167	0.65	2.1×10^{-5}
	196	----	-----
	234	1.12	7.8×10^{-6}
	260	0.60	4.9×10^{-5}
	280	1.08	1.8×10^{-5}
($\underline{Ca^{2+}}$)	125	0.97	4.0×10^{-6}
($\underline{SO_4^{2-}}$)	83	----	-----
	100	0.66	2.8×10^{-5}
	120	----	-----
	137	1.15	8.0×10^{-6}
	150	1.03	5.7×10^{-6}
	212	----	-----
	274	1.13	-----
	437	----	1.0×10^{-6}

at 1.5 r.t.u. is very much smaller than would be predicted by equation (36), again indicates that the vacancies are mainly associated. In fact, at 1.4 r.t.u. the conductivity is essentially constant and independent of impurity concentration. One possible reason for this may be that the disparity in sizes of the host and impurity ions is still of extreme significance. As the concentration of unassociated impurity ions increases the resulting increase in strain in the lattice in the neighbourhood of these ions may be such that ionic mobility is decreased in these regions. Further experimental investigation of crystals containing large amounts of sulphate ion is required.

11.4 Conductivity measurements on impurity-doped crystals in the temperature range below 300°C.

In this low temperatureregion there is a large variation in both the magnitude of conduction and its activation energy in both Ba^{2+} and SO_4^{2-}-doped crystals. This is illustrated in Table 54.

On the basis of the conductivity results for other caesium halides[55] it would have been expected that activation energies of 0.6 and 0.3eV would have been observed for $Ba^{2+}$and SO_4^{2-}-doping respectively. Three possible reasons for the non-reproducible behaviour will be discussed.

(i) The effect of dislocations.

It has been observed[49] that, in the alkali halides at low temperatures, the anion diffusion, i.e. the less mobile ion, is critically dependent upon the dislocation density. This has been attributed to the space charge around the dislocations[33]. When there is a substantial difference in anion and cation vacancy mobility, the slower moving vacancies tend to be concentrated around dislocations. While this may be valid for the other alkali halides, where the difference in anion and cation diffusion may be as great as 10^3, the existence of a significant charge on the dislocations in the caesium halides is unlikely since the anion and the cation diffusion coefficients are comparable (D_{Cl^-} / D_{Cs^+} = 0.05 in this temperature region). It would be expected that if the caesium ion diffusion was dependent on dislocations, the effects of the latter would be insignificant and so the observed disparities cannot be accounted for in this way. It should be noted that in the discussion of the conductivity results at higher temperatures the effect of dislocations was not considered for these reasons.

(ii) Electronic conductivity.

It has been suggested[53,54] that there is a substantial electronic contribution to the conductivity because of the presence of O^{2-} impurity. Although more recent results

have shown that this is unlikely at high temperatures[60], there could still be some electronic conduction at lower temperatures. Conductivity measurements on the γ-ray irradiated crystals, which did contain colour centres, (Graphs 6a and 7a), show that the activation energy for electronic conductivity is approximately 0.25eV. Consequently, a significant electronic contribution in doped crystals would have resulted in much lower activation energies than have been observed.

(iii) 'Frozen-in' defects.

It has been observed that a number of Ba^{2+}-doped crystals have a very high initial conductivity but after some heating there is a significant decrease in the conductivity (e.g. 71 ppm - Graph 13 and 153 ppm - Graph 19). Extrapolation of this anomalously high conductivity region indicates that it is an extension of region III. The Ba^{2+} solubility appears to be greatly in excess of the low temperature equilibrium solubility. Heating of the crystal restores the equilibrium as the Ba^{2+} is precipitated out as a second phase. This type of behaviour is also observed in other Ba^{2+}-doped crystals (Graphs 21 and 23). Further evidence of the possibility of producing impurity created vacancies above equilibrium concentrations is shown by the 'chilled' crystal measurements (Graphs 9 and 10). It is suggested that the anomalous behaviour of the

crystals in this low temperature region, and even at higher temperatures for crystals containing 97, 104 and 133 ppm Ba^{2+} and 100 ppm SO_4^{2-}, is associated with this non-equilibrium phenomenon.

In their preparation, substantial quantities of water are trapped in the crystals. Under these conditions the solubility of impurities in the lattice may be unusually high. During the subsequent treatment for the removal of water, the excess impurity should be precipitated out. If the crystals, however, have insufficient nucleation sites, probably dislocations, for rapid precipitation, the impurity and its vacancy may be 'frozen-in' in the lattice. The conductivity of the crystals would then be time-dependent. A time-dependent conductivity has sometimes been observed in region I, but there is no evidence of this behaviour at higher temperatures.

GRAPH 59 Variation of Transition Temperature with Impurity Concentration.

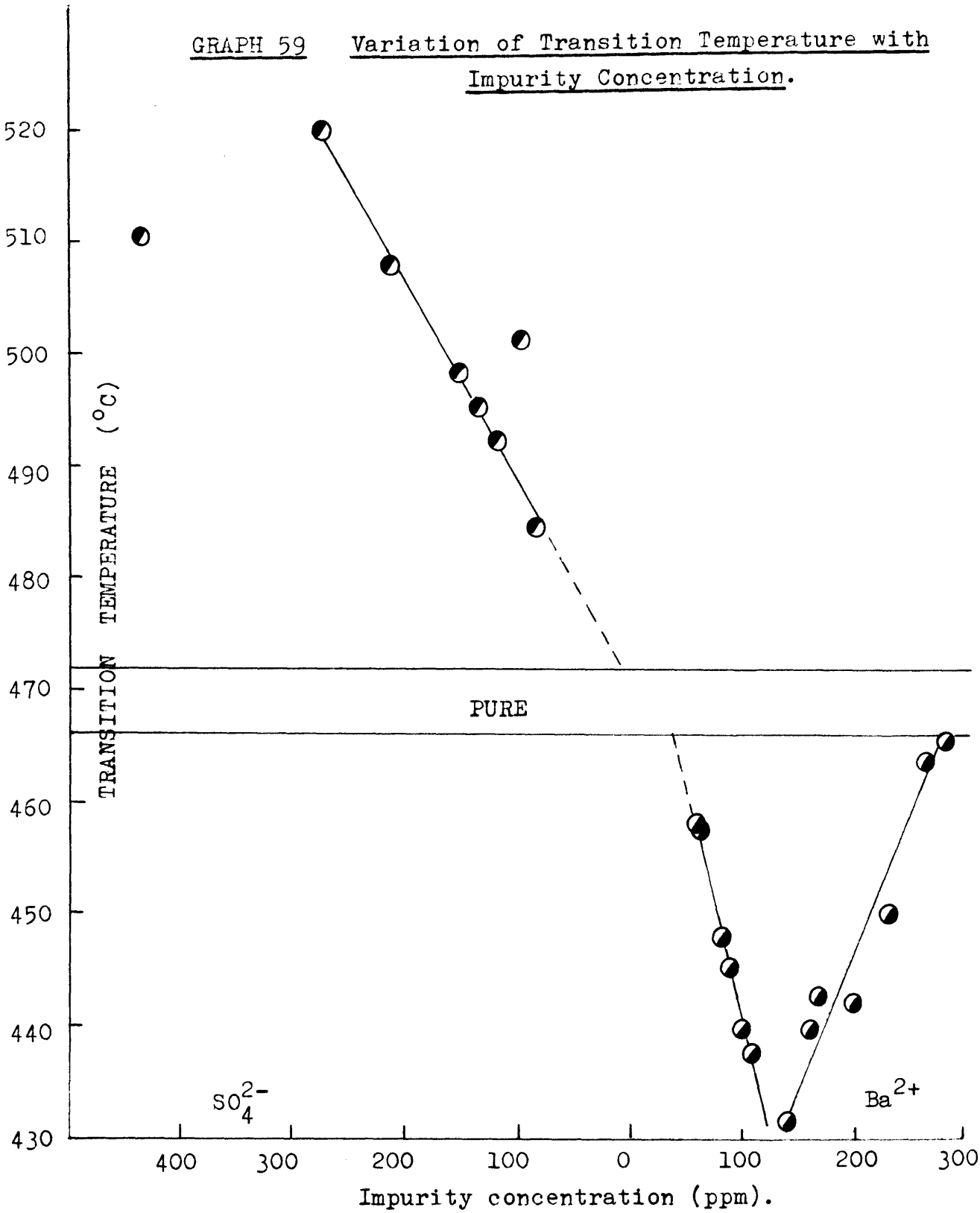

DISCUSSION. CHAPTER 12

THE PHASE TRANSITION IN CAESIUM CHLORIDE.

Studies of the effects of impurities on the transition temperature in caesium chloride have been made using ionic conductivity measurements. The results are summarized in Table 55.

The observed transition temperature in pure crystals is in good agreement with the results of the more recent investigations[60,70-72]. Both the transition temperature and the value of the conductivity at the transition are unaffected by the method of preparation of the crystal, annealing and γ-irradiation. The effect of Ba^{2+}-doping is to decrease the transition temperature, a minimum being observed at approximately 130 ppm. Further additions of Ba^{2+} reverse this trend and the transition temperature increases. The addition of SO_4^{2-} increases the transition temperature and there may be a maximum value above 300 ppm, Graph 59.

If the transition is associated with dislocations in the crystal, i.e. these gross defects acting as nucleation sites, then the effects of the impurity-doping are explicable only if there is a significant space charge on the dislocations. In sodium chloride it has been observed that the addition of divalent cation reduces the space charge and with enough impurity

TABLE 55

Crystal (ppm)	Temperature at beginning of transition (°C)	Temperature at completion of transition (°C)	σT @ beginning of transition (ohm^{-1}cm^{-1}) A.	Hysteresis range (°C)
Pure 1a	469	472	3.93×10^{-2}	21
Pure 1b	469	474	4.74×10^{-2}	20
Pure 1c	467	475	4.20×10^{-2}	16
Pure 2	472	---	3.72×10^{-2}	--
Pure 3	471	480	4.76×10^{-2}	16
Pure 4	469	475	4.40×10^{-2}	21
Pure 4a	469	473	4.57×10^{-2}	--
Pure 5	468	---	4.53×10^{-2}	--
Pure 6	467	472	4.39×10^{-2}	--
Pure 6a	466	474	4.11×10^{-2}	--
Pure 7	470	---	3.60×10^{-2}	--
Pure 7a	470	471	3.80×10^{-2}	--
Pure 8	467	471	3.79×10^{-2}	--
Ba^{2+} (57)	458	---	2.61×10^{-2}	--
Ba^{2+} (62)	456	469-484	3.27×10^{-2}	27
Ba^{2+} (71)	448	487	2.70×10^{-2}	49
Ba^{2+} (85)	445	473	2.41×10^{-2}	--
Ba^{2+} (97)	440	490	2.20×10^{-2}	--
Ba^{2+} (104)	437	460	2.04×10^{-2}	27
Ca^{2+} (125)	436	484	2.21×10^{-2}	--

TABLE 55 (continued)

Crystal (ppm)	Temperature at beginning of transition (°C)	Temperature at completion of transition (°C)	σT @ beginning of transition $(ohm^{-1}cm^{-1})^{\circ}A$	Hysteresis Range (°C)
Ba^{2+} (133)	432	---	1.76×10^{-2}	--
Ba^{2+} (?)	418	482	1.59×10^{-2}	27
Ba^{2+} (153)	439	464	1.96×10^{-2}	--
Ba^{2+} (167)	443	483	2.30×10^{-2}	52
Ba^{2+} (196)	442	479	2.38×10^{-2}	--
Ba^{2+} (234)	450	---	3.16×10^{-2}	--
Ba^{2+} (260)	463	471	3.97×10^{-2}	--
Ba^{2+} (280)	465	475	3.95×10^{-2}	--
SO_4^{2-} (83)	484	502	4.03×10^{-2}	--
SO_4^{2-} (100)	502	523	3.56×10^{-2}	--
SO_4^{2-} (120)	492	504	3.51×10^{-2}	--
SO_4^{2-} (137)	495	528	4.32×10^{-2}	55
SO_4^{2-} (150)	498	527	4.16×10^{-2}	54
SO_4^{2-} (212)	508	546	3.12×10^{-2}	--
SO_4^{2-} (274)	520	554	2.81×10^{-2}	84
SO_4^{2-} (437)	510	560	4.70×10^{-2}	62
Sr^{2+} (<5)	468	469	4.84×10^{-2}	--
KCl-CsCl	467	473	1.33×10^{-5} (1/R)	--
CsI-CsCl	466	469	3.62×10^{-5} (1/R)	--

the sign of the space charge can be reversed[33]. As shown earlier in this discussion, however, the space charge on dislocations at the transition temperature must be extremely small, if it indeed exists at all. Furthermore, the trend of transition temperature with impurity content would indicate, on this basis, that the minimum occurs when there is a maximum negative charge on the dislocations. It would also be expected that if dislocations are of major importance, that the transition temperature would be dependent upon the mechanical perfection of the crystal. The results for the pure crystals from various sources do not show evidence of any such dependence.

It has also been suggested that the phase transition temperature depends upon the fact that there is always present in the crystal, at low temperatures, a small amount of the high temperature form, and that the transition temperature is determined by the concentration of this high temperature form[102a]. While this has been shown to be possible in caesium chloride by the addition of other alkali halides[72,76], the amount of impurity required to cause comparable changes to those observed in the present investigation is approximately 50 mole per cent. We have shown that small amounts 1 of CsI (s.i.c. lattice) and KCl (f.c.c. lattice) do not cause significant changes in the transition temperature.

The results indicate, therefore, that the effect of impurity is associated solely with the difference in charge of the impurity ion from the host lattice. The size of the impurity ion cannot be significant since the Ca^{2+}-doped crystal ($R_{Ca^{2+}} = 0.99\text{Å}$) results are in good agreement with the effect of corresponding amounts of Ba^{2+}.

It is interesting to note that the reverse transition, i.e. f.c.c. to s.i.c., can be brought about in other alkali halides by application of high pressures[103]. The s.i.c. lattice must, therefore, be a much closer packed arrangement and hence it would be expected that the s.i.c. to f.c.c. transition would occur when there is a certain amount of 'free-space' in the crystal.

The addition of aliovalent impurity ions does produce vacancies, but owing to the effects discussed earlier the vacancy concentration remains constant (equation 31). The trend of transition temperature can only be explained, and then only partially, if a certain concentration of cation vacancies is required for the transition to occur. The effect of sulphate addition would be to reduce the cation vacancy concentration and therefore higher temperatures would be required before the cation vacancy concentration is sufficient to permit the transition to proceed. Ba^{2+}-doping would decrease the transition temperature but a minimum should

not be observed. Even if 130 ppm represented the maximum solubility of Ba^{2+} in the lattice, the transition temperature should then remain constant and not increase with higher Ba^{2+} concentrations. Furthermore, the low heat of transition (700 cal $mole^{-1}$)[73] would suggest that the transition requires only small readjustments of both ions and not the extensive rearrangement of only the cation lattice.

The evidence suggests that the transition requires the concerted movement of both ions and hence would be determined by the temperature at which both the cation and the anion are sufficiently mobile to take up the new f.c.c. lattice positions.

One would expect the ion movement to be related to the vacancy concentrations and the mobilities of the ions. The mobility will not be that which has been determined for the s.i.c. lattice since the ion jump is now to intermediate positions; but it is to be expected that this new jump frequency will be related to ion mobility in the s.i.c. lattice. Let us suppose that for the transition to occur, $n_1\mu_1 \geq k_1$ and $n_2\mu_2 \geq k_2$ We are imposing the condition that at the transition, the ion movement, $(n\mu)$ for both anion and cation, must be equal to or above a certain minimum value (k). Because of the small differences in ionic radii of the

Cs^+ (1.69Å) and the Cl^- (1.81Å) it would not be expected that $k_1 = k_2$, but they should not differ by a large extent.

The results of the self-diffusion studies indicate that in a pure crystal at temperature of transition,

$$D_{Cl^-} / D_{Cs^+} \simeq 3$$

We would infer from this that the rate of movement of the chloride ion is above the minimum requirements for the transition and so the transition is determined by the temperature at which the cation movement condition is satisfied, i.e. for the pure crystal at the transition,

$$n_1u_1 = k_1 \quad \text{and} \quad n_2u_2 > k_2$$

The effect of Ba^{2+}-doping is to increase n_1 and decrease n_2. Hence, the temperature at which the cation movement condition is satisfied will decrease. The transition temperature, therefore, will decrease provided the anion movement (n_2u_2) is sufficently large to be equal to or greater than (k_2) at the temperature at which $n_1u_1 = k_1$ is satisfied. On this basis, the experimentally observed lowering of the magnitude of the conductivity at the transition can be explained. However, with still larger concentrations of Ba^{2+}, n_1 will be increased and n_2 decreased to such an extent that at the temperature at which $n_1u_1 = k_1$, $n_2u_2 < k_2$. In other words, the transition temperature will then increase because higher temperatures are required before the anion movement is

condition is satisfied, i.e. in this region the transition occurs when

$$n_1\mu_1 > k_1 \qquad \text{and} \quad n_2\mu_2 = k_2$$

It follows that the minimum transition temperature will be observed when both anion and cation conditions are just satisfied, i.e.

$$n_1\mu_1 = k_1 \quad \text{and} \quad n_2\mu_2 = k_2$$

Since the conductivity is given by

$$\sigma = Ne(n_1\mu_1 + n_2\mu_2)$$

the minimum conductivity should be obtained at the minimum transition temperature. This is observed experimentally (see Table 55).

The effect of sulphate-doping will be to increase n_2 and decrease n_1. The transition, therefore, will occur at higher temperatures than in the pure crystal The transition will be determined by the temperature at which the cation condition is satisfied, i.e. for sulphate-doped crystals at the transition,

$$n_1u_1 = k_1 \qquad \text{and} \quad n_2u_2 > k_2$$

A decrease in the transition temperature would not be expected at large sulphate concentrations (437 ppm). If the solubility limit was exceeded, as the conductivity results for this crystal indicate, the transition

temperature should remain at the maximum value. More experimental observations at high concentrations are required to determine whether this one result is valid.

The presence of small amounts of divalent impurity would explain the variation in transition temperature observed by earlier workers[65-69]. It is of interest to note that the results of Ubbelohde et al[53,54] may, on the basis of the above argument, now be partially explained. Although these authors reported that the transition at 469°C was investigated, their actual conductivity plots show that the transition starts at about 460°C. Furthermore, the activation energy obtained, 1.04ev, was measured above 330°C. This corresponds approximately to what we have designated regions II and III. Our measurements have indicated that an activation energy of 1.00ev in region III precedes the transition at 458°C when 57 ppm of Ba^{2+} impurity are present.

In conclusion, we should also like to point out that the proposed mechanism could account for the effects of impurities on the transition temperature in other crystals. It has been observed that the replacement of Ti^{4+} ions by Fe^{3+} ions causes a decrease in the cubic-tetragonal transition temperature of barium titanate[104]. This substitution should lead to an increase in the

concentration of negative ion vacancies. It has also been reported recently that the rate of phase transformation from anatase to rutile is dependent upon the TiO_2 defect structure[105]. Addition of CuO accelerates the transformation possibly by the creation of O^{2-} vacancies.

APPENDIX A.

Pure CsCl. Graph 1a.

T °C	1/T x 10^{-3} °A	σ(ohm^{-1}cm^{-1})	σT(ohm^{-1}cm^{-1}) °A.
230	1.988	6.74 x 10^{-9}	3.39 x 10^{-6}
245	1.931	1.15 x 10^{-8}	5.97 x "
259	1.880	2.00 x "	1.06 x 10^{-5}
267	1.852	2.93 x "	1.58 x "
277	1.818	4.18 x "	2.30 x "
288	1.787	7.70 x "	4.32 x "
302	1.739	1.45 x 10^{-7}	8.33 x "
315	1.701	2.55 x "	1.50 x 10^{-4}
322	1.681	3.51 x "	2.14 x "
337	1.639	6.31 x "	3.85 x "
352	1.600	1.12 x 10^{-6}	6.97 x "
364	1.570	1.73 x "	1.10 x 10^{-3}
377	1.538	3.08 x "	2.00 x "
393	1.502	5.60 x "	3.73 x "
413	1.458	1.07 x 10^{-5}	7.30 x "
440	1.403	2.43 x "	1.73 x 10^{-2}
456	1.372	3.54 x "	2.58 x "
469	1.348	5.30 x "	3.93 x "
472	1.342	5.60 x 10^{-6}	4.17 x 10^{-3}
486	1.318	6.18 x "	4.70 x "
	Cooling		
467	1.351	4.67 x 10^{-6}	3.45 x 10^{-3}
455	1.374	4.12 x "	3.00 x "
451	1.381	2.76 x 10^{-5}	2.00 x 10^{-2}
436	1.410	1.93 x "	1.37 x "

.o.o.o.o.o.o.o.o.o.o.o.o.o.o.o.o.

Graph 1b. Pure CsCl

T °C	1/T x 10^{-3} °A	σ(ohm^{-1}cm^{-1})	σT(ohm^{-1}cm^{-1}) °A.
221	2.028	8.20 x 10^{-9}	4.04 x 10^{-6}
240	1.949	1.49 x 10^{-8}	7.64 x "
261	1.873	3.25 x "	1.74 x 10^{-5}
279	1.812	6.21 x "	3.43 x "
299	1.748	1.63 x 10^{-7}	9.44 x "
316	1.698	3.00 x "	1.77 x 10^{-4}
331	1.656	6.47 x "	3.91 x "
350	1.605	1.05 x 10^{-6}	6.54 x "
374	1.546	3.22 x "	2.18 x 10^{-3}
400	1.486	8.21 x "	5.56 x "
416	1.451	1.40 x 10^{-5}	9.65 x "
430	1.422	2.40 x "	1.69 x 10^{-2}
452	1.379	4.08 x "	2.98 x "
469	1.346	6.41 x "	4.74 x "
474	1.339	6.25 x 10^{-6}	4.67 x 10^{-3}
491	1.309	8.35 x "	6.38 x "
512	1.274	1.14 x 10^{-5}	9.00 x "
	Cooling		
494	1.304	9.10 x 10^{-6}	6.98 x 10^{-3}
473	1.341	6.50 x "	4.85 x "
461	1.362	5.58 x "	4.10 x "
457	1.370	3.30 x 10^{-2}	2.41 x 10^{-2}
428	1.427	2.08 x "	1.46 x "
409	1.466	1.26 x "	8.22 x 10^{-3}
381	1.529	3.98 x 10^{-6}	2.60 x "

.o.o.o.o.o.o.o.o.o.o.o.o.o.o.o.o.

Pure CsCl. Graph 1c.

T °C	1/T x 10^{-3} °A	σ(ohm^{-1}cm^{-1})	σT(ohm^{-1}cm^{-1}) °A.
190	2.160	1.38 x 10^{-9}	6.32 x 10^{-7}
203	2.101	2.70 x "	1.28 x 10^{-6}
227	2.000	6.90 x "	3.45 x "
237	1.961	9.90 x "	5.06 x "
248	1.919	1.56 x 10^{-8}	8.13 x "
265	1.859	3.00 x "	1.61 x 10^{-5}
290	1.776	1.00 x 10^{-7}	5.63 x "
313	1.706	2.52 x "	1.46 x 10^{-4}
330	1.658	5.71 x "	3.44 x "
348	1.610	1.03 x 10^{-6}	6.23 x "
358	1.585	1.81 x "	1.13 x 10^{-3}
379	1.534	4.14 x "	2.52 x "
	Left overnight		
369	1.558	3.33 x 10^{-6}	2.14 x 10^{-3}
385	1.520	5.00 x "	3.29 x "
405	1.475	9.00 x "	6.10 x "
411	1.462	1.17 x 10^{-5}	8.00 x "
427	1.429	1.82 x "	1.27 x 10^{-2}
439	1.404	2.67 x "	1.90 x "
449	1.385	3.60 x "	2.59 x "
458	1.368	4.56 x "	3.33 x "
467	1.351	5.78 x "	4.20 x "
473	1.340	1.20 x "	8.95 x 10^{-3}
475	1.337	5.25 x 10^{-6}	3.93 x "
489	1.312	6.54 x "	4.34 x "
	C6oling		
480	1.328	5.70 x 10^{-6}	4.29 x 10^{-3}
468	1.350	4.98 x "	3.69 x "
468	1.350	9.60 x "	7.08 x "
455	1.374	2.61 x 10^{-5}	1.90 x 10^{-2}
433	1.416	2.16 x "	1.52 x "

.o.o.o.o. o.o.o.o.o.o.o.o.o.o.o.

Pure CsCl. Graph 2.

$T^{o}C.$	$1/_{T} \times 10^{-3}\ ^{o}A.$	σ ($ohm^{-1}cm^{-1}$)	$\sigma T.$ ($ohm^{-1}cm^{-1}$)^{o}A
229	1.992	3.56×10^{-9}	1.79×10^{-6}
247	1.923	$8.40 \times$ "	$4.37 \times$ "
264	1.862	1.82×10^{-8}	$8.79 \times$ "
281	1.805	$3.74 \times$ "	2.07×10^{-5}
303	1.736	$9.98 \times$ "	$5.75 \times$ "
315	1.701	2.08×10^{-7}	1.18×10^{-4}
324	1.647	$3.60 \times$ "	$2.18 \times$ "
360	1.580	1.30×10^{-6}	$8.23 \times$ "
381	1.529	$2.52 \times$ "	1.05×10^{-3}
405	1.475	$5.71 \times$ "	$3.87 \times$ "
427	1.429	1.08×10^{-5}	$7.56 \times$ "
443	1.397	$1.96 \times$ "	1.40×10^{-2}
457	1.370	$3.11 \times$ "	$2.20 \times$ "
472	1.342	$5.02 \times$ "	$3.72 \times$ "
473	1.341	$3.00 \times$ "	$2.23 \times$ "
	Cooled rapidly to room temperature.		
206	2.088	4.32×10^{-9}	2.07×10^{-6}
217	2.041	$4.80 \times$ "	$2.35 \times$ "
232	1.980	$6.96 \times$ "	$3.51 \times$ "
241	1.946	$8.41 \times$ "	$4.32 \times$ "
261	1.873	1.61×10^{-8}	$8.54 \times$ "
275	1.825	$3.43 \times$ "	1.88×10^{-5}
299	1.728	$7.34 \times$ "	$4.20 \times$ "
	Left overnight in Nitrogen.		
282	1.802	5.91×10^{-8}	3.28×10^{-5}
303	1.742	1.32×10^{-7}	$7.57 \times$ "
323	1.678	$2.88 \times$ "	1.72×10^{-4}
343	1.623	$6.96 \times$ "	$4.29 \times$ "
354	1.595	1.34×10^{-6}	$7.77 \times$ "
376	1.541	$1.93 \times$ "	1.25×10^{-3}
397	1.493	$5.50 \times$ "	$3.70 \times$ "
415	1.453	1.04×10^{-5}	7.15×10^{-3}
424	1.435	$1.36 \times$ "	$9.48 \times$ "
430	1.422	$1.64 \times$ "	1.15×10^{-2}
441	1.401	$2.24 \times$ "	$1.60 \times$ "
448	1.387	$2.64 \times$ "	$1.91 \times$ "
468	1.350	$4.51 \times$ "	$3.34 \times$ "
472	1.342	5.52×10^{-6}	4.11×10^{-3}

Pure CsCl. Graph 2. (cont').

Left overnight in Nitrogen @ 370°C.

369	1.558	1.45×10^{-6}	9.30×10^{-4}
386	1.517	$2.52 \times$ "	1.66×10^{-3}
400	1.486	$3.72 \times$ "	$2.50 \times$ "
411	1.462	$6.24 \times$ "	$4.27 \times$ "
421	1.441	1.20×10^{-5}	$8.33 \times$ "
433	1.416	$1.73 \times$ "	1.22×10^{-2}
440	1.403	$2.15 \times$ "	$1.53 \times$ "
	Cooling.		
430	1.422	1.56×10^{-5}	1.10×10^{-2}
419	1.445	8171×10^{-6}	6.02×10^{-3}
405	1.475	$4.46 \times$ "	$3.03 \times$ "
392	1.504	$2.80 \times$ "	$1.88 \times$ "
366	1.565	$1.20 \times$ "	7.71×10^{-4}
349	1.608	6.37×10^{-7}	$3.97 \times$ "
325	1.672	$2.50 \times$ "	$1.50 \times$ "
310	1.715	$1.19 \times$ "	7.01×10^{-5}
295	1.760	8.90×10^{-8}	$5.05 \times$ "
285	1.792	$6.36 \times$ "	$3.55 \times$ "
273	1.828	$3.50 \times$ "	$1.91 \times$ "
264	1.862	$2.16 \times$ "	$1.16 \times$ "
249	1.916	$1.20 \times$ "	6.76×10^{-6}
237	1.960	8.52×10^{-9}	$4.34 \times$ "
230	1.988	$5.64 \times$ "	$2.84 \times$ ".

.o.o.o.o.o.o.o.o.o.o.o.o.o.o.o.o.o.o.o.o.

Pure CsCl Graph 3.

T°C	$^{1}/_{T} \times 10^{-3}$ °A	σ (ohm^{-1}cm^{-1})	σT (ohm^{-1}cm^{-1})°A.
195	2.137	2.10 x 10^{-9}	9.60 x 10^{-7}
205	2.092	2.94 x "	1.41 x 10^{-6}
213	2.058	4.00 x "	1.94 x "
234	1.972	7.56 x "	3.83 x "
246	1.927	1.26 x 10^{-8}	6.54 x "
255	1.894	1.68 x "	8.87 x "
270	1.842	3.06 x "	1.66 x 10^{-5}
278	1.815	3.86 x "	2.12 x "
297	1.754	8.39 x "	4.79 x "
307	1.724	1.40 x 10^{-7}	8.15 x "
320	1.686	2.50 x "	1.48 x 10^{-4}
328	1.664	3.84 x "	2.30 x "
342	1.626	6.80 x "	4.18 x "
346	1.616	8.79 x "	5.44 x "
362	1.575	1.86 x 10^{-6}	1.18 x 10^{-3}
373	1.548	2.91 x "	1.87 x "
390	1.508	5.17 x "	3.43 x "
400	1.486	7.67 x "	5.17 x "
420	1.443	1.46 x 10^{-5}	1.07 x 10^{-2}
440	1.403	2.73 x "	1.95 x "
457	1.370	4.20 x "	3.06 x "
471	1.344	6.40 x "	4.76 x "
480	1.328	5.84 x 10^{-6}	4.40 x 10^{-3}
494	1.304	7.35 x "	5.63 x "
513	1.272	8.40 x "	6.60 x "
528	1.248	1.18 x 10^{-5}	9.45 x "
545	1.222	1.70 x "	1.39 x 10^{-2}
	Cooling.		
531	1.244	1.31 x 10^{-5}	1.05 x 10^{-2}
513	1.272	9.40 x 10^{-6}	7.39 x 10^{-3}
504	1.287	7.35 x "	5.71 x "
495	1.302	5.67 x "	4.35 x "
477	1.333	5.00 x "	3.75 x "
475	1.337	9.71 x "	7.26 x "
464	1.357	3.61 x 10^{-5}	2.66 x 10^{-2}
456	1.372	2.58 x "	1.88 x "

o.o.o.o.o.o.o.o.o.o.o.o.o.o.o.o.o.o.o

Pure CsCl Graph 4.

$T^{\circ}C$	$^{1}/_{T} \times 10^{-3}{}^{\circ}A$	$\sigma(ohm^{-1}cm^{-1})$	$\sigma T(ohm^{-1}cm^{-1})^{\circ}A.$
216	2.045	5.35×10^{-9}	2.62×10^{-6}
229	1.992	$7.33 \times$ "	$3.68 \times$ "
243	1.538	1.32×10^{-8}	$6.80 \times$ "
259	1.880	$2.48 \times$ "	1.32×10^{-5}
283	1.799	$7.36 \times$ "	$3.09 \times$ "
303	1.736	1.43×10^{-7}	$8.21 \times$ "
326	1.669	$4.51 \times$ "	2.70×10^{-4}
352	1.600	1.28×10^{-6}	$8000 \times$ "
380	1.531	3.54×10^{-6}	2.25×10^{-3}
405	1.475	$8.35 \times$ "	$1.65 \times$ "
442	1.399	2.73×10^{-5}	1.95×10^{-2}
469	1.348	$5.93 \times$ "	$4.40 \times$ "
475	1.337	5.40×10^{-6}	4.04×10^{-3}
488	1.314	$6.64 \times$ "	$5.04 \times$ "
	Cooling for reverse transition.		
479	1.330	4.14×10^{-6}	3.11×10^{-3}
461	1.362	$3.38 \times$ "	$2.48 \times$ "
454	1.376	2.21×10^{-5}	1.61×10^{-2}
433	1.416	$1.81 \times$ "	$1.28 \times$ "
399	1.488	6.89×10^{-6}	4.63×10^{-3}
370	1.555	$2.60 \times$ "	$1.67 \times$ "
348	1.610	$1.16 \times$ "	7.20×10^{-4}
325	1.672	4.11×10^{-7}	$2.46 \times$ "
301	1.742	$1.21 \times$ "	6.93×10^{-5}
281	1.805	6.34×10^{-8}	$3.51 \times$ "
263	1.866	$3.17 \times$ "	$1.70 \times$ "
243	1.938	$1.65 \times$ "	8.51×10^{-6}
229	1.992	9.60×10^{-9}	$4.82 \times$ "
207	2.058	$6.74 \times$ "	$3.24 \times$ "

o.o.o.o.o.o.o.o.o.o.o.o.o.o.o.o.o.o.o.o.o.o.o.o.o

Pure CsCl Graph 4a.

T°C	$^{1}/_{T} \times 10^{-3}$ °A	σ (ohm^{-1}cm^{-1})	σT (ohm^{-1}cm^{-1}) °A.
231	1.984	9.29×10^{-9}	4.68×10^{-6}
247	1.923	1.66×10^{-8}	$8.60 \times$ "
267	1.825	$3.00 \times$ "	1.62×10^{-5}
279	1.812	$5.25 \times$ "	$2.90 \times$ "
295	1.761	1.01×10^{-7}	$5.74 \times$ "
310	1.715	$1.99 \times$ "	1.16×10^{-4}
327	1.667	$4.33 \times$ "	$2.60 \times$ "
342	1.626	$7.77 \times$ "	$4.78 \times$ "
361	1.577	1.80×10^{-6}	1.14×10^{-3}
391	1.506	$5.01 \times$ "	$3.39 \times$ "
422	1.439	1.40×10^{-5}	$9.72 \times$ "
446	1.391	$3.46 \times$ "	$2.49 \times$ "
461	1.362	$5.25 \times$ "	$3.85 \times$ "
469	1.348	$6.16 \times$ "	$4.57 \times$ "
471	1.344	$1.00 \times$ "	7.44×10^{-3}
473	1.340	4.89×10^{-6}	$3.66 \times$ "
484	1.321	$4.91 \times$ "	$3.72 \times$ "

o.o.o.o.o.o.o.o.o.o.o.o.o.o.o.o.o.o.o.o.o.o.o

Pure CsCl. Graph 5. Annealed 192 hrs. at 400°C.

T°C	$^{1}/_{T} \times 10^{-3}$ °A	σ (ohm^{-1}cm^{-1})	σT (ohm^{-1}cm^{-1})°A.
229	1.992	3.56×10^{-9}	1.79×10^{-6}
247	1.923	$8.40 \times$ "	$4.37 \times$ "
264	1.862	1.82×10^{-8}	$7.97 \times$ "
281	1.805	$3.74 \times$ "	2.07×10^{-5}
303	1.736	1.34×10^{-7}	$7.75 \times$ "
315	1.701	$2.08 \times$ "	1.18×10^{-4}
332	1.653	$4.63 \times$ "	$2.80 \times$ "
355	1.592	1.30×10^{-6}	$8.16 \times$ "
374	1.546	$2.52 \times$ "	1.63×10^{-3}
396	1.495	$5.70 \times$ "	$3.81 \times$ "
413	1.458	1.08×10^{-5}	$7.41 \times$ "
429	1.425	$1.96 \times$ "	1.38×10^{-2}
442	1.397	$3.10 \times$ "	$2.22 \times$ "
458	1.368	$5.02 \times$ "	$3.67 \times$ "
468	1.350	$6.11 \times$ "	$4.53 \times$ "
471	1.344	9.30×10^{-6}	6.92×10^{-3}
	Crystal chilled in liquid air.		
206	2.088	4.32×10^{-9}	2.07×10^{-6}
217	2.041	$4.80 \times$ "	$2.35 \times$ "
232	1.980	$6.96 \times$ "	$3.51 \times$ "
241	1.946	$8.40 \times$ "	$4.32 \times$ "
261	1.873	1.60×10^{-8}	$8.54 \times$ "
275	1.825	$3.43 \times$ "	$1.88 \times$ "
282	1.802	$5.91 \times$ "	$3.82 \times$ "
298	1.751	$9.40 \times$ "	5.36×10^{-5}
316	1.698	2.17×10^{-7}	1.28×10^{-4}
332	1.653	$4.35 \times$ "	$2.63 \times$ "
349	1.608	1.00×10^{-6}	$6.22 \times$ "
324	1.546	$2.72 \times$ "	1.76×10^{-3}
402	1.481	$7.41 \times$ "	$5.00 \times$ "
438	1.406	2.28×10^{-5}	1.62×10^{-2}
454	1.376	$3.92 \times$ "	$2.85 \times$ "
467	1.351	$5.80 \times$ "	$4.29 \times$ "
470	1.346	$1.35 \times$ "	$1.00 \times$ "

o.o.o.o.o.o.o.o.o.o.o.o.o.o.o.o.o.o.o.o.o

Pure CsCl. Graph 6.

$T^{\circ}C$	$^{1}/_{T} \times 10^{-3\circ} A$	$\sigma(ohm^{-1}cm^{-1})$	$\sigma T(ohm^{-1}cm^{-1})^{\circ}A$
236	1.965	6.50×10^{-9}	3.31×10^{-6}
250	1.912	1.20×10^{-8}	$6.26 \times$ "
265	1.859	$2.45 \times$ "	1.32×10^{-5}
287	1.786	$6.88 \times$ "	$3.85 \times$ "
311	1.712	2.31×10^{-7}	1.35×10^{-4}
333	1.650	$5.36 \times$ "	$3.25 \times$ "
357	1.587	1.56×10^{-6}	$9.82 \times$ "
385	1.520	$4.23 \times$ "	2.78×10^{-3}
410	1.464	$9.43 \times$ "	$6.44 \times$ "
436	1.410	2.34×10^{-5}	1.67×10^{-2}
454	1.376	$4.13 \times$ "	$3.00 \times$ "
467	1.351	$5.93 \times$ "	$4.39 \times$ "
470	1.348	8.08×10^{-6}	6.00×10^{-3}
472	1.342	$5.78 \times$ "	$4.31 \times$ "

.o.o.o.o.o.o.o.o.o.o.o.o.o.o.o.o.o.o.o.

Pure CsCl. Graph 6a. After irradation.

$T^{\circ}C$	$^{1}/_{T} \times 10^{-3\,\circ}A$	$\sigma(ohm^{-1}cm^{-1})$	$\sigma T(ohm^{-1}cm^{-1})^{\circ}A$
184	2.188	3.67×10^{-8}	1.68×10^{-5}
201	2.110	$3.33 \times$ "	$1.58 \times$ "
207	2.083	$4.06 \times$ "	$1.95 \times$ "
227	2.000	$4.60 \times$ "	$2.30 \times$ "
245	1.931	$5.06 \times$ "	$2.62 \times$ "
262	1.869	$6.11 \times$ "	$3.47 \times$ "
283	1.799	$7.19 \times$ "	$4.00 \times$ "
296	1.757	1.18×10^{-7}	$6.68 \times$ "
306	1.727	$1.81 \times$ "	1.05×10^{-4}
322	1.681	$3.36 \times$ "	$2.00 \times$ "
335	1.645	$5.95 \times$ "	$3.62 \times$ "
367	1.562	2.14×10^{-6}	1.37×10^{-3}
387	1.515	$4.00 \times$ "	$2.64 \times$ "
415	1.453	1.19×10^{-5}	$8.18 \times$ "
432	1.418	$2.28 \times$ "	1.61×10^{-2}
455	1.374	$4.94 \times$ "	$3.58 \times$ "
466	1.353	$5.56 \times$ "	$4.11 \times$ "
474	1.339	$1.00 \times$ "	7.47×10^{-3}
474	1.339	5.60×10^{-6}	$4.18 \times$ "

o.o.o.o.o.o.o.o.o.o.o.o.o.o.o.o.o.o.o.o.o.o.o

Pure CsCl. Graph 7. Melt Grown.

$T^{\circ}C$	$^{1}/_{T} \times 10^{-3\,\circ}A$	$\sigma(ohm^{-1}cm^{-1})$	$\sigma T(ohm^{-1}cm^{-1\,\circ}A$
249	1.916	1.90×10^{-8}	9.90×10^{-6}
265	1.859	$2.30 \times$ "	1.24×10^{-5}
284	1.795	$4.10 \times$ "	$2.28 \times$ "
306	1.727	1.14×10^{-7}	$6.62 \times$ "
325	1.672	$2.64 \times$ "	1.58×10^{-4}
328	1.664	$3.33 \times$ "	$2.00 \times$ "
331	1.656	$3.51 \times$ "	$2.12 \times$ "
343	1.623	$5.80 \times$ "	$3.58 \times$ "
363	1.572	1.20×10^{-6}	$7.60 \times$ "
369	1.558	$1.56 \times$ "	1.00×10^{-3}
379	1.534	$2.17 \times$ "	$1.41 \times$ "
390	1.508	$3.45 \times$ "	$2.29 \times$ "
403	1.479	$5.49 \times$ "	$3.71 \times$ "
412	1.460	$7.40 \times$ "	$5.07 \times$ "
424	1.435	1.09×10^{-5}	$7.61 \times$ "
431	1.420	$1.36 \times$ "	$9.60 \times$ "
442	1.399	$2.01 \times$ "	1.44×10^{-2}
450	1.383	$2.66 \times$ "	$1.92 \times$ "
458	1.368	$3.93 \times$ "	$2.87 \times$ "
464	1.357	$4.25 \times$ "	$3.13 \times$ "
470	1.348	$4.90 \times$ "	$3.60 \times$ "
470	1.348	$1.51 \times$ "	$1.20 \times$ "

o.o.o.o.o.o.o.o.o.o.o.o.o.o.o.o.o.o.o.o.o.o.o.o

Pure CsCl. Graph 7a. After irradation.

$T^{\circ}C$	$^{1}/_{T} \times 10^{-3}{}^{\circ}A$	$\sigma(ohm^{-1}cm^{-1})$	$\sigma T(ohm^{-1}cm^{-1})^{\circ}A.$
227	2.000	6.76×10^{-8}	3.38×10^{-5}
255	1.894	$8.36 \times$ "	$4.22 \times$ "
265	1.859	$9.80 \times$ "	$5.36 \times$ "
276	1.821	1.10×10^{-7}	$6.04 \times$ "
293	1.767	$1.22 \times$ "	$6.80 \times$ "
301	1.742	$1.41 \times$ "	$8.00 \times$ "
316	1.698	$1.92 \times$ "	1.13×10^{-4}
328	1.664	$2.71 \times$ "	$1.63 \times$ "
333	1.650	$3.55 \times$ "	$2.15 \times$ "
346	1.616	$6.19 \times$ "	$3.83 \times$ "
360	1.580	1.11×10^{-6}	$7.00 \times$ "
375	1.543	$2.10 \times$ "	1.36×10^{-3}
387	1.515	$3.46 \times$ "	$2.28 \times$ "
405	1.475	$4.47 \times$ "	$3.03 \times$ "
416	1.451	$8.71 \times$ "	$6.00 \times$ "
430	1.422	1.36×10^{-5}	$9.59 \times$ "
436	1.410	$1.80 \times$ "	1.27×10^{-2}
450	1.383	$3.03 \times$ "	$2.19 \times$ "
457	1.370	$3.68 \times$ "	$2.69 \times$ "
470	1.346	$5.11 \times$ "	$3.80 \times$ "
471	1.344	4.00×10^{-6}	2.97×10^{-3}

o.o.o.o.o.o.o.o.o.o.o.o.o.o.o.o.o.o.o

Pure CsCl. Graph 8. Melt Grown.

$T^{o}C$	$^{1}/_{T} \times 10^{-3\,o}A$	$\sigma(ohm^{-1}cm^{-1})$	$\sigma T(ohm^{-1}cm^{-1})^{o}A$
263	1.866	1.02×10^{-8}	5.46×10^{-6}
274	1.828	$1.98 \times$ "	$8.10 \times$ "
282	1.802	$2.44 \times$ "	1.35×10^{-5}
304	1.733	$7.80 \times$ "	$4.50 \times$ "
322	1.681	1.80×10^{-7}	1.07×10^{-4}
326	1.669	$3.00 \times$ "	$1.81 \times$ "
339	1.634	$3.57 \times$ "	$2.20 \times$ "
355	1.592	$8.92 \times$ "	$5.65 \times$ "
380	1.531	2.14×10^{-6}	1.42×10^{-3}
394	1.500	$5.44 \times$ "	$3.66 \times$ "
400	1.486	$7.04 \times$ "	$4.82 \times$ "
405	1.475	$8.32 \times$ "	$5.75 \times$ "
430	1.422	1.63×10^{-5}	1.17×10^{-2}
443	1.397	2.65×10^{-5}	$1.97 \times$ "
467	1.351	$5.00 \times$ "	$3.79 \times$ "
471	1.344	6.14×10^{-6}	4.51×10^{-3}
	2nd. Heating.		
293	1.767	6.28×10^{-8}	3.55×10^{-5}
318	1.695	1.76×10^{-7}	1.03×10^{-4}
338	1.637	$3.72 \times$ "	$2.27 \times$ "
344	1.621	$6.72 \times$ "	$4.15 \times$ "
346	1.616	$6.68 \times$ "	$4.15 \times$ "
380	1.530	1.87×10^{-6}	1.20×10^{-3}
397	1.493	$3.20 \times$ "	$2.14 \times$ "
415	1.456	$7.16 \times$ "	$4.98 \times$ "
430	1.420	1.17×10^{-5}	$8.30 \times$ "
438	1.406	$1.93 \times$ "	1.37×10^{-2}
456	1.372	3.18×10^{-5}	2.34×10^{-2}
469	1.351	$4.97 \times$ "	$3.66 \times$ "
470	1.348	5.65×10^{-6}	4.20×10^{-3}

o.o.o.o.o.o.o.o.o.o.o.o.o.o.o.o.o.o.o

Graph 9. Ba^{2+}-doped CsCl

T °C	1/T x 10^{-3} °A	σ(ohm^{-1}cm^{-1})	σT(ohm^{-1}cm^{-1})°A
248	1.919	4.18 x 10^{-9}	2.18 x 10^{-6}
265	1.859	7.34 x "	3.96 x "
276	1.821	2.15 x 10^{-8}	1.18 x 10^{-5}
289	1.779	4.19 x "	2.35 x "
305	1.730	1.04 x 10^{-7}	6.02 x "
315	1.701	2.00 x "	1.18 x 10^{-4}
332	1.653	4.23 x "	2.56 x "
348	1.610	8.53 x "	5.30 x "
368	1.560	1.92 x 10^{-6}	1.23 x 10^{-3}
387	1.515	4.61 x "	3.04 x "
400	1.486	1.11 x 10^{-5}	8.48 x "
407	1.471	1.82 x "	1.24 x 10^{-2}
	Chilled quickly in liquid air.		
200	2.114	7.14 x 10^{-9}	3.38 x 10^{-6}
222	2.020	1.18 x 10^{-8}	5.82 x "
237	1.961	1.82 x "	9.30 x "
252	1.905	2.68 x "	1.41 x 10^{-5}
266	1.855	4.14 x "	2.23 x "
278	1.815	5.24 x "	2.89 x "
295	1.761	7.66 x "	4.35 x "

.o.o.o.o.o.o.o.o.o.o.o.o.o.o.o.

Graph 10. Ba^{2+}-doped CsCl

t°C	$1/T \times 10^{3}$ °A	σ(ohm^{-1}cm^{-1})	σT(ohm^{-1}cm^{-1} °A
229	1.992	5.08×10^{-9}	2.55×10^{-6}
250	1.912	1.26×10^{-8}	$6.60 \times$ "
266	1.855	$2.37 \times$ "	1.28×10^{-5}
280	1.808	$4.34 \times$ "	$2.40 \times$ "
296	1.757	$8.98 \times$ "	$5.11 \times$ "
311	1.712	1.77×10^{-7}	1.04×10^{-4}
329	1.661	$4.53 \times$ "	$2.73 \times$ "
348	1.610	$9.66 \times$ "	$6.00 \times$ "
372	1.550	1.23×10^{-5}	7.92×10^{-3}

Chilled quickly in liquid nitrogen.

231	1.984	4.34×10^{-8}	2.19×10^{-5}
245	1.931	$6.10 \times$ "	$3.16 \times$ "
260	1.876	$9.44 \times$ "	$5.03 \times$ "
277	1.818	1.23×10^{-7}	$6.80 \times$ "
292	1.770	$1.77 \times$ "	1.00×10^{-4}
304	1.721	$2.72 \times$ "	$1.59 \times$ "
325	1.672	$3.81 \times$ "	$2.28 \times$ "

.o.o.o.o.o.o.o.o.o.o.o.o.o.

Ba^{2+}-doped CsCl. Graph 11. 57 ppm.

T°C.	$1/T \times 10^{-3}$ °A.	σ ($ohm^{-1}cm^{-1}$)	σT ($ohm^{-1}cm^{-1}$)
217	2.041	4.51×10^{-9}	2.19×10^{-6}
226	2.004	$5.40 \times$ "	$2.69 \times$ "
240	1.949	$8.55 \times$ "	$4.50 \times$ "
256	1.890	1.83×10^{-8}	$9.69 \times$ "
271	1.838	$3.60 \times$ "	1.96×10^{-5}
289	1.779	$6.60 \times$ "	$3.69 \times$ "
319	1.689	1.88×10^{-7}	1.11×10^{-4}
342	1.626	$4.98 \times$ "	$3.09 \times$ "
358	1.585	$9.00 \times$ "	$5.73 \times$ "
369	1.558	1.71×10^{-6}	1.11×10^{-3}
386	1.517	$5.01 \times$ "	$3.33 \times$ "
405	1.475	1.01×10^{-5}	$7.56 \times$ "
417	1.449	$1.54 \times$ "	1.08×10^{-2}
428	1.427	$1.77 \times$ "	$1.26 \times$ "
437	1.408	$2.37 \times$ "	$1.72 \times$ "
445	1.393	$2.49 \times$ "	$1.82 \times$ "
458	1.368	$3.51 \times$ "	$2.61 \times$ "
459	1.366	$2.64 \times$ "	$2.19 \times$ "
459	1.366	$2.46 \times$ "	$1.83 \times$ "

Cooled to room temperature.

2nd. Heating.

267	1.852	2.63×10^{-8}	1.13×10^{-5}
280	1.808	$4.65 \times$ "	$2.67 \times$ "
295	1.760	$7.86 \times$ "	$4.47 \times$ "
317	1.695	2.94×10^{-7}	1.39×10^{-4}
329	1.661	$3.27 \times$ "	$1.98 \times$ "
352	1.600	$7.65 \times$ "	$4.83 \times$ "
381	1.529	2.03×10^{-6}	1.34×10^{-3}
391	1.506	$3.33 \times$ "	$2.25 \times$ "
404	1.477	$5.13 \times$ "	$3.54 \times$ "
423	1.437	$8.40 \times$ "	$5.94 \times$ "
429	1.425	1.02×10^{-5}	$7.32 \times$ "
439	1.404	$1.35 \times$ "	$9.79 \times$ "
451	1.381	$1.72 \times$ "	1.27×10^{-2}
460	1.364	$1.35 \times$ "	9.51×10^{-3}
460	1.364	8.19×10^{-6}	$6.00 \times$ ".

.o.o.o.o.o.o.o.o.o.o.o.o.o.o.o.o.o.o.o.o.o.

Ba^{2+}-doped CsCl. Graph 12. 62 ppm.

$T^{\circ}C.$	$1/_T \times 10^{-3\,\circ}A.$	σ ($ohm^{-1}cm^{-1}$)	σT ($ohm^{-1}cm^{-1}{}^{\circ}A$)
183	2.193	8.00×10^{-10}	3.65×10^{-7}
195	2.137	1.20×10^{-9}	$5.71 \times$ "
207	2.083	$1.84 \times$ "	$8.83 \times$ "
219	2.033	$3.40 \times$ "	1.67×10^{-6}
230	1.988	$5.60 \times$ "	$2.82 \times$ "
246	1.927	1.04×10^{-8}	$5.39 \times$ "
262	1.869	$1.96 \times$ "	1.05×10^{-5}
275	1.825	$3.92 \times$ "	$2.14 \times$ "
290	1.776	$6.40 \times$ "	$3.60 \times$ "
296	1.757	$8.60 \times$ "	$4.90 \times$ "
320	1.686	2.54×10^{-7}	1.50×10^{-4}
332	1.653	$4.46 \times$ "	$2.70 \times$ "
355	1.592	1.22×10^{-6}	$7.66 \times$ "
372	1.550	$3.04 \times$ "	1.96×10^{-3}
383	1.524	$5.66 \times$ "	$3.71 \times$ "
393	1.502	1.18×10^{-5}	$7.86 \times$ "
410	1.464	$1.78 \times$ "	1.21×10^{-2}
432	1.418	$2.94 \times$ "	$2.07 \times$ "
441	1.401	$3.42 \times$ "	$2.45 \times$ "
449	1.385	$4.24 \times$ "	$3.05 \times$ "
456	1.372	$4.48 \times$ "	$3.27 \times$ "
460	1.364	$2.75 \times$ "	$2.02 \times$ "
469	1.348	8.60×10^{-6}	6.38×10^{-3}
484	1.321	$6.41 \times$ "	$4.51 \times$ "
	Cooling back through Transition.		
477	1.333	2.54×10^{-6}	1.90×10^{-3}
458	1.368	$4.92 \times$ "	$3.60 \times$ "
452	1.379	$9.00 \times$ "	$6.53 \times$ "
442	1.399	1.68×10^{-5}	1.20×10^{-2}
426	1.431	$1.84 \times$ "	$1.28 \times$ "
420	1.443	$1.29 \times$ "	8.94×10^{-3}
404	1.477	$1.01 \times$ "	$6.86 \times$ "
396	1.495	7.82×10^{-6}	$5.23 \times$ "
383	1.524	$4.06 \times$ "	$2.66 \times$ "

(cont' over)

Ba^{2+}-doped CsCl. Graph 12. 62ppm. (cont').

T°C.	$^{1}/_{T} \times 10^{-3}$ °A.	σ ($ohm^{-1}cm^{-1}$)	σT ($ohm^{-1}cm^{-1}$)°A
368	1.560	2.09×10^{-6}	1.34×10^{-3}
347	1.613	$1.01 \times$ "	6.26×10^{-4}
332	1.653	5.06×10^{-7}	$3.07 \times$ "
307	1.724	$1.91 \times$ "	$1.11 \times$ "
292	1.770	8.00×10^{-8}	4.52×10^{-5}
272	1.835	$3.43 \times$ "	$1.87 \times$ "
255	1.894	$2.00 \times$ "	$1.06 \times$ "
237	1.961	$1.16 \times$ "	5.90×10^{-6}
220	2.028	6.60×10^{-9}	$3.25 \times$ "

.o.o.o.o.o.o.o.o.o.o.o.o.o.o.o.o.o.o.

Ba^{2+}-doped CsCl. Graph 13. 71ppm.

T°C.	$^{1}/_{T} \times 10^{-3}$ °A.	σ ($ohm^{-1}cm^{-1}$)	σT ($ohm^{-1}cm^{-1}$°)A
203	2.101	4.51×10^{-8}	2.14×10^{-5}
217	2.041	6.30 x "	3.09 x "
227	2.000	1.06×10^{-7}	5.28 x "
249	1.916	2.00 x "	1.04×10^{-4}
276	1.821	5.43 x "	2.97 x "
285	1.792	6.15×10^{-8}	3.42×10^{-5}
299	1.748	9.63 x "	5.52 x "
313	1.706	2.22×10^{-7}	1.30×10^{-4}
324	1.675	2.52 x "	1.61 x "
352	1.600	9.60 x "	6.00 x "
	Left overnight in stream of nitrogen.		
379	1.534	2.40×10^{-6}	1.56×10^{-3}
391	1.506	8.88 x "	5.40 x "
412	1.460	1.86×10^{-5}	1.28×10^{-2}
429	1.425	2.39 x "	1.68 x "
433	1.416	2.55 x "	1.82 x "
440	1.403	2.94 x "	2.13 x "
448	1.387	3.75 x "	2.70 x "
458	1.368	2.09 x "	1.53 x "
475	1.337	1.07 x "	8.00×10^{-3}
487	1.316	4.98×10^{-6}	3.78 x "
	Cooling back through transition.		
475	1.337	7.98×10^{-6}	5.97×10^{-3}
457	1.370	8.25 x "	6.00 x "
438	1.406	1.24×10^{-5}	9.00 x "
427	1.429	1.16 x "	8.67 x "
419	1.445	1.04 x "	7.20 x "
407	1.471	8.70×10^{-6}	5.22 x "

.o.o.o.o.o.o.o.o.o.o.o.o.o.o.o.o.o.o.o.o.o.

Ba^{2+}-doped CsCl. Graph 15. 97 ppm.

T °C	1/T x 10^{-3} °A	σ(ohm^{-1}cm^{-1})	σT(ohm^{-1}cm^{-1}) °A.
236	1.965	4.60 x 10^{-8}	2.34 x 10^{-5}
253	1.901	7.60 x "	4.00 x "
278	1.815	2.01 x 10^{-7}	1.10 x 10^{-4}
302	1.740	4.86 x "	2.80 x "
330	1.658	9.08 x "	5.50 x "
346	1.616	6.20 x 10^{-6}	3.83 x 10^{-3}
370	1.555	9.60 x "	6.17 x "
382	1.527	1.41 x 10^{-5}	9.23 x "
403	1.479	1.81 x "	1.22 x 10^{-2}
420	1.443	2.30 x "	1.59 x "
440	1.403	3.07 x "	2.20 x "
447	1.390	1.80 x "	1.38 x "
465	1.355	6.40 x 10^{-6}	4.72 x 10^{-3}
479	1.330	5.42 x "	3.75 x "
490	1.311	4.70 x "	3.40 x "

.o.o.o.o.o.o.o.o.o.o.o.o.o.o.o.o.o.

Graph 14 Ba^{2+}-doped CsCl 85 ppm.

$t^{\circ}C$	$1/T \times 10^{-3}\,^{\circ}A$	$\sigma(ohm^{-1}cm^{-1})$	$\sigma T(ohm^{-1}cm^{-1})\,^{\circ}A.$
226	2.004	3.21×10^{-9}	1.60×10^{-6}
242	1.942	$5.78 \times$ "	$2.98 \times$ "
255	1.894	$9.68 \times$ "	$5.11 \times$ "
268	1.848	1.45×10^{-8}	$7.83 \times$ "
278	1.815	$2.21 \times$ "	1.22×10^{-5}
290	1.779	$4.09 \times$ "	$2.30 \times$ "
306	1.727	$7.68 \times$ "	$4.45 \times$ "
321	1.684	1.58×10^{-7}	$9.39 \times$ "
338	1.637	$4.27 \times$ "	2.61×10^{-4}
367	1.562	$8.88 \times$ "	$5.68 \times$ "
387	1.515	1.18×10^{-5}	9.96×10^{-3}
418	1.447	$2.16 \times$ "	1.49×10^{-2}
434	1.414	$2.64 \times$ "	$1.87 \times$ "
445	1.393	$3.36 \times$ "	$2.41 \times$ "
447	1.389	$1.99 \times$ "	$1.43 \times$ "
457	1.370	$1.09 \times$ "	7.94×10^{-3}
473	1.340	6.41×10^{-6}	$4.78 \times$ "
485	1.319	$6.41 \times$ "	$4.86 \times$ "

.o.o.o.o.o.o.o.o.o.o.o.o.o.o.o.

Graph 16. Ba^{2+}-doped CsCl. 104 ppm

t°C	1/T x 10^{-3} °A	σ (ohm^{-1}cm^{-1})	σT (ohm^{-1}cm^{-1})°A.
160	2.309	3.29 x 10^{-9}	1.42 x 10^{-6}
172	2.247	4.38 x "	1.95 x "
192	2.151	1.06 x 10^{-8}	4.93 x "
212	2.062	1.68 x "	8.15 x "
232	2.020	3.01 x "	1.49 x 10^{-5}
244	1.934	7.12 x "	3.68 x "
259	1.880	9.31 x "	4.95 x "
264	1.862	1.00 x 10^{-7}	5.35 x "
282	1.802	1.80 x "	9.99 x "
302	1.740	3.20 x "	1.84 x 10^{-4}
320	1.686	6.31 x "	3.74 x "
342	1.626	6.46 x 10^{-6}	3.93 x 10^{-3}
372	1.550	1.03 x 10^{-5}	6.64 x "
388	1.513	1.36 x "	9.00 x 10^{-3}
400	1.486	1.59 x "	1.07 x 10^{-2}
418	1.447	1.89 x "	1.30 x "
437	1.408	2.88 x "	2.04 x "
446	1.391	4.52 x 10^{-6}	3.25 x 10^{-3}
460	1.364	3.83 x "	2.80 x "
474	1.337	4.52 x "	3.37 x "
	Cooling.		
470	1.346	1.71 x 10^{-6}	1.27 x 10^{-3}
461	1.362	1.37 x "	1.00 x "
442	1.399	9.31 x 10^{-7}	6.64 x 10^{-4}
433	1.416	5.93 x 10^{-6}	4.18 x 10^{-3}
408	1.468	1.24 x 10^{-5}	8.44 x "
382	1.527	7.81 x 10^{-6}	5.14 x "
363	1.572	5.19 x "	3.30 x "
344	1.621	3.24 x "	2.00 x "
329	1.661	1.55 x "	9.34 x 10^{-4}
313	1.706	5.68 x 10^{-7}	3.35 x "
291	1.773	2.48 x "	1.50 x "
271	1.838	1.35 x "	7.34 x 10^{-5}
250	1.912	7.38 x 10^{-8}	3.86 x "
236	1.965	4.46 x "	2.27 x "
218	2.037	1.00 x "	4.91 x 10^{-6}

.o.o.o.o.o.o.o.o.o.o.o.o.o.o.o.o.o.o.o.

Graph 17 Ba^{2+}-doped CsCl 133 ppm

T°C	1/T x 10^{-3} °A	σ(ohm^{-1}cm^{-1})	σT(ohm^{-1}cm^{-1})°A.
318	1.690	3.85 x 10^{-7}	2.28 x 10^{-4}
324	1.675	4.48 x "	2.63 x "
333	1.650	7.84 x "	4.75 x "
342	1.625	1.81 x 10^{-6}	1.11 x 10^{-3}
351	1.603	4.56 x "	2.85 x "
358	1.585	7.26 x "	4.58 x "
361	1.575	8.10 x "	5.14 x "
364	1.570	9.90 x "	6.31 x "
370	1.555	1.04 x 10^{-5}	6.69 x "
378	1.535	1.15 x "	7.49 x "
390	1.510	1.32 x "	8.75 x "
405	1.475	1.78 x "	1.21 x 10^{-2}
412	1.460	2.01 x "	1.38 x "
425	1.435	2.33 x "	1.63 x "
432	1.418	2.50 x "	1.76 x "
438	1.406	1.64 x "	1.16 x "
447	1.389	1.37 x "	9.86 x 10^{-3}
458	1.368	1.18 x "	8.62 x "

.o.o.o.o.o.o.o.o.o.o.o.o.o.o.o.o.o.o.

Graph 18 Ba^{2+}-doped CsCl

232	1.980	9.10 x 10^{-9}	4.60 x 10^{-6}
253	1.901	1.71 x 10^{-8}	9.00 x "
271	1.838	3.06 x "	1.66 x 10^{-5}
283	1.799	4.40 x "	2.47 x "
298	1.751	5.97 x "	3.41 x "
310	1.715	1.05 x 10^{-7}	6.12 x "
335	1.645	3.08 x "	1.87 x 10^{-4}
347	1.613	4.94 x "	3.06 x "
360	1.580	1.07 x 10^{-6}	6.77 x "
376	1.541	1.40 x 10^{-5}	9.06 x 10^{-3}
389	1.511	1.70 x "	1.13 x 10^{-2}
403	1.479	1.92 x "	1.30 x "
410	1.464	2.14 x "	1.46 x "
418	1.451	2.31 x "	1.59 x "
428	1.431	1.73 x "	1.21 x "
443	1.397	1.29 x "	9.24 x 10^{-3}
468	1.350	8.00 x 10^{-6}	5.93 x "
482	1.325	6.12 x "	4.62 x "
504	1.287	8.00 x "	6.25 x "

.o.o.o.o.o.o.o.o.o.o.o.o.o.o.o.o.o.

Ba^{2+} - doped CsCl. Graph 19. 153ppm.

$T^{\circ}C$	$^{1}/_{T} \times 10^{-3\,\circ}A$	$\sigma(ohm^{-1}cm^{-1})$	$\sigma T(ohm^{-1}cm^{-1})^{\circ}A.$
172	2.247	1.50×10^{-8}	6.68×10^{-6}
190	2.160	$2.42 \times$ "	1.12×10^{-5}
209	2.075	$5.56 \times$ "	$2.68 \times$ "
218	2.037	$1.45 \times$ "	7.12×10^{-6}
230	1.988	8.71×10^{-9}	$4.38 \times$ "
242	1.942	1.23×10^{-8}	$6.33 \times$ "
259	1.880	$2.47 \times$ "	1.31×10^{-5}
274	1.828	$4.11 \times$ "	$2.25 \times$ "
301	1.702	1.21×10^{-7}	$6.95 \times$ "
313	1.704	$1.94 \times$ "	1.14×10^{-4}
347	1.613	$8.23 \times$ "	$5.10 \times$ "
361	1.577	1.61×10^{-6}	1.02×10^{-3}
377	1.538	$2.24 \times$ "	$1.46 \times$ "
385	1.520	$3.54 \times$ "	$2.33 \times$ "
392	1.504	$5.83 \times$ "	$3.88 \times$ "
407	1.411	$7.13 \times$ "	$4.85 \times$ "
414	1.456	$8.23 \times$ "	$5.65 \times$ "
422	1.439	2.13×10^{-5}	1.48×10^{-2}
439	1.404	$2.75 \times$ "	$1.96 \times$ "
443	1.385	$1.19 \times$ "	8.59×10^{-3}
453	1.377	$1.09 \times$ "	$7.91 \times$ "
459	1.370	9.68×10^{-6}	$7.07 \times$ "
464	1.357	$8.23 \times$ "	$6.12 \times$ "
471	1.344	$8.71 \times$ "	$6.58 \times$ "

Graph Ba^{2+}-doped CsCl. Graph 20. 167 ppm.

T°C	$1/T \times 10^{-3}$ °A	σ(ohm^{-1}cm^{-1})	σT(ohm^{-1}cm^{-1})°A.
186	2.179	8.76×10^{-9}	4.02×10^{-6}
207	2.083	1.31×10^{-8}	$6.26 \times$ "
227	2.000	$1.99 \times$ "	1.00×10^{-5}
245	1.931	$3.05 \times$ "	$1.58 \times$ "
261	1.876	$4.53 \times$ "	$2.42 \times$ "
273	1.832	$6.21 \times$ "	$3.38 \times$ "
285	1.792	$8.08 \times$ "	$4.51 \times$ "
302	1.739	1.18×10^{-7}	$6.80 \times$ "
311	1.712	$1.41 \times$ "	$8.22 \times$ "
318	1.692	$2.28 \times$ "	1.35×10^{-4}
333	1.650	$3.78 \times$ "	$2.29 \times$ "
348	1.610	$6.64 \times$ "	$4.12 \times$ "
363	1.572	1.57×10^{-6}	1.00×10^{-3}
379	1.534	$6.23 \times$ "	$4.06 \times$ "
391	1.506	1.16×10^{-5}	$7.71 \times$ "
407	1.471	$1.59 \times$ "	1.08×10^{-2}
429	1.425	$2.54 \times$ "	$1.78 \times$ "
443	1.397	$3.21 \times$ "	$2.30 \times$ "
462	1.381	9.99×10^{-6}	7.35×10^{-3}
483	1.323	$5.59 \times$ "	$4.23 \times$ "
483	1.393	$5.83 \times$ "	$4.41 \times$ "

•o•o•o•o•o•o•o•o•o•o•o•o•

Ba^{2+} - doped CsCl. Graph 21. 196ppm.

T°C	$^1/_T \times 10^{-3}$ °A	σ (ohm^{-1}cm^{-1})	σT (ohm^{-1}cm^{-1}) °A.
249	1.916	1.03 x 10^{-6}	5.38 x 10^{-4}
260	1.876	1.01 x "	5.38 x "
274	1.828	1.23 x "	6.72 x "
288	1.783	1.20 x "	6.72 x "
285	1.792	9.12 x 10^{-7}	5.08 x "
291	1.773	9.44 x "	5.32 x "
299	1.748	1.00 x 10^{-6}	5.72 x "
318	1.692	1.16 x "	6.88 x "
330	1.658	1.56 x "	9.40 x "
347	1.613	3.00 x "	1.86 x 10^{-3}
371	1.553	3.20 x "	2.06 x "
379	1.534	3.64 x "	2.36 x "
Cooled slowly to room temperature			
271	1.838	3.40 x 10^{-8}	1.85 x 10^{-5}
301	1.742	1.38 x 10^{-7}	7.94 x "
315	1.701	2.90 x "	1.71 x 10^{-4}
330	1.631	8.48 x "	5.20 x "
354	1.595	1.20 x 10^{-6}	7.52 x "
368	1.560	3.26 x "	2.10 x "
390	1.508	6.18 x "	4.10 x "
400	1.486	9.70 x "	6.42 x "
412	1.460	1.88 x "	1.32 x "
429	1.425	2.56 x "	1.80 x "
442	1.399	3.22 x 10^{-5}	2.38 x "
454	1.376	2.28 x "	1.66 x "
467	1.351	9.57 x 10^{-6}	7.08 x 10^{-3}
479	1.330	6.65 x "	5.00 x "

Graph 22. Ba^{2+}-doped CsCl 234 ppm

T°C	$1/T \times 10^{-3}$ °A	$\sigma(ohm^{-1}cm^{-1})$	$\sigma T(ohm^{-1}cm^{-1})$ °A.
212	2.062	2.58×10^{-9}	1.18×10^{-6}
229	1.984	$4.92 \times$ "	$2.48 \times$ "
243	1.938	1.02×10^{-8}	$5.26 \times$ "
263	1.866	$2.28 \times$ "	1.22×10^{-5}
287	1.786	1.08×10^{-7}	$6.05 \times$ "
305	1.730	$2.00 \times$ "	1.16×10^{-4}
315	1.701	$3.72 \times$ "	$2.19 \times$ "
331	1.656	$6.84 \times$ "	$4.13 \times$ "
349	1.608	1.49×10^{-6}	$8.30 \times$ "
366	1.565	$3.07 \times$ "	1.96×10^{-3}
386	1.517	1.02×10^{-5}	$6.72 \times$ "
400	1.486	$1.46 \times$ "	$9.82 \times$ "
418	1.447	$2.14 \times$ "	1.48×10^{-2}
430	1.422	$2.88 \times$ "	$2.03 \times$ "
441	1.401	$3.82 \times$ "	$2.73 \times$ "
450	1.377	$4.32 \times$ "	$3.16 \times$ "
460	1.364	3.54×10^{-6}	2.59×10^{-3}
474	1.339	$2.64 \times$ "	$1.97 \times$ "

.o.o.o.o.o.o.o.o.o.o.o.o.o.o.o.o.o.o.

Graph 23 Ba^{2+}-doped CsCl 260 ppm

T°C	1/T x 10^{-3} °A	σ(ohm^{-1}cm^{-1})	σT(ohm^{-1}cm^{-1})°A.
270	1.842	4.60 x 10^{-7}	2.50 x 10^{-4}
285	1.792	6.45 x "	3.60 x "
296	1.757	8.05 x "	4.68 x "
320	1.686	1.21 x 10^{-6}	7.20 x "
347	1.613	1.99 x "	1.24 x 10^{-3}
368	1.560	2.68 x "	1.72 x "
381	1.529	3.74 x "	2.44 x "
	2nd. Heating after slow cooling.		
224	2.012	3.89 x 10^{-8}	1.94 x 10^{-5}
237	1.957	5.98 x "	3.01 x "
251	1.908	9.00 x "	4.72 x "
264	1.862	1.32 x 10^{-7}	7.10 x "
282	1.802	2.11 x "	1.17 x 10^{-4}
291	1.773	2.62 x "	1.48 x "
313	1.704	4.51 x "	2.64 x "
327	1.667	7.80 x "	4.08 x "
342	1.626	1.32 x 10^{-6}	8.15 x "
355	1.592	2.11 x "	1.33 x 10^{-3}
376	1.541	4.40 x "	2.86 x "
392	1.504	7.20 x "	4.76 x "
404	1.477	1.12 x 10^{-5}	7.60 x "
428	1.427	2.53 x "	1.78 x 10^{-2}
445	1.393	3.74 x "	2.68 x "
456	1.372	4.97 x "	3.26 x "
463	1.359	5.40 x "	3.97 x "
471	1.344	5.83 x 10^{-6}	4.34 x 10^{-3}

.o.o.o.o.o.o.o.o.o.o.o.o.o.o.o.

Ba^{2+}-doped CsCl. Graph 24. 280 ppm.

T °C	1/T x 10^{-3} °A	σ($ohm^{-1}cm^{-1}$)	σT($ohm^{-1}cm^{-1}$)°A
172	2.247	1.20 x 10^{-9}	5.34 x 10^{-7}
185	2.188	1.54 x "	7.05 x "
200	2.114	2.32 x "	1.10 x 10^{-6}
218	2.037	6.30 x "	3.09 x "
237	1.961	1.60 x 10^{-8}	8.16 x "
255	1.894	3.75 x "	1.98 x 10^{-5}
270	1.842	7.20 x "	3.91 x "
289	1.779	1.56 x 10^{-7}	8.77 x "
299	1.748	3.92 x "	1.67 x 10^{-4}
315	1.701	4.70 x "	2.76 x "
332	1.653	9.20 x "	5.56 x "
344	1.621	1.64 x 10^{-6}	1.01 x 10^{-3}
363	1.572	3.28 x "	2.09 x "
378	1.536	6.56 x "	4.27 x "
391	1.506	1.02 x 10^{-5}	6.77 x "
405	1.475	1.71 x "	1.16 x 10^{-2}
420	1.443	2.62 x "	1.82 x "
449	1.385	4.50 x "	3.25 x "
465	1.355	5.35 x "	3.95 x "
466	1.353	1.46 x "	1.08 x "
475	1.337	2.67 x 10^{-6}	1.99 x 10^{-3}

.o.o.o.o.o.o.o.o.o.o.o.o.o.o.o.o.

Ba^{2+}-doped CsCl. Graph 25. 1000 ppm.

T °C	$1/T \times 10^{-3}$ °A	σ (ohm^{-1}cm^{-1})	σT (ohm^{-1}cm^{-1}) °A.
236	1.960	4.80×10^{-9}	1.45×10^{-6}
250	1.910	$8.48 \times$ "	$4.43 \times$ "
260	1.875	1.45×10^{-8}	$7.74 \times$ "
271	1.840	$2.67 \times$ "	1.46×10^{-5}
279	1.812	$4.32 \times$ "	$2.38 \times$ "
291	1.773	$7.92 \times$ "	$4.48 \times$ "
298	1.751	$9.60 \times$ "	$5.50 \times$ "
313	1.706	1.63×10^{-7}	$9.70 \times$ "
321	1.684	$2.62 \times$ "	1.57×10^{-4}
331	1.656	$4.08 \times$ "	$2.48 \times$ "
341	1.629	$5.92 \times$ "	$3.66 \times$ "
352	1.600	1.04×10^{-6}	$6.56 \times$ "
360	1.580	$1.60 \times$ "	1.01×10^{-3}
374	1.546	$2.56 \times$ "	$1.66 \times$ "
390	1.508	$4.43 \times$ "	$2.98 \times$ "
398	1.490	$6.40 \times$ "	$4.37 \times$ "
410	1.464	$9.84 \times$ "	$6.85 \times$ "
421	1.441	1.45×10^{-5}	1.02×10^{-2}
427	1.429	$1.92 \times$ "	$1.37 \times$ "
437	1.406	$2.61 \times$ "	$1.89 \times$ "
443	1.397	$3.30 \times$ "	$2.42 \times$ "
447	1.389	$3.58 \times$ "	$2.74 \times$ "
458	1.368	$4.68 \times$ "	$3.42 \times$ "
466	1.353	$5.95 \times$ "	$4.40 \times$ "
469	1.348	$2.25 \times$ "	$1.68 \times$ "
472	1.342	5.88×10^{-6}	4.38×10^{-3}
490	1.311	$6.19 \times$ "	$4.72 \times$ "
506	1.284	$8.61 \times$ "	$6.71 \times$ "
515	1.269	1.07×10^{-5}	$8.46 \times$ "

.o.o.o.o.o.o.o.o.o.o.o.o.o o.o.o.

Graph 26. Ba^{2+}-doped CsCl. Less than 5ppm.

n°C	$1/T \times 10^{-3}$ °A.	$\sigma(ohm^{-1}cm^{-1})$	$\sigma T(ohm^{-1}cm^{-1})$ °A.
247	1.923	7.77×10^{-9}	4.04×10^{-6}
261	1.873	1.49×10^{-8}	$7.96 \times$ "
274	1.828	3.57×10^{-8}	1.95×10^{-5}
292	1.770	$7.35 \times$ "	$4.15 \times$ "
307	1.724	1.32×10^{-7}	$7.66 \times$ "
317	1.695	$2.20 \times$ "	1.30×10^{-4}
338	1.637	$5.88 \times$ "	$3.59 \times$ "
376	1.540	1.38×10^{-6}	$8.96 \times$ "
386	1.517	$3.78 \times$ "	2.49×10^{-3}
397	1.493	$6.20 \times$ "	$4.15 \times$ "
414	1.456	1.16×10^{-5}	$7.70 \times$ "
428	1.427	$1.89 \times$ "	1.33×10^{-2}
441	1.400	$2.69 \times$ "	$1.92 \times$ "
453	1.377	$4.20 \times$ "	$3.05 \times$ "
467	1.351	$6.30 \times$ "	$4.66 \times$ "
470	1.346	$1.09 \times$ "	8.10×10^{-3}

.o.o.o.o.o.o.o.o.o.o.o.o.o.o.o.

Graph 27 . Ba^{2+}-doped CsCl Undetectable.

223	2.016	3.70×10^{-9}	1.84×10^{-6}
240	1.949	$5.91 \times$ "	$3.03 \times$ "
255	1.894	1.62×10^{-8}	$8.55 \times$ "
263	1.866	$2.64 \times$ "	1.42×10^{-5}
275	1.825	$3.40 \times$ "	$1.86 \times$ "
295	1.761	$9.60 \times$ "	$5.45 \times$ "
312	1.709	1.64×10^{-7}	$9.60 \times$ "
331	1.656	$4.54 \times$ "	2.74×10^{-4}
343	1.623	$8.77 \times$ "	$5.40 \times$ "
360	1.580	1.81×10^{-6}	1.15×10^{-3}
374	1.546	$3.01 \times$ "	$1.95 \times$ "
399	1.488	$7.80 \times$ "	$5.24 \times$ "
419	1.445	1.48×10^{-5}	1.03×10^{-2}
443	1.395	$2.90 \times$ "	$2.07 \times$ "
454	1.376	$4.20 \times$ "	$3.05 \times$ "
463	1.360	$4.90 \times$ "	$3.60 \times$ "
468	1.350	$6.00 \times$ "	$4.44 \times$ "
471	1.344	5.58×10^{-6}	4.16×10^{-3}
476	1.335	$6.02 \times$ "	$4.48 \times$ "

.o.o.o.o.o.o.o.o.o.o.o.o.o.o.o.

Graph 28. Sr^{2+}-doped CsCl

t°C	1/T x 10^{-3}° A	σ(ohm^{-1}cm^{-1})	σT(ohm^{-1}cm^{-1})° A.
235	1.969	2.48 x 10^{-9}	1.26 x 10^{-6}
266	1.855	2.15 x 10^{-8}	1.16 x 10^{-5}
279	1.812	3.24 x "	1.79 x "
290	1.776	5.42 x "	3.05 x "
304	1.733	1.22 x 10^{-7}	7.04 x "
317	1.695	2.16 x "	1.27 x 10^{-4}
337	1.639	5.40 x "	3.30 x "
352	1.600	1.12 x 10^{-6}	7.00 x "
370	1.555	2.19 x "	1.41 x 10^{-3}
388	1.513	3.80 x "	2.51 x "
406	1.473	7.45 x "	5.06 x "
422	1.439	1.36 x 10^{-5}	9.45 x "
435	1.412	2.16 x "	1.53 x 10^{-2}
451	1.381	3.74 x "	2.70 x "
468	1.350	6.54 x "	4.84 x "
468	1.350	3.37 x "	2.50 x "
469	1.348	1.88 x "	1.38 x "
469	1.348	5.39 x 10^{-6}	4.00 x 10^{-3}

.o.o.o.o.o.o.o.o.o.o.o.o.o.o.o.

Graph 29. Ca^{2+}-doped CsCl. 125 ppm.

$T^{o}C$	$1/T \times 10^{-3}$ °A	$\sigma(ohm^{-1}cm^{-1})$	$\sigma T(ohm^{-1}cm^{-1})$ °A.
227	2.000	2.86×10^{-9}	1.43×10^{-6}
258	1.880	9.41 x "	5.00 x "
274	1.828	2.02×10^{-8}	1.10×10^{-5}
297	1.754	5.29 x "	3.02 x "
309	1.718	8.23 x "	4.79 x "
325	1.672	1.65×10^{-7}	9.87 x "
343	1.623	3.76 x "	2.32×10^{-4}
354	1.595	6.40 x "	4.01 x "
371	1.553	1.18×10^{-6}	7.60 x "
395	1.497	4.24 x "	2.83×10^{-3}
407	1.471	8.23 x "	5.60 x "
410	1.464	2.07×10^{-5}	1.41×10^{-2}
426	1.431	2.50 x "	1.79 x "
436	1.410	3.12 x "	2.21 x "
440	1.403	2.80 x "	2.04 x "
461	1.362	1.00 x "	7.34×10^{-3}
484	1.321	6.60×10^{-6}	5.00 x "

.o.o.o.o.o.o.o.o.o.o.o.o.o.o.o.o.

Graph 30. SO_4^{2-}-doped CsCl. 81ppm.

$T\ ^\circ C.$	$1/T \times 10^{-3}\ ^\circ A.$	$\sigma (ohm^{-1}cm^{-1})$	$\sigma T (ohm^{-1}cm^{-1})\ ^\circ A.$
282	1.802	3.78×10^{-8}	2.10×10^{-5}
302	1.739	1.06×10^{-7}	$6.11 \times$ "
317	1.695	$1.83 \times$ "	1.08×10^{-4}
333	1.650	$3.66 \times$ "	$2.22 \times$ "
349	1.608	$7.06 \times$ "	$4.39 \times$ "
359	1.582	1.09×10^{-6}	$6.90 \times$ "
366	1.565	$1.46 \times$ "	$9.36 \times$ "
376	1.541	$2.17 \times$ "	1.41×10^{-3}
383	1.524	$4.58 \times$ "	$3.00 \times$ "
412	1.460	1.03×10^{-5}	$7.04 \times$ "
442	1.399	$2.10 \times$ "	1.50×10^{-2}
457	1.370	$2.96 \times$ "	$2.16 \times$ "
468	1.350	$3.82 \times$ "	$2.83 \times$ "
477	1.333	$4.59 \times$ "	$3.44 \times$ "
484	1.321	$5.32 \times$ "	$4.03 \times$ "
502	1.290	9.06×10^{-6}	7.02×10^{-3}
517	1.266	1.18×10^{-5}	$9.31 \times$ "

.o.o.o.o.o.o.o.o.o.o.o.o.o.o.o.

Graph 31. SO_4^{2-} -doped CsCl. 100 ppm.

T°C	$1/T \times 10^{-3}$ °A	σ (ohm^{-1}cm^{-1})	σT (ohm^{-1}cm^{-1})°A.
212	2.062	1.53×10^{-8}	7.40×10^{-6}
230	1.988	$2.56 \times$ "	1.28×10^{-5}
245	1.931	$4.76 \times$ "	$2.40 \times$ "
256	1.890	$6.44 \times$ "	$3.42 \times$ "
277	1.818	1.05×10^{-7}	$5.80 \times$ "
297	1.754	$1.56 \times$ "	$8.90 \times$ "
314	1.704	$2.36 \times$ "	1.38×10^{-4}
337	1.637	$3.09 \times$ "	$1.89 \times$ "
361	1.577	$5.10 \times$ "	$3.25 \times$ "
379	1.534	$6.80 \times$ "	$4.42 \times$ "
396	1.495	1.56×10^{-6}	1.05×10^{-3}
427	1.429	$4.70 \times$ "	$3.28 \times$ "
453	1.377	$8.25 \times$ "	$6.00 \times$ "
472	1.340	1.63×10^{-5}	1.28×10^{-2}
502	1.290	$4.60 \times$ "	$3.56 \times$ "
523	1.256	$1.70 \times$ "	$1.36 \times$ "
536	1.239	$1.80 \times$ "	$1.46 \times$ "
555	1.208	$1.95 \times$ "	$1.64 \times$ "
571	1.185	$2.08 \times$ "	$1.75 \times$ "
547	1.220	$1.50 \times$ "	$1.23 \times$ "
526	1.252	9.94×10^{-6}	7.45×10^{-3}
507	1.279	$7.20 \times$ "	$5.60 \times$ "
491	1.309	$5.35 \times$ "	$4.08 \times$ "
481	1.326	$4.00 \times$ "	$3.02 \times$ "
455	1.374	$2.04 \times$ "	$1.46 \times$ "
425	1.433	$1.44 \times$ "	$1.02 \times$ "
403	1.479	8.50×10^{-7}	5.74×10^{-4}
	Second Heating.		
333	1.650	7.20×10^{-8}	4.40×10^{-5}
349	1.608	1.16×10^{-7}	$7.70 \times$ "
365	1.567	$1.95 \times$ "	1.24×10^{-4}
375	1.543	$3.14 \times$ "	$2.03 \times$ "
400	1.486	$6.02 \times$ "	$4.00 \times$ "
423	1.437	1.20×10^{-6}	$8.31 \times$ "
447	1.387	$2.38 \times$ "	$1.70 \times$ "
478	1.332	$5.00 \times$ "	$3.75 \times$ "
503	1.289	$6.48 \times$ "	$5.02 \times$ "
540	1.230	$9.35 \times$ "	$7.60 \times$ "
574	1.181	1.34×10^{-5}	1.05×10^{-3}

o.o.o.o.o.o.o.o.o.o.o.o.o.o.o.o.o

Graph 32 SO_4^{2-}-doped CsCl 120 ppm.

$T^{\circ}C$.	$1/T \times 10^{-3}$ $^{\circ}A$.	σ (ohm^{-1}cm^{-1})	σT (ohm^{-1}cm^{-1})$^{\circ}A$
273	1.832	1.79×10^{-8}	9.76×10^{-6}
289	1.779	$3.56 \times$ "	2.00×10^{-5}
302	1.739	$6.96 \times$ "	$4.00 \times$ "
315	1.701	1.26×10^{-7}	$7.41 \times$ "
337	1.639	$3.21 \times$ "	1.96×10^{-4}
355	1.592	$8.66 \times$ "	$5.44 \times$ "
370	1.555	2.18×10^{-6}	1.40×10^{-3}
382	1.527	$4.75 \times$ "	$3.11 \times$ "
404	1.477	$8.00 \times$ "	$5.42 \times$ "
425	1.433	1.22×10^{-5}	$8.52 \times$ "
451	1.381	$2.04 \times$ "	1.48×10^{-2}
472	1.342	$3.32 \times$ "	$2.47 \times$ "
492	1.307	$4.59 \times$ "	$3.51 \times$ "
504	1.287	$1.03 \times$ "	8.00×10^{-3}
512	1.274	$1.20 \times$ "	$9.43 \times$ "

.o.o.o.o.o.o.o.o.o.o.o.o.o.o.o.o.o.o.o.

Graph 33. SO_4^{2-} - doped CsCl. 137ppm.

T°C	$^1/_T \times 10^{-3}$ ° A	σ(ohm^{-1}cm^{-1})	σT(ohm^{-1}cm^{-1}) °A.
248	1.919	1.07 x 10^{-8}	5.56 x 10^{-6}
279	1.812	4.18 x "	2.31 x 10^{-5}
296	1.757	8.90 x "	5.06 x "
323	1.678	2.72 x 10^{-7}	1.62 x 10^{-4}
338	1.637	5.21 x "	3.18 x "
352	1.600	7.72 x "	4.13 x "
382	1.527	5.90 x 10^{-6}	3.86 x 10^{-3}
405	1.473	1.02 x 10^{-5}	6.90 x "
429	1.425	1.71 x "	1.19 x 10^{-2}
452	1.779	2.58 x "	1.87 x "
468	1.351	3.35 x "	2.61 x "
478	1.322	3.91 x "	2.93 x "
495	1.302	5.62 x "	4.32 x "
498	1.297	5.41 x "	4.17 x "
506	1.284	2.60 x "	2.02 x "
528	1.248	1.16 x "	9.29 x 10^{-3}
555	1.208	1.51 x "	1.25 x 10^{-2}
581	1.177	2.26 x "	1.93 x "
	Cooling..		
541	1.229	1.29 x 10^{-5}	1.05 x 10^{-2}
516	1.267	5.94 x 10^{-6}	4.68 x 10^{-3}
491	1.309	4.18 x "	3.19 x "
473	1.340	2.80 x 10^{-5}	2.08 x 10^{-2}
456	1.372	2.30 x "	1.67 x "
438	1.406	1.38 x 10^{-5}	9.81 x 10^{-3}
416	1.451	7.66 x 10^{-6}	5.27 x "
397	1.493	4.32 x "	2.89 x "
386	1.517	2.80 x "	1.84 x "
370	1.555	1.81 x "	1.16 x "
338	1.637	5.86 x 10^{-7}	9.54 x 10^{-4}
305	1.730	1.78 x "	1.02 x "
280	1.808	7.80 x 10^{-8}	4.31 x 10^{-5}
257	1.887	2.94 x "	1.56 x "
232	1.980	1.27 x "	6.41 x 10^{-6}

o.o.o.o.o.o.o.o.o.o.o.o.o.o.o.o.o.o.o

Graph 34 SO_4^{2-}-doped CsCl 150 ppm.

$T^{\circ}C$.	$1/T \times 10^{-3}$ $^{\circ}A$.	σ(ohm^{-1}cm^{-1})	σT(ohm^{-1}cm^{-1})$^{\circ}A$
248	1.919	8.27×10^{-9}	4.31×10^{-6}
277	1.818	2.95×10^{-8}	1.62×10^{-5}
283	1.799	3.47 x "	1.93 x "
296	1.757	5.33 x "	3.03 x "
323	1.678	2.03×10^{-7}	1.21×10^{-4}
352	1.600	6.74 x "	4.21 x "
372	1.550	4.65×10^{-6}	3.00×10^{-3}
382	1.527	5.85 x "	3.83 x "
405	1.475	1.01×10^{-5}	6.82 x "
429	1.425	1.65 x "	1.16×10^{-2}
451	1.381	2.58 x "	1.87 x "
467	1.351	3.51 x "	2.60 x "
478	1.332	4.00 x "	3.01 x "
498	1.297	5.39 x "	4.16 x "
506	1.284	2.62 x "	2.04 x "
527	1.250	1.13 x "	9.04×10^{-3}
556	1.206	1.48 x "	1.23×10^{-2}
576	1.178	2.24 x "	1.90 x "
	Cooling.		
563	1.196	1.24×10^{-5}	1.04×10^{-2}
515	1.269	5.83×10^{-6}	4.59×10^{-3}
491	1.309	4.16 x "	3.18 x "
473	1.340	2.82 x "	2.10 x "
455	1.374	2.30 x "	1.67 x "
437	1.408	1.40 x "	9.94×10^{-3}
416	1.451	7.71×10^{-6}	5.31 x "
397	1.493	4.30 x "	2.88 x "
385	1.520	2.74 x "	1.80 x "
370	1.555	1.80 x "	1.16 x "
337	1.639	5.82×10^{-7}	3.60×10^{-4}
305	1.730	1.78 x "	1.02 x "
280	1.808	7.65×10^{-8}	4.23×10^{-5}
257	1.887	2.92 x "	1.55 x "
232	1.980	1.24 x "	6.36×10^{-6}

.o.o.o.o.o.o.o.o.o.o.o.o.o.o.o.o.

Graph 35 SO_4^{2-}-doped CsCl 212 ppm.

T°C	$1/T \times 10^{-3}$ °A	σ (ohm^{-1}cm^{-1})	σT (ohm^{-1}cm^{-1})°A
301	1.740	3.03×10^{-8}	1.74×10^{-5}
307	1.725	4.80 x "	2.78 x "
309	1.720	4.86 x "	2.83 x "
317	1.695	7.10 x "	4.19 x "
324	1.675	1.00×10^{-7}	5.97 x "
333	1.650	1.48 x "	9.00 x "
340	1.630	2.12 x "	1.33×10^{-4}
345	1.618	2.72 x "	1.68 x "
352	1.600	3.68 x "	2.30 x "
360	1.580	8.51 x "	5.40x "
372	1.550	4.84×10^{-6}	3.12×10^{-3}
379	1.535	5.02 x "	3.36 x "
387	1.515	5.70 x "	3.75 x "
394	1.500	6.30 x "	4.20 x "
403	1.480	7.11 x "	4.80x "
413	1.458	8.05 x "	5.50 x "
422	1.441	1.10×10^{-5}	7.65 x "
430	1.422	1.45 x "	1.02×10^{-2}
433	1.415	1.50 x "	1.06 x "
443	1.395	1.70 x "	1.22 x "
450	1.383	1.82 x "	1.32 x "
457	1.370	2.07 x "	1.51 x "
472	1.342	2.55 x "	1.89 x "
477	1.333	2.85 x "	2.14 x "
491	1.309	3.40 x "	2.69 x "
496	1.300	3.86 x "	2.97 x "
508	1.280	4.00 x "	3.12 x "
517	1.266	3.00 x "	2.37 x "
518	1.265	2.38 x "	1.88 x "
519	1.263	2.30 x "	1.82 x "
523	1.255	2.13 x "	1.60 x "
529	1.247	1.77 x "	1.42 x "
546	1.221	1.57 x "	1.28 x "

.o.o.o.o.o.o.o.o.o.o.o.o.o.o.o.

Graph 36. SO_4^{2-} -doped CsCl. 274 ppm.

T°C	$^1/_T \times 10^{-3}$ °A	σ (ohm^{-1}cm^{-1})	σT (ohm^{-1}cm^{-1})°A.
278	1.815	9.30×10^{-9}	5.12×10^{-6}
292	1.770	1.64×10^{-8}	$9.27 \times$ "
314	1.704	$3.63 \times$ "	2.13×10^{-5}
338	1.637	$8.75 \times$ "	$5.35 \times$ "
360	1.580	2.23×10^{-7}	1.41×10^{-4}
383	1.524	$5.30 \times$ "	$3.48 \times$ "
406	1.473	1.87×10^{-6}	1.26×10^{-3}
435	1.412	2.00×10^{-5}	1.42×10^{-2}
460	1.364	$2.27 \times$ "	$1.66 \times$ "
477	1.333	$2.78 \times$ "	$2.07 \times$ "
489	1.312	$2.97 \times$ "	$2.26 \times$ "
506	1.284	$3.25 \times$ "	$2.53 \times$ "
520	1.261	$3.54 \times$ "	$2.81 \times$ "
527	1.250	$1.47 \times$ "	$1.17 \times$ "
554	1.209	7.60×10^{-6}	6.29×10^{-3}
576	1.178	1.67×10^{-5}	1.42×10^{-2}
595	1.152	$3.24 \times$ "	$2.81 \times$ "
	Cooling.		
582	1.170	1.98×10^{-5}	1.69×10^{-2}
543	1.225	$8.75 \times$ "	7.14×10^{-3}
508	1.280	1.02×10^{-5}	$7.69 \times$ "
470	1.346	$1.75 \times$ "	1.30×10^{-2}
450	1.383	$1.31 \times$ "	9.47×10^{-3}
443	1.397	9.30×10^{-6}	$6.68 \times$ "
413	1.458	$5.00 \times$ "	$3.43 \times$ "
369	1.558	$1.40 \times$ "	8.90×10^{-4}
341	1.629	5.00×10^{-7}	$3.07 \times$ "
312	1.709	$1.56 \times$ "	9.12×10^{-5}
259	1.880	1.40×10^{-8}	7.45×10^{-6}

o.o.o.o.o.o.o.o.o.o.o.o.o.o.o.o.o

Graph 37 SO_4^{2-}-doped CsCl. 437 ppm.

T°C.	1/T x 10^{-3} °A.	σ(ohm^{-1}cm^{-1})	σT(ohm^{-1}cm^{-1}) °A.
239	1.953	4.40 x 10^{-10}	2.25 x 10^{-7}
262	1.869	2.20 x 10^{-9}	1.18 x 10^{-6}
281	1.805	7.21 x "	3.98 x "
307	1.724	2.57 x 10^{-8}	1.49 x 10^{-5}
329	1.661	6.31 x "	3.80 x "
332	1.653	7.20 x "	4.35 x "
340	1.631	1.10 x 10^{-7}	6.74 x "
355	1.592	2.32 x "	1.45 x 10^{-4}
364	1.570	3.53 x "	1.61 x "
383	1.524	5.85 x "	3.84 x "
392	1.504	1.01 x 10^{-6}	6.60 x "
397	1.493	1.31 x "	8.77 x "
410	1.464	2.58 x "	1.76 x 10^{-3}
406	1.473	3.00 x "	2.04 x "
422	1.439	7.82 x "	5.45 x "
465	1.355	2.25 x 10^{-5}	1.54 x 10^{-2}
477	1.344	2.71 x "	2.01 x "
496	1.300	4.19 x "	3.22 x "
510	1.277	6.02 x "	4.70 x "
538	1.233	1.40 x "	1.13 x "
560	1.200	1.20 x "	1.00 x "
582	1.170	1.20 x "	1.03 x "

.o.o.o.o.o.o.o.o.o.o.o.o.o.o.o.

Cooling.

591	1.157	1.33 x 10^{-5}	1.15 x 10^{-2}
582	1.170	9.65 x 10^{-6}	8.24 x 10^{-3}
563	1.196	6.96 x "	5.87 x "
551	1.214	5.80 x "	4.78 x "
516	1.267	1.40 x 10^{-5}	1.09 x 10^{-2}
512	1.274	1.84 x "	1.44 x "
498	1.297	3.20 x "	2.46 x "
473	1.340	2.00 x "	1.59 x "
450	1.383	1.00 x "	7.23 x 10^{-3}
432	1.418	7.00 x 10^{-6}	4.94 x "
416	1.451	3.15 x "	2.17 x "
394	1.499	1.60 x 10^{-7}	1.07 x "
372	1.550	7.50 x 10^{-7}	4.83 x 10^{-4}
350	1.605	3.30 x "	2.08 x "

m^2C.	$1/T \times 10^{-3}$ °A.	$\sigma(ohm^{-1}cm^{-1})$	$\sigma T(ohm^{-1}cm^{-1})$ °A.
328	1.664	1.05×10^{-7}	8.70×10^{-5}
304	1.733	6.50×10^{-8}	3.75 x "
277	1.818	2.80 x "	1.54 x "
263	1.836	1.80 x "	9.65×10^{-6}
242	1.942	1.16 x "	5.96 x "
227	2.000	8.00×10^{-9}	4.00 x "

.0.0.0.0.0.0.0.0.0.0.0.0.0.0.

Graph 38. Mixed crystal KCl-CsCl.

t°C	1/T x 10^{-3} °A	1/R(ohm^{-1}cm^{-1})
289	1.779	4.90 x 10^{-8}
303	1.736	8.79 x "
320	1.686	1.52 x 10^{-7}
322	1.681	1.69 x "
329	1.661	2.08 x "
341	1.629	3.16 x "
368	1.560	9.00 x "
382	1.527	1.37 x 10^{-6}
393	1.502	2.08 x "
407	1.471	3.08 x "
425	1.433	4.49 x "
440	1.403	6.42 x "
451	1.381	1.09 x 10^{-5}
467	1.351	1.33 x "
473	1.341	5.27 x 10^{-6}

.o.o.o.o.o.o.o.o.o.o.o.o.o.

Graph 39 Mixed crystal CsI-CsCl

$^{\circ}$ C	$1/T \times 10^{-3}$ $^{\circ}$A.	$1/R(ohm^{-1}cm^{-1})$
295	1.761	1.40×10^{-7}
313	1.706	2.46 x "
330	1.658	4.77 x "
350	1.605	9.40 x "
364	1.570	1.62×10^{-6}
387	1.515	3.25 x "
398	1.490	5.30 x "
414	1.456	8.70 x "
426	1.431	1.43×10^{-5}
444	1.395	2.13 x "
466	1.353	3.62 x "
469	1.348	6.00×10^{-6}

.o.o.o.o.o.o.o.o.o.o.o.o.

APPENDIX B.

CHLORIDE DIFFUSION No. 1.

Diffusion time = 71.5 hrs.

Diffusion temperature = 195 ± 3°C. i.e. at 2.137

a. PURE CsCl (unannealed)

Initial activity*	= 1238	Final activity***	= 1215
Background	= 38	Background	= 53
Corrected value**	= 1213	Corrected value	= 1174

$\log {}^{A_t}/_{A_o}$ = -0.0161

Diffusion coefficient, D (cm^2/sec) , = 8.6×10^{-13}

.....

b. PURE CsCl (annealed 'in vacuo' at 400°C. for 24 hrs.)

Initial activity	= 715	Final activity	= 704
Background	= 38	Background	= 53
Corrected value	= 681	Corrected value	= 655

$\log {}^{A_t}/_{A_o}$ = -0.0169

Diffusion coefficient, D (cm^2/sec) , = 9.4×10^{-13}

.....

* All counts expressed as counts per minute (cpm)

** Corrected for background and dead-time losses.

*** Corrected for standard deviations.

CHLORIDE DIFFUSION No. 2.

Diffusion time = 69.25 hrs.

Diffusion temperature = 228 ± 2°C. i.e. @ 1.996

a. PURE CsCl. (annealed 'in vacuo' @ 400°C. for 24 hrs.)

Initial activity	= 1373	Final activity	= 1299
Background	= 58	Background	= 60
Corrected Value	= 1331	Corrected Value	= 1253

$\log {}^{A_t}/_{A_o}$ = -0.0263

Diffusion Coefficient , D (cm^2/sec) , = 3.0×10^{-12}

.....

b. PURE CsCl. (annealed 'in vacuo' @ 400°C. for 24 hrs.)

Initial activity	= 1794	Final activity	= 1721
Background	= 58	Background	= 60
Corrected Value	= 1763	Corrected Value	= 1685

$\log {}^{A_t}/_{A_o}$ = -0.0196

Diffusion Coefficient , D (cm^2/sec) , = 1.6×10^{-12}

.....

CHLORIDE DIFFUSION No. 3.

Diffusion time = 21 hrs.

Diffusion temperature = 280 ± 2°C. i.e. @ 1.808

a. PURE CsCl. (in nitrogen).

Initial activity	= 812	Final activity	= 782
Background	= 19	Background	= 23
Corrected Value	= 798	Corrected Value	= 764

$\log {}^{A_t}/_{A_o}$ = -0.0189

Diffusion Coefficient, D (cm^2/sec) , = $\underline{5.6 \times 10^{-12}}$

.....

b. SO_4^{2-}-doped CsCl. (in nitrogen)

Initial activity	= 1315	Final activity	= 1292
Background	= 19	Background	= 23
Corrected Value	= 1310	Corrected Value	= 1283

$\log {}^{A_t}/_{A_o}$ = -0.0091

Diffusion Coefficient, D (cm^2/sec) , = $\underline{1.2 \times 10^{-12}}$

.....

c. SO_4^{2-}-doped CsCl. (in nitrogen)

Initial activity	= 555	Final activity	= 543
Background	= 19	Background	= 23
Corrected Value	= 538	Corrected Value	= 522

$\log {}^{A_t}/_{A_o}$ = -0.0131

Diffusion Coefficient, D (cm^2/sec) , = 2.5×10^{-12}

.....

d. SO_4^{2-}-doped CsCl. (in nitrogen)

Initial activity	= 2112	Final activity	= 2053
Background	= 19	Background	= 23
Corrected Value	= 2130	Corrected Value	= 2065

$\log {}^{A_t}/_{A_o}$ = -0.0134

Diffusion Coefficient, D (cm^2/sec) , = 2.5×10^{-12}

.o.o.o.o.o.o.o.o.o.o.o.o.o.o.o.o.

CHLORIDE DIFFUSION No. 4.

Diffusion time = 43 hrs.

Diffusion temperature = 320 ± 3°C. i.e. @ 1.686

a. SO_4^{2-}-doped CsCl (in nitrogen)

Initial activity	= 337	Final activity	= 286
Background	= 21	Background	= 21
Corrected Value	= 317	Corrected Value	= 266

$\log {}^{A_t}/_{A_o}$ = -0.0762

Diffusion Coefficient, D (cm^2/sec) , = 2.6×10^{-11}

.....

b. SO_4^{2-}-doped CsCl. (in nitrogen)

Initial activity	= 214	Final activity	= 205
Background	= 21	Background	= 21
Corrected Value	= 193	Corrected Value	= 184

$\log {}^{A_t}/_{A_o}$ = -0.0208

Diffusion Coefficient, D (cm^2/sec) , = 8.5×10^{-12}

.....

c. $\underline{SO_4^{2-}\text{-doped CsCl}}$. (in nitrogen)

Initial activity	= 279	Final activity	= 252
Background	= 21	Background	= 21
Corrected Value	= 258	Corrected Value	= 231

$\log {}^{A_t}/_{A_o}$ = -0.0480

Diffusion Coefficient, D (cm^2/sec) , = $\underline{1.5 \times 10^{-11}}$

.....

d. $\underline{SO_4^{2-}\text{-doped CsCl}}$. (in nitrogen)

Initial activity	= 450	Final activity	= 399
Background	= 21	Background	= 21
Corrected Value	= 430	Corrected Value	= 379

$\log {}^{A_t}/_{A_o}$ = -0.0549

Diffusion Coefficient, D (cm^2/sec) , = $\underline{1.7 \times 10^{-11}}$

.....

e. Ba^{2+}-doped CsCl. (in nitrogen) 211 ppm.

Initial activity	= 1709	Final activity	= 1527
Background	= 21	Background	= 21
Corrected Value	= 1712	Corrected Value	= 1525

$\log {}^{A_t}/_{A_o}$ = -0.0503

Diffusion Coefficient, D (cm^2/sec) , = 1.6×10^{-11}

.....

f. Ba^{2+}-doped CsCl. (in nitrogen) 48 ppm.

Initial activity	= 887	Final activity	= 775
Background	= 21	Background	= 21
Corrected Value	= 872	Corrected Value	= 759

$\log {}^{A_t}/_{A_o}$ = -0.0603

Diffusion Coefficient, D (cm^2/sec) , = 2.0×10^{-11}

.o.o.o.o.o.o.o.o.o.o.o.o.o.

CHLORIDE DIFFUSION No. 5.

Diffusion time = 20 hrs.

Diffusion temperature = 333 ± 2°C. i.e. @ 1.650

a. PURE CsCl. ('in vacuo')

Initial activity	= 777	Final activity	= 711
Background	= 37	Background	= 37
Corrected Value	= 745	Corrected Value	= 678

$\log {}^{A_t}/_{A_o}$ = -0.0410

Diffusion Coefficient, D (cm^2/sec) , = $\underline{2.8 \times 10^{-11}}$

.....

b. PURE CsCl. (in nitrogen)

Initial activity	= 1040	Final activity	= 940
Background	= 37	Background	= 37
Corrected Value	= 1012	Corrected Value	= 911

$\log {}^{A_t}/_{A_o}$ = -0.0456

Diffusion Coefficient, D (cm^2/sec) , = $\underline{3.6 \times 10^{-11}}$

.o.o.o.o.o.o.o.o.o.o.o.o.o.o.o.

CHLORIDE DIFFUSION No. 6.

Diffusion time = 20 hrs.

Diffusion temperature = 345 ± 2°C. i.e. @ 1.618

PURE CsCl. ('in vacuo')

Initial activity	= 338	Final activity	= 302
Background	= 60	Background	= 59
Corrected Value	= 279	Corrected Value	= 244

$\log {}^{A_t}/_{A_o}$ = -0.0582

Diffusion Coefficient, D (cm^2/sec) , = $\underline{5.8 \times 10^{-11}}$

.o.o.o.o.o.o.o.o.o.o.o.o.o.

CHLORIDE DIFFUSION No. 7.

Diffusion time = 29 hrs.

Diffusion temperature = 352 ± 3°C. i.e. @ 1.600

a. PURE CsCl. (in nitrogen)

Initial activity	= 1557	Final activity	= 1300
Background	= 50	Background	= 57
Corrected Value	= 1528	Corrected Value	= 1257

$\log {}^{A_t}/_{A_o}$ = -0.0874

Diffusion Coefficient, D (cm^2/sec) , = $\underline{9.2 \times 10^{-11}}$

.....

b. PURE CsCl. ('in vacuo')

Initial activity	= 1146	Final activity	= 948
Background	= 50	Background	= 57
Corrected Value	= 1107	Corrected Value	= 899

$\log {}^{A_t}/_{A_o}$ = -0.0902

Diffusion Coefficient, D (cm^2/sec) , = $\underline{9.6 \times 10^{-11}}$

.o.o.o.o.o.o.o.o.o.o.o.o.o.o.o.

CHLORIDE DIFFUSION No. 8.

Diffusion time = 20 hrs.

Diffusion temperature = 358 ± 2°C. i.e. @ 1.585

a. PURE CsCl. (in nitrogen)

Initial activity	= 354	Final activity	= 308
Background	= 17	Background	= 24
Corrected Value	= 338	Corrected Value	= 285

$\log {}^{A_t}/_{A_o}$ = -0.0741

Diffusion Coefficient, D (cm^2/sec) , = $\underline{8.2 \times 10^{-11}}$

.....

b. PURE CsCl. (in nitrogen)

Initial activity	= 429	Final activity	= 350
Background	= 17	Background	= 24
Corrected Value	= 413	Corrected Value	= 327

$\log {}^{A_t}/_{A_o}$ = -0.1015

Diffusion Coefficient, D (cm^2/sec) , = $\underline{1.2 \times 10^{-10}}$

.....

c. Ba^{2+}-doped CsCl. (in nitrogen) 77ppm.

Initial activity	= 548	Final activity	= 488
Background	= 17	Background	= 24
Corrected Value	= 533	Corrected Value	= 466

$\log {}^{A_t}/_{A_o}$ = -0.0583

Diffusion Coefficient, D (cm^2/sec) , = 5.7×10^{-11}

.....

d. Ba^{2+}-doped CsCl. (in nitrogen) 162 ppm.

Initial activity	= 581	Final activity	= 549
Background	= 17	Background	= 24
Corrected Value	= 567	Corrected Value	= 527

$\log {}^{A_t}/_{A_o}$ = —0.0318

Diffusion Coefficient, D (cm^2/sec) , = 2.0×10^{-11}

.....

e. SO_4^{2-}-doped CsCl. (in nitrogen)

Initial activity	= 350	Final activity	= 321
Background	= 17	Background	= 17
Corrected Value	= 334	Corrected Value	= 298

$\log {}^{A_t}/_{A_o}$ = -0.0495

Diffusion Coefficient, D (cm^2/sec) , = 4.0×10^{-11}

.....

f. SO_4^{2-}-doped CsCl. (in nitrogen)

Initial activity	= 214	Final activity	= 203
Background	= 17	Background	= 24
Corrected Value	= 197	Corrected Value	= 179

$\log {}^{A_t}/_{A_o}$ = -0.0416

Diffusion Coefficient, D (cm^2/sec) , = 3.5×10^{-11}

.o.o.o.o.o.o.o.o.o.o.o.o.o.o.o.

CHLORIDE DIFFUSION No. 9.

Diffusion time = 4 hrs.

diffusion temperature = 358 ± 3°C. i.e. @ 1.585

a. PURE CsCl.

Initial activity	= 832	Final activity	= 765
Background	= 55	Background	= 55
Corrected Value	= 783	Corrected Value	= 715

$\log {}^{A_t}/_{A_o} = -0.0395$

Diffusion Coefficient, D (cm^2/sec) , = $\underline{1.2 \times 10^{-10}}$

.....

b. PURE CsCl.

Initial activity	= 875	Final activity	= 805
Background	= 55	Background	= 55
Corrected Value	= 827	Corrected Value	= 755

$\log {}^{A_t}/_{A_o} = -0.0396$

Diffusion Coefficient, D (cm^2/sec) , = $\underline{1.2 \times 10^{-10}}$

.o.o.o.o.o.o.o.o.o.o.o.o.o.o.

CHLORIDE DIFFUSION No. 10.

Diffusion time = 24 hrs.

Diffusion temperature = 360 ± 2°C. i.e. @ 1.580

a. SO_4^{2-}-doped CsCl. ('in vacuo')

Initial activity	= 625	Final activity	= 535
Background	= 27	Background	= 29
Corrected Value	= 601	Corrected Value	= 508

$\log {}^{A_t}/_{A_o}$ = -0.0730

Diffusion Coefficient, D (cm^2/sec) , = 8.0×10^{-11}

.....

b. SO_4^{2-}-doped CsCl. ('in vacuo')

Initial activity	= 4271	Final activity	= 3751
Background	= 27	Background	= 29
Corrected Value	= 4396	Corrected Value	= 3853

$\log {}^{A_t}/_{A_o}$ = -0.0576

Diffusion Coefficient, D (cm^2/sec) , = 4.7×10^{-11}

.o.o.o.o.o.o.o.o.o.o.o.o.o.o.o.

c. SO_4^{2-}-doped CsCl. ('in vacuo')

Initial activity	= 621	Final activity	= 517
Background	= 27	Background	= 29
Corrected Value	= 597	Corrected Value	= 490

$\log {}^{A_t}/_{A_o}$ = -0.0858

Diffusion Coefficient, D (cm^2/sec) , = 1.1×10^{-10}

.....

d. SO_4^{2-}-doped CsCl. ('in vacuo') 162 ppm.

Initial activity	= 737	Final activity	= 646
Background	= 27	Background	= 29
Corrected Value	= 714	Corrected Value	= 621

$\log {}^{A_t}/_{A_o}$ = -0.0606

Diffusion Coefficient, D (cm^2/sec) , = 5.4×10^{-11}

.....

e. SO_4^{2-}-doped CsCl. ('in vacuo') 123 ppm.

Initial activity	= 1829	Final activity	= 1560
Background	= 27	Background	= 29
Corrected Value	= 1829	Corrected Value	= 1553

$\log {}^{A_t}/_{A_o} = -0.0711$

Diffusion Coefficient, D (cm^2/sec) , = 7.4×10^{-11}

.....

f. SO_4^{2-}-doped CsCl. ('in vacuo').

Initial activity	= 3829	Final activity	= 3272
Background	= 27	Background	= 29
Corrected Value	= 3926	Corrected Value	= 3331

$\log {}^{A_t}/_{A_o} = -0.0715$

Diffusion Coefficient, D (cm^2/sec) , = 7.5×10^{-11}

.o.o.o.o.o.o.o.o.o.o.o.o.o.

CHLORIDE DIFFUSION No. 11.

Diffusion time = 6 hrs.

Diffusion temperature = 370°C. i.e. @ 1.555

a. PURE CsCl. (in nitrogen)

Initial activity	= 489	Final activity	= 434
Background	= 58	Background	= 60
Corrected Value	= 433	Corrected Value	= 376

$\log {}^{A_t}/_{A_o}$ = -0.0613

Diffusion Coefficient, D (cm^2/sec) , = 2.2×10^{-10}

.....

b. PURE CsCl. (in nitrogen)

Initial activity	= 622	Final activity	= 547
Background	= 58	Background	= 60
Corrected Value	= 567	Corrected Value	= 489

$\log {}^{A_t}/_{A_o}$ = -0.0643

Diffusion Coefficient, D (cm^2/sec) , = 2.5×10^{-10}

.....

c. Ba^{2+}-doped CsCl. (in nitrogen) 128 ppm.

Initial activity	= 940	Final activity	= 876
Background	= 58	Background	= 60
Corrected Value	= 889	Corrected Value	= 823

$\log {}^{A_t}/_{A_o}$ = -0.0335

Diffusion Coefficient, D (cm^2/sec) , = 6.3×10^{-11}

.....

d. Ba^{2+}-doped CsCl. (in nitrogen).

Initial activity	= 601	Final activity	= 557
Background	= 58	Background	= 60
Corrected Value	= 545	Corrected Value	= 500

$\log {}^{A_t}/_{A_o}$ = -0.0374

Diffusion Coefficient, D (cm^2/sec) , = 7.7×10^{-11}

.....

e. SO_4^{2-}-doped CsCl. (in nitrogen)

Initial activity	= 458	Final activity	= 389
Background	= 58	Background	= 60
Corrected Value	= 402	Corrected Value	= 330

$\log {}^{A_t}/_{A_o}$ = -0.0857

Diffusion Coefficient, D (cm^2/sec) , = 4.4×10^{-10}

.....

f. SO_4^{2-}-doped CsCl. (in nitrogen) 180 ppm.

Initial activity	= 488	Final activity	= 420
Background	= 58	Background	= 60
Corrected Value	= 432	Corrected Value	= 361

$\log {}^{A_t}/_{A_o}$ = -0.0780

Diffusion Coefficient, D (cm^2/sec) , = 3.7×10^{-10}

.o.o.o.o.o.o.o.o.o.o.o.o.o.

CHLORIDE DIFFUSION No. 12.

Diffusion time = 21.75 hrs.

Diffusion temperature = 380 ± 3°C. i.e. @ 1.531

a. PURE CsCl. (in nitrogen)

Initial activity	= 1354	Final activity	= 1042
Background	= 32	Background	= 30
Corrected Value	= 1338	Corrected Value	= 1021

$\log {}^{A_t}/_{A_o}$ = -0.1174

Diffusion Coefficient, D (cm^2/sec) , = 2.4×10^{-10}

.....

b. PURE CsCl.

Initial activity	= 1419	Final activity	= 1076
Background	= 32	Background	= 30
Corrected Value	= 1404	Corrected Value	= 1055

$\log {}^{A_t}/_{A_o}$ = -0.1241

Diffusion Coefficient, D (cm^2/sec) , = 2.7×10^{-10}

.o.o.o.o.o.o.o.o.o.o.o.o.o.o.o.

c. Ba^{2+}-doped CsCl. 97 ppm.

Initial activity	= 254	Final activity	= 227
Background	= 32	Background	= 30
Corrected Value	= 223	Corrected Value	= 197

$\log {}^{A_t}/_{A_o} = -0.0538$

Diffusion Coefficient, D (cm^2/sec) , = $\underline{7.2 \times 10^{-11}}$

.....

d. Ba^{2+}-doped CsCl.

Initial activity	= 443	Final activity	= 367
Background	= 32	Background	= 30
Corrected Value	= 412	Corrected Value	= 338

$\log {}^{A_t}/_{A_o} = -0.0860$

Diffusion Coefficient, D (cm^2/sec) , = $\underline{1.3 \times 10^{-10}}$

.o.o.o.o.o.o.o.o.o.o.o.o.o.o.

CHLORIDE DIFFUSION No. 13.

Diffusion time = 4 hrs.

Diffusion temperature = 388 ± 2°C. i.e. @ 1.513

a. PURE CsCl. (in nitrogen)

Initial activity	= 521	Final activity	= 457
Background	= 58	Background	= 57
Corrected Value	= 465	Corrected Value	= 382

$\log {}^{A_t}/_{A_o}$ = -0.0854

Diffusion Coefficient, D (cm^2/sec) , = 3.4×10^{-10}

.....

b. PURE CsCl. (in nitrogen)

Initial activity	= 832	Final activity	= 652
Background	= 58	Background	= 57
Corrected Value	= 780	Corrected Value	= 600

$\log {}^{A_t}/_{A_o}$ = -0.1109

Diffusion Coefficient, D (cm^2/sec) , = 4.3×10^{-10}

.....

c. Ba^{2+}-doped CsCl. (in nitrogen) 116 ppm.

Initial activity	= 737	Final activity	= 667
Background	= 58	Background	= 57
Corrected Value	= 683	Corrected Value	= 614

$$\log {}^{A_t}/_{A_o} = -0.0464$$

Diffusion Coefficient, D (cm^2/sec) , = 1.7×10^{-10}

.....

d. Ba^{2+}-doped CsCl. (in nitrogen)

Initial activity	= 588	Final activity	= 539
Background	= 57	Background	= 57
Corrected Value	= 533	Corrected Value	= 484

$$\log {}^{A_t}/_{A_o} = -0.0419$$

Diffusion Coefficient, D (cm^2/sec) , = 1.4×10^{-10}

.....

e. SO_4^{2-}-doped CsCl. (in nitrogen)

Initial activity	= 882	Final activity	= 720
Background	= 58	Background	= 57
Corrected Value	= 829	Corrected Value	= 667

$\log {}^{A_t}/_{A_o} = -0.0945$

Diffusion Coefficient, D (cm^2/sec) , = 3.7×10^{-10}

.....

f. SO_4^{2-}-doped CsCl. (in nitrogen)

Initial activity	= 707	Final activity	= 535
Background	= 58	Background	= 57
Corrected Value	= 653	Corrected Value	= 480

$\log {}^{A_t}/_{A_o} = -0.1337$

Diffusion Coefficient, D (cm^2/sec) , = 5.0×10^{-10}

.o.o.o.o.o.o.o.o.o.o.o.o.o.

CHLORIDE DIFFUSION No. 14.

Diffusion time = 4 hrs.

Diffusion temperature = 404 ± 3°C. i.e. @ 1.477

a. PURE CsCl.

Initial activity	= 673	Final activity	= 572
Background	= 54	Background	= 54
Corrected Value	= 623	Corrected Value	= 522

$\text{Log } {}^{A_t}/_{A_o} = -0.0768$

Diffusion Coefficient, D (cm^2/sec) , = 4.9×10^{-10}

.....

b. PURE CsCl.

Initial activity	= 831	Final activity	= 705
Background	= 54	Background	= 54
Corrected Value	= 783	Corrected Value	= 655

$\log {}^{A_t}/_{A_o} = -0.0774$

Diffusion Coefficient, D (cm^2/sec) , = 5.0×10^{-10}

.o.o.o.o.o.o.o.o.o.o.o.o.o.

CHLORIDE DIFFUSION No. 15.

Diffusion time = 2.5 hrs.

Diffusion temperature = 420 $\pm$ 2°C. i.e. @ 1.443

a. PURE CsCl. (in nitrogen)

Initial activity	= 809	Final activity	= 702
Background	= 58	Background	= 58
Corrected Value	= 756	Corrected Value	= 648

$\log {}^{A_t}/_{A_o}$ = -0.0669

Diffusion Coefficient, D (cm^2/sec) , = 6.0×10^{-10}

.....

b. PURE CsCl. (in nitrogen)

Initial activity	= 1286	Final activity	= 1078
Backgound	= 54	Background	= 54
Corrected Value	= 1242	Corrected Value	= 1030

$\log {}^{A_t}/_{A_o}$ = -0.0713

Diffusion Coefficient, D (cm^2/sec) , = 8.8×10^{-10}

.o.o.o.o.o.o.o.o.o.o.o.o.o.

CHLORIDE DIFFUSION No. 16.

Diffusion time = 65 hrs.

Diffusion temperature = 429 ± 3°C. i.e. @ 1.425

a. PURE CsCl.

Initial activity	= 566	Final activity	= 235
Background	= 34	Background	= 15
Corrected Value	= 535	Corrected Value	= 220

$\log {}^{A_t}/_{A_o} = -0.3860$

Diffusion Coefficient, D (cm^2/sec) , = $\underline{1.1 \times 10^{-9}}$

.....

b. Ba^{2+}-doped CsCl. 88 ppm.

Initial activity	= 1560	Final activity	= 950
Background	= 35	Background	= 20
Corrected Value	= 1546	Corrected Value	= 938

$\log {}^{A_t}/_{A_o} = -0.2170$

Diffusion Coefficient, D (cm^2/sec), = $\underline{5.8 \times 10^{-10}}$

c. $\underline{SO_4^{2-}\text{-doped CsCl}}$.

Initial activity	= 684	Final activity	= 314
Background	= 35	Background	= 40
Corrected Value	= 653	Corrected Value	= 275

$\log {}^{A_t}/_{A_o}$ = -0.3756

Diffusion Coefficient, D (cm^2/sec) , = $\underline{1.0 \times 10^{-9}}$

.o.o.o.o.o.o.o.o.o.o.o.o.o.

CHLORIDE DIFFUSION No. 17.

Diffusion time = 70.75 hrs.

Diffusion temperature = $440^{o} \pm 3^{o}C$. i.e. @ 1.403

a. PURE CsCl.

Initial activity	= 2498	Final activity	= 1129
Background	= 32	Background	= 20
Corrected Value	= 2519	Corrected Value	= 1116

$\log {}^{A_t}/_{A_o} = -0.3525$

Diffusion Coefficient, D (cm^2/sec) , = $\underline{1.3 \times 10^{-9}}$

.....

b. PURE CsCl.

Initial activity	= 2143	Final activity	= 825
Background	= 30	Background	= 18
Corrected Value	= 2152	Corrected Value	= 812

$\log {}^{A_t}/_{A_o} = \rightarrow 0.4167$

Diffusion Coefficient, D (cm^2/sec), = $\underline{1.5 \times 10^{-9}}$

.o.o.o.o.o.o.o.o.o.o.o.o.o.

CHLORIDE DIFFUSION No. 18.

Diffusion time = 3 hrs.

Diffusion temperature = 450 ± 2°C. i.e. at 1.383

a. PURE CsCl (in nitrogen)

Initial activity	= 1014	Final activity	= 772
Background	= 63	Background	= 65
Corrected value	= 959	Corrected value	= 712

$\log {}^{A_t}/_{A_o}$ = -0.1293

Diffusion coefficient, D (cm^2/sec) , = 2.3×10^{-9}

.....

b. PURE CsCl (in nitrogen)

Initial activity	= 343	Final activity	= 281
Background	= 63	Background	= 65
Corrected value	= 281	Corrected value	= 217

$\log {}^{A_t}/_{A_o}$ = -0.1122

Diffusion coefficient, D (cm^2/sec) , = 1.6×10^{-9}

.o.o.o.o.o.o.o.o.o.o.o.o.o.

CHLORIDE DIFFUSION No. 19.

Diffusion time = 18 hrs.

Diffusion temperature = 456 ± 3°C. i.e. at 1.372

a. PURE CsCl

Initial activity	= 974	Final activity	= 510
Background	= 58	Background	= 58
Corrected value	= 924	Corrected value	= 454

$\log {}^{A_t}/_{A_o}$ = -0.3086

Diffusion coefficient, D (cm^2/sec) , = $\underline{3.0 \times 10^{-9}}$

.....

b. Ba^{2+}-doped CsCl.

Initial activity	= 1222	Final activity	= 913
Background	= 58	Background	= 58
Corrected value	= 1176	Corrected value	= 862

$\log {}^{A_t}/_{A_o}$ = -0.1350

Diffusion coefficient, D (cm^2/sec) , = $\underline{1.6 \times 10^{-10}}$

.....

c. Ba^{2+}-doped CsCl

Initial activity	= 792	Final activity	= 636
Background	= 58	Background	= 58
Corrected value	= 739	Corrected value	= 561

$\log {}^{A_t}/_{A_o}$ = -0.1196

Diffusion coefficient, D (cm^2/sec) , = $\underline{1.2 \times 10^{-10}}$

.o.o.o.o.o.o.o.o.o.o.o.o.o.o.

CAESIUM DIFFUSION No. 1.

Diffusion time = 116.5 hrs.

Diffusion temperature = 248 ± 3 °C. i.e. at 1.919

a. PURE CsCl unannealed (in nitrogen)

Initial total activity	= 1102	Final total activity	= 1072
Background	= 51	Background	= 46
Corrected value*	= 1062	Corrected value	= 1036
γ-contribution	= 440	γ-contribution	= 438
β-contribution	= 622	β-contribution	= 598

$\log {}^{A_t}/_{A_o} = -0.0171$

Diffusion coefficient, D (cm^2/sec) , = 8.2×10^{-14}

.....

b. PURE CsCl annealed (in nitrogen)

Initial total activity	= 921	Final total activity	= 881
Background	= 51	Background	= 46
Corrected value	= 878	Corrected value	= 842
γ-contribution	= 369	γ-contribution	= 369
β-contribution	= 509	β-contribution	= 473

$\log {}^{A_t}/_{A_o} = -0.0318$

Diffusion coefficient, D (cm^2/sec) , = 3.4×10^{-13}

.o.o.o.o.o.o.o.o.o.o.o.o.o.

CAESIUM DIFFUSION No. 2.

Diffusion time = 66.5 hrs.

Diffusion temperature = 290 ± 3 °C. i.e. at 1.776

a. PURE CsCl annealed.

Initial total activity	= 773	Final total activity**	= 750
Background	= 47	Background	= 47
Corrected value*	= 733	Corrected value*	= 710
γ-contribution	= 306	γ-contribution	= 306
β-contribution	= 427	β-contribution	= 404

$\log {}^{A_t}/_{A_o}$ = -0.0240

Diffusion coefficient, D (cm^2/sec) , = $\underline{3.4 \times 10^{-13}}$

.....

b. PURE CsCl unannealed.

Initial total activity	= 927	Final total activity	= 893
Background	= 47	Background	= 47
Corrected value	= 888	Corrected value	= 854
γ-contribution	= 368	γ-contribution	= 365
β-contribution	= 520	β-contribution	= 489

$\log {}^{A_t}/_{A_o}$ = -0.0267

Diffusion coefficient, D (cm^2/sec) , = $\underline{3.8 \times 10^{-13}}$

.o.o.o.o.o.o.o.o.o.o.o.o.o.o.o.o.o.o.

*Corrected for dead-time losses and background radiation.

**Corrected for standard deviations, and when ratio of γ-contributions is outwith 1%.

CAESIUM DIFFUSION No. 3.

Diffusion time = 91.5 hrs.

Diffusion temperature = 307 ± 2 °C. i.e. at 1.724

a. PURE CsCl (in nitrogen)

Initial total activity	= 999	Final total activity	= 928
Background	= 72	Background	= 68
Corrected value	= 936	Corrected value	= 867
γ-contribution	= 392	γ-contribution	= 392
β-contribution	= 544	β-contribution	= 475

$\log {}^{A_t}/_{A_o}$ = -0.0589

Diffusion coefficient, D (cm^2/sec) , = $\underline{1.4 \times 10^{-12}}$

.....

b. PURE CsCl (in nitrogen)

Initial total activity	= 1142	Final total activity	= 1064
Background	= 72	Background	= 68
Corrected value	= 1081	Corrected value	= 1006
γ-contribution	= 462	γ-contribution	= 462
β-contribution	= 619	β-contribution	= 544

$\log {}^{A_t}/_{A_o}$ = -0.0561

Diffusion coefficient, D (cm^2/sec) , = $\underline{1.2 \times 10^{-12}}$

.....

c. Sr^{2+}-doped CsCl

Initial total activity	= 843	Final total activity	= 779
Background	= 72	Background	= 68
Corrected value	= 776	Corrected value	= 715
γ-contribution	= 320	γ-contribution	= 320
β-contribution	= 456	β-contribution	= 395

$\log {}^{A_t}/_{A_o}$ = -0.0624

Diffusion coefficient , D (cm^2/sec) , = $\underline{1.6 \times 10^{-12}}$

.....

d. Ba^{2+}-doped CsCl

Initial total activity	= 698	Final total activity	= 594
Background	= 72	Background	= 68
Corrected value	= 630	Corrected value	= 539
γ-contribution	= 262	γ-contribution	= 262
β-contribution	= 368	β-contribution	= 277

$\log {}^{A_t}/_{A_o}$ = -0.1233

Diffusion coefficient , D (cm^2/sec) , = $\underline{6.5 \times 10^{-12}}$

.....

e. Ca^{2+}-doped CsCl

Initial total activity	= 602	Final total activity	= 441
Background	= 72	Background	= 68
Corrected value	= 533	Corrected value	= 374
γ-contribution	= 228	γ-contribution	= 228
β-contribution	= 305	β-contribution	= 146

$\log {}^{A_t}/_{A_o}$ = -0.3199

Diffusion coefficient , D (cm^2/sec) , = $\underline{8.4 \times 10^{-11}}$

f. SO_4^{2-}-doped CsCl

Initial total activity	= 586	Final total activity	= 544
Background	= 72	Background	= 68
Corrected value	= 517	Corrected value	= 478
γ-contribution	= 224	γ-contribution	= 224
β-contribution	= 293	β-contribution	= 254

$\log {}^{A_t}/_{A_o}$ = -0.0621

Diffusion coefficient, D (cm^2/sec) , = $\underline{1.6 \times 10^{-12}}$

.....

g. SO_4^{2-}-doped CsCl

Initial total activity	= 851	Final total activity	= 823
Background	= 72	Background	= 68
Corrected value	= 784	Corrected value	= 760
γ-contribution	= 333	γ-contribution	= 330
β-contribution	= 451	β-contribution	= 430

$\log {}^{A_t}/_{A_o}$ = -0.0207

Diffusion coefficient, D (cm^2/sec) , = $\underline{2.1 \times 10^{-13}}$

.o.o.o.o.o.o.o.o.o.o.o.o.o.o.

CAESIUM DIFFUSION No. 4.

Diffusion time = 68.75 hrs.

Diffusion temperature = 320 ± 2 °C. i.e. at 1.686

a. PURE CsCl annealed (in nitrogen)

Initial total activity	= 907	Final total activity	= 842
Background	= 70	Background	= 74
Corrected value	= 844	Corrected value	= 774
γ-contribution	= 361	γ-contribution	= 361
β-contribution	= 483	β-contribution	= 413

$\log {}^{A_t}/_{A_o}$ = -0.0679

Diffusion coefficient, D (cm^2/sec) , = $\underline{2.7 \times 10^{-12}}$

.....

b. PURE CsCl unannealed (in nitrogen)

Initial total activity	= 736	Final total activity	= 680
Background	= 71	Background	= 74
Corrected value	= 669	Corrected value	= 609
γ-contribution	= 281	γ-contribution	= 281
β-contribution	= 388	β-contribution	= 328

$\log {}^{A_t}/_{A_o}$ = -0.0729

Diffusion coefficient, D (cm^2/sec) , = $\underline{3.0 \times 10^{-12}}$

.....

c. Sr^{2+}-doped CsCl annealed (in nitrogen)

Initial total activity	= 850	Final total activity	= 796
Background	= 71	Background	= 74
Corrected value	= 786	Corrected value	= 727
γ-contribution	= 336	γ-contribution	= 336
β-contribution	= 450	β-contribution	= 391

$\log {}^{A_t}/_{A_o}$ = -0.0610

Diffusion coefficient, D (cm^2/sec) , = $\underline{2.0 \times 10^{-12}}$

.....

d. Sr^{2+}-doped CsCl unannealed (in nitrogen)

Initial total activity	= 966	Final total activity	= 865
Background	= 71	Background	= 74
Corrected value	= 903	Corrected value	= 796
γ-contribution	= 384	γ-contribution	= 384
β-contribution	= 519	β-contribution	= 412

$\log {}^{A_t}/_{A_o}$ = -0.1003

Diffusion coefficient, D (cm^2/sec) , = $\underline{5.8 \times 10^{-12}}$

.....

e. SO_4^{2-}-doped CsCl

Initial total activity	= 921	Final total activity	= 895
Background	= 71	Background	= 74
Corrected value	= 857	Corrected value	= 828
γ-contribution	= 360	γ-contribution	= 360
β-contribution	= 491	β-contribution	= 468

$\log {}^{A_t}/_{A_o}$ = -0.0209

Diffusion coefficient, D (cm^2/sec) , = $\underline{3.1 \times 10^{-13}}$

CAESIUM DIFFUSION No. 5.

Diffusion time = 66.25 hrs.

Diffusion temperature = 364 ± 3 °C. i.e. at 1.570

a. PURE CsCl (in nitrogen)

Initial total activity	= 709	Final total activity	= 598
Background	= 57	Background	= 61
Corrected value	= 656	Corrected value	= 540
γ-contribution	= 274	γ-contribution	= 274
β-contribution	= 382	β-contribution	= 266

$\log {}^{A_t}/_{A_o} = -0.1572$

Diffusion coefficient, D (cm^2/sec) , = $\underline{1.6 \times 10^{-11}}$

.....

b. Ca^{2+}-doped CsCl (in nitrogen)

Initial total activity	= 843	Final total activity	= 604
Background	= 57	Background	= 61
Corrected value	= 793	Corrected value	= 546
γ-contribution	= 335	γ-contribution	= 335
β-contribution	= 458	β-contribution	= 211

$\log {}^{A_t}/_{A_o} = -0.3366$

Diffusion coefficient, D (cm^2/sec) , = $\underline{1.0 \times 10^{-10}}$

.o.o.o.o.o.o.o.o.o.o.o.o.o.o.o.

CAESIUM DIFFUSION No. 6.

Diffusion time = 19 hrs.

Diffusion temperature = 383 ± 3 °C. i.e. at 1.524

a. PURE CsCl annealed (in nitrogen)

Initial total activity	= 750	Final total activity	= 634
Background	= 54	Background	= 52
Corrected value	= 700	Corrected value	= 585
γ-contribution	= 294	γ-contribution	= 294
β-contribution	= 406	β-contribution	= 291

$\log {}^{A_t}/_{A_o}$ = -0.1446

Diffusion coefficient, D (cm^2/sec) , = $\underline{4.5 \times 10^{-11}}$

.....

b. PURE CsCl unannealed (in nitrogen)

Initial total activity	= 842	Final total activity	= 711
Background	= 54	Background	= 52
Corrected value	= 793	Corrected value	= 663
γ-contribution	= 336	γ-contribution	= 336
β-contribution	= 457	β-contribution	= 327

$\log {}^{A_t}/_{A_o}$ = -0.1454

Diffusion coefficient, D (cm^2/sec) , = $\underline{4.6 \times 10^{-11}}$

.....

c. Ba^{2+}-doped CsCl (in nitrogen)

Initial total activity	= 639	Final total activity	= 478
Background	= 54	Background	= 52
Corrected value	= 588	Corrected value	= 428
γ-contribution	= 246	γ-contribution	= 246
β-contribution	= 342	β-contribution	= 182

$\log {}^{A_t}/_{A_o}$ = -0.2739

Diffusion coefficient, D (cm^2/sec) , = $\underline{1.9 \times 10^{-10}}$

.....

d. SO_4^{2-}-doped CsCl (in nitrogen)

Initial total activity	= 786	Final total activity	= 701
Background	= 54	Background	= 52
Corrected value	= 737	Corrected value	= 653
γ-contribution	= 315	γ-contribution	= 315
β-contribution	= 422	β-contribution	= 338

$\log {}^{A_t}/_{A_o}$ = -0.0964

Diffusion coefficient, D (cm^2/sec) , = $\underline{1.9 \times 10^{-11}}$

.o.o.o.o.o.o.o.o.o.o.o.o.o.o.o.

CAESIUM DIFFUSION No. 7.

Diffusion time = 5 hrs.

Diffusion temperature = 402 ± 2 °C. i.e. at 1.481

a. PURE CsCl (in nitrogen)

Initial total activity	= 676	Final total activity	= 586
Background	= 57	Background	= 58
Corrected value	= 623	Corrected value	= 531
γ-contribution	= 258	γ-contribution	= 258
β-contribution	= 365	β-contribution	= 273

$\log {}^{A_t}/_{A_o}$ = -0.1261

Diffusion coefficient, D (cm^2/sec) , = $\underline{\underline{1.2 \times 10^{-10}}}$

.....

b. PURE CsCl (in nitrogen)

Initial total activity	= 596	Final total activity	= 517
Background	= 57	Background	= 58
Corrected value	= 542	Corrected value	= 461
γ-contribution	= 222	γ-contribution	= 222
β-contribution	= 320	β-contribution	= 239

$\log {}^{A_t}/_{A_o}$ = -0.1268

Diffusion coefficient, D (cm^2/sec) , = $\underline{\underline{1.2 \times 10^{-10}}}$

.....

c. Ba^{2+}-doped CsCl (in nitrogen)

Initial total activity	= 779	Final total activity	= 674
Background	= 57	Background	= 58
Corrected value	= 727	Corrected value	= 620
γ-contribution	= 305	γ-contribution	= 305
β-contribution	= 422	β-contribution	= 315

$\log {}^{A_t}/_{A_o} = -0.1270$

Diffusion coefficient, D (cm^2/sec) , = $\underline{1.2 \times 10^{-10}}$

.....

d. Ba^{2+}-doped CsCl (in nitrogen)

Initial total activity	= 1177	Final total activity	= 992
Background	= 57	Background	= 58
Corrected value	= 1133	Corrected value	= 943
γ-contribution	= 487	γ-contribution	= 487
β-contribution	= 646	β-contribution	= 456

$\log {}^{A_t}/_{A_o} = -0.1512$

Diffusion coefficient, D (cm^2/sec) , = $\underline{1.9 \times 10^{-10}}$

.o.o.o.o.o.o.o.o.o.o.o.o.o.o.

CAESIUM DIFFUSION No. 8

Diffusion time = 2.5 hrs.

Diffusion temperature = 449 °C i.e. at 1.385

a. PURE CsCl

Initial total activity	= 803	Final total activity	= 657
Background	= 61	Background	= 58
Corrected value	= 747	Corrected value	= 603
γ-contribution	= 313	γ-contribution	= 313
β-contribution	= 434	β-contribution	= 290

$\log {}^{A_t}/_{A_o} = -0.1751$

Diffusion coefficient, D (cm^2/sec) , = 4.5×10^{-10}

.....

b. PURE CsCl

Initial total activity	= 670	Final total activity	= 570
Background	= 61	Background	= 58
Corrected value	= 613	Corrected value	= 515
γ-contribution	= 263	γ-contribution	= 263
β-contribution	= 350	β-contribution	= 252

$\log {}^{A_t}/_{A_o} = -0.1472$

Diffusion coefficient, D (cm^2/sec) , = 2.9×10^{-10}

.....

c. Ba^{2+}-doped CsCl

Initial total activity	= 682	Final total activity	= 610
Background	= 58	Background	= 58
Corrected value	= 631	Corrected value	= 559
γ-contribution	= 266	γ-contribution	= 266
β-contribution	= 365	β-contribution	= 293

$\log {}^{A_t}/_{A_o} = -0.0954$

Diffusion coefficient, D (cm^2/sec) , = $\underline{1.2 \times 10^{-10}}$

.....

d. Ba^{2+}-doped CsCl

Initial total activity	= 993	Final total activity	= 923
Background	= 58	Background	= 58
Corrected value	= 947	Corrected value	= 877
γ-contribution	= 419	γ-contribution	= 419
β-contribution	= 528	β-contribution	= 458

$\log {}^{A_t}/_{A_o} = -0.0627$

Diffusion coefficient, D (cm^2/sec) , = $\underline{5.3 \times 10^{-11}}$

.o.o.o.o.o.o.o.o.o.o.o.o.o.o.o.

CAESIUM DIFFUSION No. 9.

Diffusion time = 2.0 hrs

Diffusion temperature = 481 ± 2 °C. i.e. at 1.326

a. PURE CsCl (in nitrogen)

Initial total activity	= 541	Final total activity	= 465
Background	= 78	Background	= 78
Corrected value	= 465	Corrected value	= 388
γ-contribution	= 187	γ-contribution	= 187
β-contribution	= 278	β-contribution	= 201

$\log {}^{A_t}/_{A_o}$ = -0.1415

Diffusion coefficient, D (cm^2/sec) , = $\underline{4.6 \times 10^{-10}}$

.....

b. PURE CsCl (in nitrogen)

Initial total activity	= 548	Final total activity	= 462
Background	= 78	Background	= 78
Corrected value	= 473	Corrected value	= 386
γ-contribution	= 189	γ-contribution	= 189
β-contribution	= 284	β-contribution	= 197

$\log {}^{A_t}/_{A_o}$ = -0.1588

Diffusion coefficient, D (cm^2/sec) , = $\underline{5.5 \times 10^{-10}}$

.....

c. SO_4^{2-}-doped CsCl (in nitrogen)

Initial total activity	= 538	Final total activity	= 426
Background	= 78	Background	= 78
Corrected value	= 462	Corrected value	= 349
γ-contribution	= 176	γ-contribution	= 176
β-contribution	= 286	β-contribution	= 173

$\log {}^{A_t}/_{A_o}$ = -0.2184

Diffusion coefficient, D (cm^2/sec) , = $\underline{9.7 \times 10^{-10}}$

.....

d. SO_4^{2-}-doped CsCl (in nitrogen)

Initial total activity	= 872	Final total activity	= 684
Background	= 78	Background	= 78
Corrected value	= 799	Corrected value	= 610
γ-contribution	= 314	γ-contribution	= 314
β-contribution	= 485	β-contribution	= 296

$\log {}^{A_t}/_{A_o}$ = -0.2144

Diffusion coefficient, D (cm^2/sec) , = $\underline{9.4 \times 10^{-10}}$

.....

CAESIUM DIFFUSION No. 10.

Diffusion time = 120 hrs.

Diffusion temperature = 233 ± 3°C. i.e. @ 1.972

a. IURI CsCl (in nitrogen)

Initial total activity	= 1910	Final total activity**	= 1850
Background	= 61	Background	= 58
Corrected value*	= 1880	Corrected value	= 1823
γ-contribution	= 760	γ-contribution	= 753
β-contribution	= 1120	β-contribution	= 1070

$\log {}^{A_t}/_{A_o}$ = -0.0198

Diffusion coefficient, D (cm^2/sec) , = $\underline{1.0 \times 10^{-13}}$

.....

b. PURE CsCl (in nitrogen)

Initial total activity	= 830	Final total activity	= 808
Background	= 61	Background	= 58
Corrected value	= 775	Corrected value	= 755
γ-contribution	= 332	γ-contribution	= 332
β-contribution	= 443	β-contribution	= 423

$\log {}^{A_t}/_{A_o}$ = -0.0201

Diffusion coefficient, D (cm^2/sec) , = $\underline{1.2 \times 10^{-13}}$

.....

*Values corrected for background radiation and dead-time losses.

**Corrected for Standard deviations and also corrected when the initial and final γ-contributions differ by more than 1%.

APPENDIX D.

'Pure' CsCl from Graph 2

Wt of crystal = 0.4100 g

Dissolved in cell and 4 drops of NH_3 buffer added

titrated against 1.03 mM EDTA

RESULTS	Ml of EDTA added	Absorbance
	0.00	0.087
	0.02	0.098
	0.04	0.115
	0.06	0.132
	0.08	0.147
	0.10	0.166

End point occurs below 0.009 ml

Now 1 ml of ImM EDTA = 0.137 mg Ba^{2+}

$\therefore$ 0.009 ml of 1.03mM EDTA = 0.00127 mg Ba^{2+}

$$\therefore \frac{Ba^{2+}}{Cs^{+}} = \frac{0.00127 \times 168.4 \times 10^6}{0.4100 \times 137.4 \times 10^6}$$

= less than 4 ppm

'Pure' CsCl from Graph 4 and 4a

Wt of crystal = 0.4170 g

Dissolved in 2 ml of distilled H_2O and 4 drops NH_3 buffer added titrated against 1.03mM EDTA

Results	Ml of EDTA added	Absorbance
	0.00	0.066
	0.02	0.077
	0.04	0.098
	0.06	0.115
	0.08	0.132
	0.10	0.150
	0.12	0.167
	0.14	0.185

End point occurs at 0.009 ml

Now 1 ml of EDTA (1.03mM) = 0.137 mg Ba^{2+}

$\therefore$ 0.009 ml of 1.03mM EDTA = 0.00127 mg Ba^{2+}

$\therefore \frac{Ba^{2+}}{Cs^{+}} = \frac{0.00127 \times 10^{6} \times 168.4}{0.4170 \times 137.4 \times 10^{3}}$

$= 3.7$ ppm

Ba^{2+} -doped CsCl from Graph 11

Wt of crystal = 0.2336 g

Dissolved in distilled water and 10 drops of NH_3 buffer added. Solution made up to 5 ml and 2 ml titrated against 1.03mM EDTA solution.

Results	Ml EDTA added	Absorbance
	0.000	0.044
	0.012	0.050
	0.025	0.053
	0.040	0.061
	0.065	0.080
	0.080	0.094
	0.095	0.105
	0.115	0.120

End point is at 0.031 ml

Now 1 ml of ImM EDTA = 0.137 mg Ba^{2+}

$\therefore$ 0.031 ml 1.03 mM = 0.00437 mg Ba^{2+} in 2 ml

= 0.0109 mg in 5 ml

$\therefore \frac{Ba^{2+}}{Cs^+}$ = $\frac{0.0109 \times 168.4 \times 10^6}{0.2336 \times 167.4}$

= 57 ppm

Ba^{2+} -doped CsCl from Graph 12

Wt of crystal 0.2917 g

Dissolved in distilled water, 10 drops NH_3 buffer added made up to 5 ml. 2 ml titrated with 1.03 mM EDTA

Results	Ml EDTA added	Absorbance
	0.00	0.085
	0.02	0.091
	0.04	0.097
	0.06	0.115
	0.08	0.131
	0.10	0.148
	0.12	0.166
	0.14	0.180

End point occurs at 0.042 ml

Now 1 ml mM EDTA = 0.137 mgs Ba^{2+}

0.042 ml of 1.03 mM EDTA = 0.00593 mgs Ba^{2+} in 2 ml

$\therefore$ in 5 ml = 0.0148 mgs Ba^{2+}

$$\therefore \frac{Ba^{2+}}{Cs^{+}} = \frac{0.0148 \times 168.4 \times 10^{6}}{0.2917 \times 137.4 \times 10^{3}}$$

$$= \underline{\underline{62 \text{ ppm}}}$$

Ba^{2+} -doped CsCl from Graph 13

Wt of crystal 0.4420 g

Dissolved in 2 ml made up to 5 ml with buffer 10 drops of buffer added 2 ml titrated against 1.78 mM EDTA

Results	ml EDTA added	Absorbance
	0.00	0.107
	0.02	0.115
	0.04	0.120
	0.06	0.147
	0.08	0.178
	0.10	0.200

End point is at 0.040 ml

Now 1 ml of 1 mM EDTA = 0.137 mg Ba^{2+}

$\therefore$ 0.040 ml of 1.78mM EDTA = 0.0103 mg Ba^{2+} in 2 ml

$\therefore$ in 5 ml = 0.0258 mg Ba^{2+}

$$\therefore \frac{Ba^{2+}}{Cs^{+}} = \frac{0.0258 \times 168.4 \times 10^{6}}{0.4420 \times 137.4 \times 10^{3}}$$

$$= \underline{\underline{71 \text{ ppm}}}$$

Ba^{2+}-doped CsCl from Graph 14

Wt of crystal = 0.2036 g

Dissolved in distilled water 10 drops NH_3 buffer added and made up to 5 ml. 2 ml titrated against 1.03mM EDTA

Results	Ml EDTA added	Absorbance
	0.00	0.061
	0.02	0.074
	0.04	0.078
	0.06	0.096
	0.08	0.120
	0.10	0.137
	0.12	0.153

End point occurs at 0.040 ml

1 ml of 1 mM EDTA = 0.137 mg Ba^{2+}

$\therefore$ 0.040 ml of 1.03mMEDTA = 0.00564 mg Ba^{2+} in 2 ml

= 0.0141 mg Ba^{2+} in 5 ml

$$\therefore \frac{Ba^{2+}}{Cs^{+}} = \frac{0.0141 \times 168.4 \times 10^{6}}{0.2036 \times 137.4 \times 10^{3}}$$

= 85 ppm

Ba^{2+} -doped CsCl from Graph 15

Wt of crystal = 0.2086 g

Dissolved in distilled H_2O, 10 drops ammonia buffer added and made up to 5 ml. 2 ml titrated against 1.03 mM EDTA

Results	Ml of EDTA added	Absorbance
	0.00	0.032
	0.02	0.040
	0.04	0.043
	0.06	0.057
	0.08	0.080
	0.10	0.095
	0.12	0.111

End point occurs at 0.047 ml

Now 1 ml of 1 mM EDTA = 0.137 mg Ba^{2+}

$\therefore$ 0.047 ml of 1.03mM EDTA = 0.0066 mg Ba^{2+} in 2 ml

= 0.0165 mg Ba^{2+} in 5 ml

$$\therefore \frac{Ba^{2+}}{Cs+} = \frac{0.0165 \times 168.4 \times 10^6}{0.2086 \times 137.4 \times 10^3}$$

= 97 ppm

Ba^{2+}-doped CsCl from Graph 16

Wt of crystal = 0.2906 g

Dissolved in distilled water, 10 drops NH_3 buffer added and made up to 5 ml. 2 ml titrated using 1.78 mM EDTA

Results	ml EDTA added	Absorbance
	0.00	0.065
	0.02	0.073
	0.04	0.075
	0.06	0.105
	0.08	0.126
	0.10	0.150
	0.12	

End point occurs at 0.040 ml

Now 1 ml mM EDTA = 0.137 mg Ba^{2+}

$\therefore$ 0.040 ml of 1.78 mM EDTA = 0.0098 mg Ba^{2+} in 2 ml

in 5 ml = 0.0245 mg Ba^{2+}

$$\therefore \frac{Ba^{2+}}{Cs^{+}} = \frac{0.0245 \times 168.4 \times 10^{6}}{0.2906 \times 137.4 \times 10^{3}}$$

$$= 104 \text{ ppm}$$

Ba^{2+} -doped CsCl from Graph 17

Wt of crystal = 0.1017 g

Dissolved in cell and 4 drops NH_3 buffer added

titrated against 1.03 mM EDTA.

Results	ml EDTA added	Absorbance
	0.00	0.132
	0.02	0.142
	0.04	0.145
	0.06	0.148
	0.08	0.154
	0.10	0.175
	0.12	0.191
	0.14	0.208

End point occurs at 0.078 ml

Now 1 ml or 1 mM EDTA = 0.137 mg Ba^{2+}

$\therefore$ 0.078 ml or 1.03 mM EDTA = 0.011 mg Ba^{2+}

$$\therefore \quad \frac{Ba^{2+}}{Cs^{+}} = \frac{0.0110 \times 168.4 \times 10^{6}}{0.1017 \times 137.4 \times 10^{3}}$$

$$= 133 \text{ ppm}$$

Ba^{2+} -doped CsCl from Graph 19

Wt of crystal = 0.2350 g

Dissolved in distilled water, 10 drops NH_3 buffer added and made up to 5 ml. 2 ml titrated with 1.03mM EDTA.

Results	ml EDTA added	Absorbance
	0.00	0.083
	0.025	0.095
	0.050	0.097
	0.075	0.105
	0.100	0.120
	0.125	0.142
	0.150	0.162

End point occurs at 0.084 ml

1 ml of 1 mM EDTA = 0.137 mg Ba^{2+}

$\therefore$ 0.084 ml of 1.03mM EDTA = 0.0119 mg Ba^{2+} in 2 ml

= 0.0298 mg Ba^{2+} in 5 ml

$$\therefore \frac{Ba^{2+}}{Cs^{+}} = \frac{0.0298 \times 168.4 \times 10^{6}}{0.2350 \times 137.4 \times 10^{3}}$$

= 153 ppm

Ba^{2+}-doped CsCl from Graph 20

Wt of crystal = 0.2460 g

Dissolved in distilled water 10 drops NH_3 buffer added and solutions made up to 5 ml. 2 ml titrated against 1.03 mM EDTA.

Results	ml EDTA added	Absorbance
	0.00	0.101
	0.02	0.115
	0.04	0.118
	0.06	0.122
	0.08	0.130
	0.10	0.138
	0.12	0.158
	0.14	0.175
	0.16	0.192

End point occurs at 0.095 ml

1 ml of 1 mM EDTA = 0.137 mg Ba^{2+}

$\therefore$ 0.095 ml of 1.03 mM EDTA = 0.134 mg Ba^{2+} in 2 ml

= 0.0335 mg Ba^{2+} in 5 ml

$$\therefore \quad \frac{Ba^{2+}}{Cs^{+}} = \frac{0.0335 \times 168.4 \times 10^6}{0.2460 \times 137.4 \times 10^3}$$

= 167 ppm

Ba^{2+}-doped CsCl from Graph 21

Wt of crystal = 0.2682 g

Dissolved in distilled water 10 drops of NH_3 buffer added and solution made up to 5 ml. 2 ml titrated against 1.78 mM EDTA.

Results	ml EDTA added	Absorbance
	0.000	0.113
	0.025	0.121
	0.050	0.127
	0.075	0.138
	0.100	0.172
	0.125	0.204

End point occurs at 0.070 ml

1 ml of 1 mM EDTA = 0.137 mg Ba^{2+}

$\therefore$ 0.070 ml of 1.78mM EDTA = 0.017 mg Ba^{2+} in 2 ml

= 0.043 mg Ba^{2+} in 5 ml

$$\therefore \frac{Ba^{2+}}{Cs^{+}} = \frac{0.043 \times 168.4 \times 10^{6}}{0.2682 \times 137.4 \times 10^{3}}$$

= 196 ppm

Ba^{2+}-doped CsCl from Graph 22

Wt of crystal = 0.1830 g

Dissolved in distilled water, 10 drops NH_3 buffer added made up to 5 ml. 2 ml titrated against 1.03 mM EDTA.

Results	ml of EDTA added	Absorbance
	0.00	0.220
	0.025	0.225
	0.04	0.227
	0.06	0.230
	0.08	0.236
	0.10	0.240
	0.12	0.258
	0.14	0.275
	0.16	0.295
	0.18	0.310

End point occurs at 0.10 ml

Now 1 ml of 1 mM EDTA = 0.137 mg Ba^{2+}

$\therefore$ 0.10 ml of 1.03 mM EDTA = 0.0141 mg Ba^{2+} in 2 ml

= 0.0352 mg Ba^{2+} in 5 ml

$$\therefore \frac{Ba^{2+}}{Cs^{+}} = \frac{0.0352 \times 168.4 \times 10^{6}}{0.1830 \times 137.4 \times 10^{3}}$$

= 234 ppm

Ba^{2+} -doped CsCl from Graph 23

Wt of crystal = 0.2588 g

Dissolved in distilled water, 10 drops NH_3 buffer added and solution made up to 5 ml. 2 ml titrated against 1.03 mM EDTA.

Results	ml of EDTA added	Absorbance
	0.00	0.045
	0.02	0.055
	0.04	0.056
	0.06	0.058
	0.08	0.060
	0.10	0.061
	0.12	0.066
	0.14	0.068
	0.16	0.075
	0.18	0.095

End point occurs at 0.155 ml

Now 1 ml of 1 mM EDTA = 0.137 mg Ba^{2+}

$\therefore$ 0.155 ml of 1.03 mM EDTA = 0.0219 mg Ba^{2+} in 2 ml

= 0.0547 mg Ba^{2+} in 5 ml

$$\therefore \frac{Ba^{2+}}{Cs^{+}} = \frac{0.0547 \times 168.4 \times 10^{6}}{0.2588 \times 137.4 \times 10^{3}}$$

= 260 ppm

Ba^{2+} -doped CsCl from Graph 24

Wt of crystal = 0.3756 g

Dissolved in distilled water, 10 drops NH_3 buffer added made up to 5 ml. 2 ml titrated against 1.03 mM EDTA.

Results	ml EDTA added	Absorbance
	0.00	0.070
	0.05	0.079
	0.10	0.080
	0.15	0.088
	0.20	0.092
	0.25	0.100
	0.30	0.135
	0.35	0.170

End point occurs at 0.245 ml

Now 1 ml of 1 mM EDTA = 0.137 mg Ba^{2+}

$\therefore$ 0.245 ml of 1.03 mM EDTA = 0.0346 mg Ba^{2+} in 2 ml

= 0.0864 mg Ba^{2+} in 5 ml

$$\therefore \frac{Ba^{2+}}{Cs^{+}} = \frac{0.0864 \times 168.4 \times 10^{6}}{0.3756 \times 137.4 \times 10^{3}}$$

= 280 ppm

Ca^{2+} -doped CsCl from Graph 29

Wt of crystal = 0.4120 g

Dissolved in distilled water, 10 drops buffer added, made up to 5 ml. 2 ml titrated against 1.03 mM EDTA.

Results	ml of EDTA added	Absorbance
	0.00	0.035
	0.02	0.043
	0.04	0.048
	0.06	0.050
	0.08	0.053
	0.10	0.055
	0.12	0.060
	0.14	0.079
	0.16	0.096

End point occurs at 0.120 ml

Now 1 ml of 1 mM EDTA = 0.040 mg Ca^{2+}

$\therefore$ 0.12 ml of 1.03 mM EDTA = 0.0049 mg Ca^{2+} in 2 ml

= 0.0124 mg Ca^{2+} in 5 ml

$$\therefore \frac{Ca^{2+}}{Cs^{+}} = \frac{0.0124 \times 168.4 \times 10^{6}}{0.4120 \times 40.08 \times 10^{3}}$$

= 125 ppm

Ba^{2+}-doped CsCl (^{36}Cl diffusion No.4e)

Wt of crystal = 0.3250 g

Dissolved in distilled water, 10 drops of NH_3 buffer added. Solution made up to 5 ml and 2 ml titrated against 1.78 mM EDTA.

Results	ml of EDTA added	Absorbance
	0.00	0.074
	0.025	0.083
	0.055	0.088
	0.075	0.094
	0.100	0.107
	0.130	0.144
	0.160	0.181

End point occurs at 0.092 ml

Now 1 ml of 1 mM EDTA = 0.137 mg Ba^{2+}

$\therefore$ 0.092 ml of 1.78 mM EDTA = 0.0224 mg Ba^{2+} in 2 ml

= 0.0561 mg Ba^{2+} in 5 ml

$$\therefore \frac{Ba^{2+}}{Cs^{+}} = \frac{0.0561 \times 168.4 \times 10^{6}}{0.3250 \times 137.4 \times 10^{3}}$$

= 211 ppm

Ba^{2+} -doped CsCl (from Cl^{36} diffusion No. 4f)

Wt of crystal = 0.3128 g

Dissolved in cell, 4 drops of ammonia buffer added and titrated against 1.78 mM EDTA.

Results	ml of EDTA added	Absorbance
	0.00	0.180
	0.025	0.187
	0.050	0.191
	0.080	0.230
	0.10	0.255
	0.13	0.285

End point occurs at 0.050 ml

Now 1 ml of 1 mM EDTA = 0.137 mg Ba^{2+}

$\therefore$ 0.050 ml of 1.78 mM EDTA = 0.0122 mg Ba^{2+}

$$\frac{Ba^{2+}}{Cs^{+}} = \frac{0.0122 \times 168.4 \times 10^{6}}{0.3128 \times 137.4 \times 10^{3}}$$

$$= 48 \text{ ppm}$$

Ba^{2+} -doped CsCl (from Cl^{36} diffusion No. 8c)

Wt of crystal = 0.2808 g

Dissolved in distilled water and 10 drops of NH_3 buffer added. Solution made up to 5 ml and 2 ml titrated against 1.03 mM EDTA.

Results	ml of EDTA added	Absorbance
	0.00	0.043
	0.02	0.048
	0.04	0.054
	0.06	0.066
	0.08	0.085
	0.10	0.105
	0.12	0.122

End point occurs at 0.050 ml

Now 1 ml of 1 mM EDTA = 0.137 mg Ba^{2+}

$\therefore$ 0.050 ml of 1.03 mM EDTA = 0.00706 mg Ba^{2+} in 2 ml

= 0.01765 mg Ba^{2+} in 5 ml

$$\therefore \frac{Ba^{2+}}{Cs^{+}} = \frac{0.01765 \times 168.4 \times 10^{6}}{0.2808 \times 137.4 \times 10^{3}}$$

= 77 ppm

Ba^{2+}-doped CsCl from Cl^{36} diffusion No. 8d

Wt of crystal = 0.1870 g

Dissolved in distilled water and 10 drops of ammonia buffer added. Made up to 5 ml and 2 ml titrated against 1.03 mM EDTA.

Results	ml of EDTA added	Absorbance
	0.00	0.082
	0.02	0.092
	0.04	0.096
	0.06	0.100
	0.08	0.112
	0.10	0.130
	0.12	0.150

End point occurs at 0.070 ml

Now 1 ml of 1 mM EDTA = 0.137 mg Ba^{2+}

$\therefore$ 0.070 ml of 1.03 mM EDTA = 0.00988 mg Ba^{2+} in 2 ml

= 0.0247 mg Ba^{2+} in 5 ml

$$\therefore \frac{Ba^{2+}}{Cs^{+}} = \frac{0.0247 \times 168.4 \times 10^{6}}{0.1870 \times 137.4 \times 10^{3}}$$

= 162 ppm

Ba^{2+}-doped CsCl (^{36}Cl diffusion No. 11c)

Wt of crystal = 0.1655 g

Dissolved in distilled water and 10 drops of NH_3 buffer added. Solution made up to 5 ml and 2 ml titrated against 1.03 mM EDTA.

Results	ml of EDTA added	Absorbance
	0.00	0.047
	0.02	0.050
	0.04	0.053
	0.06	0.065
	0.08	0.083
	0.10	0.101
	0.12	0.116

End point occurs at 0.049 ml

Now 1 ml of 1 mM EDTA = 0.137 mg Ba^{2+}

$\therefore$ 0.049 ml of 1.03 mM EDTA = 0.00691 mg Ba^{2+} in 2 ml

= 0.01728 mg Ba^{2+} in 5 ml

$$\therefore \frac{Ba^{2+}}{Cs^{+}} = \frac{0.01728 \times 168.4 \times 10^{6}}{0.1655 \times 137.4 \times 10^{3}}$$

= 128 ppm

Ba^{2+}-doped CsCl (from Cl^{36} diffusion No.12c)

Wt of crystal = 0.2722 g

Dissolved in distilled water, and 10 drops of NH_3 buffer added. Made up to 5 ml and 2 ml titrated against 1.03 mM EDTA.

Results	ml of EDTA added	Absorbance
	0.00	0.062
	0.02	0.067
	0.04	0.069
	0.06	0.073
	0.08	0.090
	0.10	0.108
	0.12	0.125
	0.14	0.140

End point occurs at 0.061 ml

Now 1 ml of 1 mM EDTA = 0.137 mg Ba^{2+}

$\therefore$ 0.061 ml of 1.03 mM EDTA = 0.00861 mg Ba^{2+} in 2 ml

= 0.02152 mg Ba^{2+} in 5 ml

$$\therefore \frac{Ba^{2+}}{Cs^{+}} = \frac{0.02152 \times 168.4 \times 10^{6}}{0.2722 \times 137.4 \times 10^{3}}$$

= 97 ppm

Ba^{2+}-doped CsCl (from Cl^{36} diffusion No. 13c)

Wt of crystal = 0.2445 g

Dissolved in distilled water and 10 drops of NH_3 buffer added. Solution made up to 5 ml and 2 ml titrated against 1.78 mM EDTA.

Results	ml of EDTA added	Absorbance
	0.00	0.077
	0.02	0.082
	0.04	0.088
	0.065	0.121
	0.085	0.147
	0.115	0.179

End point occurs at 0.038 ml

Now 1 ml of 1 mM EDTA = 0.137 mg Ba^{2+}

$\therefore$ 0.038 ml of 1.78 mM EDTA = 0.00926 mg Ba^{2+} in 2 ml

= 0.02315 mg Ba^{2+} in 5 ml

$$\therefore \frac{Ba^{2+}}{Cs^{+}} = \frac{0.02315 \times 168.4 \times 10^{6}}{0.2445 \times 137.4 \times 10^{3}}$$

= 116 ppm

Ba^{2+}-doped CsCl (from Cl^{36} diffusion No.16b)

Wt of crystal = 0.2296 g

Dissolved in distilled water and 10 drops of NH_3 buffer added. Solution made up to 5 ml and 2 ml titrated against 1.78 mM EDTA.

Results	ml of EDTA added	Absorbance
	0.00	0.068
	0.02	0.074
	0.04	0.094
	0.06	0.120
	0.08	0.147
	0.10	0.166

End point occurs at 0.027 ml

Now 1 ml of 1 mM EDTA = 0.137 mg Ba^{2+}

$\therefore$ 0.027 ml of 1.78 mM EDTA = 0.00659 mg Ba^{2+} in 2 ml

= 0.01646 mg Ba^{2+} in 5 ml

$$\therefore \frac{Ba^{2+}}{Cs^{+}} = \frac{0.01646 \times 168.4 \times 10^{3}}{0.2296 \times 137.4 \times 10^{3}}$$

= 88 ppm

SO_4^{2-}-doped CsCl from Graph 30

Wt of crystal = 0.3845 g

Dissolved in 2 ml of $BaSO_4$ solution. Centrifuged with 2 ml of standard $BaCl_2$ solution. 2 ml of resulting solution titrated against 1.03 mM EDTA in the presence of NH_3 buffer.

Results	ml of EDTA added	Absorbance
	0.00	0.142
	0.030	0.153
	0.050	0.159
	0.070	0.164
	0.100	0.170
	0.125	0.177
	0.155	0.179
	0.180	0.184
	0.205	0.201
	0.225	0.220
	0.260	0.248

End point occurs at 0.188 ml

In absence of SO_4^{2-} end point occurs at 0.280 ml

$\therefore$ Amount of Ba^{2+} reacting with SO_4^{2-} = 0.092 ml EDTA

Now 1 ml of 1 mM EDTA = 0.096 mg SO_4^{2-}

$\therefore$ 0.092 ml of 1.03 mM EDTA = 0.00907 mg SO_4^{2-} in 2 ml

= 0.01814 mg SO_4^{2-} in 4 ml

$$\frac{SO_4^{2-}}{Cl} = \frac{0.01814 \times 168.4 \times 10^6}{0.3845 \times 96.07 \times 10^3} = 83 \text{ ppm}$$

SO_4^{2-}-doped CsCl from Graph 31

Wt of crystal = 0.2073

Dissolved in 2 ml of $BaSO_4$ solution. Centrifuged with 2 ml of standard $BaCl_2$ solution. 2 ml of resulting solution titrated against 1.03 mM EDTA.

Results	ml of EDTA added	Absorbance
	0.00	0.083
	0.025	0.091
	0.050	0.092
	0.070	0.099
	0.105	0.102
	0.140	0.106
	0.160	0.113
	0.180	0.116
	0.200	0.120
	0.220	0.125
	0.240	0.142
	0.260	0.158
	0.295	0.186

End point occurs at 0.220 ml

End point in absence of SO_4^{2-} occurs at 0.280 ml.

$\therefore$ Amount of Ba^{2+} reacting with SO_4^{2-} = 0.060 ml EDTA

1 ml of 1 mM EDTA = 0.137 mg Ba^{2+} = 0.096 mg SO_4^{2-}

$\therefore$ 0.060 ml of 1.03 mM EDTA = 0.00593 mg SO_4^{2-} in 2 ml

= 0.01186 mg SO_4^{2-} in 4 ml

$$\therefore SO_4^{2-} = \frac{0.01186 \times 168.4 \times 10^6}{0.2073 \times 96.07 \times 10^3} = 100 \text{ ppm}$$

SO_4^{2-}-doped CsCl from Graph 32

Wt of crystal = 0.2955 g

Dissolved in 2 ml of $BaSO_4$ solution centrifuged with 2 ml of standard $BaCl_2$ solution. 2 ml of resulting solution titrated against 1.03 mM EDTA.

RESULTS	ml of EDTA added	Absorbance
	0.00	0.122
	0.02	0.129
	0.04	0.131
	0.06	0.132
	0.08	0.137
	0.10	0.144
	0.12	0.144
	0.14	0.148
	0.16	0.151
	0.18	0.156
	0.20	0.173
	0.22	0.190
	0.24	0.206

End point occurs at 0.178 ml

End point, in absence of SO_4^{2-} occurs at 0.28 ml.

$\therefore$ Amount of Ba^{2+} reacting with SO_4^{2-} = 0.102 ml EDTA

Now 1 ml of 1 mM EDTA = 0.137 mg Ba^{2+} = 0.096 mg SO_4^{2-}

$\therefore$ 0.102 ml of 1.03 mM EDTA = 0.01009 mg SO_4^{2-} in 2 ml

= 0.02018 mg SO_4^{2-} in 4 ml

$$\therefore \frac{SO_4^{2-}}{Cl^-} = \frac{0.02018 \times 168.4 \times 10^6}{0.2955 \times 96.07 \times 10^3} = 120 \text{ ppm}$$

SO_4^{2-}-doped CsCl from Graph 33

Wt of crystal = 0.1122 g

Dissolved in 2 ml of $BaSO_4$ solution. Centrifuged with 2 ml of $BaCl_2$ solution 2 ml of resulting solution titrated against 1.03 mM EDTA in the presence of NH_3 buffer.

RESULTS	ml of EDTA added	Absorbance
	0.00	0.032
	0.02	0.041
	0.04	0.042
	0.06	0.042
	0.08	0.046
	0.10	0.049
	0.12	0.052
	0.14	0.052
	0.16	0.055
	0.18	0.057
	0.20	0.060
	0.22	0.060
	0.24	0.066
	0.26	0.084
	0.28	0.103
	0.30	0.120
	0.32	0.134

End point occurs at 0.237 ml

End point, in absence of SO_4^{2-} occurs at 0.280 ml

$\therefore$ amount of Ba^{2+} reacting with SO_4^{2-} = 0.043 ml EDTA

1 ml of 1 mM EDTA = 0.096 mgs SO_4^{2-}

$\therefore$ 0.043 ml of 1.03 mM EDTA = 0.00425 mg SO_4^{2-} in 2 ml

= 0.00850 mg SO_4^{2-} in 4 ml

$$\therefore \quad \frac{SO_4^{2-}}{Cl^-} = \frac{0.00850 \times 168.4 \times 10^6}{0.1122 \times 96.07 \times 10^3} = 137 \text{ ppm}$$

SO_4^{2-} -doped CsCl from Graph 34

Wt of crystal = 0.1779 g

Dissolved in 2 ml of $BaSO_4$ solution. Centrifuged with 2 ml of $BaCl_2$ solution. 2 ml of resulting solution titrated against 1.03 mM EDTA in the presence of NH_3 buffer.

RESULTS	ml of EDTA added	Absorbance
	0.00	0.100
	0.03	0.109
	0.06	0.115
	0.09	0.121
	0.12	0.127
	0.15	0.130
	0.18	0.136
	0.21	0.148
	0.24	0.174
	0.27	0.196
	0.30	0.317

End point occurs at 0.203 ml

End point, in the absence of SO_4^{2-} occurs at 0.280 ml

$\therefore$ Amount of Ba^{2+} reacting with SO_4^{2-} = 0.077 ml EDTA

Now 1 ml of 1 mM EDTA = 0.096 mg SO_4^{2-}

$\therefore$ 0.077 ml of 1.03 mM EDTA = 0.00761 mg SO_4^{2-} in 2 ml

= 0.01522 mg SO_4^{2-} in 4 ml

$$\therefore \quad \frac{SO_4^{2-}}{Cl^-} = \frac{0.01522 \times 168.4 \times 10^6}{0.1779 \times 96.07 \times 10^3} = 150 \text{ ppm}$$

SO_4^{2-}-doped CsCl from Graph 35

Wt of crystal = 0.1880 g

Dissolved in 2 ml of $BaSO_4$ solution. Centrifuged with 2 ml of $BaCl_2$ standard. 2 ml of resulting solution titrated against 1.03 mM EDTA in the presence of NH_3 buffer.

RESULTS	ml of EDTA added	Absorbance
	0.00	0.077
	0.03	0.085
	0.06	0.089
	0.09	0.096
	0.12	0.099
	0.15	0.105
	0.18	0.120
	0.21	0.143
	0.24	0.167
	0.27	0.186

End point occurs at 0.165 ml

End point, in absence of SO_4^{2-} occurs at 0.280 ml

$\therefore$ Amount of Ba^{2+} reacting with SO_4^{2-} = 0.115 ml EDTA

1 ml of 1 mM EDTA = 0.096 mg SO_4^{2-}

$\therefore$ 0.115 ml of 1.03 mM EDTA = 0.01137 mg SO_4^{2-} in 2 ml

= 0.02274 mg SO_4^{2-} in 4 ml

$$\therefore \frac{SO_4^{2-}}{Cl^-} = \frac{0.02274 \times 168.4 \times 10^6}{0.1880 \times 96.07 \times 10^3} = 212 \text{ ppm}$$

SO_4^{2-}-doped CsCl From Graph 36

Wt of crystal = 0.1265

Dissolved in 2 ml of $BaSO_4$ solution. Centrifuged with 2 ml of $BaCl_2$ standard solution. 2 ml of resulting solution titrated against 1.03 mM EDTA in the presence of NH_3 buffer.

Results

ml of EDTA added	Absorbance
0.00	0.092
0.04	0.102
0.08	0.110
0.12	0.117
0.16	0.128
0.20	0.146
0.24	0.175
0.28	0.202

End point occurs at 0.18 ml

End point, in absence of SO_4^{2-} occurs at 0.28 ml

$\therefore$ Amount of Ba^{2+} reacting with SO_4^{2-} = 0.10 ml EDTA

Now 1 ml of 1 mM EDTA = 0.096 mg SO_4^{2-}

$\therefore$ 0.10 ml of 1.03 mM EDTA = 0.00988 mg SO_4^{2-} in 2 ml

= 0.01976 mg SO_4^{2-} in 4 ml

$$\therefore \frac{SO_4^{2-}}{Cl^-} = \frac{0.01976 \times 168.4 \times 10^6}{0.1265 \times 96.07 \times 10^3} = 274 \text{ ppm}$$

SO_4^{2-}-doped CsCl from Graph 37

Wt of crystal = 0.1363 g

Dissolved in 2 ml of $BaSO_4$ solution. Centrifuged with 2 ml of standard $BaCl_2$ solution. 2 ml of resulting solution titrated against 1.03 mM EDTA in the presence of NH_3 buffer.

RESULTS	ml of EDTA added	Absorbance
	0.000	0.063
	0.025	0.074
	0.055	0.080
	0.080	0.086
	0.115	0.098
	0.135	0.114
	0.160	0.133
	0.190	0.153

End point occurs at 0.108 ml

End point, in absence of SO_4^{2-} occurs at 0.280 ml

$\therefore$ Amount of Ba^{2+} reacting with SO_4^{2-} = 0.172 ml EDTA

Now 1 ml of 1 mM EDTA = 0.096 mg SO_4^{2-}

$\therefore$ 0.172 ml of 1.03 mM EDTA = 0.0170 mg SO_4^{2-} in 2 ml

= 0.0340 mg SO_4^{2-} in 4 ml

$$\therefore \frac{SO_4^{2-}}{Cl^-} = \frac{0.0340 \times 168.4 \times 10^6}{0.1363 \times 96.07 \times 10^3} = 437 \text{ ppm}$$

SO_4^{2-}-doped CsCl (from Cl^{36} diffusion No. 10d

Wt of crystal = 0.2600 g

Dissolved in 2 ml of $BaSO_4$ solution. Centrifuged with 2 ml of standard $BaCl_2$ solution. 2 ml of resulting solution titrated against 1.78 mM EDTA in presence of NH_3 buffer.

RESULTS	ml of EDTA added	Absorbance
	0.00	0.123
	0.030	0.128
	0.055	0.130
	0.075	0.135
	0.095	0.148
	0.115	0.172
	0.135	0.198
	0.155	0.212

End point occurs at 0.085 ml

End point, in absence of SO_4^{2-} occurs at 0.155 ml

$\therefore$ amount of Ba^{2+} reacting with SO_4^{2-} = 0.070 ml EDTA

1 ml of 1 mM EDTA = 0.096 mg SO_4^{2-}

$\therefore$ 0.070 ml of 1.78 mM EDTA = 0.0120 mg SO_4^{2-} in 2 ml

= 0.0240 mg SO_4^{2-} in 4 ml

$$\therefore \frac{SO_4^{2-}}{Cl^-} = \frac{0.0240 \times 168.4 \times 10^6}{0.2600 \times 96.07 \times 10^3} = 162 \text{ ppm}$$

SO_4^{2-}-doped CsCl (from Cl^{36} diffusion No.10e)

Wt of crystal = 0.1948 g

Dissolved in 2 ml of $BaSO_4$ solution. Centrifuged with 2 ml of standard $BaCl_2$ solution. 2 ml of resulting solution titrated against 1.78 mM EDTA in the presence of NH_3 buffer.

Results	ml of EDTA added	Absorbance
	0.000	0.140
	0.025	0.150
	0.055	0.153
	0.080	0.157
	0.100	0.160
	0.120	0.180
	0.140	0.208
	0.160	0.232

End point occurs at 0.105 ml

End point, in absence of SO_4^{2-} occurs at 0.155 ml

$\therefore$ Amount of Ba^{2+} reacting with SO_4^{2-} = 0.040 ml EDTA

Now 1 ml of 1 mM EDTA = 0.096 mg SO_4^{2-}

$\therefore$ 0.040 ml of 1.78 mM EDTA = 0.00684 mg SO_4^{2-} in 2 ml

= 0.01368 mg SO_4^{2-} in 4 ml

$\therefore$ $\dfrac{SO_4^{2-}}{Cl^-} = \dfrac{0.01368 \times 168.4 \times 10^6}{0.1948 \times 96.07 \times 10^3} =$ 123 ppm

SO_4^{2-}-doped CsCl (from ^{36}Cl diffusion No. 11 f)

Wt of crystal = 0.1601 g

Dissolved in 2 ml of $BaSO_4$ solution. Centrifuged with 2 ml of $BaCl_2$ standard solution. 2 ml of resulting solution titrated against 1.03 mM EDTA in the presence of NH_3 buffer.

Results	ml of EDTA added	Absorbance
	0.00	0.088
	0.03	0.095
	0.06	0.103
	0.09	0.108
	0.12	0.117
	0.15	0.120
	0.18	0.127
	0.21	0.140
	0.24	0.164
	0.27	0.186

End point occurs at 0.196 ml

End point, in absence of SO_4^{2-} occurs at 0.280 ml

$\therefore$ Amount of Ba^{2+} reacting with SO_4^{2-} = 0.084 ml EDTA

Now 1 ml of 1 mM EDTA = 0.096 mg SO_4^{2-}

$\therefore$ 0.084 ml of 1.03 mM EDTA = 0.00832 mg SO_4^{2-} in 2 ml

= 0.01664 mg SO_4^{2-} in 4 ml

$$\therefore \frac{SO_4^{2-}}{Cl^-} = \frac{0.01644 \times 168.4 \times 10^6}{0.1601 \times 96.07 \times 10^3} = 180 \text{ ppm}$$

REFERENCES.

1. FRENKEL , Z. Physik. , 35 , 652 , (1926).
2. COMPTON , Phys. Rev. , 101 , 1209 , (1956).
3. FRIAUF , Phys. Rev. , 105 , 843 , (1957).
4. SCHOTTKY , Z. Phys. Chem. , 29B , 335 , (1935).
   WAGNER & SCHOTTKY , ibid. , 11B , 163 , (1930).
5. See for example ,
Garner " Chemistry of the Solid State " (Butterworths , 1955)
Chapter 2 by F.S. Stone.
Flugge " Handbuch der Physik " XX , (1957) , (Springer-Verlach)
Chapter 2 by A.B. Lidiard.
6. Mott & Gurney , " Electronic Processes in Ionic Crystals "
Oxford University Press , (1940).
7. TUBANDT & EGGERT , Z. Anorg. Chem. , 110 , 196 , (1920).
ibid. , 115 , 105 , (1921).
8. LEHFELDT , Z. Phys. , 85 , 717 , (1933).
9. SMEKAL , Z. Electrochem. , 34 , 476 , (1928).
Handbuch der Physik , XXIV/2 , 876 , (1933).
10. Jost , " Diffusion und Chemische Reaktion in Festen Stoffen "
(Steinkopff , Dresden) , 77 , (1937).
11. KOCH & WAGNER , Z. Phys. Chem. , 38B , 295 , (1937).
12. KELTING & WITT , Z. Physik , 126 , 697 , (1949).
13. ETZEL & MAURER , J. Chem. Phys. , 18 , 1003 , (1950).
14. POHL , Z. Physik , 39 , 36 , (1938).
15. ESTERMANN , LEIVO & STERN , Phys. Rev. , 75 , 627 , (1949).
16. SEITZ , Rev. Mod. Phys. , 18 , 384 , (1946).
17. See for example ,
Van Bueren , " Imperfections in Crystals " ,
(North - Holland Publishing Co.) , 548 , (1961).

18. MAPOTHER , CROOKS & MAURER , J.Chem. Phys. , 18 , 1231 , (1950).
19. ASCHNER , Phys. Rev. , 94 , 771 , (1954).
20. CHEMLA , Ann. de Phys. , 1 , 988 , (1956).
21. BRECKENBRIDGE , J. Chem. Phys. , 16 , 959 , (1948).
ibid. , 18 , 913 , (1950).
22. HENVIS , DAVISSON & BURSTEIN , Phys. Rev. , 82 , 774 , (1951).
23. BURSTEIN , DAVISSON & SCLAR, Phys. Rev. , 96 , 819 , (1954).
24. TETLOW & WILKE , Naturwiss , 41 , 423 , (1954).
25. JACOBS , ibid. , 42 , 575 , (1955).
26. DRYDEN &MEAKINS , Disc. Far. Soc. , 23 , 39 , (1957).
27. JACOBS , VANDEWIELE & HAMERLINCK, J. Chem. Phys. , 36 , 2946 , (1962).
28. DRYDEN , J. Phys. Soc. Japan , 18 , Suppl.3 , 129 , (1963).
29. ECONOMOU , Phys. Rev. , 135 , 1020 , (1964).
30. WATKINS , ibid. , 113 , 79 , 91 , (1959).
31. SCHNEIDER , Disc. Far. Soc. , 28 , 122 , (1959).
32. Garner , " Chemistry of the Solid State " , (Butterworths , 1955) , Chapter 1 by F.C. Frank.
33. LEHOVEC , J. Chem. Phys. , 21 , 1123 , (1953).
ESHELBY , NEWEY , PRATT & LIDIARD , Phil. Mag. , 3 , 75 , (1958).
34. FISHBACH & NOWICK , J. Phys. Chem. Solids , 5 , 302 , (1958).
35. HOODLESS & THOMSON, Phil. Mag. , 4 , 431 , (1959).
36. SUZUOKA , Trans. Japan Inst. Metals , 2,25, (1961).
37. DREYFUS & NOWICK , Phys. Rev. , 126 , 1367 , (1962).

38. ALLNATT & JACOBS , Trans. Far. Soc. , 58 , 116 , (1962).
39. JAIN & DAHAKE , Phys. letters , 3 , 308 , (1963).
40. JAIN & DAHAKE , Indian J. Pure & Appl. Phys. , 2 , 71 , (1964).
41. JAIN & PARASHAR , ibid. , 3 , 164 , (1965).
42. KENESHEA & FREDERICKS , J. Phys. Chem. Solids , 26 , 501 , (1965).
43. KENESHEA & FREDERICKS , J. Chem. Phys. , 38 , 1952 , (1963).
44. KESSLAR , MARIANI & PUALING - TOTHOV'A , Czech. J. Phys. , 14 , 34 , (1964).
45. REISFELD , GLASNER & HONIGBAUM , J. Chem. Phys. , 42 , 1892 , (1965).
46. BANASEVICH , LUR'E & MURIN , Fiz. Tverd. Tela. , 2 , 80 , (1960).
47. HARRISON , MORRISON & RUDHAM , Trans. Far. Soc. , 54 , 106 , (1958).
48. LAURENT & BENARD , J. Phys. Chem. Solids , 3 , 7 ,(1957).
49. BARR , HOODLESS , MORRISON & RUDHAM , Trans. Far. Soc. , 56 , 697 , (1960).
50. LIDIARD , J. Phys. Chem. Solids , 6 , 298 , (1958).
51. LAURANCE , Phys. Rev. , 120 , 57 , (1960).
52. BARR , MORRISON & SCHROEDER , J. Appl. Phys. , 36 , 624 , (1965).
53. HARPUR , MOSS & UBBELOHDE , Proc. Roy. Soc. , A232, 196 , (1955).
54. MOSS & UBBELOHDE , ibid. , A232, 310 , (1955).
55. LYNCH , Phys. Rev. , 118 , 468 , (1960).
56. HAUFFE , GRIESSBACH - VIERCH , Z. Electrochem. , 57 , 248 , (1953).

57. FRIAUF , Bull. Am. Phys. Soc. , 3 , 127 , (1958).
58. FRIAUF , J. Phys. Chem. Solids , 18 , 203 , (1961).
59. HERMANN , Z. Phys. Chem. , 227 , 338 , (1964).
60. HOODLESS & MORRISON , J. Phys. Chem. , 66 , 557 , (1962).
61. BESSON , CHAUVY & ROSSEL , Helv. Phys. Acta. , 35,211 , (1962).
62. ECKLIN , NADLER & ROSSEL , ibid. , 37,692 , (1964).
63. M^{c}NICOL , Private communication.
64. HERRINGTON & STAVELEY , J. Phys. Chem. Solids , 25 , 921 , (1964).
65. ZEMEZUZNY & RAMBACH , Z. Anorg. Chem. , 65, 418 , (1910).
66. SANDONINI & SCARPA , Mem. Accad. Lincei , (5) 21 , 77 , (1912).
67. KORRANG , Z. Anorg. Chem. , 91 , 194 , (1915).
68. WAGNER & LIPPERT ,Z. Phys. Chem. , B21 , 471 , (1933).
69. WAGNER & LIPPERT , ibid. , B31 , 263 , (1936).
70. MENARY , UBBELOHDE & WOODWARD , Proc. Roy. Soc. , A208 , 158 , (1951).
71. JOHNSON , AGRON & BREDIG , J. Amer. Chem. Soc. , 77 , 2734 , (1955).
72. WOOD , SECUNDA & M^{c}BRIDE , ibid. , 80 , 307 , (1958).
73. CLARK , J. Chem. Phys. , 31 , 1526 , (1959).
74. DINICHERT , Helv. Phys. Acta. , 15 , 462 , (1942).
75. THOMAS & STAVELEY , J. Chem. Soc. , 1420 & 2572 , (1951).
76. WOOD , SWEENY & DERBES , J. Amer. Chem. Soc. , 81 , 6148 , (1959).

77. HEDVALL & HEUBERGER , Z. agnew. Chem. , 140 , 251 , (1924).

78. HEDVALL & HEUBERGER , Z. anorg. Chem. , 197 , 399 , (1931).

79. HEDVALL & SJOMAN , Z. Electrochem. , 37 , 130 , (1931).

80. LINDNER , Acta Chem. Scanda. , 5 , 735 , (1951).

81. LANTELME & PAULY , Compt. rend. , 249 , 677 , (1959).

82. HARPUR & UBBELOHDE , Nature , 170 , 975 , (1952).

83. See for example,
Buerger , " Phase Transformations in Solids ", John Wiley & Sons, Inc. , New York , p183 , (1951).

84. AVIAKAN & SMAKULA , J. Appl. Phys. , 31 , 1720 , (1960).

85. See for example,
"Handbook of Chemistry and Physics" , (Chemical Rubber Publishing Company), 43rd. edition , p.2672 , (1961-62).

86. FICK , Pogg. Ann. , 94 , 59 , (1855).

87. SCHAMP & KATZ , Phys. Rev. , 94 , 828 , (1954).

88. SHIRN , WAJDA & HUNTINGDON , Acta Meta. , 1 , 513 , (1953).

89. PATTERSON , ROSE & MORRISON , Phil. Mag. , 1 , 393 , (1956).

90. STEIGMANN , SCHOCKLEY & NIX , Phys. Rev. , 56 , 13 , (1939).

91. PARRY & DOLLMAN , J. Analy. Chem. , 36 , 1783 , (1964).

92. FRIAUF , J. Appl. Phys. , 33 , 494 , (1962).

93. DOWNING JR. , U.S. At. Energy Comm. COO-1197-9, 61pp,(1965).
Chem. Abstracts , 63 , 3721d , (1965).

94. BANSIGIR & SCHNEIDER , J.Appl. Phys. , 33 , 383 , (1962).

95. LIDIARD , J.Appl. Phys. , 33 , 414 , (1962).

96. See for example,
Kroger , "Chemistry of Imperfect Crystals" , (North-Holland Publishing Company) , p.637 , (1964).

97. CAFFYN & SCHNEIDER , Phys. Soc. (London) , p.74 , (1955).

98. See for example,
Van Bueren , "Imperfections in Crystals" , (North-Holland Publishing Company) , p.513 , (1960).

99. See for example,
Mott and Gurney , "Electronic Processes in Ionic Crystals" , 2nd. edition , (Oxford, Clarendon Press) , Chapters I & II , (1946).

100. JACOBS & TOMPKINS , Quart. Rev. , 6 , 258 , (1952).

101. KAPUSTINSKI , Quart. Rev. , 10 , 283 , (1956).

102. GRUZENSKY & SCOTT , J. Phys. Chem. Solids , 21 , 128 , (1961).

102a. COHEN & KOOY , Z. Phys. Chem. , 109 , 81 , (1924).

103. PISTORIUS , J. Phys. Chem. Solids , 26 , 1003 , (1965).

104. ELLIOT & BJORKSTAM, J. Phys. Chem. Solids , 25 , 1273 , (1964).

105. SHANNON , See Chem. Abstracts , 63 , 2468b , (1965).